Synthesis of polyaniline-based conducting polymer and their hydrogels. Electrochemical applications

Chahineze Nawel Kedir

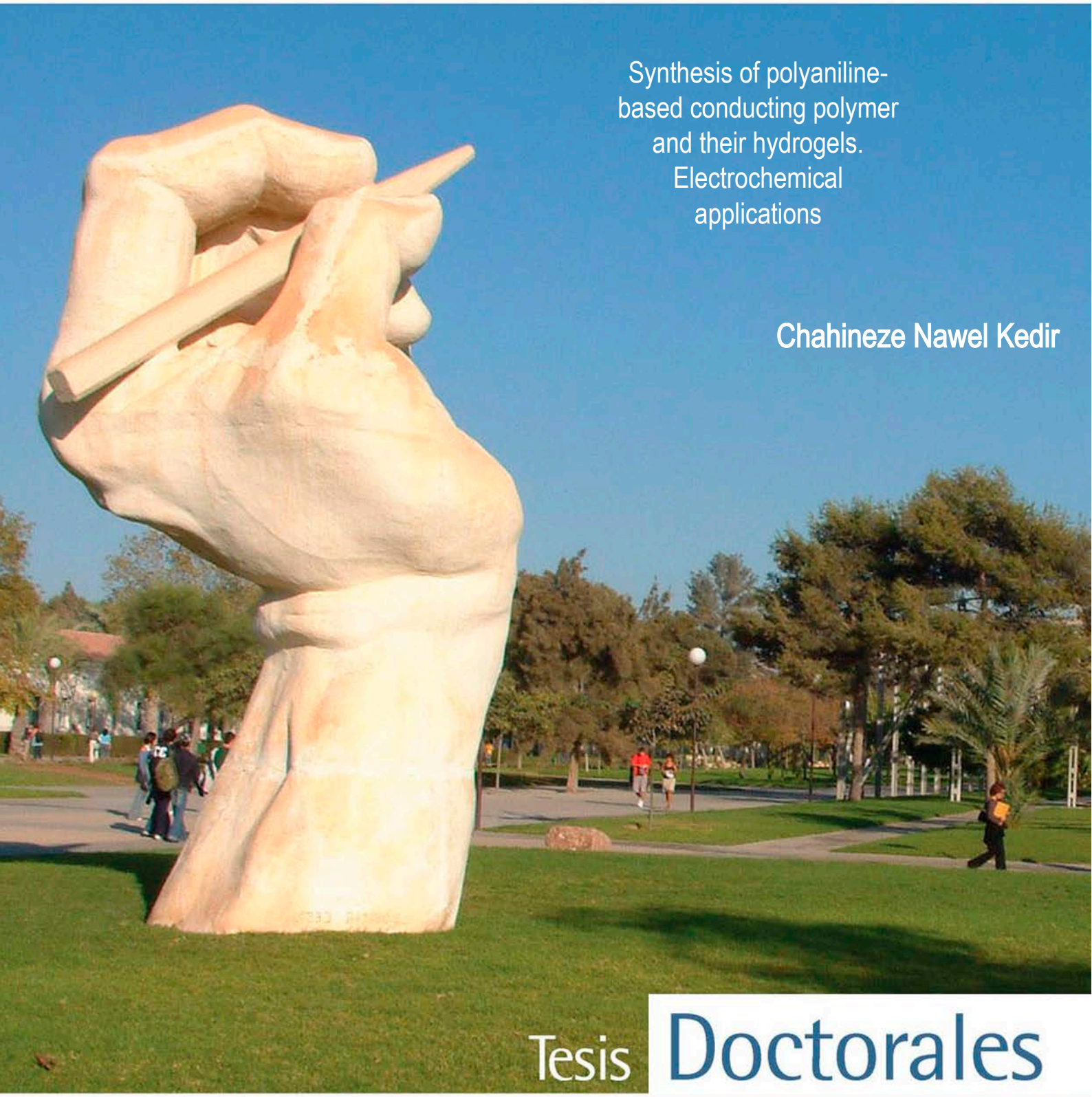

Synthesis of polyaniline-based conducting polymer and their hydrogels. Electrochemical applications

Chahineze Nawel Kedir

Doctoral Thesis

University of Mascara
faculty of science and technology
University of Alicante
University Institute of materials

Synthesis of polyaniline-based conducting polymer and their hydrogels. Electrochemical applications

Doctoral thesis presented by

Chahineze Nawel Kedir

To obtain the international doctorate degree from
University of Alicante and
University of Mascar

Directed by:

Emilia Morallón Núñez
Professor of physical chemistry

Abdelghani Benyoucef
Professor of Chemistry

Universidad de Mascara
Facultad de ciencia y tecnología
Universidad de Alicante
Instituto Universitario de Materiales

Synthesis of polyaniline-based conducting polymer and their hydrogels. Electrochemical applications

Chahineze Nawel Kedir

Tesis presentada para aspirar al grado de
DOCTORA por la UNIVERSIDAD DE ALICANTE y por la
UNIVERSIDAD DE MASCARA (Mustapha Stambouli)
En régimen de cotutela.
Programa de doctorado CIENCIA DE MATERIALES

Dirigida por:

Emilia Morallón Núñez
Catedrática de Química Física

Abdelghani Benyoucef
Prof. Ingeniería de procesos

« La mesure de l'intelligence est la capacité à changer »

Albert Einstein

ACKNOWLEDGMENT

Ma thèse

A été réalisée,
Avec la collaboration de groupes de recherche
Electrocatalyse et Electrochimie des Polymères (GEPE)
et l'Institut des Matériaux de l'Université d'Alicante, Espagne (IUMA)
et Laboratoire de Chimie Organique, et Matériaux Macromoléculaires de Mascara, Algérie (LCOMM).
de l'Université Mustapha Stambouli, Mascara Cette thèse de doctorat opte pour la mention
"International Ph.D"

C'est l'aboutissement, de plusieurs années de travail acharné,
afin de développer le thème proposé dans les règles de l'art et de la science, en proposant des solutions pratiques et efficaces,
je souhaiterais aussi rendre hommage et remercier du fond du cœur, Toutes les personnes qui m'ont permis, de mener à bien ce travail, dans d'excellentes conditions.

A madame **Emilia MORALLON**,
Professeur Département de Chimie Physique,
Directrice du Laboratoire de d'Electrocatalyse & Electrochimie des Polymères GEPE
Université d'Alicante

Ma profonde gratitude,
de m'avoir ouvert les portes de votre laboratoire,
pour l'accueil chaleureux, abstraction faite de tout protocole,
j'étais toujours la bienvenue au sein de votre équipe
et ça me réjouit.
vous m'avez fait profiter de votre savoir- faire extraordinaire,
votre aide m'était précieuse.

A *Monsieur* **Abdelghani BENYOUCEF**,
Professeur Département de Chimie Université Mustapha Stambouli de Mascara

Merci infiniment,
de votre contribution à l'accomplissement
de ce travail de recherche. Votre assistance était prépondérante à l'achèvement de ce dur labeur, Je tiens à vous remercier pour l'opportinité que vous m'avez accordez, La Cotutelle entre l'université
Algerienne et Espagnole.

A **Tous Mes Enseignants**

Du primaire à l'université, en passant par le CEM et le lycée

Merci d'avoir fait de moi ce que je suis maintenant.
vous m'avez transmis les bases solides du
savoir et des connaissances, pour évoluer

et faire évoluer.

A **mes amis et collègues**

Du Laboratoire d'Alicante en Espagne,
votre bonne humeur intacte à toute épreuve,pour votre aide inconditionnelle,la courtoisie et l'amour du savoir,
Mille merci a Andrés Felipe Quintero Jaime tu es la personne qui ne dit jamais Non !
Tu es disponible pour toutes personnes qui a besoin d'aide tu as le sense de partage et de transfert de savoir ;
Tes nobles valeurs font de toi une personne unique !
Je me souviendrai de toi à jamais.

De la Faculté de Technologie De la Faculté des Sciences Exactes
je vous suis reconnaissante, d'être toujours à mes côté
à chaque fois que j'en avez besoin.
Mes Sincère Amitié.

A **MA FAMILLE**

A la mémoire de mon Frère que je n'oublierai jamais,
A mes grands parents,
A ***Mes chers Parents****,*

Ma mère et mon père,
source inépuisable d'amour et d'affection qui m'ont toujours aidé et soutenu, même dans les moments de détresse, vous êtes ma source d'inspiration et d'équilibre je leur dédie spécialement ce travail
je vous Aime plus que tout au Monde !

A ***Mes adorables Frères et Soeur****,*

merci beaucoup
pour tout ce que vous avez fait pour moi,
sacrifices et temps accordez pour chaque main tendue, pour chaque instant passer a mes cotés vos Rire et Delire
me rende plus forte
je vous Adore !

A ***Mon Mari,***

Ta présence et ton encouragement,
me font pousser des ailes ! Tu es un modèle à méditer Amour ; Attention ;Douceur et Gentillesse ; et le plus c'est le Temps que tu m'as consacré et la prommesse tenue.
J'espère te combler et te rendre heureux et fière de moi pour un long commun serein.
Je te dédis ce travail et qu'il soit le témoignage de
ma reconnaissance et De mon amour sincère ;
A nos futures enfants.
Ti amo Vita mia. . .

A ***<u>Mes Amis</u>***

A ma très chère copine Halima Djelad sans toi je n'en serai pas là ! Ta présence, ton attention ont été si importantes dans la réalisation de notre objectif LMD.
Je dédie ce travail à notre sincère amities et aux années de moments inoubliables.
A ma très chère Amie Zoubida Taleb dont la présence, la disponibilté .À tout moment ont été si importantes dans
la réalisation de ce modeste travail.
Vous etes des perles Rares !

.... Et à tous ceux qui me sont chers.

Pour vous...

Maman

Papa

INDEX

STRUCTURE AND OBJECTIVE OF THE DOCTORAL THESIS

CHAPTER 1: GENERAL INTRODUCTION

CHAPTER 2: MATERIALS, METHODS AND EXPERIMENTAL TECHNIQUES

CHAPTER 3: AN ELECTROCHEMICAL STUDY ON THE COPOLYMERS FORMED FROM 2-AMINOTEREPHTHALIC ACID, PIPERAZINE, AND ANILINE MONOMERS TESTING THEIR SENSITIVITY TOWARDS DOPAMINE AND ASCORBIC ACID

CHAPTER 5: SYNTHESIS AND CHARACTERIZATION OF HYDROGELS OBTAINED FROM ANILINE AND AMINOTEREPHTHALIC ACID AND PIPERAZINE MONOMERS

CHAPTER 6: HYBRID SUPERCAPACITORS FROM SUPRAMOLECULAR HYDROGELS

CHAPTER 7: GENERAL CONCLUSIONS

CHAPTER 8: RESUMEN Y CONCLUSIONES GENERALES.

STRUCTURE AND OBJECTIVE OF THE DOCTORAL THESIS

1 Introduction

The polymerization of aniline with other monomers is of great importance in the synthesis of new conducting polymers that improve the properties and characteristics of polyaniline. Thus, the use of aminoterephthalic acid and piperazine together with aniline is of great interest because aminoterephthalic acid contributes with two carboxylic groups to the polymer and piperazine can act as a complexing agent. Moreover, the so-called hydrogels can have numerous applications. Then, the electrochemical applications of these conducting polymers as sensors and supercapacitors are growing in recent years. Then, the present PhD thesis focuses on the synthesis of polyaniline-based conducting polymer and conducting polymer hydrogels based on piperazine and aminoterephthalic acid, and their electrochemical applications.

2 Objectives of the PhD Thesis

The main objective of this PhD Thesis is the synthesis of polyaniline-based conducting polymer with piperazine and aminoterephthalic acid and conducting polymer hydrogels and their electrochemical applications. The performance in electrochemical sensors and as electrodes in supercapacitors has been studied. The following specific objectives are presented:

- To study the electrochemical behaviour of piperazine and 2-aminoterephthalic acid in acid medium.
- To study the electrochemical method for synthesis of conducting polymer from aniline and monomers (piperazine and 2-aminoterephthalic acid) in acid medium using a platinum electrode.
- To synthesize conducting polymer hydrogels using polystyrene sulfonate as crosslinker. Then, polyaniline-poly(styrene sulfonate) and different hydrogels poly(Ani-co-2ATA)/PSS) and poly(Ani-co-PIP)/PSS have been studied.
- The chemical, morphological and electrochemical characterization of the different synthesized conducting polymers and copolymer hydrogels.
- To evaluate the applicability of the electrochemically copolymers as electrochemical sensors for the detection of dopamine and ascorbic acid.
- To evaluate the applicability of the different hydrogels as electrodes in supercacitors.

3 Structure of the PhD Thesis

The present PhD Thesis has been performed in the research groups of Electrocatalysis and Polymer Electrochemistry (GEPE) and the Materials Institute of the University of Alicante, Spain (IUMA) and Laboratory of Organic Chemistry, Macromolecular Materials University of Mascara, Algeria (LCOMM) in cotutele international.

- Chapter 1: General Introduction.

In this chapter an introduction of the main concepts and a specific description of conducting polymers is performed. Moreover, the description of the different electrochemical sensors and supercapacitor application in several fields are included.

- Chapter 2: Materials, methods and experimental techniques.

This chapter describes the different reagents, techniques and methods employed during this PhD Thesis. A summary of the main concepts for each technique employed for physicochemical, morphological and electrochemical characterization is presented. Moreover, the different procedures, the accurate determination of the species of interest, different equations and statistical methods employed for the validation and reliability of the results obtained, are described in detail in this chapter.

- Chapter 3: An Electrochemical Study on the Copolymers formed from 2-Aminoterephthalic Acid, Piperazine, and Aniline Monomers Testing their Sensitivity towards Dopamine and AscorbicAcid

In this chapter, a study on the electrochemical oxidation of piperazine, 2-aminoterephthalic acid and their electrochemical copolymerization with aniline in acidic medium is presented. It was found that the homopolymerization of piperazine cannot be achieved under electrochemical conditions. A combination of electrochemistry, in situ Fourier transform infrared (FTIR), and ex situ X-ray photoelectron spectroscopy (XPS) spectroscopies was used to characterize both the chemical structure and the redox behavior of an electrochemically synthesized copolymers. The electrochemical sensing properties of the deposited materials on platinum electrode were also tested against ascorbic acid and dopamine as redox probes.

Results of this chapter have been published in:
Dkhili, S.; López-Bernabeu, S.; Kedir, C.N.; Huerta, F.; Montilla, F.; Besbes-Hentati, S.; Morallon, E. An Electrochemical Study on the Copolymer Formed from Piperazine and Aniline Monomers. *Materials* **2018**, *11*, 1012. https://doi.org/10.3390/ma11061012

- Chapter 4: Synthesis and Characterization of Hydrogels Obtained from Aniline and Aminoterephthalic Acid and Piperazine Monomers

In this chapter, the chemical synthesis of hydrogels from aniline and 2-aminoterephthalic acid or aniline and piperazine have been studied. These copolymer hydrogels can improve the properties of polyaniline hydrogel like solubility and interaction with other compounds. Then the copolymers (poly(ANI-co-2ATA)/PSS)and poly(Ani-co-PIP)/PSS) have been characterized using different techniques. A combination of X-ray photoelectron spectroscopy (XPS), Thermogravimetric analyses (TGA) and Fourier transform infrared (FTIR) spectroscopy have been used for the characterization of the hydrogels. Electrochemical techniques have been used to analyze the redox behavior of the copolymer. Finally, The conductive properties of the hydrogels have been tested with four-point probe method. The mass swelling ratio was measured by comparing the hydrated weight with the dehydrated weight.
Some of the results of this chapter have been submitted for publication in Journal of Molecular Structure.

- Chapter 5: Hybrid Supercapacitors from Supramolecular Hydrogels

In this chapter, the applicability of different hydrogels prepared in the previous chapter as electrodes in capacitors in aqueous solution have been evaluated. Modification of hydrogel copolymers with multi wall carbon nanotubes (MWCNTs) and carbon black (Vulcan) has been also studied.

- Chapter 6: General Conclusions

In this chapter the main conclusions of the PhD Thesis are presented.

- Chapter 7: Conclusiones generales

En este capítulo se presentan las principales conclusiones de la Tesis Doctoral.

- Chapter 8: Resumen y conclusiones generales.

Este capítulo contiene un resumen del trabajo de Tesis Doctoral que incluye una introducción general, un resumen de los resultados y de la discusión organizada de acuerdo con los capítulos presentados, incluyendo también las conclusiones generales de la tesis

Chapter 1

GENERAL INTRODUCTION

1 Introduction

Nowadays, it is impossible to ignore the importance of polymers in the development of new technologies, they are present in all areas, from food to aerospace through cosmetics. They are light, simple to implement and have a much lower cost than most of their competitors; some even consider that they will be at the heart of the next industrial revolution. A considerable number of articles, reviews, books and PhD Thesis have been written on conducting polymers (CPs), often incorporating different perspectives from chemistry and from physics to materials science and engineering[1]. As if often done in this area, a look at nature for inspiration indicates that complexity, rather that simplicity, is often the evolutionary result. A revision of the Faraday Discussion section of the Chemical Society regarding the charge transfer in polymers from almost two decades ago suggests that polymers with the same composition rarely behave in exactly the same way [2]. However, the research on new materials based on CPs and a better understanding of the properties and characteristics of these kind of polymers will allow the development of new applications.

CPs are the most recent and promising generation of polymers. They have many desirable properties generally associated with conventional polymers but also exhibit electrical properties similar to those of metals and inorganic semiconductors. CPs have played a central role in the latest technological development, and the expansion of polymer properties which is gaining unprecedented fields of application. The number of articles has increased considerably over the past twenty years, as shown in (Figure 1.1), which shows a great interest in this field.

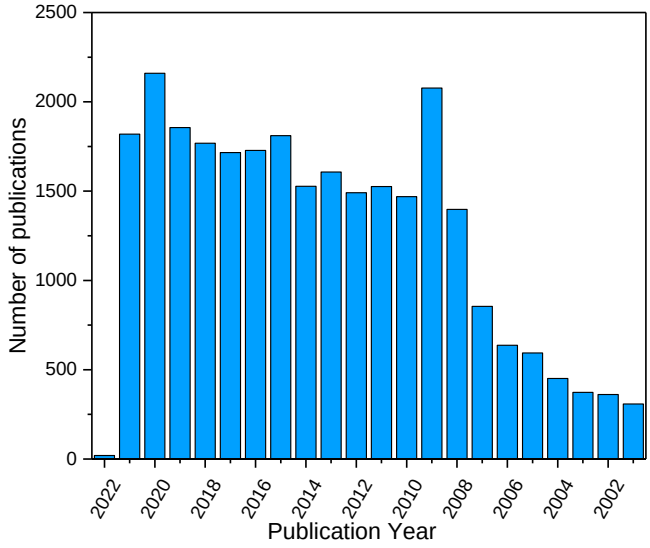

Figure 1.1: Number of publications on conducting polymers in Scopus.

Conducting organic polymers are a new class of "synthetic metals" that can, for some, combine the chemical and physical properties of polymers with the conductive properties of metals and semiconductors[3,4] However, the main disadvantages were the difficulties of implementation and their low chemical stability. In 1979, the electrochemical approach for the synthesis of CPs was reported by Diaz et al., who synthesized electrochemically polypyrrole (PPy) films with good electrical and mechanical properties [5]. Simultaneously, Heeger et al. reported that CPs submitted to chemical and electrochemical redox processes yield materials with relatively high electric conductivities [6]. In 1985, MacDiarmid et al. developed the synthesis of polyaniline (Pani) [7]. The latter is increasingly used, because of its low cost of synthesis compared to other conductive polymers, its doping and its easy implementation, its good stability to ambient air and especially its good conductivity which could reach values close to 100 $S.cm^{-1}$. In addition, polyaniline is a case apart among the conductive polymers since it has the distinction of being able to go from a semiconductor state to a conductive state not only by redox doping, but also by acid-base doping. In 2000, Heeger, MacDiarmid and Shirakawa were distinguished with the Nobel Prize in Chemistry for the discovery and development of CPs [8].

Polyaniline is one of the most common conducting polymers, which can be synthesized either by chemical oxidation polymerization [9,10] or electropolymerization [11]. In 1862, Letherby reported the anodic oxidation of aniline (Ani) in dilute sulphuric acid, which yielded an insoluble deep-blue shiny powdered deposit on a platinum electrode[8]. That was the first reference describing the synthesis of a CP. From such initial discovery, further studies were reported [11–14].In recent

decades, CPs have attracted great interest within the scientific community and, as a result, a large number of these chemical compounds have been developed and extensively investigated [5,8,12,15,16].

1.1 Conducting polymers

1.1.1 Definition of polymer

A polymer is a chemical molecule, natural or synthetic, composed of a large number of covalently-bonded repeating structural units; the word polymer comes from the combination of the two Greek words "Poly" (many) and "mer" (parts) [17]. In this definition such once you would have to change chemical compound by macromolecule, but it explains well how polymer is made up of smaller units called monomers, attached through the polymerization process. In nature, we can find natural polymers such as cellulose, wool, silk and rubber. In the case of synthetic polymers, they are obtained by chemical reactions and some examples are polyvinylchloride (PVC), nylon, polyethylene, polypropylene, polyamides, polycarbonates, etc[18]. Polymers are materials in continuous development in the field of Materials Science, discovering more applications every day (e.g., plastics, rubbers, fibers, paints, adhesives, etc.) to cutting-edge uses (aircraft, bullet-proof vests, artificial joints, etc.).

In the case of small molecules it is possible to assign a molecular weight [19,20] but this is not so easy in the case of polymers, because the reactions of polymerization generally do not tend to produce chains of the same length. In samples, there are chains that have the same molar weight and will not necessarily have the same dimensions or molecular forms, due to conformational isomerism, which it can exist. Finally, it is unlikely that all the chains that are formed are completely linear, some reactions can also occur that, and they can cause branched chains, being able to reach extreme cases where they can even obtain three-dimensional networks by the intersection of two different chains through some of its ramifications (Figure 1.2).

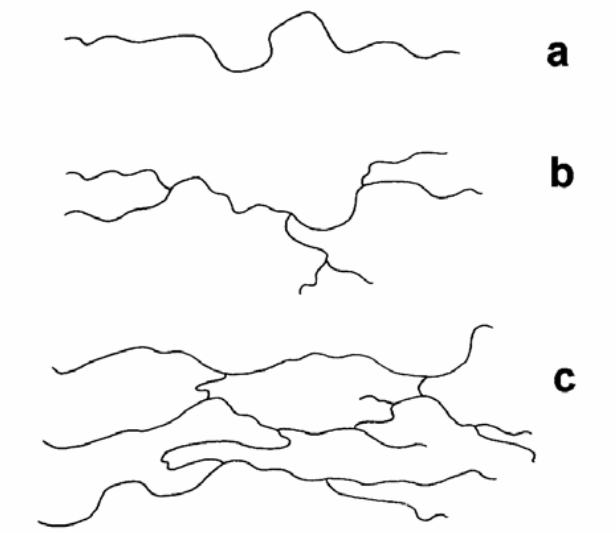

Figure 1.2: Representation of the different types of polymers, a) Linear, b) Branched, c) Crosslinked.

The polymers formed by two types of monomers are called copolymers (Figure 1.3) and they can be classified as i) alternating, in which the repeating units alternate consecutively to the chain length, ii) random, in which there is not defined a sequence in the ordering of the units repeat along the chain, iii) in block, in which a complete sequence of a single repeating unit is observed, followed by sequence from other repeat unit and iv) grafted in which there is a main chain consisting of a single type of unit repeating, which has grafted blocks of chain laterally to form strings by the other repeat unit.

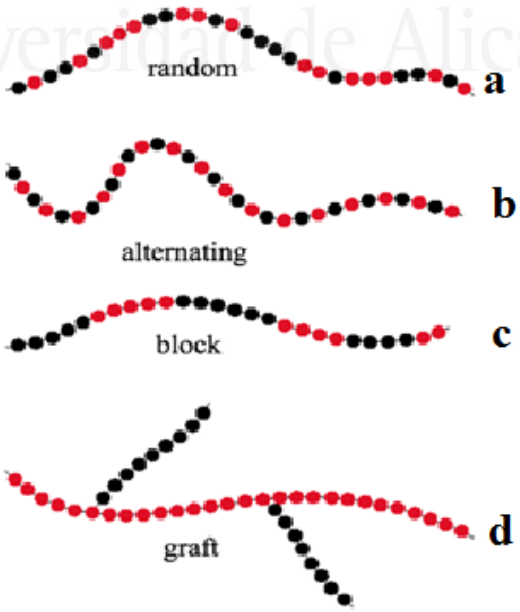

Figure 1.3: Scheme of different types of copolymers, a) random, b) alternated, c) blocks and d) grafted.

1.1.2 Classification of polymers

Polymers are used for many applications replacing materials traditional as wood, iron, steel, cardboard, etc. The materials that can be manufactured with polymers can be divided into three broad categories (Figure 1.4):

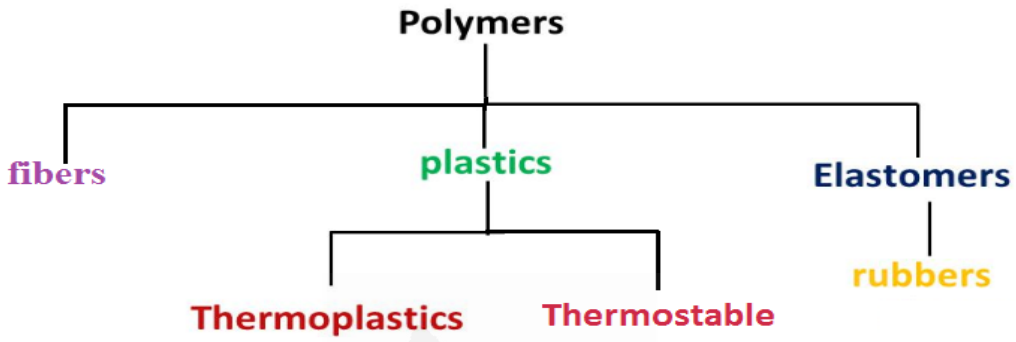

Figure 1.4: scheme of general classification of polymers

1.1.2.1 Fibers

This type of materials is characterized by the existence of an order monoaxial at the molecular level with direction parallel to the axis of the filament, and they usually have a high degree of crystallinity, although they can be obtained with amorphous phases. At the macroscopic level a fiber is defined as a flexible and homogeneous object that has a length / diameter ratio minimum of 100; however, it will only be fiber if it has order at the molecular level. Therefore, the defining physical parameter of the fiber structure is the degree of orientation, which can be determined by different methods: microscopy optics, x-rays and infrared dichroism. Similarly, another fundamental parameter of the fiber is crystallinity, whose evaluation is difficult, if you want to get information about the distribution of the amorphous and crystalline phases. There are several methods for its determination, being the most useful X-ray diffractometry, IR spectroscopy and calorimetry sweep differential (DSC).

1.1.2.2 Plastics

All those polymers whose properties are intermediate between elastomers and fibers and it can be divided taking into account their use in:

- General use: They are manufactured in high quantities and are dedicated to multiple applications. They have intermediate properties that can be partially modified for a specific application by additives or proper processing.
- Engineering plastics: They have significantly better prices such as a consequence of its lower production volume. They are characterized by special properties for demanding applications, usually they have a high crystallinity. They compete with mechanical materials and with ceramics with the advantage of its lower density and ease of processing.
- Advanced polymers: They are designed to satisfy a concrete application they usually present some exceptional property such as high electrical conductivity, biocompatibility or formation of liquid crystals.

The transformations of synthetic polymers give two kinds of polymer:

- Thermoplastic polymers: are soften with heat and harden by cooling, they have a similar structure before and after processing (reversibility), and have physical interactions between polymer chains.
- Thermostable polymers: after thermal treatment they acquire an irreversible structure, as a consequence of crosslinking reactions between the polymer chains.

The same polymer can be thermoplastic or thermostable (e.g. rubbers with poly-isoprene chains are thermoplastic but when we add a sulfur becames thermostable by vulcanization), this process gives us the elastomers.

1.1.2.3 Elastomers

Those materials which have elasticity as their distinctive quality snapshot, which must be recovered and unlimited at high deformations, normally polymers that meet these requirements have high molecular weight, and a very low glass transition temperatures and are amorphous in the relaxed state. However, a fundamental requirement is the existence of crosslinking between polymer chains, which prevent molecular displacement. The more representatives of this type of materials are rubbers.

1.1.3 Classification of Conducting Polymers

In recent decades, CPs have attracted great interest within the scientific community and, as a result, a large number of these chemical compounds have been developed and extensively investigated[12,15]. (Figure 1.5) shows a simple classification of CPs according to their chemical structure.

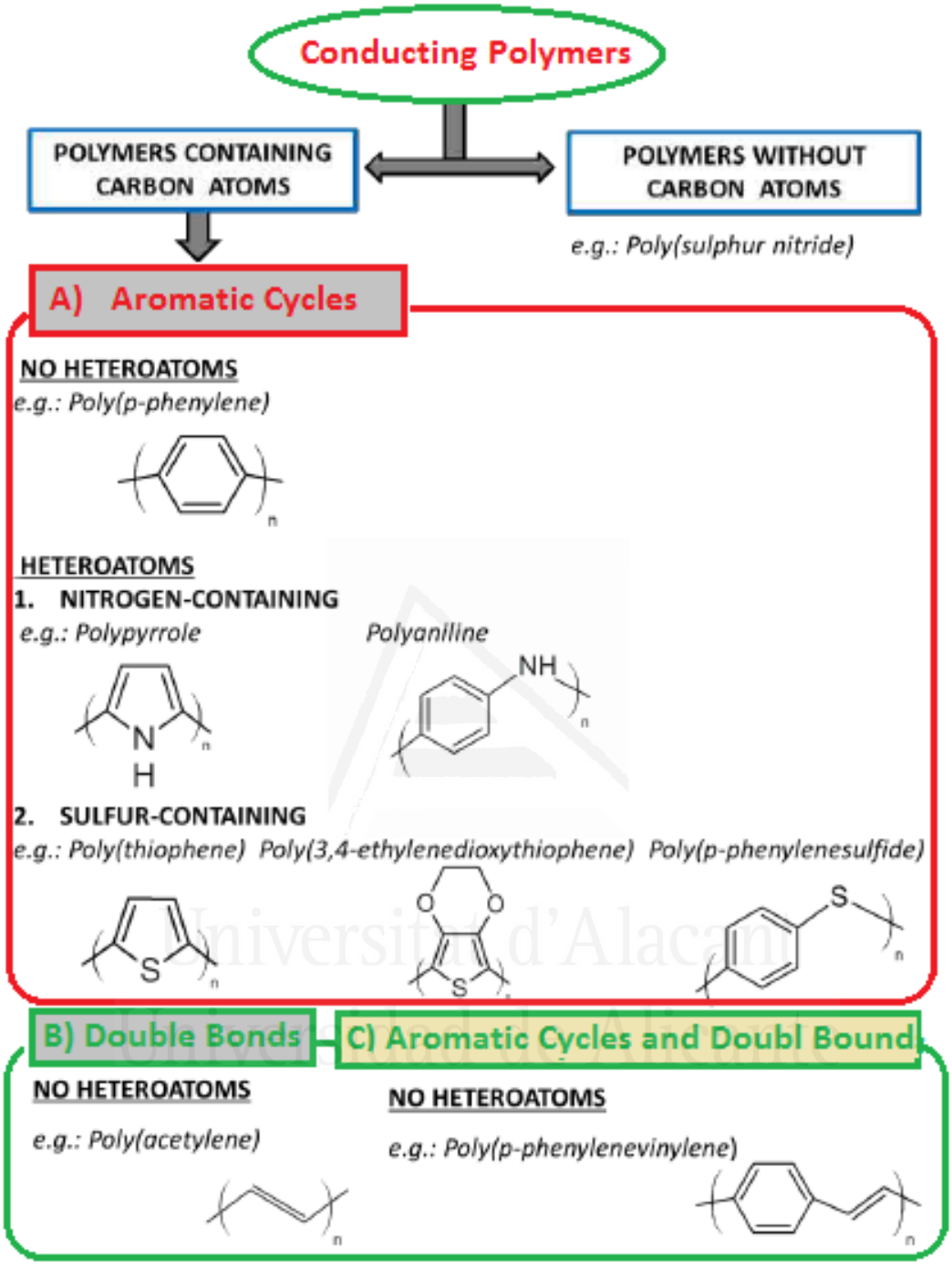

Figure 1.5: General classification of CPs according to their chemical structure.

Moreover, conducting polymers can be classified depending on the i) nature of polymer and dopant (Figure 1.6) and ii) conduction mechanism (Figure 1.7)

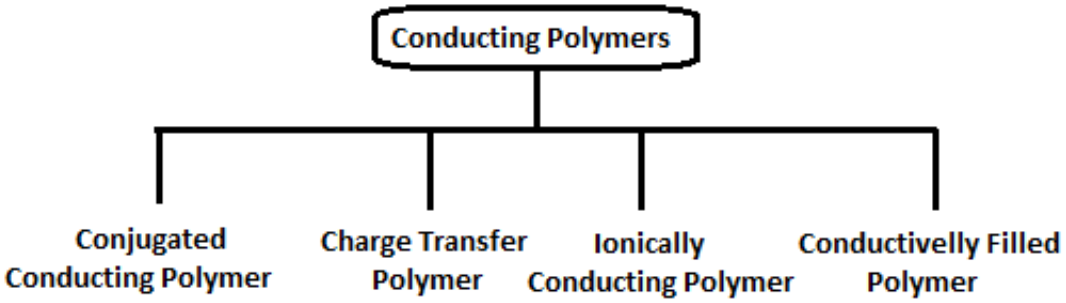

Figure 1.6: Classification of conducting polymers based on nature of matrix and dopant

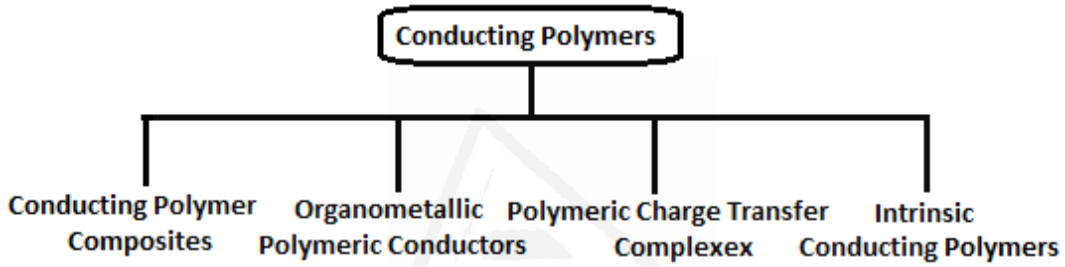

Figure 1.7: Classification of conducting polymers based on Conduction Mechanism

1.1.4 Synthesis of Conducting Polymers

Conducting polymers may be synthesized by any one of the following methods [21].

i) Chemical polymerization

ii) Electrochemical polymerization

iii) Photochemical polymerization

iv) Metathesis polymerization

v) Concentrated emulsion polymerization

vi) Inclusion polymerization

vii) Solid-state polymerization

viii) Plasma polymerization

ix) Pyrolysis

x) Soluble precursor polymerization

xi) Microwave polymerization

The most used technique is based on the oxidative coupling which involves oxidation of monomers to form a cation radical followed by coupling to form a di-cation. This can be performed by chemical or electrochemical polymerization.

In chemical polymerization, a monomer, a dopant, and an oxidant are dissolved in a solution kept at a certain temperature. The polymerization mechanism is still uncertain. Many research groups have adopted the cation-radical mechanism even though there is disagreement about the steps involved in chain growth.[22,23] The monomer is first oxidized into a radical cation, which has several resonance forms of cations. The coupling of two radical cations results in a dimer. The dimer can then be oxidized into a dimer radical cation and propagation of these reactions produces oligomers followed by polymers until termination of the chain. The polymerization time ranges from minutes up to a few days, depending on reaction conditions. The mixture is then filtered, washed, and dried to yield pure conducting polymers.

Similar to chemical polymerization, in the electrochemical polymerization the radical cation is generated at the initial step via an applied potential within an electrolytic solution of the monomer. Electrochemical polymerization is convenient, since the polymer does not need to be isolated and purified.

As discussed above, in both polymerization synthesis (chemical and electrochemical), the initial step is the formation of the radical cation (Figure 1.8), followed by coupling reaction of radical cations[24]. These both strategies have advantages and disadvantages, which are summarized in Table 1.1.

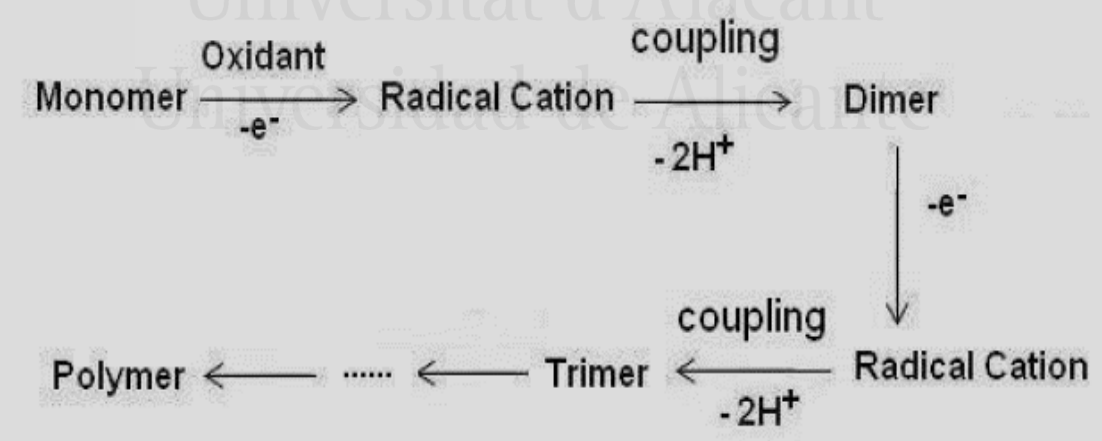

Figure 1.8. Polymerization scheme of a conducting polymer.

Polymerization Method	Advantages	Disadvantages
Chemical polymerization	a) Larger-scale production b) Post-covalent modification of bulk CPs c) More options to modify CPs backbone covalently	a) Synthesis more complicated b) Difficult to make thin films
Electrochemical polymerization	a) Ease of synthesis b) Entrapment of molecules in polymer network c) Doping and synthesis are simultaneous d) Easy to make thin films	a) Difficult to remove film from electrodes surface b) Post-covalent modification of bulk CPs is difficult

Table 1.1. Comparison of chemical and electrochemical CPs polymerization. [25]

1.1.5 Structure and Properties of conducting polymers

1.1.5.1 Electrical conductivity

The electrical conductivity of CPs results from mobile charge carriers introduced into the π-conjugated system that is formed by the continuous overlap of extended and delocalized p-orbitals along the polymer chain's backbone. However, conducting polymers without doping generally exhibit very low conductivity at room temperature. Their conductivity can be varied by adding a dopant to change the charge carrier density on the polymer backbone

Table 1.2 lists the conductivities and Energy gap for some common conjugated polymers[26]. As can be seen in Table 1.2, the conjugated structure with alternating single and double bonds or conjugated segments coupled with atoms providing p-orbitals for a continuous orbital overlap (e.g. N, S) seems to be necessary for polymers to become intrinsically conducting.

Polymer (Conductivity discovered)	Energy gap (eV)	Conductivity (S/cm)
Polyacetylene (1977)	1.5	$10^3 – 1.7\times10^5$
Polypyrrole (1979)	3.1	$10^2 – 7.5\times10^3$
Polythiophene (1981)	2.0	$10 – 10^3$
Poly(p-phenylene vinylene) (1979)	2.5	$3 – 5\times10^3$
Polyaniline (1980)	3.2	30 – 200

Table 1.2: conductivity of some conjugated conducting polymers[29].

Materials are divided into three different types, metals, semiconductors and insulators (Figure 1.9) [27,28]. For a long time metals were considered as dominant area of electrical conductivity until the discovery of semiconductors which opened a new field for basic scientific and applied science researches. Two categories are now available, one is melt-processable and thus highly efficient at creating conductive networks when alloyed with a thermoplastic polymer which is under research and development and the other is coating which is utilizing in some industrial purpose and considered as a useful method in some industrial application.

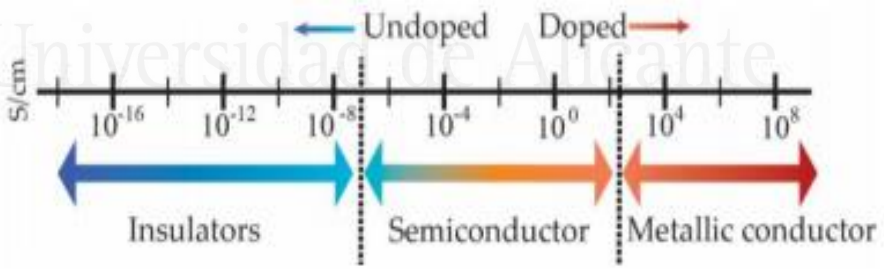

Figure 1.9**:** conductivity range of conducting polymers (CPs).[27,28]

From Figure 1.9, CPs with a theoretical conductivity between from 10^{-8} S/m to 10^8 S/cm could be obtained. In the literature CPs with conductivity as high as 10^4 S/cm has been synthesized. However, the typical values are in the range of 1-100 S/cm. [29]

1.1.5.2 Doping of Conducting Polymers

Conducting polymers show poor electrical conductivity in the undoped state; however, they should be treated with an appropriate oxidation (p-doing) or reduction (n-doping) treatments to increase their conductivities to the metallic region. These processes have been named as "Doping". Doping results in exciting changes in the electrical, optical, and structural characteristic of the polymer but this process is not precisely the same as that in inorganic semiconductors. The doping method in CPs is reversible. Both doping and undoping forms, including dopant counter particles which settle the doped case, might be done chemically or electrochemically. Doping in inorganic semiconductors makes either holes in the valence band or electrons in the conduction band; however, doping in CPs offers an increase in the arrangement of conjugation deformations, in other words, solitons, polarons or bipolarons in the polymer chain (Figure 1.10).

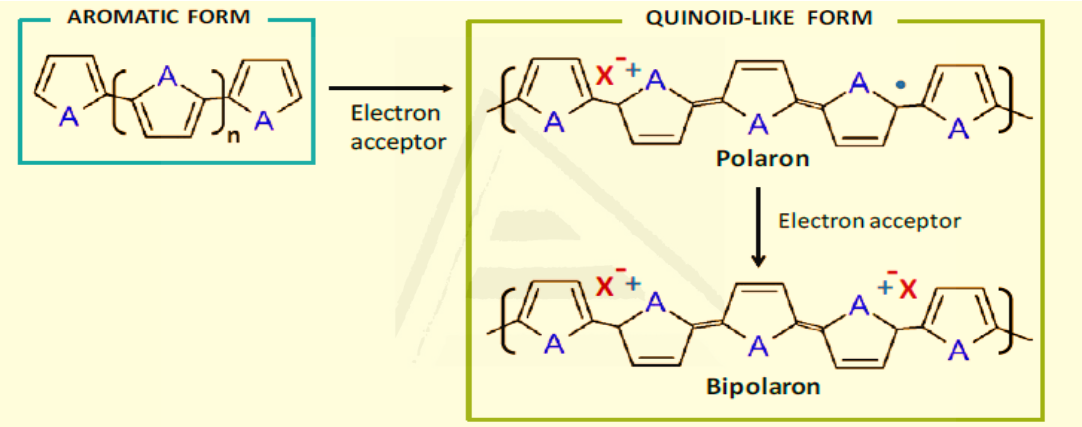

Figure 1.10. Formation of polarons and bipolarons (p-type doping) in polyheterocycles. A = S, NH or O.

Dopants in conducting polymers may be classified as ionic dopants, organic dopants, and polymeric dopants. The dopants are incorporated into the polymer during the oxidizing or reducing processes to make the polymer electrically neutral. Organic dopants are anionic dopants generally incorporated into polymers from aqueous electrolytes during anodic deposition of the polymer.

1.1.6 Functionalized conducting polymers

The modification of CPs at chemical and biological level has become the most popular choice for many applications. CPs exhibit many advantages over other electroactive materials or other semiconductors and metals (e.g. silicon and gold). Specifically, CPs are inexpensive, easy to synthesize and versatile. In recent years, most research has been focused on improving their

electrochemical properties, morphology and biological characteristics, allowing the achievement of specific materials for the intended applications. The main strategies developed to design such improvements are classified in two groups, which correspond to those involving non-covalent and covalent modifications. As shown in (Figure 1.11) non-covalent modifications include adsorption, physical entrapment and affinity binding while covalent modifications include chemical bond and copolymerization. Other strategies used to change physical properties are micro- or nano-patterning, which include the use of templates that can be removed to yield free-standing structures, and modification of the parameters used for the electrochemical synthesis of CPs (e.g. dopant and deposition charge).

Also, CPs can be combined with a wide variety of materials (e.g. metal nanoparticles, living cells, polymers) to enhance the desired properties. As a result of these combinations, CPs can be categorized into five groups: basic polymers, substituted polymers, self-doped polymers, copolymers and composites.

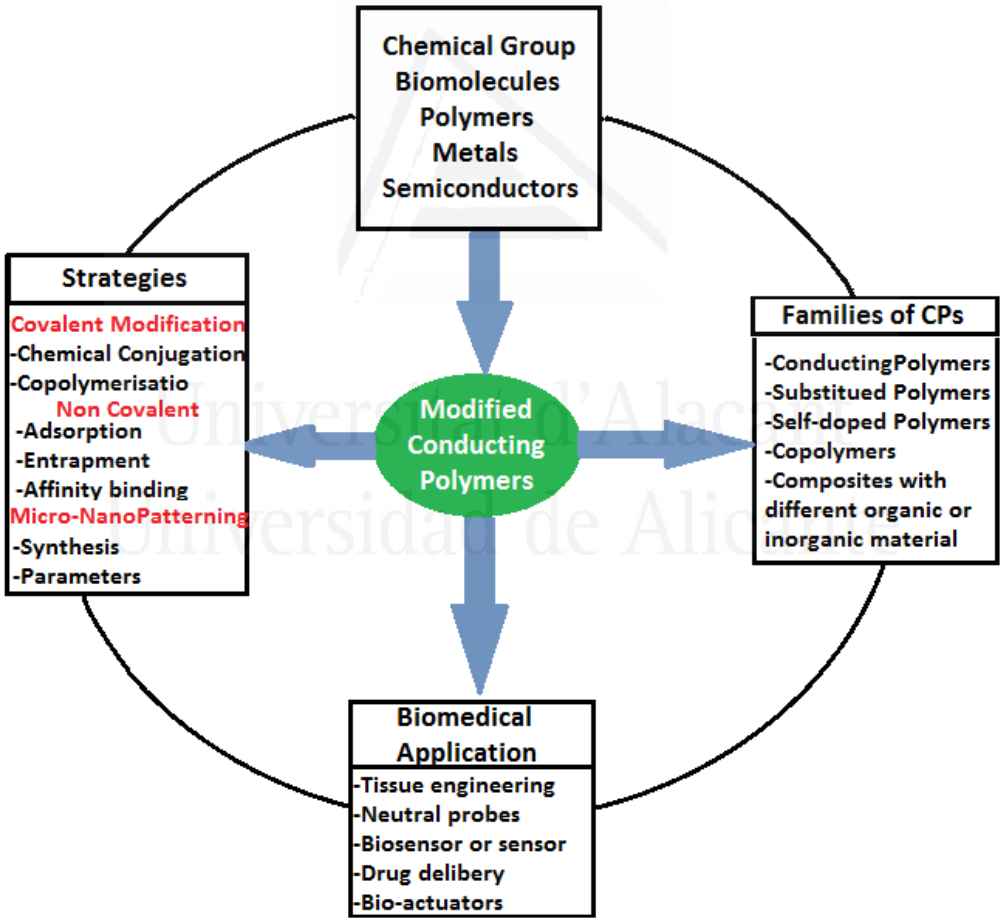

Figure 1.11: Principal strategies to modify CPs for biomedical applications.

The copolymers have expanded the range of electronic and electrochemical applications of the polymer family in several fields[30–32]. These copolymers have an interest in renewable energy[33], electrochemical capacitors [34], sensors [35], magnetic shielding [36], and corrosion [37].

Electrochemical copolymerization reactions offer a fairly clean way, using only electrons as oxidizing agents, to lead copolymers with interesting properties. Copolymers based on aniline can be exploited in the field of detection of compounds that are useful in environmental fields and health [38], and the combination with other compounds can provide some catalytic activity [37–39]. In addition, to benefit from the use of copolymers based on aniline as bioelectrochemical sensors, the electroactivity at physiological pH is recommended and then, the introduction of some groups with acido-basic properties, such as 2-aminoterephthalic acid is recommended [40].

1.2 Polyaniline

Polyaniline (Pani) is one of the most widely studied conducting polymers because of its inexpensive cost, facile synthesis, and easy doping/dedoping. Pani, it was discovered in 1934 also known as aniline black, was first discovered as a dye and has been studied over 100 years. Also exists naturally as part of a mixed copolymer with polyacetelene and polypyrroles[41–43].

Polyaniline has multiple structural forms, accepts special doping mechanisms to produce high conductivity, and retains good environmental stability in air[44].Moreover, it can be easily synthesized by either chemical or electrochemical oxidation of aniline[45]. And then processed into powder, films fibres and composites with other materials.

Pani is phenylene rings-based polymer having a chemically flexible –NH– group in a polymer chain flanked either side by a phenylene rings. They provide precisely controlled electrical conductivity over a wide range, improve phase compatibility and thus blendability with bulk polymers, and provide easier means of processing and forming conductive products which could be future development in this area[46].

Pani can exist in several different oxidation states[47]. From a series of electrochemical studies where taken a discrete structural unit (4 units), have been identified the different oxidation states of polyaniline. The electrochemical response of Pani is presented in Figure 1.12, in which the voltammogram of the Pani in acidic medium shows two redox processes corresponding to the different oxidation states of the polymer [42]. The oxidized form is called pernigraniline and the reduced is known as leucoemeraldine, while the intermediate state is called emeraldine, which presents the higher conductivity values. Figure 1.13 shows the different structures of the oxidation states of Pani from the leucoemeraldine to pernigraniline.

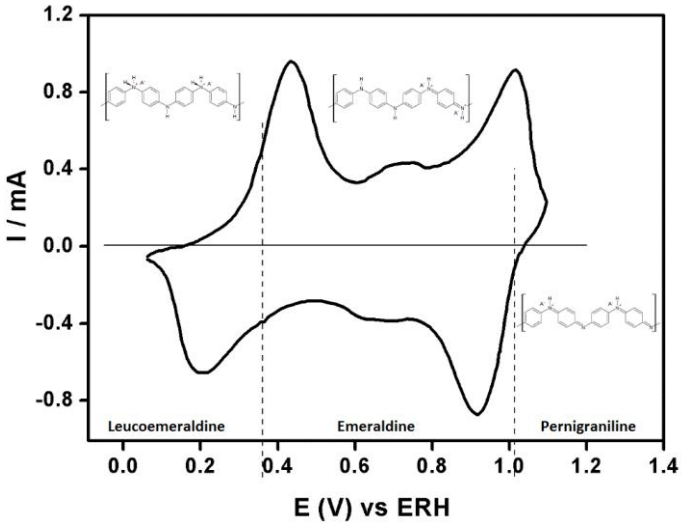

Figure 1.12: Cyclic voltagram of polyaniline in acidic medium and its structures [42].

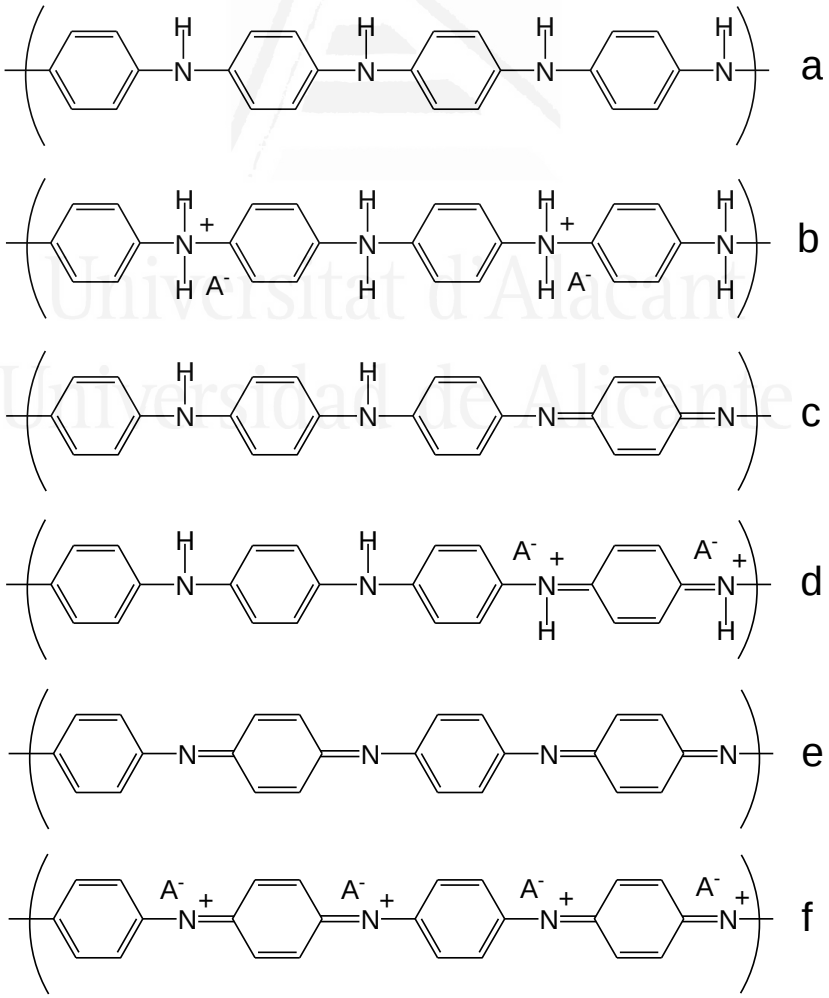

Figure 1.13. Different Pani structures according to the oxidation state. a) Leucoemeraldine base, b) Leucoemeraldine salt, c) Emeraldine base, d) Emeraldine salt, e) Pernigraniline base, f) Pernigraniline salt.

1.2.1 Synthesis methods

The polymerization of Pani proceeds by oxidation of the aniline monomer preferably in aqueous acidic medium, although the polymerization in neutral and basic medium is also produced[48].

1.2.1.1 Chemical synthesis

The chemical synthesis consists to add an oxidizing species to an aqueous acidic solution of aniline, the most commonly used is the ammonium persulfate ($(NH_4)_2S_2O_8$) [24], ferric trichloride ($FeCl_3$) [49] or potassium dichromate ($K_2Cr_2O_7$)[50]. The amount of the oxidant is usually stoichiometric in relation to that of monomer, although some authors have reported on the convenience of adding the oxidant in defect to minimize the appearance of defects due to over-oxidation of the polymer[50]; also the temperature at which the reaction proceeds is important for higher quality of Pani. The product is an insoluble polymer in aqueous medium that must be purified, by successive filtering and washing of soluble oligomers.

1.2.1.2 Electrochemical synthesis

The electrochemical polymerization of aniline can be carried out in acidic media by constant potential, constant current, and potential cycling (potentiodynamic) between two selected potentials. These electrochemical polymerization methods offer the possibility of conveniently investigating various chemical and physical properties of Pani in spectroscopic techniques and electrical properties.

The electrochemical synthesis also starts from acidic aqueous solutions of the monomer, but in this case at room temperature. The monomer oxidation and growth of polymer occur at the interface of an anodic polarized inert electrode and the electrolyte. Using these methods, "clean" polymeric films with good adherence to the substrate is obtanied[51]. The potentiodynamic regime (cyclic voltammetry) leads to homogeneous deposits[52], using a typical potential window of 0.0 - 1.0 V against the normal hydrogen electrode (NHE) for usual values of the scan rate (50-100 mV/s).

1.2.1.3 Functionalized polyaniline

Polyaniline has many inconvenient, low solubility in commonly organic solvents and therefore its low processing. To avoid these problems, the inlusion of functional groups in the polymer chain

have been studied, diminishing strong interactions between chains and increasing the solubility. There are three methods to introduce functional groups:

(i) Post-functionalization of the Pani once synthesized.

(ii) Homopolimerization of substituted anilines

(iii) Co-polymerization of aniline with substituted anilines.

Since it is not possible to control the degree of modification with the post-modification, the last two methods seem to be the most effective for obtaining a polymer with the desired properties. By choosing between one and the other, the chemical properties (mainly reactivity) of the monomer must be taken into account. Copolymerization in principle is normally used for the synthesis of aniline derivatives when it is not possible to obtain them by homopolymerization. In general, the monomers used to obtain modified polyaniline can be classified into three categories, according to the position occupied by the functional groups, substituted cycle, N-substituted and the ring melts. In all cases, the polymerization method is similar, but the properties of the obtained polymers are very diverse.

1.2.2 Copolymerization of aniline with other monomers.

The aniline co-polymerisation with substituted monomers can be carried out by chemicals and electrochemicals methods [53–57]. This copolymerization is an interesting alternative to obtain functionalized polyaniline that extend its electroactivity at higher pH than 3 decreasing the degradation.

During the electrochemical growth of the copolymer some authors have pointed out that the presence of the comonomer greatly reduces the speed of polymer growth [58] Copolymers obtained by both chemical and electrochemical synthesis have significantly lower molecular weights than those of Pani, due to limitations on the incorporation of the monomer into chain growth. Other properties of this type of copolymers are very similar to those prepared by Yue et al.[59]. In bibliography it can find a lot of work in which synthesize aniline copolymers with aniline derivatives with certain functional groups. For example, by introducing alkyl [60], alkoxy [61] groups into the chain, hydroxyl [62], methoxy [63], sulfonic [64], alkoxysulfonic [65], carboxyl [66] or nitrile [67]. The inclusion of these groups produce different effects according to their tendency to assign electrons or take them, and also according to their size. The copolymerization produces materials with a gradual variation of its properties, such as solubility, conductivity, electroactivity, etc.

1.2.3 Piperazine

Piperazine, also known as hexahydropyrazine (Figure 1.14), consists of a saturated cycle containing two nitrogen atoms on different sides of the cycle, which can be found in many drugs[38–40,68].

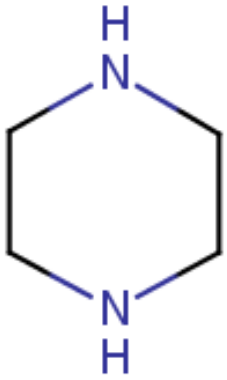

Figure 1.14: Structure of Piperazine

Molecular compounds containing the piperazine group attracted great attention, due to their different applications in the industrial and drug fields [69–71]. Heterocyclic compounds containing nitrogen show particular importance because of their ability to form hydrogen bonds thus generating supramolecular structures [72,73]. Piperazine-based compounds are used as chelating agents because of their ability to form a complex with metal ions [74]. Polypiperazin polymers were synthesized, such as poly(methyl-para-piperazine-hydroxybenzoic) acid, polyethylene polypiperazine, polypiperazinephosphonamide, poly (iodideperfluorohexylpiperazine) [75,76]. These polypiperazine have several applications. They are used as flocculation agents and polyamine synthesis products [77],as ultrafiltration and reverse osmosis membranes [78]. And for different applicationsss in industry and medicine [79–81]. The effects of sweep speed, pH and concentration on the voltammetric response of sodium 4-benzyl piperazine-1-carbodithioate and sodium 4-benzhydryl piperazine-1-carbodithioate have been studied for assess the electrochemical and kinetic parameters of electron transfer processes [1]. Afzal Shah et al carry out the voltammetric study of compounds containing piperazine under acidic, neutral and basic pH conditions[82]. The electropolymerization of piperazine compounds has been the subject of many of attention of several researchers due to the different fields of applications piperazine. It is then reported that the chemical copolymerization of 1,4-bis (3-aminopropyl) piperazine with N-methyl-2-pyrrolidone (NMP), catalyzed by a ionic liquid , produces polymers with controlled molecular weights and low polydispersity [83]. The chemical copolymerization of p-cresol and piperazine was also studied [84]. New catalysts in the form of functionalized mesoporous polymers by piperazine have been chemically synthesized according to a self-assembly between the phenol, piperazine and formaldehyde; these present a strong catalytic reactivity as well as good selectivity in an aqueous

medium[85].The chemical copolymerization of aniline and piperazine has been studied by Ramachandran et al [86], the copolymer exhibited electrochemical activity. The proposed chemical structure consists of fragments in alternation, piperazine and aniline linked in ortho and para positions (Figure 1.15).

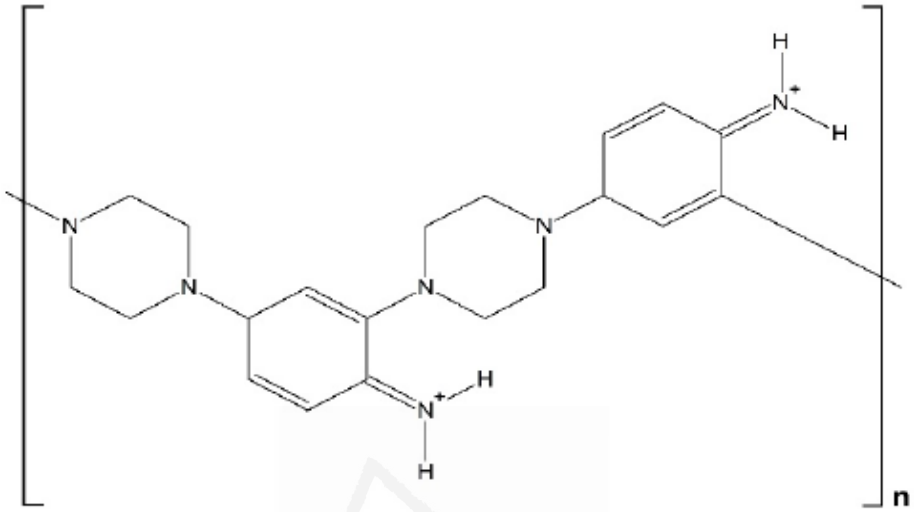

Figure 1.15 : Structure of the piperazine-aniline copolymer[86] .

It was then shown that the delocalization of the filler in this polymer includes also oxidized piperazine centers, however extensive conjugation has not not been observed. The electrical conductivity of the material was between 10^{-7} and 10^{-9} S cm^{-1}.

1.2.4 -2-Aminoterephthalic acid

2-aminoterephthalic acid (2ATA) also knows as (2-amino 1,4-benzenedicarboxylic acid), (Figure 1.16), it could be an interesting monomer for its copolymerization with aniline. 2ATA contains two carboxylic groups, which may be ionized by proton transfer, which may react by positions 2 or 3 in relation to the COOH groups, and constitutes an attractive monomers that can provide self-doped copolymers, thus avoiding the use of external dopants [40]. In a previous work, copolymers from aniline and 2ATA monomers by chemical oxidative polymerization have been obtained[87]. It was found that 2ATA monomers were four times less reactive than aniline in the conditions of chemical polymerization, because of the deactivating effect of the carboxylic groups attached to the aromatic ring.

Sensors based on conductive polymers generally offer high sensitivity, fast response but also fairly low conductivity when the active material is in the undoped state. Despite this, the conductivity values can be easily and reversibly multiplied by a factor of 10, after chemical oxidation or

electrochemical, both called oxidative doping [88]. It is well established that the electrical conductivity of Pani is influenced by both the state oxidation of its skeleton and its level of protonation [89]. Such behavior limits most of the applications, especially those related to biological sensors, since this polymer is almost electrochemically inactive at physiological pH [90]. The most followed strategy to overcome this problem involves the chemical modification of its structure to include some ionizable carboxylic, sulfonic, etc. groups having acid-base properties. Polyanilines containing such groups are called self-doped polyanilines [91,92], where the pH range of polymer electroactivity is widened, thus giving an appropriate electrochemical response, to become potential candidates for biosensors. Then, 2ATA is an interesting aniline co-monomer for copolymerization with aniline. 2ATA is used in a new synthesis approach hydrothermal coordination polymers based on rare earths [93]. On the other hand, copolymers of aniline and 2ATA showing good electroactivity in an aqueous acid medium, have been prepared by oxidation chemical by varying the feed ratio of the two monomers [87]. He has been verified that the 2ATA units are indeed included in the polymer backbone, as shown in (Figure 1.16).

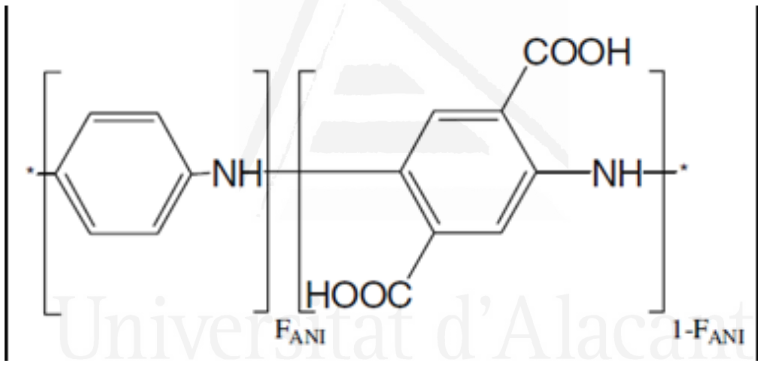

Figure 1.16: Poly(aniline-co-2-aminotherphthalic acid) [90].

The research group maintains an active line of research concerning the synthesis of self-doped polyanilines for electrochemical sensors[94–99]. Chemical synthesis is preferable when high amounts of the polymer are required. However, electrochemical synthesis has two important advantages. The first one, it avoids the use of chemical oxidants leading to a product of high purity and, the second one, the polymer material is generally obtained on a surface, no further handling or transfer of the sample is necessary. The electrochemical polymerization can be carried out on electrodes of different nature and morphologies that constitutes another advantage, but is always limited to conductive substrates, while chemical polymerization can be successfully driven on non-conductive surfaces [100]. A copolymer of Ani and 2ATA monomers was obtained by chemical oxidative polymerization [101]. It was then found that the monomers of 2ATA were four times less

reactive than aniline under the conditions of chemical polymerization, due to the deactivating effect of the linked carboxylic group in the aromatic ring. Therefore, controlling the monomer ratio was a key parameter for obtaining a true copolymerization product and for modulating the composition and properties of the material. In a preliminary study of copolymer obtained on platinum were developed, in potentiodynamic conditions and in an acid medium [40]. It has been shown that the material obtained has significant electroactivity (Figure 1.16).

1.3 Hydrogels

When the liquid in a gel is water, the networked polymer structure is made of either chemically or physically cross-linked waters-soluble polymers, the material is called as "Hydrogel"[102]. Then, a hydrogel is a three-dimensional macromolecular network composed of hydrophilic polymer chains, interconnected by chemical or physical crosslinking nodes. The high hydrophilicity of hydrogels is due to the presence of hydrophilic functional groups such as carboxylic, amide, amino and hydroxyl groups distributed throughout the structure of the polymer chains, which are capable of ionizing in the presence of water. Hydrogels are swollen in water, which generally represents more than 80% of the total mass of the gel, which gives biocompatibility properties [103,104]. Conducting polymer hydrogels are gels, which are swollen with water, and contain a conducting polymer along with a supporting polymer as constituents [105].

Hydrogels contain different properties: i) mixed electrical conductivity (electronic and ionic conductivity); ii) electrochemical reversibility between oxidized and reduced forms of CPs; iii) transition between conductor (salt form) and insulator (base form) in the CPs; iv) good flexibility and mechanical integrity; v) non-toxic and compatible tissue or cell; vi) high porosity and specific surface; vii) macroscopic homogeneity and controlled morphology[106].

The synthesis of hydrogels can be envisaged according to two main routes. The first is obtained by simultaneous polymerization and crosslinking of a monomer (Figure 1.17a). The gel can also be prepared by crosslinking of preformed linear macromolecules, possibly functionalized during a first synthesis step by reactive chemicals functions (Figure 1.17b). The structure obtained is more homogeneous but the method is less versatile and more difficult than synthesis of copolymers.

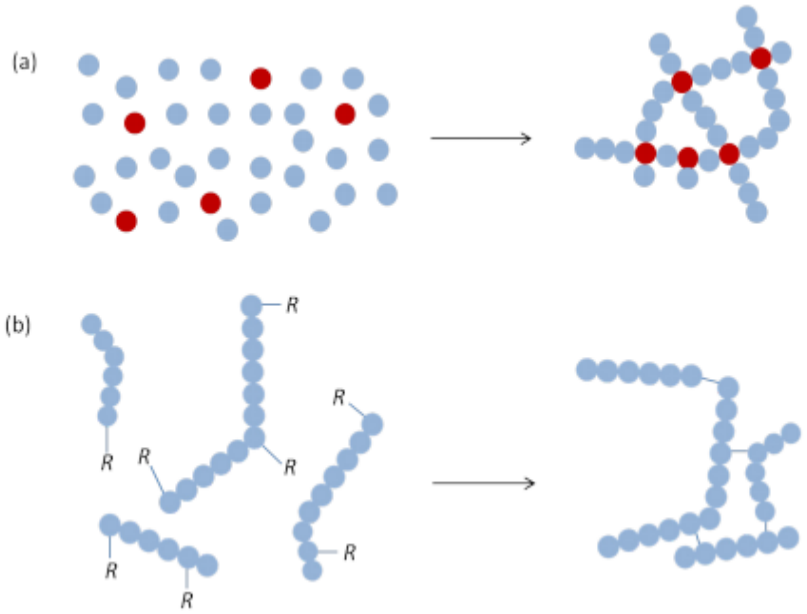

Figure 1.17. Synthesis of hydrogels by (a) simultaneous polymerization and crosslinking from monomers ;(b) by crosslinking of functionalized polymer chains.

In both cases, the structure of the hydrogel obtained after synthesis (Figure 1.18) varies with the nature of the polymer, the crosslinking density, the size of the mesh or (loops, free end, tangles, junction, etc.). These parameters contribute to the thermodynamic and kinetic swelling properties of hydrogels.

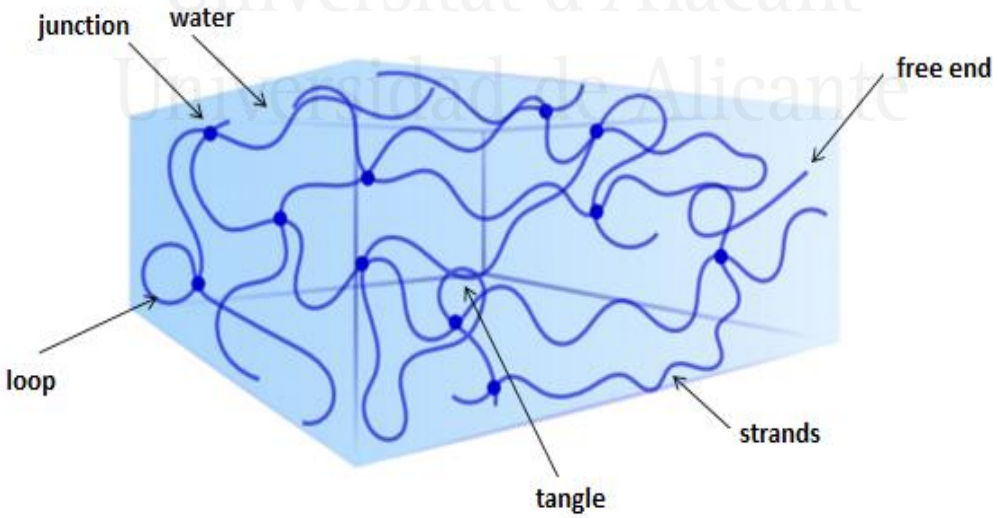

Figure 1.18: structure of the hydrogel obtained after synthesis

Different strategies have been used in the preparation of hydrogels with the incorporation of the conducting polymers. The most frequently reported approach was based on the preparation of hydrogel of supporting polymer, which was subsequently used as a matrix for the preparation of the conducting polymer. Then, the conducting hydrogel was sometimes obtained even if the supporting polymer has not been gelled prior to the synthesis of conducting polymers. The most frequent approach is to prepare hydrogel of supporting polymer followed by the preparation of CPs in the same hydrogel matrix. The insulating polymer forms the aqueous gel and the CPs imparts conductivity to the gel [105].

The use of hydrogels in new technologies explains their presence in many areas of application. If their biocompatibility and in some cases, their transparency are especially used for visual correction using contact lenses [107,108]. Moreover, the large absorption capacity gives them the status of super-absorbent materials [109]. They can be synthesized for the encapsulation of active ingredients [110]or for the design of microfluidic systems [111].

Conducting polymer hydrogels are used in many applications in two main research streams: the first concern Biosciences and the second energy conversion and storage. The areas of research in biomedicine concern biosensors, drug delivery devices, etc. [112]. They are very environmentally stable [113], and can be combined with biodegradable polymers [114]. Many energy conversion/storage devices are based on the electrical and electrochemical properties of CPs [115,116]. Some of their applications are in batteries that convert the chemical energy into electrical energy or in supercapacitors that store the electric energy. The incorporation of electrolyte in conducting polymer hydrogels offers them an ionic conductivity in addition to electronic conductivity due to conducting polymers. Pani has been widely used for the synthesis of hydrogels for its properties [117,118].

Many investigations have evaluated Pani combined with other monomers to develop new materials and test them as supercapacitors with improved conductivity [119]. In this PhD Thesis, the synthesis and characterization of the obtained conducting polymer hydrogels in supercapacitors applications have been studied.

1.4 Applications of Conducting Polymers

The synthesis, characterization and application of conducting polymers in a wide range of fields are a subject of great research. CPs have important applications in molecular electronics, electrical displays, electromagnetic shielding, printed circuit boards, rechargeable batteries, solid electrolytes and optical computers [120]. Other potential applications of these conducting polymers are in sensors [121,122], artificial nerves, drug release systems, antistatic clothing, capacitors ion

exchange membranes [123], solar cell and fuel cell [124,125], corrosion protection, electromechanical actuators and "smart" structures [126].

The interest in CPs has its origin in the possible commercial applications of these materials, which are based on the combination of light weight, processibility and electrical conductivity. Some of the CPs can change their optical properties on applications of current or voltage and therefore may find useful applications as heat shutter and light emitting diode (LED).

1.4.1 Sensors

A sensor is a device that can detect a physical, chemical, or biochemical quantity and transduce it into a signal, which can be analyzed by an observer or an instrument [127]. Sensors have been widely used in many areas, such as environmental monitoring, imaging, manufacturing, medical and biological applications[128]. Some of the classification of sensors is the following: 1) electrochemical, 2) optical, 3) electromechanical, and 4) thermal. The working sequence and classification of sensors are shown in (Figure 1.19).

Sensors have been fabricated using a variety of candidate materials, such as metal oxide[100], carbon nanotube[129], and polymers[130], etc. Recently conducting polymers, especially Pani, have been investigated for sensor application because of their fast response and sensitivity to many chemical species [131,132].

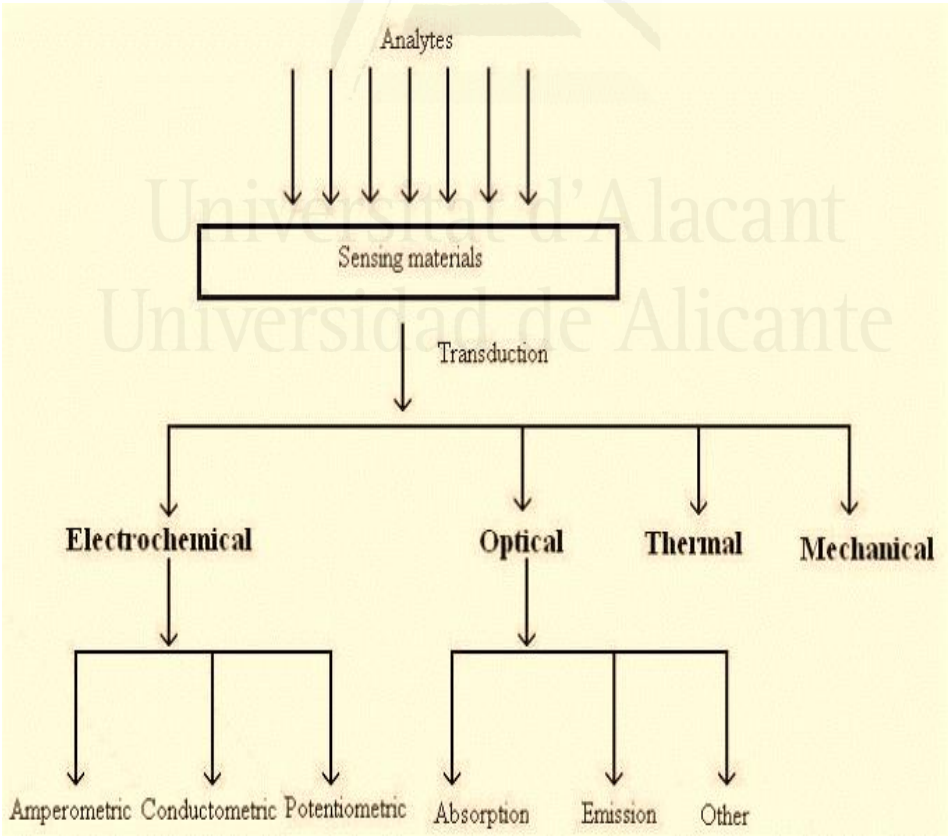

Figure 1.19: Working sequence and classification of sensors.

Although, various kinds of new sensor devices and principles have been proposed not all of them have been successfully commercialized. Some of the problems for this commercialization is the fact that, not just high performance but reasonable productions are required for a successful device. Moreover, new devices must be introduced at the right time to meet social needs. However, fundamental understanding of the sensor remains far from being satisfactory. There is increasing need of new sensors capable of detecting humidity, various toxic gases and smell components

1.4.1.1 Types of sensors

Generally, sensors can be classified into many types based upon the applications, input signal, and conversion mechanism, material used in sensor, production technologies or sensor characteristics such as cost, accuracy or range. They are classified as follows:

- Humidity sensors: These are based on change in electrical properties of the material due to the absorption of water vapor. Hydrophilic polymers are used for resistance type humidity sensors, while hydrophobic polymers are preferred for capacitance type sensors.

- Liquid and solid electrolyte-electrochemical sensors: These are based on Faraday's law. Because of the ionic nature, the ionic conductivity in the electrolytes for any current passing through it will carry a corresponding flux of matter. Therefore, the measurement of current provides an easy and accurate determination of the quantity of matter being transferred from one electrode to other.

- Catalytic sensors: In catalytic sensor, the gases react on a catalytic filament via an exothermic process. The resulting temperature increase is being monitored by a corresponding resistance change in the filament.

- Electronic conductive devices-semiconductor sensors: In these sensors, reversible reaction of the gas at the semiconductor surface results in a change of one of its electronic properties usually conductance.

- Calorimetric sensors: Detect change in temperature.

- Optochemical sensors: Chemical and biological changes are sensed in the form of optical signals.

- Mass sensitive microbalance sensors: Here gases are adsorbed on to a coated piezoelectric crystal. The resulting weight change causing a frequency shift from the fundamental.

- Biosensors: These sensors make the measurements on biological systems such as biologically based molecules, enzymes, amino acids, etc. as systems for improving selectivity of devices.
- Electrochemical sensors.

1.4.1.2 Electrochemical sensors of ascorbic acid and dopamine.

1.4.1.2.1 Oxidation of ascorbic acid

The electrochemical oxidation of ascorbic acid (AA) has been extensively studied [133–135], because of the importance of its detection in biochemistry, and for application in clinical diagnostics. Electrochemical oxidation in conventional electrodes is very documented [136]. Low reproducibility of direct electrochemical oxidation of ascorbate over conventional electrodes have led to study the use of mediators and modified electrodes to improve and catalyze the electrochemical oxidation [133–135].

1.4.1.2.2 Oxidation of dopamine

Dopamine (DA) is produced in many parts of the nervous system, especially the black substance, in a wide variety of animals, vertebrates and invertebrates [137]. Pani arises in these studies as the most effective electrochemical catalyst for the oxidation of ascorbic acid and dopamine, in which it accepts a proton and two electrons in one-step and therefore proves to be a potential transducer for the development of sensors [138].

1.4.2 Electrochemical capacitors.

Electrochemical capacitors (also called supercapacitors) are a class of electrochemical energy storage devices well suited to the rapid storage and release of energy [139]. There are three main categories used as electrode materials in this application: activated carbon, metallic oxides, and conducting polymers [140].

Supercapacitors or electrochemical capacitors are high-power energy storage systems consisting of two electrodes in contact with an electrolyte and separated by a porous membrane. The energy is store due to the formation of electrical double layer at the interface electrode-dissolution. Figure 1.20 shows a supercapacitor scheme, it can be seen a negative electrode (cathode in the charging process), where the adsorption of the cations is produced and a positive electrode (anode in the process of discharge) on which the anions are adsorbed. Then, the charge is accumulated by the adsorption of the ions of the electrolyte at the electrode/electrolyte interface [139,141]. This mechanism is the predominant when we use carbon materials of high porosity as electrodes. In the case of pseudocapacitance, the energy storage is given by reversible faradic reactions that occur on

the surface of the electrode. This process is governing the charge storage mechanism when used metallic oxides or conductive polymers as electrodes of the electrochemical capacitor.

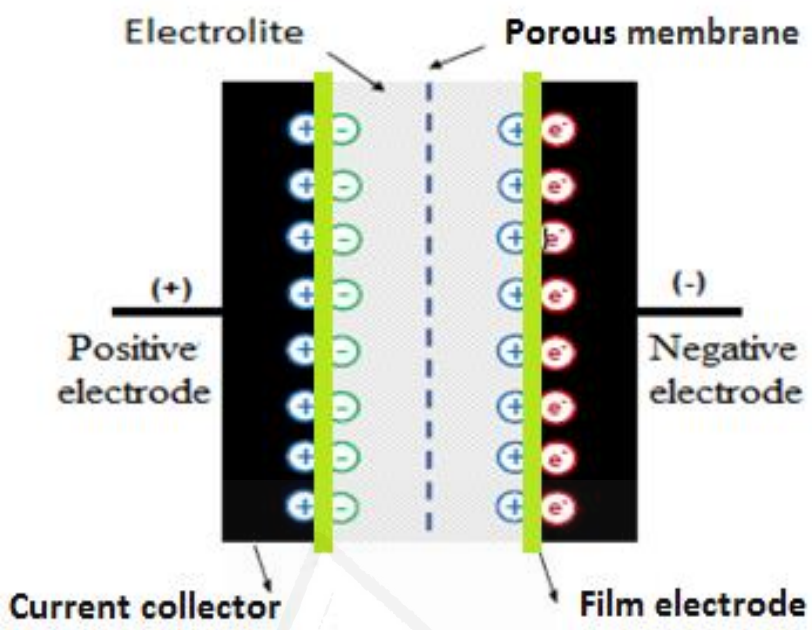

Figure 1.20**:** Supercapacitor or electrochemical capacitor.

The primary advantages of supercapacitors involve high power density and almost unlimited cycle life, etc. Furthermore, they provide higher energy density than conventional capacitors while higher power density than batteries. To clearly compare their power and energy capabilities, summarizes power and energy relations in a Ragone plot for supercapacitors and batteries (Figure 1.21). These devices have a wide range of applications: electric cars, digital devices, etc. Compared to conventional capacitors, these devices provide higher energy densities, due to the use of electrodes allowing superior charge storage. The Ragone diagram shows the main devices of storage and power generation (Figure 1.21) [142]. Compared to batteries and fuel cells, supercapacitors have much higher power, but limited power density. For these reasons, it is necessary to continue researching in order to achieve energy densities that allow its use to be extended to battery applications [141,143–145].The two most important parameters in an electrochemical capacitor witch can determine its possible uses are energy and specific power.

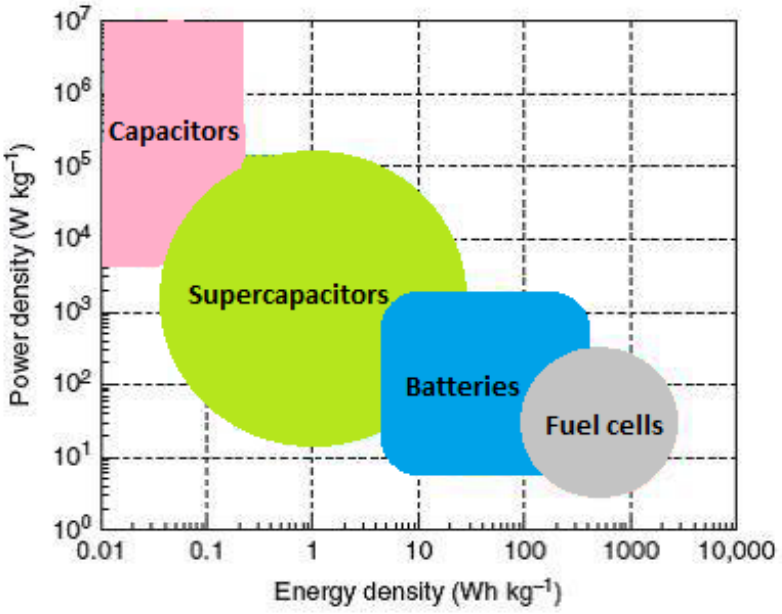

Figure 1.21: Ragone plot for energy storage and conversion devices [142].

A symmetric capacitor is obtained when the device is made up of two electrodes of equal materials and masses. This is the most frequent and simplest industrial implementation format, although it does not have to be the most optimal in terms of energy and power for the material used as an electrode. and for an asymmetric capacitor, an electrode material has a different capacity depending on the potential window in which it will work once arranged as a positive or negative electrode in the supercapacitor; this is especially marked on materials with pseudo-capacitive behavior, where capacitance depends on potential, but it also occurs when the size of the cation and the anion it differs a lot and the porous structure of the material has sizes similar to ions [146].

1.4.2.1 Properties of electrochemical capacitors.

The electrical double-layer mechanism, which arises from the electrostatic attraction between the electrode surface and charges in the electrolyte, plays the major role in supercapacitors. The capacitance in a capacitor is defined considering that the charge separation takes place on polarization at the electrode-electrolyte interface with a double layer distance ***d*** , leading to a capacitance ***C*** (equation 1):

$$C = \frac{\varepsilon_r \varepsilon_0 A}{d} \quad (1)$$

Where ε_r and ε_O are the dielectric constants of the electrolyte and vacuum, respectively, and ***A*** is the surface area of electrode/electrolyte interface (accessible surface area).

Overall, the desirable properties of an electrolytic system for supercapacitors are: high ionic conductivity, wide voltage, and high electrochemical and thermal stability, low viscosity, low toxicity, low cost, etc[147]. The currently used electrolytes are aqueous electrolytes (H_2SO_4 and KOH), organic electrolytes (propylene carbonate and acetonitrile), and recently ionic liquids [148]. Compared with non-aqueous electrolytes, the aqueous medium provides a much higher conductivity leading to higher power density. The conductivity (25 ^oC) of 6 mol L^{-1} KOH exceeds 600 mS cm^{-1} while it is only 20 mS cm^{-1} for tetraethylammonium tetrafluoroborate in propylene carbonate and ~10 mS cm^{-1} for typical room temperature ionic liquids [149]. On the other hand, low cost and easy manipulation could be further advantages for aqueous electrolytes.

The contribution of fast redox processes on the surface is an important factor that has become relevant in research on new materials for supercapacitors, for the determination of the possible applications that can be generated and used in a material. The addition of functional groups on the CPs can have different beneficial effects such as: increase the wettability of the material, contribute to the capacitance for phenomena of pseudocapacitance. On the contrary, they can also negatively impact the behavior of the material by reducing material stability and decrease electrical conductivity [150,151].

1.4.2.2 Application of hydrogels on electrochemical capacitors.

The possibility of introducing positive charge in the CPs by oxidation has generated that these materials have attracted interest to be used in supercapacitors. Furthermore, the presence of redox processes contributes to pseudocapacitance and makes the storage of energy in these materials as a consequence of the combination of a capacitive process with a faradic process. Then, conducting polymers have reached high values of capacitance than metal oxides [152,153].

However, the application of continuous charge-discharge cycles causes swelling and contraction phenomena in the conducting polymer that impact on their stability, and degradation occurs after several charge-discharge cycles. So, in order to find a solution to this problem; the electrochemical study of these conducting polymer hydrogel alone and mixed with carbon materials will be studied in this PhD Thesis.

2 References:

[1] T. Skotheim; Handbook of Conducting Polymers. Second Edition, Eds. Marcel Dekker New York, 1998.

[2] A. Kowal, K. Doblhofer, S. Krause and G. Weinberg, J. Appl. Electrochem. 1987, 17, 1246.

[3] M. Kurian, A. Dasgupta, M.E. Galvin, C.R. Ziegler, F.L. Beyer. A Novel Route to Inducing Disorder in Model Polymer-Layered Silicate Nanocomposites, Macromolecules. 2006, 1864–1871.

[4] M. Alexandre, P. Dubois. Polymer-layered silicate nanocomposites : preparation , properties and uses of a new class of materials. 2000, 28, 1–63.

[5] J. A. F. Diaz, K. K. Kanasawa and G. P. Gradini. Electrochemical Polymerization of Pyrrole. Chem Soc. Chem. Comm. 1979, 635, 635–636.

[6] K. Lee, S. Cho, H.P. Sung, A.J. Heeger, C.W. Lee, S.H. Lee, Metallic transport in polyaniline, Nature. 2006, 441, 65–68. doi:10.1038/nature04705.

[7] A. G. McDiarmid, A. J. Heeger, Molecular Metals, Springer US, Plenum, New York, 1979. doi:10.1007/978-1-4684-3480-4.

[8] G. Inzelt. Conducting Polymers: A new era in electrochemestry, Springer Berlin Heidelberg, 2008. doi:10.1007/978-3-540-75930-0.

[9] D.S. Sutar, N. Padma, D.K. Aswal, S.K. Deshpande, S.K. Gupta, J. V. Yakhmi, Preparation of nanofibrous polyaniline films and their application as ammonia gas sensor, Sensors Actuators, B Chem. 2007, 128, 286–292. doi:10.1016/j.snb.2007.06.015.

[10] H. Liu, C.H. Reccius, H.G. Craighead, Single electrospun regioregular poly(3-hexylthiophene) nanofiber field-effect transistor, Appl. Phys. Lett. 2005, 87, 1-3. doi:10.1063/1.2149980.

[11] M.M. Alam, J. Wang, Y. Guo, S.P. Lee, H.R. Tseng, Electrolyte-gated transistors based on conducting polymer nanowire junction arrays. J. Phys. Chem. B. 2005, 109, 12777-12784. doi:10.1021/jp050903k.

[12] H. S. Nalwa. Handbook of Advanced Electronic and Photonic Materials and Devices. Academic P, USA. 2011.

[13] B.A. Bolto, R. McNeil, D.E. Weiss. Electronic Conduction in Polymers. III. Electronic Properties of Polypyrrole, Aust. J. Chem. 1963, 16, 1090–1103.

[14] Z. P. Li, B. H. Liu. The use of macrocyclic compounds as electrocatalysts in fuel cells. J. Appl. Electrchem. 2010, 475–483. doi:10.1007/s10800-009-0028-7.

[15] H. Peng, L. Zhang, C. Soeller, J. Travas-sejdic. Biomaterials Conducting polymers for electrochemical DNA sensing, Biomaterials. 2009, 30, 2132–2148. doi:10.1016/j.biomaterials.2008.12.065.

[16] G.G. Wallace, G.M. Spinks, L.A.P. Kane-Maguire, P. R. Teasdale. Conducting Electroactive Polymers: Intelligent Polymer Systems. CRC Press, New York, 2008.

[17] M. Manoj Prabhakar, A.K. Saravanan, A. Haiter Lenin, I. Jerin leno, K. Mayandi, P. Sethu Ramalingam. A short review on 3D printing methods, process parameters and materials. Materials Today: Proceedings. 2021, 45, 6108–6114.

[18] C. E. Carraher. Carraher's Polymer Chemistry. Ninth Edition. CRC Press, Boca Raton, 2014.

[19] M.P. Stevens. Polymer Chemistry: An Introduction. Third Edition, Oxford Uni, New York, 1999.

[20] J.M.G. Cowie. Polymers: chemistry and physics of modern materials. Blackie Ac, London, 1996.

[21] D. Kumar, R.C. Sharma. Advances in conductive polymers. Eur. Polym. J. 1998, 34, 1053–1060.

[22] Y. Ding, A.B. Radias, H.K. Hall. Chemical trapping experiments support a cation-radical mechanism for the oxidative polymerization of aniline. J. Polym. Sci. Part A Polym. Chem. 1999, 37, 2569–2579.

[23] S. Sadki, P. Schottland, N. Brodie, G. Sabouraud. The mechanisms of pyrrole electropolymerization. Chem. Soc. Rev. 2000, 29, 283–293.

[24] A.G. Macdiarmid, J. Chiang, W. Huang, S. Mu. Molecular Crystals and Liquid Crystals " Polyaniline ": Interconversion of Metallic and Insulating Forms. 1985, 37–41.

[25] N.K. Guimard, N. Gomez, C.E. Schmidt. Conducting polymers in biomedical engineering, Prog. Polym. Sci. 2007, 32, 876–921.

[26] L. Dai. Conjugated and fullerene-containing polymers for electronic and photonic applications: Advanced syntheses and microlithographic fabrications. J. Macromol. Sci. - Polym. Rev. 39 (1999) 273–387. doi:10.1081/MC-100101421.

[27] J. Tsukamoto, Recent advances in highly conductive polyacetylene, Adv. Phys. 41 (1992) 509–546. doi:10.1080/00018739200101543.

[28] J. Tsukamoto, A. Takahashi, K. Kawasaki, Structure and Electrical Properties of Polyacetylene Yielding a Conductivity of 105S/cm, Jpn. J. Appl. Phys. 29, 1990, 125–130. doi:10.1143/JJAP.29.125.

[29] D.S. Park, Y.B.Shin, S.M. Park, Degradation of Electrochemically Prepared Polypyrrole in Aqueous Sulfuric Acid, J. Electrochem. Soc. 1993, 140, 609. doi:10.1149/1.2056130.

[30] W.Z. and S.D. l Zhuang Li. Electrolyte effects on the electrochemical polymerization of IV-benzylaniline. J. Elecrroanal. Chem. 1991, 317, 109–116. doi:10.1002/cphc.201900680.

[31] L. Niu, Q. Li, F. Wei, S. Wu, P. Liu, X. Cao. Electrocatalytic behavior of Pt-modified polyaniline electrode for methanol oxidation: Effect of Pt deposition modes, J. Electroanal. Chem. 2005, 578, 331–337. doi:10.1016/j.jelechem.2005.01.014.

[32] L.M. Peter, K.G.U. Wijayantha, Electron transport and back reaction in dye sensitized nanocrystalline photovoltaic cells, Electrochim. Acta. 2000, 45, 4543–4551. doi:10.1016/S0013-4686(00)00605-8.

[33] M.M. Gvozdenović, B.Z. Jugović, T.L. Trišović, J.S. Stevanović, B.N. Grgur. Electrochemical characterization of polyaniline electrode in ammonium citrate containing electrolyte, Mater. Chem. Phys. 2011, 125, 601–605. doi:10.1016/j.matchemphys.2010.10.011.

[34] H.R. Ghenaatian, M.F. Mousavi, S.H. Kazemi, M. Shamsipur. Electrochemical investigations of self-doped polyaniline nanofibers as a new electroactive material for high performance redox supercapacitor, Synth. Met. 2009, 159, 1717–1722. doi:10.1016/j.synthmet.2009.05.014.

[35] D. Jambrec, M. Antov, B. Grgur. Electrochemically Deposited Nano Fibrous Polyanilne For Amperometric Determination Of Glucose. Dig. J. Nanomater. Biostructures. 2012, 7, 785–794.

[36] A. Kaur, S.K. Dhawan. Tuning of EMI shielding properties of polypyrrole nanoparticles with surfactant concentration. Synth. Met. 2012, 162, 1471–1477. doi:10.1016/j.synthmet.2012.05.012.

[37] B.G. A. Elkais, M. Gvozdenović, B. Jugović, T. Trišović, M. Maksimović. Electrochemical synthesis andcorrosion behavior of thin polyaniline film on mild steel, copper and aluminum, Hem. Ind. 2012, 65, 15–21. doi:10.2298/HEMIND100901069E.

[38] R.F. Staack, G. Fritschi, H.H. Maurer. Studies on the metabolism and toxicological detection of the new designer drug N -benzylpiperazine in urine using gas chromatography – mass

spectrometry q. J. Chromatogr. B. 2002, 773, 35–46.

[39] D. De Boer, I.J. Bosman, E. Hidvégi, C. Manzoni, A.A. Benkö, L.J.A.L. Dos Reys, R.A.A. Maes. Piperazine-like compounds: A new group of designer drugs-of-abuse on the European market, Forensic Sci. Int. 2001, 121, 47–56. doi:10.1016/S0379-0738(01)00452-2.

[40] M. Abidi, S. López-Bernabeu, F. Huerta, F. Montilla, S. Besbes-Hentati, E. Morallón. Spectroelectrochemical study on the copolymerization of o-aminophenol and aminoterephthalic acid. Eur. Polym. J. 2012, 91,386–395. doi:10.1016/j.eurpolymj.2017.04.024.

[41] J.-C. Chiang, A.G. MacDiarmid. Polyaniline: protonic acid doping of the emeraldine form to the metallic regime. Synt. Met. 1986, 13, 193–205.

[42] W. Huang, B.D. Humphrey, A.G. Macdiarmid, Polyaniline , a Novel Conducting Polymer. Chem. Soc,Faraday Trans. 1986, 1, 2385–2400.

[43] W.P. Wuelfing, S.J. Green, J.J. Pietron, D.E. Cliffel, R.W. Murray. Electronic conductivity of solid-state, mixed-valent, monolayer-protected Au clusters. J. Am. Chem. Soc. 2000, 122, 11465–11472. doi:10.1021/ja002367+.

[44] J.M. Ko, R.Y. Song, H.J. Yu, J.W. Yoon, B.G. Min, D.W. Kim. Capacitive performance of the composite electrodes consisted of polyaniline and activated carbons powder in a solid-like acid gel electrolyte. Electrochim. Acta. 2004, 50, 873–876. doi:10.1016/j.electacta.2004.02.064.

[45] C.C. Hu, J.Y. Lin, Effects of the loading and polymerization temperature on the capacitive performance of polyaniline in $NaNO_3$. Electrochim. Acta. 2002, 47, 4055–4067. doi:10.1016/S0013-4686(02)00411-5.

[46] Y. -H Liao, K. Levon. Doping of polyaniline with polymeric dopants in solid state, gel state and solutions, Polym. Adv. Technol. 1995, 6, 47–51. doi:10.1002/pat.1995.220060107.

[47] E.T. Kang, K.G. Neoh, K.L. Tan, Polyaniline: A polymer with many interesting intrinsic redox states, Prog. Polym. Sci. 1998, 23, 277–324. doi:10.1016/S0079-6700(97)00030-0.

[48] A. Volkov, G. Tourillon, P.C. Lacaze, J.E. Dubois. Electrochemical polymerization of aromatic amines. IR, XPS and PMT study of thin film formation on a Pt electrode, J. Electroanal. Chem. 1980, 115, 279–291. doi:10.1016/S0022-0728(80)80332-9.

[49] K. Nishio, M. Fujimoto, N. Yoshinaga, O. Ando, H. Ono, T. Murayama. Electrochemical characteristics of polyaniline synthesized by various methods. J. Power Sources. 1995, 56,

189–192. doi:10.1016/0378-7753(95)80032-C.

[50] E.M. Geniès, C. Tsintavis, A.A. Syed. Molecular Crystals and Liquid Crystals Electrochemical Study Of Polyaniline In Aqueous And Organic Medium. Redox And Kinetic Properties. Mol. Cryst, Liq. Cryst. 1985, 121, 181.

[51] E.M. Genies, C. Tsintavis, Redox mechanism and electrochemical behaviour or polyaniline deposits, J. Electroanal. Chem. 1985, 195, 109–128. doi:10.1016/0022-0728(85)80009-7.

[52] A. Thyssen, A. Hochfeld, R. Kessel, A. Meyer, J.W. Schultze. Anodic polymerisation of aniline and methylsubstituted derivatives: ortho and para coupling. Synth. Met. 1989, 29, 357–362. doi:10.1016/0379-6779(89)90318-4.

[53] C. Sanchís, H.J. Salavagione, J. Arias-Pardilla, E. Morallón. Tuning the electroactivity of conductive polymer at physiological pH. Electrochim. Acta. 2007, 52, 2978–2986. doi:10.1016/j.electacta.2006.09.031.

[54] A. Benyoucef, F. Huerta, J.L. Vázquez, E. Morallon. Synthesis and in situ FTIRS characterization of conducting polymers obtained from aminobenzoic acid isomers at platinum electrodes. Eur. Polym. J. 2005, 41, 843–852. doi:10.1016/j.eurpolymj.2004.10.047.

[55] A. Benyoucef, F. Huerta, M.I. Ferrahi, E. Morallon. Voltammetric and in situ FT-IRS study of the electropolymerization of o-aminobenzoic acid at gold and graphite carbon electrodes: Influence of pH on the electrochemical behaviour of polymer films. J. Electroanal. Chem. 2008, 624, 245–250. doi:10.1016/j.jelechem.2008.09.013.

[56] C. Sanchis, M.A. Ghanem, H.J. Salavagione, E. Morallón, P.N. Bartlett. The oxidation of ascorbate at copolymeric sulfonated poly(aniline) coated on glassy carbon electrodes, Bioelectrochemistry. 2011, 80, 105–113. doi:10.1016/j.bioelechem.2010.06.006.

[57] A.A. Karyakin, I.A. Maltsev, L. V Lukachova. The influence of defects in polyaniline structure on its electroactivity : optimization of ' self-doped ' polyaniline synthesis. J.Electroanal. Chem. 1996, 402, 217–219.

[58] J.Y. Lee, C.Q. Cui. Electrochemical copolymerization of aniline and metanilic acid. J. Electroanal. Chem. 1996, 403, 109–116. doi:10.1016/j.synthmet.2003.12.008.

[59] J. Yue, A.J. Epstein. Synthesis of Self-Doped Conducting Polyaniline. J. Am. Chem. Soc. 1990, 112, 2800–2801. doi:10.1021/ja00163a051.

[60] Y. Wei, R. Hariharan, S.A. Patel. Chemical and electrochemical copolymerization of aniline with alkyl ring-substituted anilines. Macromolecules. 1990, 23, 758–764.

doi:10.1021/ma00205a011.

[61] S.S. Pandey, S. Annapoorni, B.D. Malhotra. Synthesis and characterization of a conducting copolymer. Macromolecules. 1993, 26, 3190–3193. doi:10.1016/s0379-6779(98)80012-x.

[62] S. Mu. Electrochemical copolymerization of aniline and o -aminophenol, Synth. Met. 2004, 143, 259–268. doi:10.1016/j.synthmet.2003.12.008.

[63] P. Mokreva, D. Tsocheva, G. Ivanova, L. Terlemezyan. Copolymers of Aniline and o-Methoxyaniline : Synthesis and Characterization. J. Appl. Polym. Sci. 2005, 98, 1822. doi:10.1002/app.22226.

[64] M.Y.T. Nguyen, P. Kasai, J.L. Miller, A.F. Diaz. Synthesis and Properties of Novel Water-Soluble Conducting Polyaniline Copolymers, Macromolecules. 1994, 27, 3625–3631. doi:10.1021/ma00091a026.

[65] V. Prevost, A. Petit, F. Pla. Studies on chemical oxidative copolymerization of aniline and o -alkoxysulfonated anilines : I . Synthesis and characterization of novel self-doped polyanilines. Synth. Met. 1999, 104, 79–87.

[66] H.J. Salavagione, D.F. Acevedo, M.C. Miras, A.J. Motheo, C. A. Barbero. Comparative study of 2-amino and 3-aminobenzoic acid copolymerization with aniline synthesis and copolymer properties. J. Polym. Sci. Part A Polym. Chem. 2004, 42, 5587–5599. doi:10.1002/pola.20409.

[67] K.H. M. Sato, S. Yamanaka, J. Nakay., Electrochemical copolymerization of aniline with o-aminobenzonitrile, Electrochim. Acta. 39 (1994) 2159.

[68] C. Balmelli, H. Kupferschmidt, K. Rentsch, M. Schneemann. Tödliches Hirnödem nach Einnahme von Ecstasy und Benzylpiperazin, Dtsch. Med. Wschr. 2001, 126, 809–811.

[69] M. Yarim, M. Koksal, I. Durmaz, R. Atalay. Cancer Cell Cytotoxicities of 1-(4-Substitutedbenzoyl)-4-(4-chlorobenzhydryl)piperazine Derivatives, Int. J. Mol. Sci. 2012, 13, 8071–8085. doi:10.3390/ijms13078071.

[70] F.J. Schwinn, Ergosterol Biosynthesis Inhibitors. An Overview of Their History and Contribution to Medicine and Agriculture". Pestic. Sci. 1984, 15 , 40–47.

[71] C.S. Ananda Kumar, S. Nanjunda Swamy, N.R. Thimmegowda, S.B. Benaka Prasad, G.W. Yip, K.S. Rangappa. Synthesis and evaluation of 1-benzhydryl-sulfonyl-piperazine derivatives as inhibitors of MDA-MB-231 human breast cancer cell proliferation. Med. Chem. Res. 2007, 16, 179–187. doi:10.1007/s00044-007-9022-y.

[72] N. Jamai, M. Rzaigui, S.A. Toumi, Piperazine-1,4-diium bis(hexahydroxidoheptaoxidohexaborato- κ3O,O′,O″) cobaltate (II) hexahydrate. Acta Crystallogr. Sect. E Struct. Reports Online. 2014, 70 m167–m168. doi:10.1107/S1600536814007090.

[73] L. Zhang, X.M. Peng, G.L.V. Damu, R.X. Geng, C.H. Zhou, Comprehensive Review in Current Developments of Imidazole-Based Medicinal Chemistry, Med. Res. Rev. 2014, 34, 340–437. doi:10.1002/med.21290.

[74] D.A.W. D.K. Crump, J. Simon, Bis (aminoalkyl) piperazine derivatives and their use as metalion control agents, GooglePatents. 1987.

[75] J. Duchet, R. Legras, S. Demoustier-champagne, Chemical synthesis of polypyrrole : structure – properties relationship, Synth. Met. 1998, 98, 113–122.

[76] C.D. Djamila, R Meghabar, M.Belbachr. Piperazine Polymerization Catalyzed by Maghnite-H Journal of Environmental Analytical Piperazine Polymerization Catalyzed by Maghnite-H^+. J Env. Anal Chem. 2017, 4, 208. doi:10.4172/2380-2391.1000208.

[77] C. P. Reghunadhan Nair, G. Clouet & J. Brossas. Thermal Functional Polymeric " Iniferters " Based on Phosphorus- Containing Poly (Thiuram Disulfides); Synthesis and Characterization. J. Macromol. Sci.Chem.Ed A. 1988, 25(9), 1089–1126. doi:10.1080/00222338808053409.

[78] L. Credali, G. V. Baruzzi. Reverse Osmoss Ansotropic Membranes Based On Polypperazine Am Des, U.S. Pat. No. 4,129,559 to Montedison SPA, Milan, IT, USA. 1978.

[79] P. Danielsson, J. Bobacka, A. Ivaska. Electrochemical synthesis and characterization of poly(3,4- ethylenedioxythiophene) in ionic liquids with bulky organic anions. J. Solid State Electrochem. 2004, 8, 809–817. doi:10.1007/s10008-004-0549-2.

[80] X. Tu, X. Fu, Q. Jiang. The synthesis and electrochemical properties of anodic electrochromic materials phenothiazine derivatives and their electrochromic devices. Displays. 2010, 31, 150–154. doi:10.1016/j.displa.2010.05.001.

[81] J. Kawahara, P.A. Ersman, I. Engquist, M. Berggren, Improving the color switch contrast in PEDOT:PSS-based electrochromic displays, Org. Electron. 13, 2012, 469–474. doi:10.1016/j.orgel.2011.12.007.

[82] A. Shah, A.H. Shah, N. Parveen, Z. ur Rehman, S.Z. Khan, U.A. Rana, S.U.D. Khan, J. Nisar, A. Lashin, R. Qureshi. Synthesis and electrochemical investigations of piperazines. Electrochim. Acta. 2016, 220, 705–711. doi:10.1016/j.electacta.2016.10.165.

[83] B. Alici, S. Köytepe, T. Seçkin. Synthesis of piperazine based polyimide in the presence of ionic liquids, Turkish J. Chem. 2007, 31, 569–578.

[84] P. Chutayothin, H. Ishida. Polymerization of p-cresol, formaldehyde, and piperazine and structure of monofunctional benzoxazine-derived oligomers. Polymer (Guildf). 2011, 52, 3897–3904. doi:10.1016/j.polymer.2011.07.006.

[85] R.Z. and H.L. Fang Zhang, Xushi Yang, Chao Liang. Piperazine-functionalized Ordered Mesoporous Polymer as Highly Active and Reusable Organocatalyst for Water-medium Organic Synthesis. Green Chem. 2013, 15, 1665–1672. doi:10.1039/C3GC40215K.

[86] R. Ramachandran, S. Balasubramanian, G. Aridoss, P. Parthiban. Polymer Synthesis and studies of semiconducting piperazine – aniline copolymer. 2006, 42, 1885–1892. doi:10.1016/j.eurpolymj.2006.02.010.

[87] J. Arias-Pardilla, H.J. Salavagione, C. Barbero, E. Morallón, J.L. Vázquez. Study of the chemical copolymerization of 2-aminoterephthalic acid and aniline. Synthesis and copolymer properties. Eur. Polym. J. 2006. 42, 1521–1532. doi:10.1016/j.eurpolymj.2006.02.003.

[88] X. Lu, W. Zhang, C. Wang, T.C. Wen, Y. Wei, One-dimensional conducting polymer nanocomposites: Synthesis, properties and applications, Prog. Polym. Sci. 2011, 36, 671–712. doi:10.1016/j.progpolymsci.2010.07.010.

[89] R. Saraswathi, S. Kuwabata, H. Yoneyama. Influence of basicity of dopant anions on the conductivity of polyaniline. J. Electroanal. Chem. 1992, 335, 223–231. doi:10.1016/0022-0728(92)80244-X.

[90] H.D. Nguyen, T.H. Nguyen, N.V. Hoang, N.N. Le, T.N.N. Nguyen, D.C.T. Doan, M.C. Dang, pH sensitivity of emeraldine salt polyaniline and poly(vinyl butyral) blend, Adv. Nat. Sci. Nanosci. Nanotechnol. 2014, 5. doi:10.1088/2043-6262/5/4/045001.

[91] T.K. Das, S. Prusty. Review on Conducting Polymers and Their Applications, Polym. - Plast. Technol. Eng. 2012, 51, 1487–1500. doi:10.1080/03602559.2012.710697.

[92] P. Chandrasekhar, Conducting Polymers, Fundamentals and Applications. Second Edition, Springer International Publishing, 2018. doi:10.1007/978-3-319-69378-1.

[93] S. Petrosyants, Z. Dobrokhotova, A. Ilyukhin, A. Gavrikov, N. Efimov, V. Novotortsev. Coordination polymers of rare-earth elements with 2-aminoterephthalic acid, Russ. J. Coord. Chem. Khimiya. 2017, 43, 770–779. doi:10.1134/S1070328417110069.

[94] S. Dkhili, S. López-bernabeu, F. Huerta, F. Montilla, S. Besbes-hentati, E. Morallón. A self-

doped polyaniline derivative obtained by electrochemical copolymerization of aminoterephthalic acid and aniline. Synth. Met. 2018, 245, 61–66. doi:10.1016/j.synthmet.2018.08.005.

[95] B. Martínez-Sánchez, A.F. Quintero-Jaime, F. Huerta, D. Cazorla-Amorós, E. Morallón, Synthesis of phosphorus-containing polyanilines by electrochemical copolymerization, Polymers (Basel). 12 (2020). doi:10.3390/POLYM12051029.

[96] J. Quílez-bermejo, A. Ghisolfi, D. Grau-marín, E. San-fabián, E. Morallón, D. Cazorla-amorós. Post-synthetic efficient functionalization of polyaniline with phosphorus- containing groups . Effect of phosphorus on electrochemical properties. Eur. Polym. J. 2019, 119, 272–280. doi:10.1016/j.eurpolymj.2019.07.048.

[97] S. Benykhlef, A. Bekhoukh, R. Berenguer, A. Benyoucef, E. Morallon, PANI-derived polymer/Al_2O_3 nanocomposites: synthesis, characterization, and electrochemical studies, Colloid Polym. Sci. 2016, 294, 1877–1885. doi:10.1007/s00396-016-3955-y.

[98] N. Saidani, E. Morallón, F. Huerta, S. Besbes-Hentati, F. Montilla. Electrochemical synthesis of fluorinated polyanilines. Electrochim. Acta. 2020, 348. doi:10.1016/j.electacta.2020.136329.

[99] M. Porcel-Valenzuela, J. Ballesta-Claver, I. De Orbe-Payá, F. Montilla, L.F. Capitan-Vallvey. Disposable electrochromic polyaniline sensor based on a redox response using a conventional camera: A first approach to handheld analysis, J. Electroanal. Chem. 2015, 738, 162–169. doi:10.1016/j.jelechem.2014.12.002.

[100] D. Nicolas-Debarnot, F. Poncin-Epaillard. Polyaniline as a new sensitive layer for gas sensors. Anal. Chim. Acta. 2003, 475, 1–15. doi:10.1016/S0003-2670(02)01229-1.

[101] A.G. Asturias, G. E.; Macdiarmid. Synthetic Metals, , Synth. Met. 1989, 29, 157–162.

[102] S.P. Ansari, A. Anis, Conducting polymer hydrogels, Elsevier Ltd, 2018. doi:10.1016/b978-0-08-102179-8.00018-1.

[103] N.A. Peppas, A.S. Hoffman, Biomaterials Science:1.3.2E Hydrogels, Biomateria, Elsevier, 2020. doi:10.1016/B978-0-12-816137-1.00014-3.

[104] Nikolaos A. Peppas and Richard W. Korsmeyer, Dynamically Swelling Hydrogel in Controlled Release Application, Volume III: Proprieties and applications, 1986.

[105] J. Stejskal, Conducting polymer hydrogels. Chem. Pap. 2017, 71, 269–291. doi:10.1007/s11696-016-0072-9.

[106] A. Malti, J. Edberg, H. Granberg, Z.U. Khan, J.W. Andreasen, X. Liu, D. Zhao, H. Zhang, Y. Yao, J.W. Brill, I. Engquist, M. Fahlman, L. Wågberg, X. Crispin, M. Berggren, An organic mixed ion-electron conductor for power electronics. Adv. Sci. 2016, 3, 1–9. doi:10.1002/advs.201500305.

[107] A.M. Oelker, M.W. Grinstaff, Ophthalmic adhesives: A materials chemistry perspective, J. Mater. Chem. 2008, 18, 2521–2536. doi:10.1039/b719791h.

[108] M.S. Lord, M.H. Stenzel, A. Simmons, B.K. Milthorpe. The effect of charged groups on protein interactions with poly(HEMA) hydrogels, Biomaterials. 2006, 27, 567–575. doi:10.1016/j.biomaterials.2005.06.010.

[109] K. Kabiri, S. Faraji-Dana, M.J. Zohuriaan-Mehr. Novel sulfobetaine-sulfonic acid-contained superswelling hydrogels. Polym. Adv. Technol. 2005, 16, 659–666. doi:10.1002/pat.637.

[110] D.M. Headen, G. Aubry, H. Lu, A.J. García, Microfluidic-based generation of size-controlled, biofunctionalized synthetic polymer microgels for cell encapsulation, Adv. Mater. 2014, 26, 3003–3008. doi:10.1002/adma.201304880.

[111] S. Cosson, M.P. Lutolf, Hydrogel microfluidics for the patterning of pluripotent stem cells, Sci. Rep. 2014, 4, 1–6. doi:10.1038/srep04462.

[112] T.F. O'Connor, K.M. Rajan, A.D. Printz, D.J. Lipomi, Toward organic electronics with properties inspired by biological tissue. J. Mater. Chem. B. 2015, 3, 4947–4952. doi:10.1039/c5tb00173k.

[113] J. Stejskal, M. Exnerová, Z. Morávková, M. Trchová, J. Hromádková, J. Prokeš. Oxidative stability of polyaniline. Polym. Degrad. Stab. 2012, 97, 1026–1033. doi:10.1016/j.polymdegradstab.2012.03.006.

[114] H.B. Zhao, L. Yuan, Z.B. Fu, C.Y. Wang, X. Yang, J.Y. Zhu, J. Qu, H.B. Chen, D.A. Schiraldi. Biomass-Based Mechanically Strong and Electrically Conductive Polymer Aerogels and Their Application for Supercapacitors, ACS Appl. Mater. Interfaces. 2016, 8, 9917–9924. doi:10.1021/acsami.6b00510.

[115] B.C. Kim, J.Y. Hong, G.G. Wallace, H.S. Park, Recent Progress in Flexible Electrochemical Capacitors: Electrode Materials, Device Configuration, and Functions, Adv. Energy Mater. 2015, 5, 1500959. doi:10.1002/aenm.201500959.

[116] Y. Shi, G. Yu, Designing Hierarchically. Nanostructured Conductive Polymer Gels for Electrochemical Energy Storage and Conversion. Chem. Mater. 2016, 28, 2466–2477. doi:10.1021/acs.chemmater.5b04879.

[117] W. Li, F. Gao, X. Wang, N. Zhang, M. Ma. Strong and Robust Polyaniline-Based Supramolecular Hydrogels for Flexible Supercapacitors. Angew. Chemie. 2016, 128, 9342–9347. doi:10.1002/ange.201603417.

[118] A. Szöllősi, Á. Hoschke, J.M. Rezessy-Szabó, E. Bujna, S. Kun, Q.D. Nguyen. Formation of novel hydrogel bio-anode by immobilization of biocatalyst in alginate/polyaniline/titanium-dioxide/graphite composites and its electrical performance, Chemosphere. 2017, 174 58–65. doi:10.1016/j.chemosphere.2017.01.095.

[119] B.W. Walker, R. Portillo Lara, E. Mogadam, C. Hsiang Yu, W. Kimball, N. Annabi. Rational design of microfabricated electroconductive hydrogels for biomedical applications, Prog. Polym. Sci. 2019, 92, 135–157. doi:10.1016/j.progpolymsci.2019.02.007.

[120] S. Bahceci, B. Esat. A polyacetylene derivative with pendant TEMPO group as cathode material for rechargeable batteries, J. Power Sources. 2013, 242, 33–40. doi:10.1016/j.jpowsour.2013.05.051.

[121] S.T. Navale, A.T. Mane, G.D. Khuspe, M.A. Chougule, V.B. Patil. Room temperature NO_2 sensing properties of polythiophene films, Synth. Met. 2014, 195, 228–233. doi:10.1016/j.synthmet.2014.06.017.

[122] K.P. Sambasevam, S. Mohamad, S. Phang. Enhancement of polyaniline properties by different polymerization temperatures in hydrazine detection. J. Appl. Polym. Sci. 2015, 41746, 1–8. doi:10.1002/app.41746.

[123] E. Grodzka, K. Winkler, B.M. Esteban, C. Kvarnstrom. Capacitance properties of electrochemically deposited polyazulene films. Electrochim. Acta. 2010, 55, 970–978. doi:10.1016/j.electacta.2009.09.054.

[124] D. Song, M. Li, T. Wang, P. Fu, Y. Li, B. Jiang, Y. Jiang, X. Zhao. Dye-sensitized solar cells using nanomaterial/PEDOT-PSS composite counter electrodes: Effect of the electronic and structural properties of nanomaterials. J. Photochem. Photobiol. A Chem. 2014, 293, 26–31. doi:10.1016/j.jphotochem.2014.07.014.

[125] J. Jurga, A. Woźniak-Braszak, Z. Fojud, K. Jurga, Proton longitudinal NMR relaxation of poly(p-phenylene sulfide) in the laboratory and the rotating frames reference, Solid State Nucl. Magn. Reson. 2004, 25, 47–52. doi:10.1016/j.ssnmr.2003.03.014.

[126] C. Nguyen Van, K. Potje-Kamloth. The influence of thickness and preparation temperature of doped polypyrrole films on the electrical and chemical sensing properties of polypyrrole/gold Schottky barrier diodes. J. Phys. D. Appl. Phys. 2000, 33, 2230–2238.

doi:10.1088/0022-3727/33/18/305.

[127] J. Li, Y. Lu, Q. Ye, M. Cinke, J. Han, M. Meyyappan. Carbon nanotube sensors for gas and organic vapor detection. Nano Lett. 2003, 3, 929–933. doi:10.1021/nl034220x.

[128] N. Guernion, R.J. Ewen, K. Pihlainen, N.M. Ratcliffe, G.C. Teare. The fabrication and characterisation of a highly sensitive polypyrrole sensor and its electrical responses to amines of differing basicity at high humidities, Synth. Met. 2002, 126, 301–310. doi:10.1016/S0379-6779(01)00572-0.

[129] J. Huang, S. Virji, B.H. Weiller, R.B. Kaner, Polyaniline nanofibers: Facile synthesis and chemical sensors, J. Am. Chem. Soc. 2003, 125, 314–315. doi:10.1021/ja028371y.

[130] G.K. Prasad, T.P. Radhakrishnan, D.S. Kumar, M.G. Krishna, Ammonia sensing characteristics of thin film based on polyelectrolyte templated polyaniline, Sensors Actuators, B Chem. 2005, 106, 626–631. doi:10.1016/j.snb.2004.09.011.

[131] S.K. Dhawan, D. Kumar, M.K. Ram, S. Chandra, D.C. Trivedi. Application of conducting polyaniline as sensor material for ammonia, Sensors Actuators, B Chem. 1997, 40, 99–103. doi:10.1016/S0925-4005(97)80247-X.

[132] V. V. Chabukswar, S. Pethkar, A.A. Athawale, Acrylic acid doped polyaniline as an ammonia sensor, Sensors Actuators. B Chem. 2001, 77, 657–663. doi:10.1016/S0925-4005(01)00780-8.

[133] P.N. Bartlett, E.N.K. Wallace. The oxidation of ascorbate at poly(aniline)-poly(vinylsulfonate) composite coated electrodes. Phys. Chem. Chem. Phys. 2001, 3, 1491–1496. doi:10.1039/b009377g.

[134] A.M. Bonastre, P.N. Bartlett. Electrodeposition of Pani films on platinum needle type microelectrodes. Application to the oxidation of ascorbate in human plasma. Anal. Chim. Acta. 2010, 676, 1–8. doi:10.1016/j.aca.2010.07.003.

[135] A.M. Bonastre, M. Sosna, P.N. Bartlett. An analysis of the kinetics of oxidation of ascorbate at poly(aniline)-poly(styrene sulfonate) modified microelectrodes. Phys. Chem. Chem. Phys. 2011, 13, 5365–5372. doi:10.1039/c0cp02327b.

[136] I. Koshiishi, T. Imanari. Measurement of ascorbate and dehydroascorbate contents in biological fluids. Anal. Chem. 1997 69, 216–220. doi:10.1021/ac960704k.

[137] S.J. Cragg, J. Baufreton, Y. Xue, J.P. Bolam, M.D. Bevan. Synaptic release of dopamine in the subthalamic nucleus. J. Physiol. 1910, 41, 19–59. doi:10.1111/j.1460-9568.2004.03629.x.

[138] F.M. Benes. Carlsson and the discovery of dopamine. Trends Pharmacol. Sci. 2001, 22, 46–47.

[139] B.E. Conway. Electrochemical Supercapacitors: Scientific Fundamentals and Technological Applications, Springer Science & Business Media: Berlin, Germany, 2013.

[140] R.Z. Ma, J. Liang, B.Q. Wei, B. Zhang, C.L. Xu, D.H. Wu. Study of electrochemical capacitors utilizing carbon nanotube electrodes. J. Power Sources. 1999, 84, 126–129. doi:10.1016/S0378-7753(99)00252-9.

[141] F. Béguin, E. Frackowiak, Carbons for Electrochemical Energy Storage and Conversion Systems, First Edition, CRC Press, 2009.

[142] K.M. Ajay, M.N. Dinesh. Influence of various Activated Carbon based Electrode Materials in the Performance of Super Capacitor, IOP. Conf. Ser. Mater. Sci. Eng. 2018, 310. doi:10.1088/1757-899X/310/1/012083.

[143] E. Frackowiak, Q. Abbas, F. Béguin, Carbon/carbon supercapacitors, J. Energy Chem. 2013, 22, 226–240. doi:10.1016/S2095-4956(13)60028-5.

[144] B.E. Conway. Transition from "supercapacitor" to "battery" behavior in electrochemical energy storage. J. Electrochem. Soc. 1991, 138, 1539–1548. doi:10.1109/ipss.1990.145856.

[145] P. Simon, Y. Gogotsi, Materials for electrochemical capacitors, Nat. Mater. 2008, 7, 845–854.

[146] G. Salitra, A. Soffer, L. Eliad, Y. Cohen, D. Aurbach. Carbon Electrodes for Double-Layer Capacitors I. Relations Between Ion and Pore Dimensions. J. Electrochem. Soc. 2000, 147, 2486-2493. doi:10.1149/1.1393557.

[147] G. Wang, L. Zhang, J. Zhang, A review of electrode materials for electrochemical supercapacitors, Chem. Soc. Rev. 2012, 41, 797–828. doi:10.1039/c1cs15060j.

[148] A. Burke, R&D considerations for the performance and application of electrochemical capacitors, Electrochim. Acta. 2007, 52, 1083–1091. doi:10.1016/j.electacta.2007.01.011.

[149] P.J. Hall, M. Mirzaeian, S.I. Fletcher, F.B. Sillars, A.J.R. Rennie, G.O. Shitta-Bey, G. Wilson, A. Cruden, R. Carter. Energy storage in electrochemical capacitors: Designing functional materials to improve performance, Energy Environ. Sci. 2010, 3, 1238–1251. doi:10.1039/c0ee00004c.

[150] M.J. Bleda-Martínez, J.A. Maciá-Agulló, D. Lozano-Castelló, E. Morallón, D. Cazorla-Amorós. A. Linares-Solano, Role of surface chemistry on electric double layer capacitance

of carbon materials, Carbon N. Y. 2005, 43, 2677–2684. doi:10.1016/j.carbon.2005.05.027.

[151] Q.T. Qu, Y. Shi, L.L. Li, W.L. Guo, Y.P. Wu, H.P. Zhang, S.Y. Guan, R. Holze, $V_2O_5 \cdot 0.6H_2O$ nanoribbons as cathode material for asymmetric supercapacitor in K_2SO_4 solution. Electrochem. Commun. 2009, 11, 1325–1328. doi:10.1016/j.elecom.2009.05.003.

[152] K.S. Ryu, K.M. Kim, N.G. Park, Y.J. Park, S.H. Chang, Symmetric redox supercapacitor with conducting polyaniline electrodes, J. Power Sources. 103 (2002) 305–309. doi:10.1016/S0378-7753(01)00862-X.

[153] H. Zhou, H. Chen, S. Luo, G. Lu, W. Wei, Y. Kuang. The effect of the polyaniline morphology on the performance of polyaniline supercapacitors. J. Solid State Electrochem. 2005, 9, 574–580. doi:10.1007/s10008-004-0594-x.

Chapter 2

Materials, Methods and Experimental Techniques

1 Introduction

This Chapter presents the reagents, materials and synthesis methods used during this PhD Thesis. Moreover, the different experimental techniques used for the physicochemical, morphological and electrochemical characterization, employed during the PhD Thesis.

2 Materials and methods used.

The water used for the preparation of all solutions was obtained from an *ELGA Lab Water Purelab* system with a resistivity of 18.2 MΩ • cm measured at 25 ° C. The electrolytes used were solutions prepared with perchloric acid ($HClO_4$, 60%) and sulfuric acid (H_2SO_4, 98%) supplied by *Merck and Sigma-Aldrich*, respectively. The working solutions were deoxygenated before the beginning of the experiments by bubbling, for about 15 minutes, nitrogen gas (99.999%) supplied by *Air Liquide*.

The reagents used were: Piperazine (98.8%), aniline (99.5%), 2-Aminoterephthalic acid (Aldrich, 98%). They were used without further purification (all were supplied by Aldrich) and ammonium per sulphate (APS) and hydrochloric acid (HCl, 37%) (Merck, p.a.), Poly(sodium 4-styrenesulfonate) (NaPSS, Mw 70,000) was purchased from Aldrich, potassium permanganate ($KMnO_4$, 99%), hydrogen peroxide (H_2O_2, 20%) supplied by *VWR International*, ascorbic acid (AA, 98.9%), and dopamine (DA, 97.9%) were purchased from Merck. In the case of aniline, it was destiled under vacuum in order to remove the oligomer produced during its storage.

The working electrodes used were a platinum polycrystalline electrode, glassy carbon supplied by Carbone Lorraine. As auxiliary electrode a platinum wire was used as counter electrode and as reference electrodes, two were used: Ag/AgCl/Cl^-(sat), and a reversible hydrogen electrode (RHE), which consists in a platinum wire with a deposit of black platinum introduced in a hydrogen saturated solution of the same working electrolyte. The hydrogen gas (99.999%) supplied by *Air Liquide*.

3 Characterization techniques.

3.1 Microscopic techniques

3.1.1 Transmission electron microscopy (TEM)

In transmission electron microscopy (TEM), a thin sample is irradiated with an electron beam, whose energy is within the range of 100 to 200 keV. Part of these electrons are transmitted, another part is scattered and another part gives rise to interactions that produce different phenomena such as light emission, secondary electrons and Auger, X-rays, etc. The transmission electron microscope uses the transmission/dispersion otf the electrons to form images [1].

A condition for the transmission of electrons through the sample is that it is thin, that is, transparent to electrons. It is recommended not to use samples of more than 10 nm in thickness since the smaller the thickness of the sample, the better the quality of the images obtained.

The simplest electron microscopes consist of two imaging lenses much like conventional optical microscopes. The illumination comes from cannon of electrons emitted by a filament of W or LaB6. The electrons are accelerated by applying a negative potential and focused by two condensing lenses on a thin sample, transparent to the electrons.

After passing through the sample the electrons are picked up and focused by the objective lens within an enlarged intermediate image. The image is further enlarged thanks to the projecting lenses, which control the magnification of the image on the fluorescent screen. The final image is projected on a fluorescent screen or a photographic film.

The preparation of the samples consists in the dispersion in ethanol. Subsequently, the dispersion is deposited on a carbon or metal grid and is introduced directly into the microscope.

In the present PhD Thesis, a JEOL 120 kV transmission electron microscope model JEM-1400 Plus has been used. The source of electrons used consists of a hot filament of tungsten that, by thermionic effect, emits electrons, which are accelerated by a potential of 100 to 200 kV. A resolution between lines of 0.2 nm and between points of 0.38 nm is obtained. The camera of acquisition of images is of the brand GATAN model ORIUS SC600. It is mounted on axis with the microscope at the bottom and is integrated into the image acquisition and treatment program GATAN Digital Micrograph 1.80.70 for GMS 1.8.0. The equipment used is installed in Research Technical Services of the University of Alicante.

3.1.2 Scanning electron microscopy (SEM)

Scanning electron microscopy is a technique that allows the visualization of the morphology of solid samples on the physical limit of the optics, allowing a resolution of a few thousand Å, depending on the nature of the sample [2]. The technique employs a source of electron emission,

usually tungsten or lanthanum, and an accelerated electron beam of between 5 and 30 keV. This consists, mainly, in sending a beam of electrons to the surface of the sample and, by means of an appropriate detector, to register the secondary electrons and backscattered. The beam moves on the sample by scanning in the X and Y directions, so that the intensity of the image varies at each point with the intensity of the electron beam generated on the surface.

The electrons from the atoms of the sample, product of the bombardment of electrons of the primary beam, are called secondary electrons. These provide information about the surface topography, and it is the signal with which an image of the sample is obtained. Due to the low energy of the secondary electrons (less than 50 eV), in their trip towards the outside of the sample they lose energy by different interactions, so that only those that are very close to the surface have some probability of escaping the material and get to the detector. Therefore, the signal of the secondary electrons comes from the same surface and from a very small area below it, around a few nanometers (of the order of 5 to 10 nm).

Electrons that bounce elastically on the surface are called backscattered electrons. Its energy is greater than 50 eV and the depth of the site from which they come (of the order of hundreds of nanometers) is greater than that of the secondary electrons. The intensity of the signal of backscattered electrons, for a given energy of the beam, depends on the atomic number of the atoms of the material. This fact allows, from differences in intensity, distinguish phases of material of different chemical composition.

Samples that are to be analyzed by scanning electron microscopy must be dried before being introduced into the microscope; otherwise the low pressure in the microscope will cause water (and other volatile liquids) to evaporate, violently leaving the sample, altering the structure of it. When it is desired to visualize a sample in a scanning electron microscope, it must be conductive, then for no conducting samples should be cover with a conductive film, with a thickness between 10 and 25 nm.

The scanning electron microscope used in this PhD Thesis was JEOL JSM-840, installed in Research Technical Services of the University of Alicante. This equipment consists of a detector of secondary electrons type scintillate photomultiplier with resolution of 4 to 3.5 nm and a backscattered electron detector type Si P-N with resolution of 10 to 5 nm.

3.1.3 Scanning electron microscopy of field emission (FESEM)

Field Emission Scanning Electron Microscopy is a technique for morphological and chemical characterization of the material surface with higher resolution than the conventional SEM. In this case, a field emission canyon produces a highly focused beam of high and low energy electrons using low voltages (0.02-5 kV), in comparison with the thermionic system in the conventional SEM, avoiding over heating of the samples and possible sample damages.

The equipment installed in the Research Technical Services of the University of Alicante and used in this PhD Thesis is a scanning electron microscope of emission of field (FESEM) mark ZEISS model Merlin VP Compact equipped with a system of microanalysis by EDX brand BRUKER model Quantax 400 The resolution it reaches is 0.8 nm at 15 kV and 1.6 nm at 1 kV.

3.2 Thermogravimetric techniques

Thermal analysis is a series of techniques that measure the evolution, depending on temperature, time and atmosphere, of a sample specimen.

Thermogravimetry (TGA) is defined as the technique in which the weight of a sample is measured against time or temperature while the sample is subjected to a temperature controlled program in a specific atmosphere [3].

The temperature program can be kept at a constant temperature (isothermal), heating at a constant speed (the most usual next to the isotherm), cooling or any combination of them. During thermal treatment there is a loss of weight, but it is also possible that there is a gain of it. The atmosphere can be static or dynamic at a given flow rate (reduced pressure conditions are also used) and the most common gases are N_2, air, Ar, CO_2. H_2, Cl_2, or SO_2 are also used.

A fundamental characteristic of the TGA is that it only allows to detect processes in which there is a variation of weight such as decompositions, sublimations, reduction, desorption, absorption, etc. while it does not allow studying processes such as mergers, phase transitions, etc.

All TGA in this PhD Thesis were conducted by thermogravimetric equipment (TA Instruments, SDT Q600 Simultaneous) from the Research Technical Services of the University of Alicante.

3.3 Spectroscopic techniques

3.3.1 Fourier transformed infrared spectroscopy (FTIR)

In infrared spectroscopy the vibrational spectrum of a compound is obtained by exposing the sample to infrared radiation. FTIR spectroscopy uses a Michelson Interferometer that produces an interferogram from the splitted beam, which contains information about the whole range of IR frequencies coming from the source. The analysis of the interferogram resulting from the interaction with the sample permits to obtain the IR spectrum [4]. The infrared spectroscopy extends from 4000 to 400 cm^{-1} and informs about the molecular vibration.

In the experiment, after the signal is processed, the spectrum of the absorbed/transmitted IR radiation fraction as a function of the frequency or wavenumber is obtained. Bands will appear at certain wavelengths where the sample has absorbed IR radiation. This absorption of IR radiation is related to the excitation of the different vibrational modes of a molecule and different bands will

appear depending on the specific chemical bonds in the sample, which allows to identify them in the material.

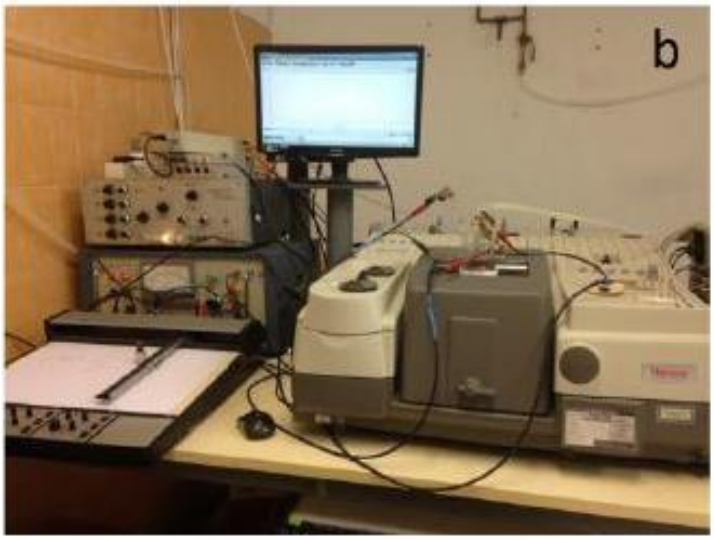

Figure 2.1: Equipment for in situ FTIR spectroscopy.

There are different configurations for obtaining infrared spectra, of among which the transmission, the diffused reflectance (DRIFT), the reflection-absorption (IRRAS) and the attenuated total reflectance (ATR). Each of these configurations is based on the different modes of interaction of the light beam with the sample, as shown in Figure 2.2.

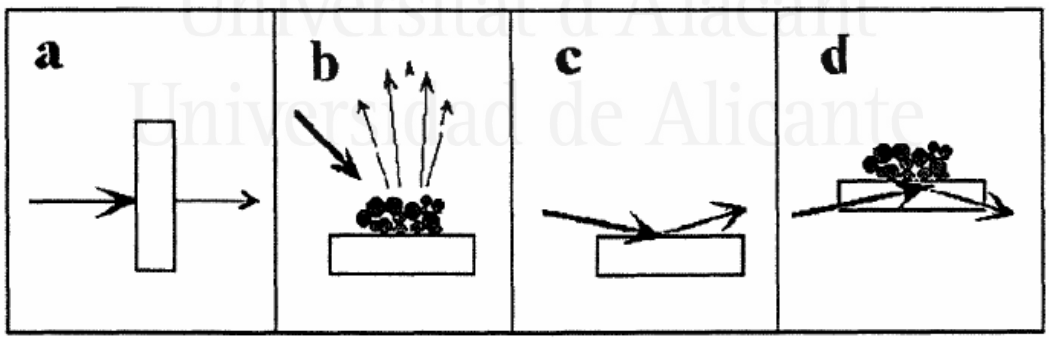

Figure 2.2: Different configurations to obtain a spectrum of infrared. a) Transmission, b) Diffused reflectance, c) Reflection-absorption and d) attenuated total reflectance.[5]

The main method of obtaining the in situ FTIR spectra in this PhD Thesis has been the external reflection [6]. The infrared spectrum of a sample is constituted by a variation of the transmittance versus the frequency of the incident radiation. The equipment used in the characterization of

copolymers obtained by electrochemical methods was a Nicolet 5700 FTIR spectrophotometer with mercury cadmium telluride (MCT) cooled with liquid nitrogen (Figure 2.1). The key to success in this spectroscopy is to minimize the signal losses due to the strong infrared absorption of water. This requires working with a thin layer configuration, in which the path of the beam going through the solution has to be minimal. It is also advisable to use a working electrode with a mirror finish such as Pt or Au to maximize the reflection of the beam. To achieve the configuration of thin electrolyte layer, the strategy is to press the electrode against the bottom of the electrochemical cell on which it is affected by infrared beam, this latter was then accomplished by threaded the plunger that acts on the body of the working electrode (Figure 2.3). The bottom of the cell is a triangular CaF_2 prism with angles of 60°. The beam is controlled by a system of mirrors in order to have an approximately perpendicular path on the side, so the electrode reaches an angle of 60 ° about the normal. The use of prismatic window improves significantly the signal quality than the use of flat windows. The resolution used in *in situ* FTIR spectroscopy was $8cm^{-1}$.

In situ FTIR analysis is performed potentiostatically, namely, leaving the electrode balanced each potential before acquire the spectrum. For each spectrum 100 averaged interferograms are taken. The result is a single beam spectrum (R), which is equivalent to the transmittance. Due to the distortion of the spectrum caused by the solvent, it is necessary working with a reference spectrum obtained in the same configuration but a different potential (R_0). The result is the spectrum subtraction: $(R-R_0)/R_0$. By processing this signal, two kind of band it can be observed: a monopolar band (positive that indicates disappearance of the species at the sample potential and negative, that indicates appearance of the species at the sample potential) and bipolar band by the presence of two modes the negative mode (appearance at sample potential) and the positive mode (disappearance at the sample potential) (Figure 2.4).

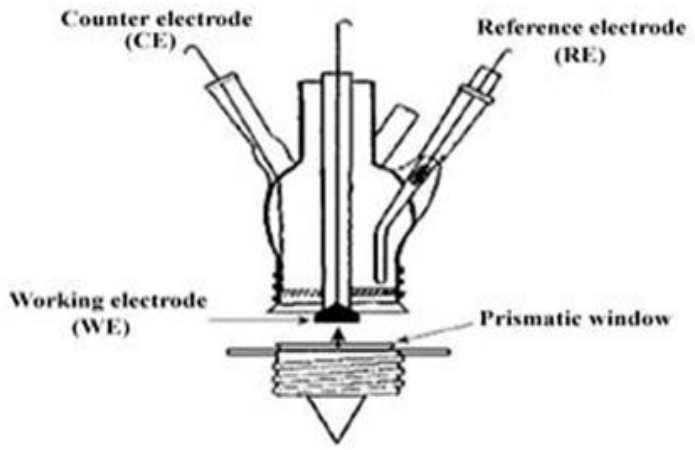

Figure 2.3: Electrochemical cell used in the in situ FTIR spectroscopy.

In general, the final in situ FTIR spectra are represented by negative absorption bands (downward) corresponding to species that appear by changing the potential value and other positive bands (upward) showing species that disappear by modifying the potential values (Figure 2.4).

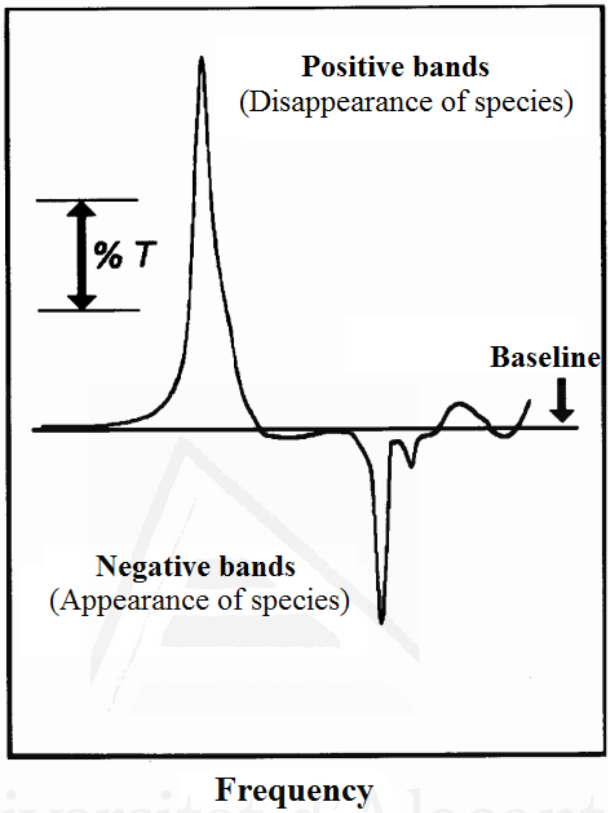

Figure 2.4: representation of a in situ FTIR spectrum.

3.3.2 X-ray photoelectron spectroscopy (XPS)

The X-ray photoelectron spectroscopy is a quantitative detection technique useful for determining the nature of the chemical species and their oxidation states on the surface of a material. This technique is considered as a surface characterization technique due to its low penetration power (1-3 nm) [7].

The technique consists in the determination of the kinetic energy of the emitted electrons when the samples are irradiated with a monochromatic X-ray beam. The irradiation can produce the emission of valence or inner electrons from the sample atoms. The electron emission has a specific kinetic energy which is related to the electron configuration of the elements and consequently to the binding energy of the ejected electron. The binding energy can be calculated from the energy of the X-ray source by subtracting to the energy of the incident radiation, the kinetic energy of the emitted electron and the work function, which is a characteristic of the apparatus and the sample [8]. The

obtained spectrum shows the number of counts or intensity recorded in a range of binding energies. Generally, the binding energy increases for the higher oxidation states of the elements, and these changes can be seen as a shift of the binding energy of the XPS peak.

The experimental setup has an X-ray source, an electron detector and the energy analyzer. All the experiments are performed at ultrahigh vacuum (5 x 10^{-7} Pa) in order to avoid the collision between the ejected electrons and residual molecules, which can affect the signal quality.

The surface composition and oxidation states of the species in the materials were studied using a VG-Microtech Mutilab 3000 spectrometer and Mg Ka radiation (1253.6 eV). The C1s peak position was set at 284.6 eV and used as reference to shift the position of the whole spectrum. Deconvolution of the XPS spectra was done by least squares fitting, using Gaussian-Lorentzian curves, while a Shirley line was used for the background determination.

In this PhD Thesis the XPS technique has been used in order to determine the surface composition of the different polymers. For this, the transitions have been followed C (1s), O (1s) and N (1s), S (2p). XPS spectra were obtained with a spectrometer electron Multi lab VG Microtech 3000, equipped with Mg source $K_{\alpha 1,2}$ 1253.6 eV X-Ray of the Research Technical Services of the University of Alicante.

3.4 Measurement of electrical conductivity

As definition conductivity characterizes the ability of a material or a solution to let the electric charges move freely and thus allow an electric current. The conductivity, σ, is a physical property inherent to homogeneous material and is expressed in S cm^{-1}. Its inverse is the resistivity, ρ, which can be obtained from experimental measurements of the material resistance, R. in fact, the conductivity.

According to Ohm's law, the simplest method of measuring resistance in a material is to apply a current between two metallic points in contact with the piece of material and measure the potential difference that is established between them. However, in the case of semiconductor materials, a high contact resistance is established between the metal tips and the sample which contributes significantly to the measured resistance values, so this method is no longer adequate. The four-point in-line configuration (Figure 2.5) is an alternative for the measurement of resistance in semiconductor materials between the end points a current is passed and the voltage established between the intermediate points is recorded. It is assumed that the tip pressure on the material breaks the crystal structure of the semiconductor material. So, in order to promote the establishment of an ohmic contact, and to avoid the formation of a Schottky barrier this is typical to the contacts between metallic and semiconductor. The piece of semiconductor material must rest on an insulating surface

during the measurement, to prevent the formation of external alternative conduction paths to the material of interest. The electric current spreads concentrically around each point, so that the geometry of the sample has important implications in the results of resistance obtained. The ideal sample is that of semi-infinite geometry, which means with a flat surface and of unlimited dimensions in the rest of directions. In this case, the resistivity is obtained by an integrating equation for the distance between the inner points. In the most common case, the four tips are equidistant at a spacing s = 1591 mm. In fact to consider semi-infinite, the diameter or dimension representative of the geometry of the sample must be in order of 100s (~ 16 cm) and its thickness greater than 5s (~ 1 cm).

In the present PhD Thesis, the pellet is prepared from each of the synthesized materials using a steel mold, which is subjected for at least 10 min to 45 MPa pressure. The experimental device used was the S-302-4 model of the Lucas Labs equipment, with a four-point equidistant head of tungsten carbide. The sample was placed according to the configuration of (Figure 2.5), by means of which a potential difference was applied using a potentiostat-galvanostat AutoLab PGSTATG302.

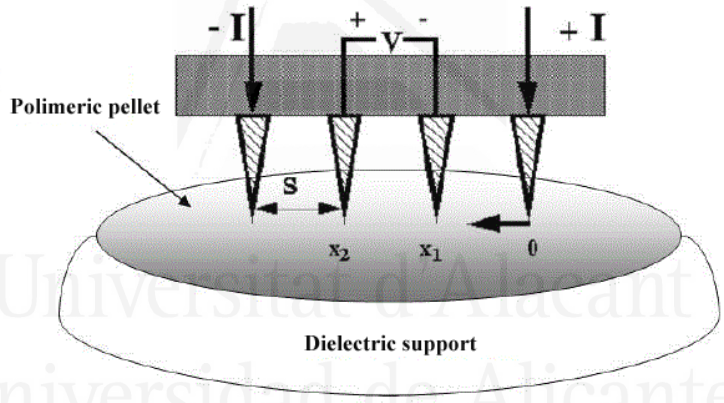

Figure 2.5**:** Conductivity measurement with the methods of four-points in line.

3.5 Electrochemical characterization.

The electrochemical characterization of the synthesized materials has been performed using mainly cyclic voltammetry. The electrochemical techniques allow the analysis of the processes that occur on the electrode/electrolyte interface. In the following sections, the cell configurations and the fundamentals of electrochemical techniques are described.

3.5.1 Cyclic voltammetry (CV)

Cyclic voltammetry is a very useful technique for assessing the electrochemical behavior of an interface electrode/electrolyte [13]. It is possible to get information about electrochemical reactions, thermodynamics of redox processes, and kinetics of electron-transfer reactions, capacitive currents, and adsorption processes, among others.

Cyclic voltammetry experiments consist in a linear scanning of the potential of a working electrode. In the experiment, the current flowing through the working electrode (WE) and the counterelectrode (CE) is measured during a potential change with time using a constant potential scan rate[13]. The applied potential to the WE is measured against a reference electrode (RE). At the beginning, the WE is introduced in the electrolyte at an initial potential E_i, where no reaction occurs. Figure 2.6 shows the theoretical cyclic voltammetry measurements of potential vs. time and current vs. potential (cyclic voltammogram) for a redox reversible reaction.

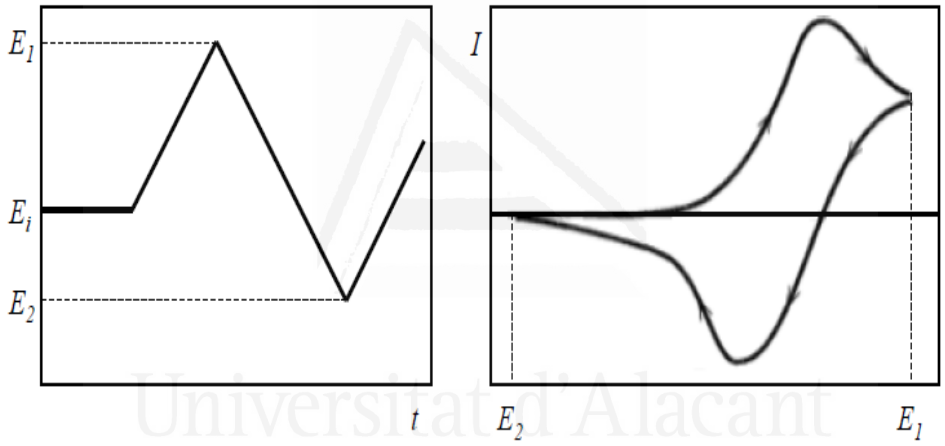

Figure 2.6: Cyclic potential sweep (left) and the resulting cyclic voltammogram (right)

The response of each material is different and depends on the combined action of capacitive currents delivered during the formation of the electrical double layer over the surface of the electrode and possible faradic reactions that can occur on the electrode/electrolyte interface.

3.5.2 Chronopotentiometry

Chronopotentiometry is a galvanostatic technique that is based on the measure of the potential or voltage as a function of time at constant current [13]. The use of this technique allows register the galvanostatic charge-discharge cycles, and after reaching a potential the sign of the current is reversed until potential/voltage reached the initial value. From them, parameters like capacitance, reversibility, durability, ohmic drop, specific energy, specific power, etc can be determined [10]. Figure 2.7.a shows the current program over time during a galvanostatic charge-discharge cycle. The

Figure 2.7b shows the charge-discharge curve obtained for a no faradic process typical for a capacitor [17].

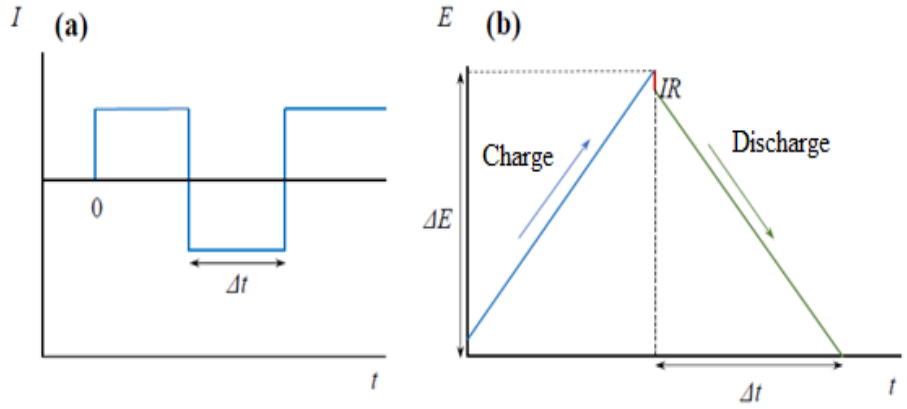

Figure 2.7: (a) Variation of the current over time during a galvanostatic charge/discharge cycle (b) galvanostatic charge-discharge cycle for a capacitor.

We can determine the specific capacitance of an electrode or a capacitor using the following equation (1)[17].

$$C = \frac{I\Delta t}{m\Delta E} \qquad (1)$$

Where I is the current (A), Δt is the discharge time (s), ΔE is the potential window when the a material is characterized or voltage when a capacitor is testing (V) and m is the electrode mass or that of both electrodes when it comes to the supercapacitor.

The galvanostatic charge-discharge cycles allow to determine the ohmic drop, which is related to the resistance of the material and the device. In this PhD Thesis, all the specific capacitances have been calculated including the ohmic drop in the value of the applied potential window or voltage. [18].

3.5.3 Electrochemical cell configurations.

A standard three electrode cell was used for the electrochemical synthesis and characterization by cyclic voltammetry. The cell is filled with an electrolyte in order to ensure sufficient conductivity, and it consists of a reference electrode (RE); working electrode (WE), which corresponds to the material to be measured; and a counter electrode (CE) which is an inert material with high surface area [12].

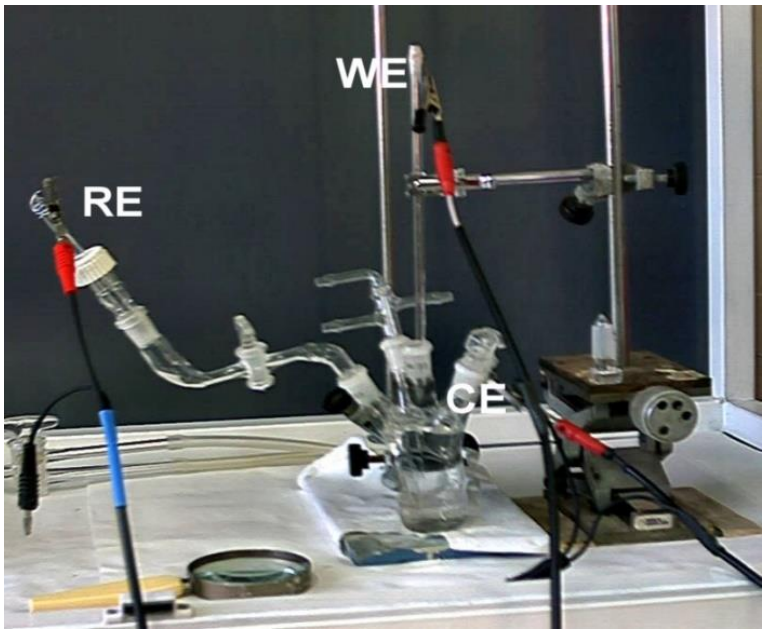

Figure 2.8: Electrochemical cell of three electrodes.

As can be seen in Figure 2.8, in addition to the three electrodes already described, a gas connector is used to eliminate oxygen dissolved in solution by purging N_2 (g). This is usually done through a constant bubbling for at least 10 minutes before starting the experiment, and then it is passed to keep the internal environment of the cell purged with N_2, with the aim of maintaining an inert atmosphere during the electrochemical measurements.

Another common accessory is the Luggin capillar that allows the reference electrode to be kept in a small compartment and oblivious to possible changes in the composition of the working solution. The use of a Pt wire in which a deposit of platinum black within a solution saturated with H_2(g) as reversible hydrogen electrode (RHE) as reference electrode. Figure 2.9 shows the diagram of the electrochemical cell with three electrodes used in the cyclic voltammetry experiments.

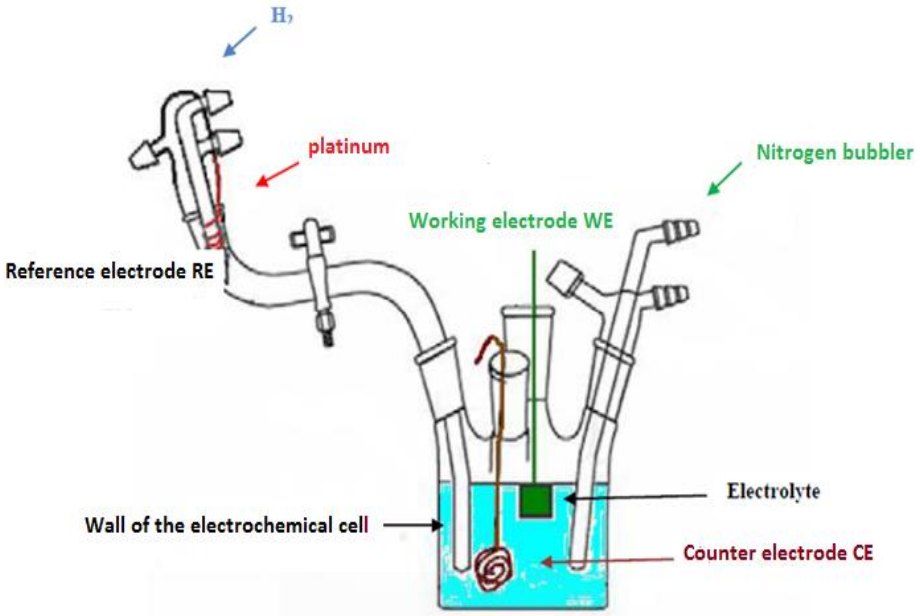

Figure 2.9:

Diagram of the electrochemical cell used of three electrodes

The electrochemical cells of two electrodes are used for the characterization of the supercapacitors [10]. They are composed of two active materials (positive and negative electrodes), two current collectors, one separator and an electrolyte. The current collectors are conductive electric that guarantee the transfer of electrons. The separator must be an ionic conductor (allowing keep the flow of current in the cell) and electrical insulator to avoid the device short circuit. The separator and the active materials must be in a conductive medium, such as a liquid electrolyte, solid or polymeric.

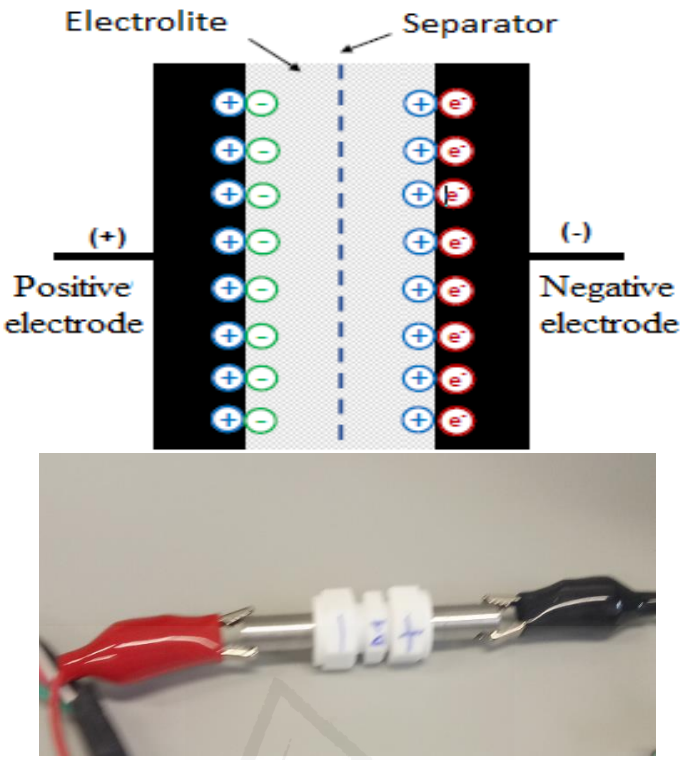

Figure 2.10: Electrochemical cell of two electrodes.

Figure 2.10 shows a cell of two electrodes used to characterize a supercapacitor. In this system, the current or the voltage between the positive and negative electrodes are recorded or controlled to assess the behavior of the capacitor [11].

In this PhD Thesis different types of cells have been used, in each Chapter specifies the details concerning: (i) configuration of cell; (ii) construction of the working electrode; (iii) type of electrode

3.6 Synthesis methods.

3.6.1 Electrochemical polymerization

Cyclic voltammetry experiments were carried out in a conventional three-electrode cell under N_2 atmosphere. The working electrode was a spherical platinum polycrystalline surface with an area of about 15 mm^2, and a platinum wire was used as the counter electrode. All of the potentials were measured against the reversible hydrogen electrode (RHE) immersed in the same electrolyte through a Luggin capillary. Cyclic voltammograms were recorded at a constant scan rate of 50 mV s^{-1} and at room temperature. The platinum electrodes were thermally cleaned and subsequently protected from the laboratory contaminations with a droplet of ultrapure water.

3.6.2 Synthesis of hydrogel

Various strategies have been used in the preparation hydrogels of copolymers formed from piperazine, aniline and sodium poly(styrene sulfonate) (PSS) (poly(Ani-co-PIP)/PSS) and copolymers formed from with 2-aminoterephthalic acid, aniline and PSS (poly(Ani-co-2ATA)/PSS) prepared at different monomer molar ratios (Ani/PIP or Ani/2ATA) in concentrated solutions (0.25/0.25) =1; (0.38/0.12) =3; (0.42/0.08) =5. The hydrogels were synthesized in 1M HCl, and different quantities of monomers to obtain a concentration of 0.5 M were added into 20 mL of 1M HCl and 0.5M PSS. After stirring for 10 min, 10 mL of APS (oxidant) solution, with a concentration to maintain a molar ratio monomers/APS of 1, was added to initiate the polymerization. The resulting solution was stirred for 1 min and then the reaction was allowed to proceed without agitation for 12 h at room temperature. Hydrogel products were purified in a large amount of distilled water for 1 week to eliminate low molecular weight components.

3.6.3 Cleaning the glass material

In cyclic voltammetry the cleaning of the glass material that is in contact with the solutions is quite important. The cleaning protocol is as follows:

- The glass material is immersed in a concentrated acid solution of $KMnO_4$ for about 12 hours. The recipe for preparing the oxidant solution is the following: 30 g of $KMnO_4$ + 5 mL H_2SO_4 (98%) in 2 L of H_2O. In this way it is possible to oxidize the organic matter present to simpler species to be eliminated.
- The glass material is then removed from the oxidant mixture and rinsed with an acidic H_2O_2 solution. With this solution, the remains of MnO_4^- that have not reacted are reduced. Then the material is washed with abundant ultrapure water (18.2 MΩ • cm) to eliminate salts, residues and oxidation products.
- After the washing, the glassware is boiled repeatedly in heating plates or in microwaves with ultrapure water, thus eliminating substances that may still be adhered to the walls of the material. Finally, the material is rinsed with ultrapure water and it is ready to be used.

3.6.4 Cleaning platinum electrodes

In both the cyclic voltammetry and IR-in-situ experiences, a heat treatment to the working electrode in order to obtain a clean surface and neat. This heat treatment, proposed by J. Clavilier et al. [19,20] for single crystals of platinum, consists on heating the platinum electrode in a flame of propane / air for a few seconds at a temperature close to 1300 ° C, leaving it then cool to about 300 ° C in the air and then protect it from contamination atmospheric with a drop of ultrapure water. This temperature of 300ºC is what low enough to contact the drop of water at temperature environment does not cause tensions that can damage the electrode, but sufficiently high to achieve catalytic oxidation of any impurity present on the electrode surface.

Figure 2.11 shows a voltammogram for a heat-treated platinum electrode immersed in a solution of 0.5 M H_2SO_4. The characteristic zone generally known as adsorption desorption of hydrogen (1.2 and 3.4 in Figure 2.11) is observed, although that the adsorption-desorption of the anion electrolytic. The no faradic zone completely horizontal (7 on the Figure 2.11) and the surface oxidation-reduction process of platinum (5, 6 in Figure 2.11). This shows that the cleaning level of the cell is enough to work. In addition, this last step is used to calibrate the reference electrode (RHE, Ag/AgCl, pseudo-reference), taking into account that the Hydrogen production with a Pt electrode takes place at 0.0 V vs NHE.

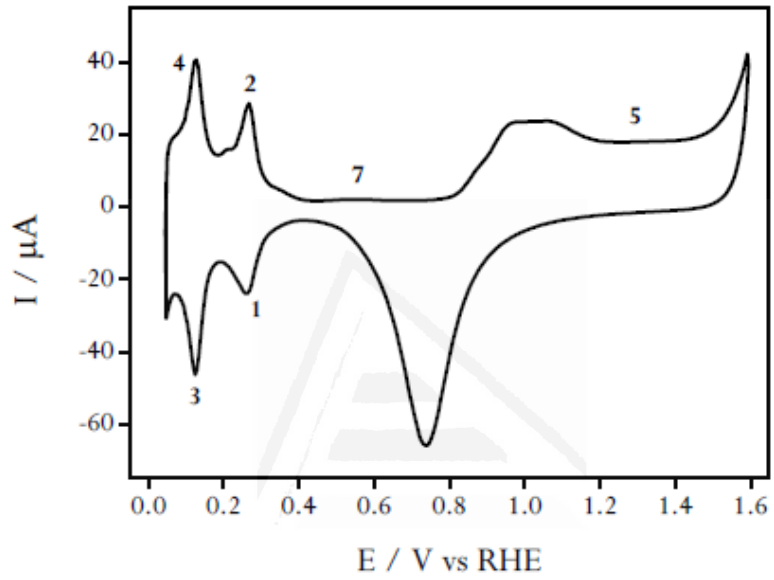

Figure 2.11: Cyclic voltammetry of a clean polycrystalline electrode of Pt immersed in 0.5M H_2SO_4 solution.

3.6.5 Preparation of the electrodes for capacitor cell.

Due to the nature of the samples intended to know their electrochemical behavior (capacitance, stability, resistance ...), which are mostly in the form of powder, it is necessary to form a film (disc) that will be attached to the current collector. The materials of the collectors depend on the electrolytic medium where they will be studied. Preparation of electrodes during development of this PhD Thesis have generally followed the method showed in Figure 2.12a; b; c.

The mixture of the active material with a binder and a conductivity promoter, in our case is Teflon (PTFE). The weight ratio of each of them is detailed in each chapter. In this part, we will build the cell of two electrode in other to characterize a supercapacitor with the dried hydrogels (powder), they will be used to prepare a film electrode with mixture of Teflon; the cell was containing

a drop of 1M H_2SO_4 as electrolyte and Nylon membrane as separator. The conditions of these experiments are detailed in Chapter 3.

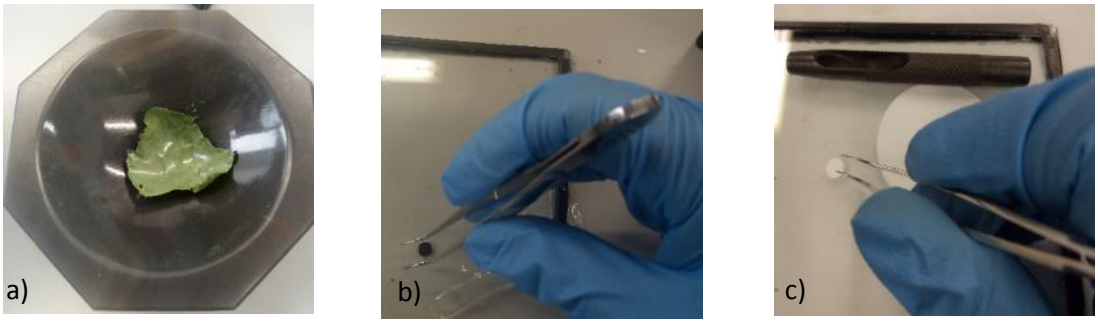

Figure 2.12: a) Forming the film electrode; b) Disc film electrode; c) separator Nylon membrane

4 References

[1] Y. Leng. Materials characterization: Introduction to microscopic and spectroscopic methods: Second edition. Wiley Online Library, 2013. doi:10.1002/9783527670772.

[2] R. Wiesendanger. Scanning probe microscopy and spectroscopy : methods and applications, Cambridge University Press, 1994.

[3] T. Hatakeyama, F.X. Quinn. Thermal analysis : fundamentals and applications to polymer science, Wiley, 1999.

[4] B.C. Smith. Fundamentals of Fourier Transform Infrared Spectroscopy. CRC Press, 2011.

[5] F. Montilla, E. Morallón, J.L. Vázquez. Evaluation of the electrocatalytic activity of antimony-doped tin dioxide anodes toward the oxidation of phenol in aqueous solutions. J. Electrochem. Soc. 2005, 152, 0–6. doi:10.1149/1.2013047.

[6] T. Iwasita, F.C. Nart. In situ infrared spectroscopy at electrochemical interfaces. Prog. Surf. Sci. 1997, 55, 271–340. doi:10.1016/S0079-6816(97)00032-4.

[7] D.A. Skoog, F.J. Holler, S.R. Crouch, Principles of instrumental analysis, Thomson, Brooks/Cole, Belmont, CA, 2007.

[8] C.R. Brundle, C.A. Evans, S. Wilson. Encyclopedia of materials characterization : surfaces, interfaces, thin films, Butterworth-Heinemann, 1992.

[9] E. Raymundo-Piñero, D. Cazorla-Amorós, A. Linares-Solano, J. Find, U. Wild, R. Schlögl. Structural characterization of N-containing activated carbon fibers prepared from a low softening point petroleum pitch and a melamine resin. Carbon N. Y. 2002, 40, 597–608. doi:10.1016/S0008-6223(01)00155-5.

[10] P.S. J.-F. Fauvarque, Principles of Electrochemistry and Electrochemical Methods. Carbons, 2009. doi:10.1201/9781420055405.

[11] S. Shiraishi, Electrochemical Performance, Materials Science and engineering of carbon, 2016. doi:10.1016/b978-0-12-805256-3.00010-6.

[12] M. Inagaki, H. Konno, O. Tanaike, Carbon materials for electrochemical capacitors, J. Power Sources. 195 , 2010, 7880–7903. doi:10.1016/j.jpowsour.2010.06.036.

[13] A.J. Bard, L.R. Faulkner, Basic Potential Step Methods, in: D. Harris (Ed.), Electrochem. Methods Fundam. Appl., Second, John Wiley & Sons, Texas, 2001, 156–225.

[14] J.Wang. Analytical electrochemistry. Third Edition, John Wiley & Sons, New York, 2006.

[15] D. Pletcher, R. Greff, R. Peat, L.M. Peter, J. Robinson. Instrumental methods in electrochemistry, First Edition, Woodhead Publishing Limited, Oxford, 2001. doi:10.1533/9781782420545.

[16] J. Rouquerol, F. Rouquerol, P. Llewellyn, G. Maurin, K.S.W. Sing. Adsorption by Powders and Porous Solids: Principles, Methodology and Applications, Second Edition, Elsevier,

Oxford, 2013. doi:10.1016/C2010-0-66232-8.

[17] B.E. Conway, Electrochemical Supercapacitors, Springer US, 1999. doi:10.1007/978-1-4757-3058-6.

[18] B.E. Conway, Introduction and Historical Perspective, in: Electrochem. Supercapacitors, Springer US, Boston, MA, 1999, 1–9. doi:10.1007/978-1-4757-3058-6_1.

[19] J. Clavilier, The role of anion on the electrochemical behaviour of a {111} platinum surface; an unusual splitting of the voltammogram in the hydrogen region, J. Electroanal. Chem. 1980, 107, 211–216. doi:10.1016/S0022-0728(79)80023-6.

[20] J. Clavilier, R. Faure, G. Guinet, R. Durand. Preparation of monocrystalline Pt microelectrodes and electrochemical study of the plane surfaces cut in the direction of the {111} and {110} planes. J. Electroanal. Chem. 1980, 107, 205–209. doi:10.1016/S0022-0728(79)80022-4.

Chapter 3

An Electrochemical Study on the Copolymers formed from 2-Aminoterephthalic Acid, Piperazine, and Aniline Monomers Testing their Sensitivity towards Dopamine and Ascorbic Acid

1 Introduction

In recent years nanostructured materials, and particularly those based on conducting polymers, have received great attention for a variety of applications including chemical and biological sensors [1]–[3] . Sensors based on conducting polymers offer typically high sensitivity and fast response but, also, quite a low conductivity when the active material is in the undoped state. In spite of this, conductivity values can be easily (and reversibly) multiplied by a 10^5 factor after chemical or electrochemical oxidation, a process also known as oxidative doping. It is well established that, contrary to other conducting polymers such as polypyrrole or polythiophene, the electrical conductivity of polyaniline is influenced by both, the oxidation state of the polymer backbone and its protonation level [4].

Moreover, the electrochemical devices based on conducting polymers, either working as sensors or as systems taking advantage of other electrocatalytic effects, have become a topic of growing interest for molecular electrochemistry during the last decades [5]–[10] . It is known that conducting polymers show the ability to incorporate catalytic molecules, and numerous works based on this particular property led to interesting applications in the field of bioelectrochemical sensing. The polymer constitutes an organic matrix where catalytic molecules, such as enzymes, may preserve its activity better, and where the conducting surroundings may electrically wire it to the metal electrode surface [16–19]. Besides the incorporation of catalytic species, the pristine conducting polymers (polyaniline, polypyrrole, etc.) can be also chemically modified to gain further catalytic capabilities. The most classical way to perform chemical modification is to copolymerize aniline or pyrrole, for example, with monomers that are able to provide the final material with the desired catalytic features.

2-Aminoterephthalic acid (2ATA) could be an interesting co-monomer for the aniline copolymerization because it contains two –COOH groups linked to the aromatic ring. The use of 2ATA can be attractive in order to yield soluble self-doped polyaniline avoiding the use of external

dopants. Furthermore, 2-aminotherephthalic acid could react through either the 2- or 3-position in relation to the COOH group [11]. In a previous contribution, a copolymer from aniline (ANI) and aminoterephthalic acid (ATA) monomers by chemical oxidative polymerization has been studied [11]. It was found that ATA monomers were four times less reactive than aniline in the conditions of chemical polymerization, because of the deactivating effect of the carboxylic group attached to the aromatic ring. Therefore, controlling the monomer ratio was a key parameter to obtain a true copolymerization product and to modulate the material composition and properties.

Chemical derivatives of piperazine (diethylenediamine) constitute a promising group of catalytic molecules that have been successfully applied in chemical and electrochemical sensing [2], [10], [12]–[14] . In spite of this, few studies exist that are devoted to the exploration of the catalytic properties of polymer systems containing the parent piperazine molecule. Among them, it has been reported that a novel piperazine-functionalized mesoporous organic polymer exhibited highly catalytic activity and selectivity for some organic synthesis reactions in aqueous medium [15] . The electrochemical sensing ability of piperazine in combination with inorganic polymers has been explored recently in the selective detection of ascorbic acid [16] . The sensing system was a piperazine-functionalized mesoporous silica, and the results show that this type of hybrid material is a potential candidate for the construction of bioelectrochemical sensors.

The chemical copolymerization of aniline and piperazine was studied by Ramachandran et al. [17] . Although the catalytic properties of the obtained material were not analyzed, the copolymer showed electrochemical activity. The chemical structure proposed (see Scheme 3.1) seems constituted by alternated piperazine and aniline moieties, which are bound through aniline *ortho*- and *para*- positions. It was shown that charge delocalization in this polymer includes also oxidized piperazine centers, but extended conjugation was not observed. The electrical conductivity of the material was in the range of 10^{-7}–10^{-9} S cm^{-1}.

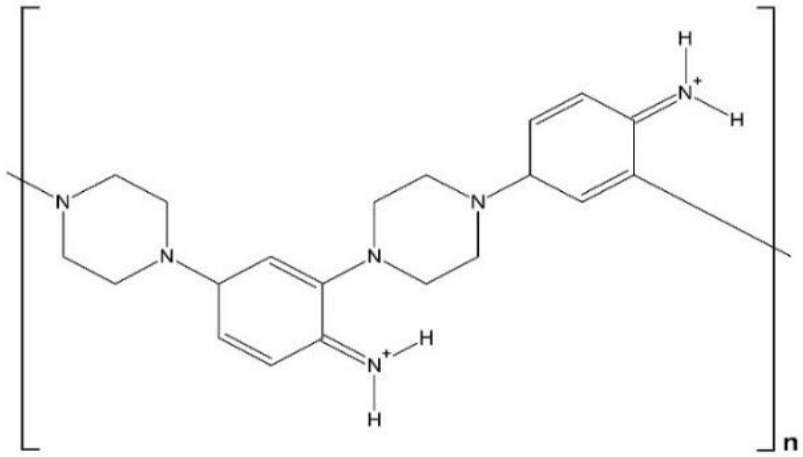

Scheme 3.1. Model structure proposed by Kabilan et al [17] for the chemically synthesized piperazine–aniline copolymer in the doped state

In this context, the aim of this chapter thesis is to investigate the possibility of electrochemically synthesizing electroactive copolymer containing aniline and aminoterephthalic acid units (see Scheme 3.2) Moreover, the electrochemical oxidation of piperazine in acidic medium and, additionally, its electrochemical copolymerization with aniline. A combination of in situ Fourier transform infrared (FTIR) spectroscopy and electrochemical techniques will be used to characterize the redox behavior of the copolymer, while X-ray photoelectron spectroscopy (XPS) will shed more light on the chemical structure of the electrochemically synthesized materials. Finally, the electrochemical sensing properties of the all the synthesized copolymers will be tested for ascorbic acid and dopamine.

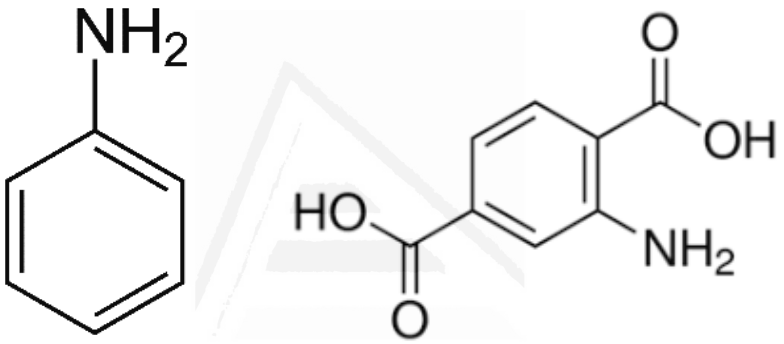

Scheme 3.2. Chemical structures of aniline, and aminoterephthalic acid.

2 Experimental

Aniline monomer was distilled previously and aminoterephthalic acid was used without further purification (both were supplied by Aldrich). The ultrapure water (18.2MΩ cm) employed in all the experiments were obtained from an Elga Labwater Purelab system. Piperazine (98.8%), aniline (99.5%), 2-Aminoterephthalic acid (Aldrich, 98%) and ammonium persulphate (Merck, p.a.), ascorbic acid (AA, 98.9%), and dopamine (DA, 97.9%) were purchased from Merck.

Cyclic voltammetry experiments were carried out in a conventional three-electrode cell under N_2 atmosphere. The working electrode was a spherical platinum polycrystalline surface with an area of about 15 mm^2. The counter electrode was a platinum wire. All potentials were measured against a reversible hydrogen electrode (RHE) immersed in the working solution. The Pt working electrode

was thermally cleaned and subsequently protected from the laboratory atmosphere by a droplet of ultrapure water. Then, it was transferred to the working solution (previously deaerated by bubbling N_2) where it was immersed at controlled potential (0.05 V/RHE). Cyclic voltammograms were recorded at 50 mV s^{-1} and at room temperature. The electrochemical copolymerization of aniline and aminoterephthalic acid was carried out in 1M $HClO_4$ (Merck,p.a.) medium containing 30 mM aniline and 70 mM aminoterephthalic acid (Aldrich); a monomer ratio (ANI/ATA=3/7). In the case of electrochemical copolymerization of aniline with piperazine different monomer ratios have been studied (ANI/PIP= 0.2, 0.3, 1, 3 and 5).

A Nicolet 5700 spectrometer (Thermo Electron Scientific Instruments, Madison, USA) equipped with an N_2-cooled mercury cadmium telluride detector was employed for the in situ FTIR experiments. The working Pt disc electrode was mirror-polished with alumina powder, and the spectroelectrochemical cell used a prismatic CaF_2 window beveled at 60° in order to increase the beam intensity reaching the infrared (IR) detector. All the spectra were collected at the same 8 cm^{-1} resolution using deuterated water (99.9% D) as the solvent. The processed spectra have been presented in the standard mode $\Delta R/R$.

AVG-Microtech Multilab 3000 electron spectrometer (VG Microtech Ltd., Uckfield, UK) was employed to acquire the ex situ XPS spectra. The 300-W power radiation source was a non-monochromatized Mg-Kα, and the analysis was performed under 5×10^{-7} Pa pressure. The high-resolution spectra were acquired at 50 eV pass energy, and are presented as a combination of Lorentz (30%) and Gaussian (70%) curves. The C 1s line at 284.4 eV has been employed as the reference for the experimental binding energies, which were obtained with 0.2 eV accuracy.

The scanning electron micrographs were acquired by means of an ORIUS-SC600 Field Emission Scanning Electron Microscope (FE-SEM) (Gatan Inc., Pleasanton, USA), which was equipped with a ZEISS microscope (Carl Zeiss Microscopy Ltd, Cambridge, UK).

3 Results and discussion

3.1 Polymerization of Aniline and Aminoterephthalic Acid monomers on Pt electrode.

3.1.1 Electrochemical Behavior of Aminoterephthalic Acid on Pt.

In this section, the electrochemical response of 2-aminoterephthalic acid has been studied. The oxidation of the monomer will demonstrate the choice of suitable conditions for copolymer formation, particularly when setting the higher potential limit during electropolymerization. In addition, the recorded voltammetric profiles of the monomer will be used to define the redox behavior of the resulting copolymer.

The electrooxidation of 10 mM 2ATA was carried out on a platinum electrode in 1M $HClO_4$ by cyclic voltammetry between 0.06 and 1.45 V. Figure 3.1a shows that the oxidation of ATA starts at of potential as high as 1.18 V and displays a maximum at 1.34 V which decreases continuously with the number of cycles. Then, it seems that this intense anodic peak yields some non-electroactive adsorbed product on the electrode surface, as deduced from the absence of any coupled reduction wave during subsequent reverse scans. In fact, after the experiment, the surface of the platinum electrode appeared covered by a yellowish film that was then washed with ultrapure water and transferred to a new test solution containing 1 M $HClO_4$ as the background electrolyte. A cyclic voltammogram recorded for this film in the absence of monomer species is presented in Figure 3.1b, where the characteristic profile of a platinum electrode covered with an almost electroinactive thin layer of polymeric product can be clearly observed (the curve is similar to the polycrystalline electrode without a deposit) [18] . Therefore, it can be inferred that contrary to its parent compound o-aminobenzoic acid [19] , the electrochemical oxidation of aminoterephthalic acid does not yield an electroactive polymer on the electrode surface.

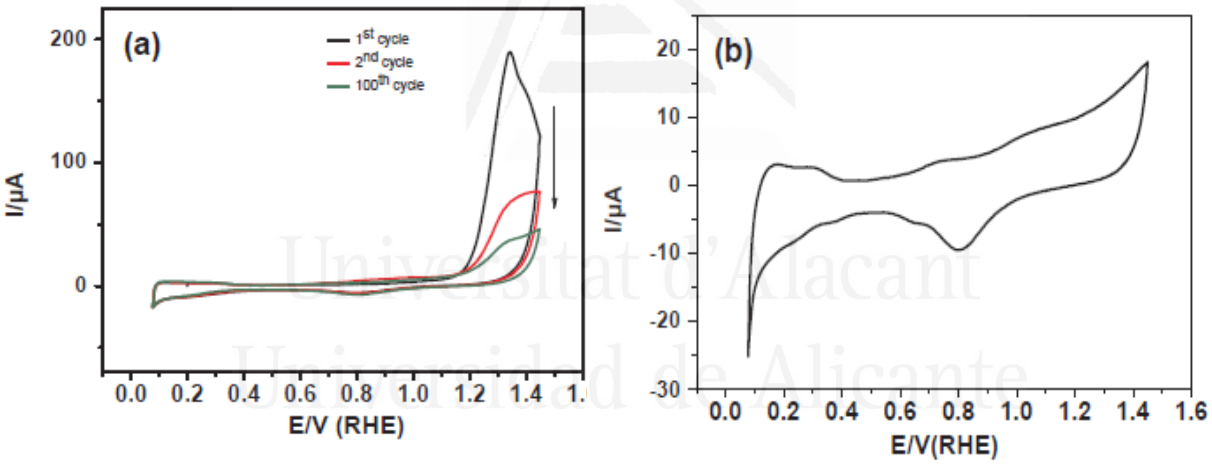

Figure 3.1. (a) Cyclic voltammograms recorded for a Pt electrode during the electrochemical oxidation of 10 mM ATA in 1 M $HClO_4$ solution. 1st cycle (black line), 2nd cycle (red line), 100th cycle (green line). (b) Voltammetric response of the modified electrode in 1 M $HClO_4$ background solution free of monomer. (For interpretation of the references to colour in this figure legend, the reader is referred to the web version of this article.) [18]

3.1.2 Copolymerization of Aniline and Aminoterephthalic Acid.

It is reported that the chemical oxidation of 2-aminoterephthalic acid (ATA) and aniline (ANI) mixtures does not yield any copolymerization product for aniline-aminoterephthalic acid monomer feed ratios below 0.3 (aniline mole fraction in the feed, $f_{ANI}<0.3$) [11] . Besides, the copolymer obtained using a f_{ANI} = 0.3 feed ratio shows an aniline mole fraction within the polymerization product, F_{ANI}, close to 0.5 as determined by XPS and elemental analysis [11] . Therefore, to achieve the parallel electrochemical copolymerization, the particular $f_{ANI}=0.3$ value seems a lower limit that should not be exceeded. Nevertheless, the use of large aniline relative concentrations during electro-copolymerization usually gives rise to polyaniline deposits with no (or little) incorporation of the other co-monomer, due to the higher electrochemical reactivity of aniline. Taking these two factors into account, the use of a feed mole fraction f_{ANI} around 0.3 seems a compromise solution to ensure an eventual incorporation of 2ATA molecules to the growing polymer and, accordingly, this will be the value employed in the chapter thesis.

On the other hand, it is also known that electrochemically deposited copolymers show physicochemical properties strongly affected by the upper inversion potential employed during the synthesis. To gain insight into this point, ANI-ATA copolymers have been deposited using four different upper potential limits comprised from 1.1 V and 1.4 V for the first scan, and at 1 V for the subsequent ones and all cycles at the upper potential limit. The lower potential value corresponds to the onset of reported oxidation for aminoterephthalic acid molecules, although they can be incorporated in their unoxidized state to the growing polymer chains to create copolymer structures [18] . Figure 3.2a shows the first direct scan for a platinum electrode in a strongly acidic solution containing a mixture of aniline: amino-terephthalic acid with a monomer ratio of 3:7. The arrows denote the three different higher potentials used to perform electropolymerization in this monomer ratio.

Figure 3.2b shown the experiment carried out to during the consecutives cycles until 1.4V, in order to achieve electropolymerization under the established premises. Figure 3.2c to e, show the electrochemical responses in 1 M $HClO_4$ solutions free of monomers, of the different ANI-ATA copolymers deposited by cycling up to 1.4 V (c), 1.2 V (d) and 1.2 V for the first scan, and at 1 V for the subsequent ones (e) after ten voltametric cycles. It is observed in these figures that the voltammograms of the copolymer materials show three redox transitions, regardless of the higher potential limit used during the polymerization. The first, at about 0.3-0.5 V, and the latter, centered around 0.9 V, are clearly attributed to the leucoemeraldine to emeraldine and emeraldine to pernigraniline transformations, respectively. The potential of the average peak corresponds well to those usually attributed to the presence of crosslinked or superoxidized sites in the polyaniline chains, which are favored when aniline is copolymerized with other aromatic amines [20], [21] . The

comparison of the voltammograms of Figure 3.2c and Figure 3.2d show that the amount of material deposited on the electrode surface is significantly lower when the electropolymerization potential limit is below 1.4 V, Figure 3.2e shows the voltammograms when the upper potential limit is 1.2V during the first cycle but the subsequent is 1V. It can be observed the low amount of copolymer obtained. Then, this result indicates that the potential of 1.2V is too low to produce the oxidation of ATA and the concentration of ANI is also low to polymerize in large extension.

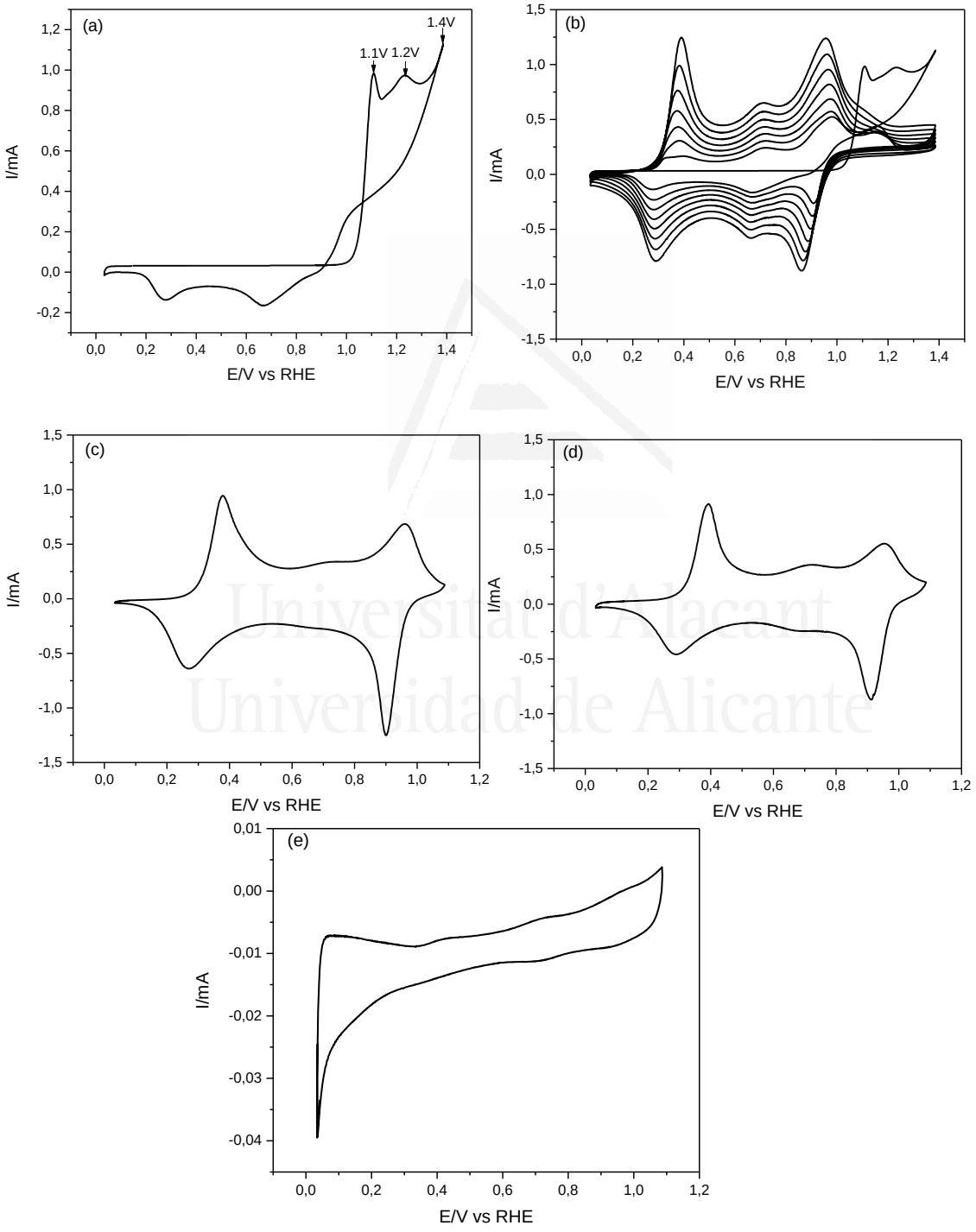

Figure 3.2. (a) Cyclic voltammogram recorded for a Pt electrode in 1M $HClO_4$ aniline (0.3mM) and aminoterephthalic acid (0.7mM) in 3:7 monomer ratio until 1.4V; steady state cyclic voltammograms for the polymeric materials in 1M $HClO_4$ obtained after ten cycles up to 1.2 V(c) and (d) 1.4 V; (e) 1.1 V for the first scan, and at 1 V for the subsequent ones . 50 mV s^{-1}.

3.2 Polymerization of Aniline and Piperazine monomers on Pt electrodes.

3.2.1 Electrochemical Behavior of Piperazine on Pt

Cyclic voltammetry (CV) curves recorded for a polycrystalline platinum electrode immersed in 1 M of $HClO_4$ + 10 mM piperazine solution are illustrated in Figure 3.3. The electrode was immersed at a controlled potential of 0.1 V, and the response was firstly examined in the 0.05–0.5 V potential range (Figure 3.3a). Two oxidation peaks were observed at 0.18 and 0.30 V during the forward scan up to 0.5 V. Both features are related with the electrochemistry of partially blocked adsorption sites at the platinum surface in perchloric medium [22] , which reveals that piperazine strongly adsorbs on this electrode. In a new experiment, the clean electrode was immersed at 0.1 V, and the potential was scanned up to 1.4 V to examine the anodic behavior of piperazine. The onset of oxidation occurs at about 0.5 V, but the electrochemical process appears more clear at potentials higher than, roughly, 1.0 V in the form of a broad current, with no well-defined peaks. The voltammetric profile recorded during the reverse scan does not reach the characteristic shape of a Pt electrode (Figure 3.3b, dashed line). This result indicates that some adsorbed species coming from piperazine oxidation still remain on the electrode surface and block part of Pt adsorption sites. However, as expected, no electropolymerization of piperazine is observed after continuous potential cycling, with the voltammetric profile being almost equivalent to that shown in the solid line of Figure 3.3b.

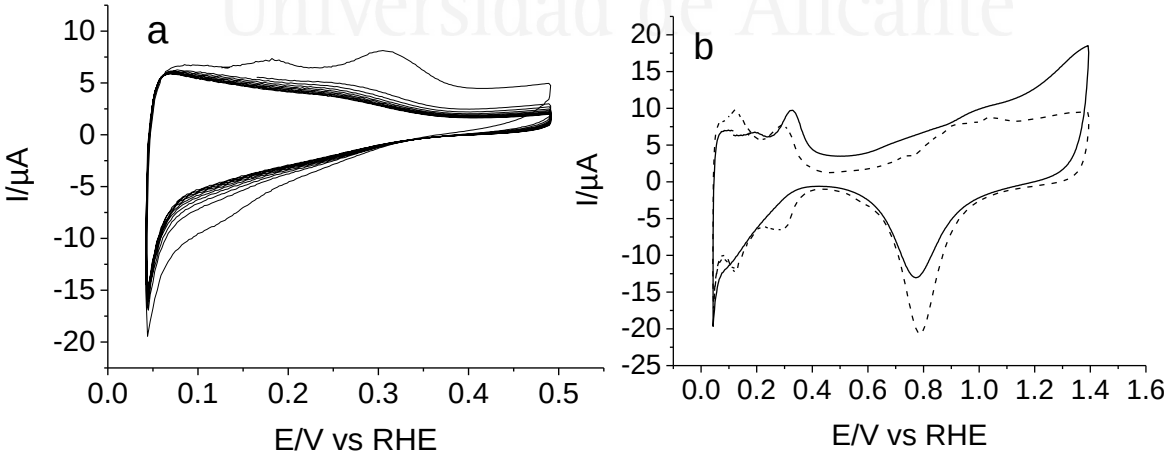

Figure 3.3. Cyclic voltammograms recorded for a Pt electrode in 1 M of $HClO_4$ solution containing 10 mM of piperazine. (**a**) Electrochemical behavior within the potential region 0.05–0.5 V (10 cycles); (**b**) Electrochemical response obtained during the first excursion of up to 1.4 V (solid line), and for clean Pt, in 1 M of $HClO_4$ free of piperazine (dashed line) in the same potential window. v = 50 mV s^{-1} in all cases.

In situ FTIR spectroscopy has been used to increase the understanding of the piperazine oxidation process. Figure 3.4 shows a set of spectra obtained for a Pt electrode immersed in 10 mM of piperazine + 0.1 M $HClO_4$, using D_2O as the solvent. The mirror-polished platinum electrode was transferred to the spectroelectrochemical cell, which was immersed at 0.1 V into the solution, and its surface was pressed against the CaF_2 window. In this case, the concentration of perchloric acid was 0.1 M in order to avoid the damage of the spectroscopic window. The reference spectrum was collected at 0.1 V, and then, the potential was stepped up to 1.4 V to collect several sample spectra. By referring each sample to the unique reference, the information on the redox transformations undergone by the piperazine as a function of the applied potential can be obtained. A positive-going absorption feature appears at 1502 cm^{-1} in the spectrum obtained at 0.4 V, whose intensity rises significantly at higher applied potentials. This means that the species giving rise to this vibrational mode disappears upon oxidation. The frequency of 1502 cm^{-1} is compatible with the $–ND_2^+$ stretching vibration of deuterated piperazine [28], which occurs because of the proton–deuterium exchange equilibrium in D_2O solvent. The electrochemical oxidation of piperazine at higher potential values results in the formation of different carbonyl groups within the piperazine ring, as deduced from the C=O stretching vibrations appearing at around 1570 and 1630 cm^{-1} [23], [24] .

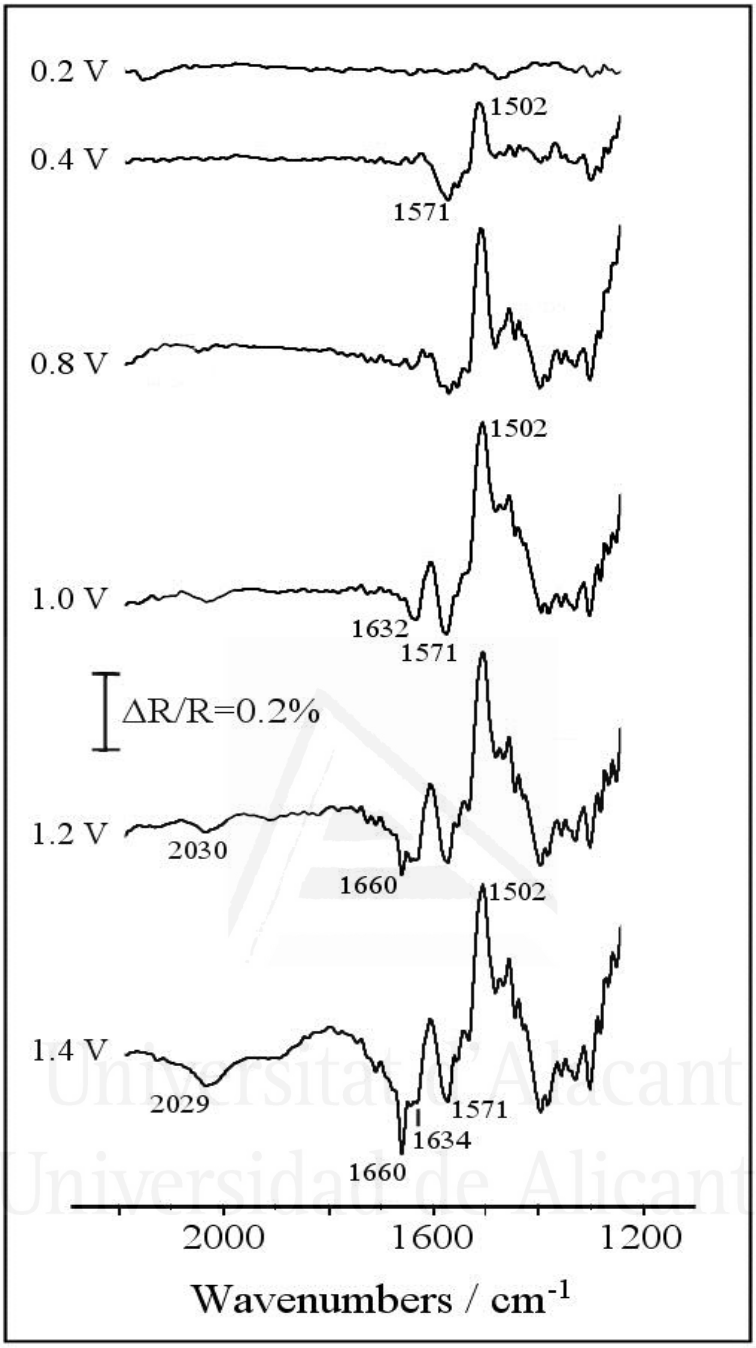

Figure 3.4. Set of in situ Fourier transform infrared (FTIR) spectra collected during the oxidation of 10 mM of piperazine in 0.1 M of $HClO_4/D_2O$ solution. Reference potential: 0.1 V. Sample potential labeled for each spectrum: 100 interferograms at each potential.

Finally, the spectra collected at large anodic potentials display two additional negative bands at 1660 and 2030 cm^{-1}. The former seems related with the occurrence of C=O in amide species, while the frequency of the latter strongly suggests the formation of multiple C-N bonds, probably as

isocyanates [25] . It is known that piperazine N-oxides obtained from the oxidation of piperazine show N-O stretching frequencies at around 1350 cm^{-1} [26] . The presence of this kind of structure cannot be ruled out during the electrochemical oxidation, because the frequency region between 1250 and 1450 cm^{-1} is altered in the spectra of Figure 4 due to the presence of diverse C-N, CH_2, CND, and N-D absorptions. Anyway, from the results presented in this section, it is derived that the electrochemical oxidation of piperazine on Pt electrodes yields some kind of ketopiperazine species at moderate potentials and, at more positive potential values, the ring could open to produce both amide groups and isocyanates.

3.2.2 Electrochemical Copolymerization of Piperazine and Aniline

The results in the previous section strongly suggest that the copolymerization of piperazine with aniline should be carried out using as low a potential as possible, in order to minimize the irreversible oxidation of the former. However, it is known that anilinium cations (which originate at potentials beyond 1.2 V versus RHE) are needed to trigger the deposition of polyaniline-derived polymers. A compromise is then needed between the most favorable polymerization conditions to obtain a little degraded material, and the actual conditions to obtain a deposit. Figure 3.5 shows the experiment carried out to achieve electropolymerization under the established premises. Owing to the higher reactivity of aniline monomer, the copolymerization solution contained a aniline: piperazine relative concentration as low as 0.2 in 1 M of $HClO_4$. The first potential scan was carried out up to 1.3 V to generate an adequate amount of anilinium radicals, while the inversion potential was set at 0.9 V for the subsequent scans to ensure that the piperazine unbroken rings can be incorporated to the growing polymer. The development of new redox processes within the 0.05–0.9 V potential region evidences the growth of an electroactive polymeric species. After 10 potential cycles, the Pt electrode was removed from the solution, and its surface appeared covered by a dark blue film.

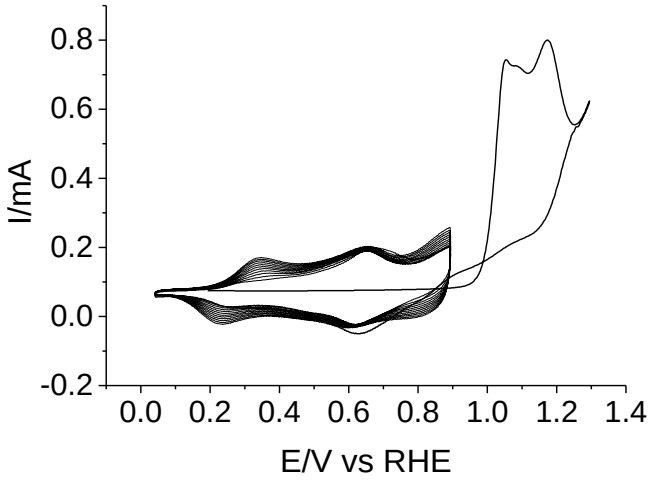

Figure 3.5. Cyclic voltammograms recorded for a Pt electrode during the electrochemical copolymerization of 0.5 M of piperazine and 0.1 M of aniline (PIP/Ani=5) in 1 M of $HClO_4$ solution. The upper potential limit was set at 1.3 V for the first scan, and at 0.9 V for the subsequent ones. v = 50 mV s^{-1}.

The electrochemical behavior of the deposited copolymer was tested in an acidic background solution that was free of any monomer species, and the result is shown in Figure 6 (solid line). CV shows three redox transitions centered at around 0.33, 0.68, and 0.97 V. The first one can be assigned to a leucoemeraldine–emeraldine transformation similar to that of pristine polyaniline. The second one, which is broader and less intense, has been usually interpreted in terms of the presence of different quinoid structures [33, 34]. For the copolymer studied here, the formation of ketopiperazines upon piperazine oxidation at very low anodic potentials (see Figure 4) demonstrates that the deposited material could incorporate a little amount of those previously formed quinoid structures. However, the high relative intensity of the voltammetric wave at 0.68 V strongly suggests a main contribution of active redox centers involving piperazine units which are oxidized *after* they are incorporated to the copolymer chain. Accordingly, the second redox peak may be related to the existence of redox transitions involving hydroxypiperazine ⇌ ketopiperazine species within the copolymer structure [27]. With regard to the pair of redox peaks centered at 0.97 V in the CV of Figure 3.6, they can be clearly related to the emeraldine–pernigraniline transition of the copolymer, which is similar to that undergone by polyaniline under the same experimental conditions (dashed line).

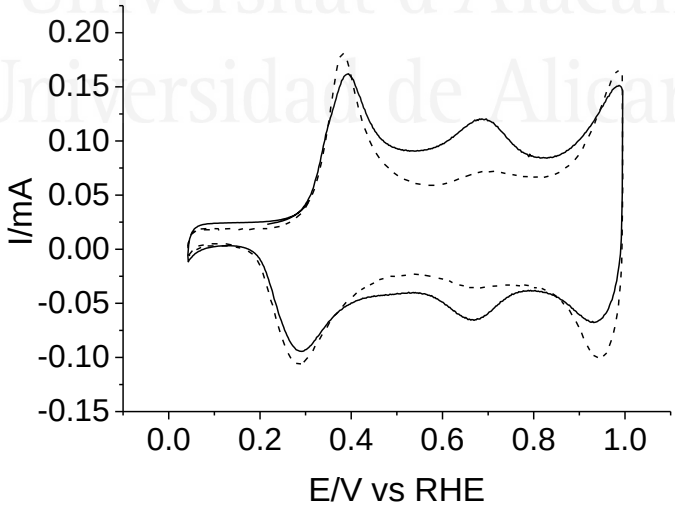

Figure 3.6. Electrochemical response in 1 M of $HClO_4$ medium of a Pt electrode covered with either polyaniline (dashed line) or an aniline–piperazine copolymer (ANI/PIP=0.2)

(solid line), which were deposited under the potential program used in Figure 5. v = 50 mV $s^{-1.}$

In order to monitor the redox behavior of the copolymer and analyze the chemical nature of the species involved in the redox transitions (particularly the existence of a keto-hydroxypiperazine transformation), in situ FTIR spectroscopy experiments were performed for the copolymer. The Pt-modified electrode was transferred to the IR spectroelectrochemical cell, which contained a perchloric acid solution that was free of monomers and prepared with D_2O to facilitate assignments in the 1500–1700 cm^{-1} spectral range. After some potential cycles within the stability window of the copolymer, the Pt surface was pressed against the prismatic CaF_2 window, and a reference spectrum was collected at 0.1 V. Finally, the potential was stepped to higher values to collect sample spectra, and the results are displayed in Figure 3.7. Three main positive bands at 1516, 1436, and 1212 cm^{-1}, and three clear negative bands at 1630, 1580, and 1170 cm^{-1} can be observed together with several features in the 1300–1400 cm^{-1} region. Some of the referred absorptions can be unambiguously assigned to the presence of a polyaniline skeleton. Particularly, the complete disappearance of the leucoemeraldine state at 0.6 V is evidenced by the vanishing of the aromatic C-C stretching mode at 1516 cm^{-1} and of the C-N-C stretching at 1212 cm^{-1} [28], [29] . The formation of oxidized emeraldine (0.6 V) and pernigraniline (1.0 V) structures is also supported by the development of quinoid C=C stretching vibrations at 1580 cm^{-1} [29], [30] , by the -CH in-plane bending at oxidized aniline rings at 1170 cm^{-1}, and, finally, by the generation of several intermediate-order C-N vibrations in the 1300–1400 cm^{1} frequency window [30], [31] . On the other hand, the successful incorporation of piperazine structures to the polyaniline chain is evidenced by two representative bands, which cannot be observed for a pristine polyaniline. These absorptions correspond to the activation of the CH_2 bending upon oxidation (positive-going feature at 1435 cm^{-1} [32] , and to the carbonyl C=O stretching at 1630 cm^{-1}. This latter band supports the voltammetric result in Figure 3.5, and confirms that a significant fraction of piperazine rings are present in the form of electroactive ketopiperazines (C=O ⇌ C-OH). The absence of additional vibrations at around 1660 and 2030 cm^{-1} shows that neither amide structures nor isocyanates are formed and, consequently, that piperazine was not overoxidized during the electropolymerization process under the experimental conditions employed. FTIR assignments are collected in Table 3.1.

Table 3.1. Observed frequencies and proposed assignments for the vibrational bands derived from Figure 3.4 and Figure 3.7.

	Frequency / cm^{-1}		**Suggested Assignment**
	Piperazine (Figure 3.2)	**Copolymer (Figure 3.5)**	
Reduced	1502		$–ND_2^+$ str.
		1212	C-N-C str.
		1436	CH_2 bend.
		1516	C–C str. Aromatic rings
Oxidized	1570-1630	1630	C=O str. Carbonyl
		1170	-CH bend.
		1580	C=C str. Quinoid rings
	1660		C=O str. Amide
	1250-1450	1300-1400	Overlapped bands: C-N (intermediate order) - CND-, N-D, Possible N-O in oxidized piperazine
	2030		C≡N str. Isocyanate

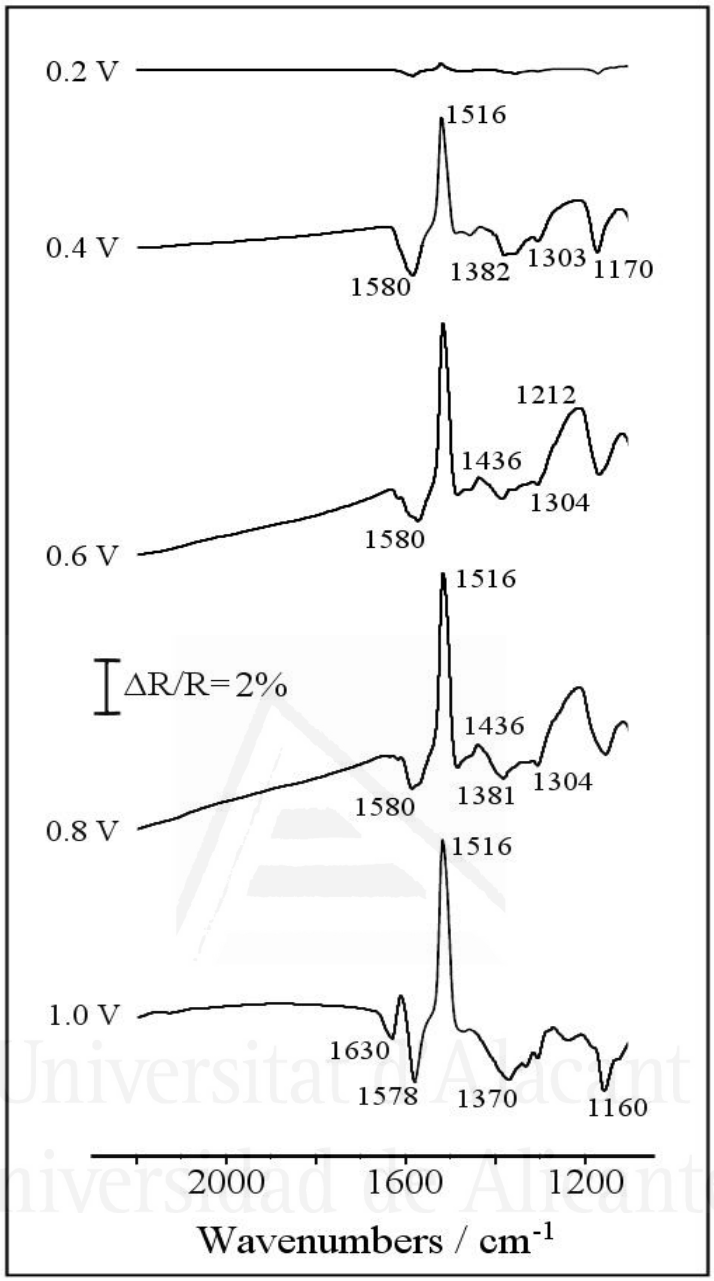

Figure 3.7. Set of in situ FTIR spectra collected during the oxidation of an electrochemically obtained poly(Ani-co-PIP) film in 0.1 M of $HClO_4/D_2O$ test solution. Reference potential 0.1 V. Sample potential labeled for each spectrum: 100 interferograms at each potential.

Additionally, the electrodeposited copolymer was examined by ex situ XPS in order to analyze its surface composition, and also to give support to the chemical structures suggested by in situ FTIR

spectroscopy. A film grown after 10 voltammetric cycles as in Figure 3.5 was rinsed with ultrapure water, dried under nitrogen, stored in a dry place for 24 h, and then analyzed by XPS. Figure 3.8 shows the photoelectronic spectra of C 1s and N 1s core levels. The C 1s signal can be fitted with four peaks at 284.5, 285.4, 286.6, and 288.7 eV. Both the high energy level and the weak intensity of the latter contribution is compatible with the presence of a small amount of carbonyl carbon, which was probably associated to the ketopiperazine centers. On the other hand, there are two major signals that were undoubtedly associated to aromatic carbon, and hence to aniline rings. This is the main peak at 284.6 eV, which was attributed to plain aromatic carbon, and the signal at 285.4 eV, which was due to aromatic carbon bonded to neutral nitrogen. On the other hand, binding energies at around 286.6 eV are characteristic of carbon bonded to positive nitrogen [33], and consequently, this peak is compatible with the presence of piperazine rings within the polymer backbone. The best fit for the N1s spectrum shows only two contributions at 399.6 and 401.6 eV, but unfortunately, it is not possible to distinguish signals coming from the piperazine and aniline environments. The peak at 399.6 eV is clearly attributed to neutral nitrogen, but it could be associated to any of the amine, imine or even amide groups, as these species do not show significantly different chemical shifts. In the same way, the higher binding energy signal at 401.6 eV is compatible with the presence of piperazine within the material. That peak is assigned to positively charged nitrogen atoms resulting from the protonation of imine centers (located exclusively at aniline rings) and secondary amine positions (at both piperazine and aniline rings) [33] .

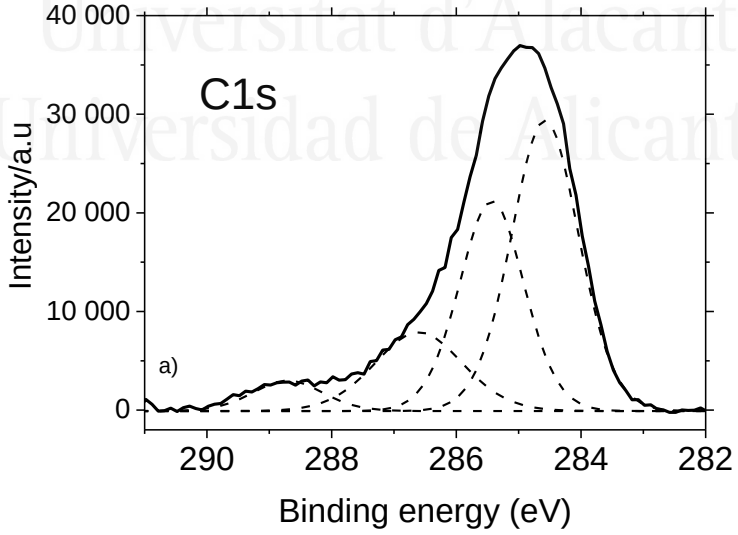

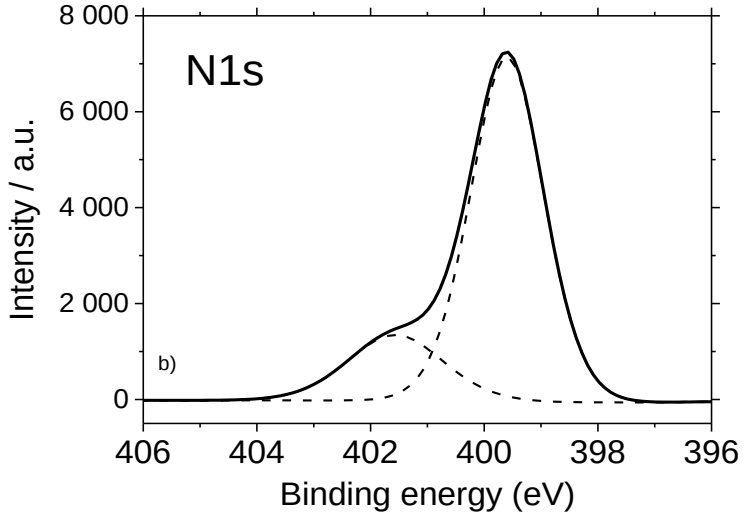

Figure 3.8. Deconvoluted (**a**) C 1s and (**b**) N 1s X-ray photoelectron spectroscopy (XPS) core-level spectra of an electrodeposited aniline–piperazine copolymer. The sample was obtained as in Figure 5.

Chemically obtained polyanilines are usually amorphous solids, but more or less ordered structures can also be obtained depending on the synthesis conditions [34] . In general, better ordering is observed for electrochemically-prepared thin films [35] . The surface morphology of the aniline–piperazine copolymer electrodeposited on platinum after 10 cycles has been examined by SEM. The top image in Figure 3.9 shows how this organic coating is completely distributed over the surface in the form of flat ribbon strings with a width of about 3–5 μm. These structures are quite different from those detected for unmodified polyaniline deposited on Pt under similar experimental conditions, for which a uniformly distributed, smooth film is obtained (Figure 3.9b). According to these observations, the presence of a significant amount of piperazine units is seen at the origin of the particular morphologic features shown by the copolymer material.

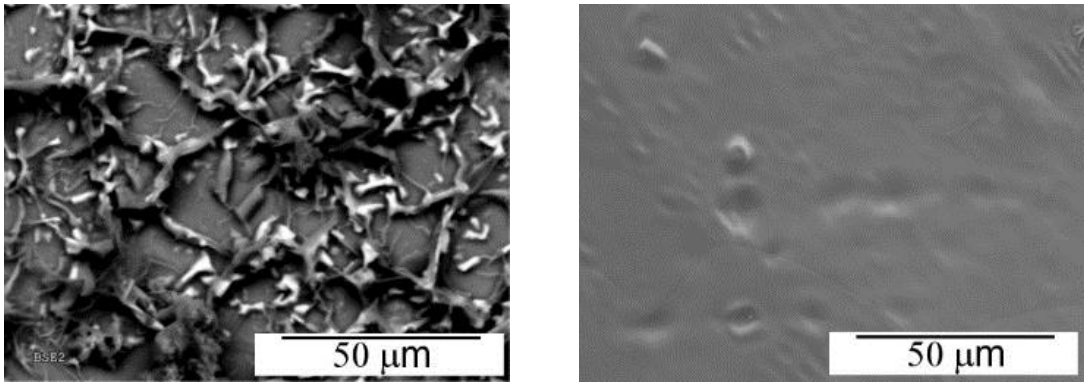

(a) **(b)**

Figure 3.9. Scanning electron micrographs at 1000× magnification of copolymer (**a**) and polyaniline (**b**) deposited under the same experimental conditions.

3.2.3 Effect of polymerization potential

Figure 3.10a shows the voltamogram during the oxidation in solution of both monomers with a monomer ratio of 5. Two clear oxidation peaks are observed in the positive potential scan, the arrows indicate the potentials used for the copolymerization. In other to understand in this point, the aniline-Piperazine copolymers were deposited using four different upper potential limits 1.2 V; 1.3V; 1.4 V and 1.1 V for the first scan and 0.9 V for the subsequent ones. The lower potential value corresponds to the beginning of the oxidation reported for the results of the previous section (In situ FTIR spectroscopy) strongly suggest that the copolymerization of Piperazine with aniline should be carried out using as little potential as possible, in order to minimize the irreversible oxidation of the former. However, it is known that anilinium cations (which originate at potentials beyond 1.2 V versus RHE) are necessary to trigger the deposition of polymers derived from polyaniline. Figure 3.10a shows the first forward scan for a Pt in a monomer ratio of 5 (0.5M: 0.1M). There, arrows designate the four upper potentials limits used to achieve electropolymerization. The electrochemical behavior of the deposited copolymers was tested in an acidic background solution during the electrochemical copolymerization of aniline and Piperazine in a monomer ratio of 5, the result is shown in Figure 3.10.b we can be observed that the electrochemical behavior of the copolymers strongly affected by the higher inversion potential used during synthesis. Equilibrium electrochemical response of deposited copolymers after ten voltametric cycles at each potential limit in 1M $HClO_4$; the background solution is shown in Figure 3.10b. It is observed in this figure that the cyclic voltammograms of the copolymer materials show three redox transitions, regardless of the upper potential limit used during the polymerization. The first, at about 0.3-0.5 V, the second, broader and less intense, has generally been interpreted in terms of the presence of different quinoid structures [36], [37] , and the last one, centered near 0,97 V, are clearly attributed to leucoemeraldine-

emeraldine and emeraldine-pernigraniline transformations, respectively. The potential of the average peak agrees well with those usually attributed to the presence of crosslinked or overoxidized sites in polyaniline chains, which are favored when the aniline is copolymerized with other aromatic amines [20][21]. The voltametric profiles of Figure 3.10b also show that the amount of material deposited on the surface of the electrode is significantly higher when the electropolymerization potential limit is higher than 1.3V.

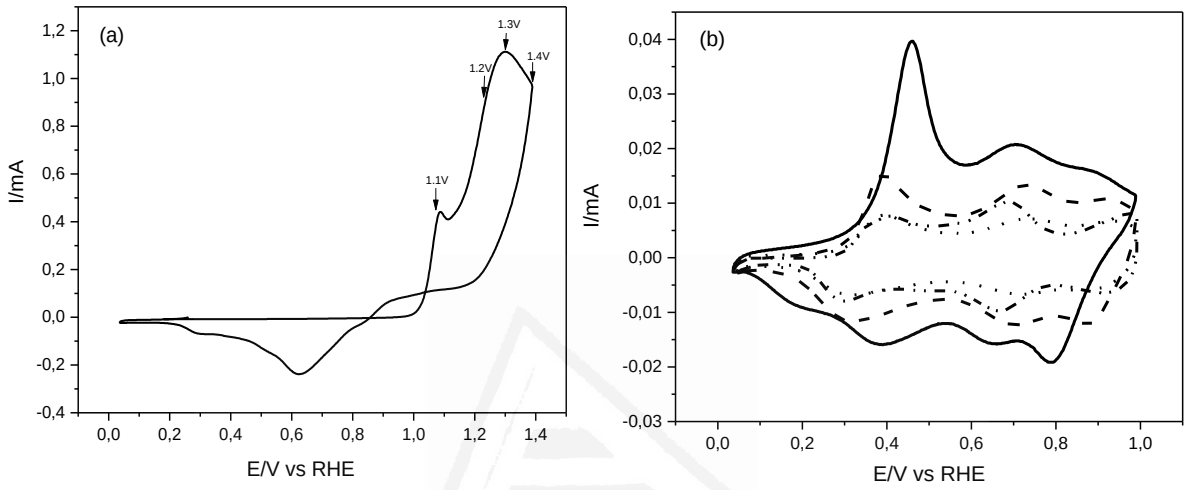

Figure 3.10. (a) First forward scan recorded for a Pt electrode during the electrochemical copolymerization of aniline and Piperazine in monomer ratio of 5; (b) Steady state cyclic voltammograms for the polymeric materials obtained after ten cycles up to the potential marked in: 1.4 V (solid line); 1.3 V (dashed line) 1.2 V (dotted line); and 1.1 V for the first scan, and at 0.9 V for the subsequent ones (dashed-dotted line). Background electrolyte 1M $HClO_4$ and scan rate 50 mV s^{-1} in all cases.

Additionally, the electrodeposited copolymer was examined during the electrochemical copolymerization of aniline and Piperazine in a monomer ratio of 0.5M: 0.5M (Ani/PIP=1). The result is shown in Figure 3.11. In this case, three oxidation peaks appear in the voltammograms (Figure 3.11a) at 1V; 1.12 V; 1.2V, the oxidation peak at 1.12V could be associated to the oxidation of Piperazine as a consequence of the increase in concentration (Figure 3.5). Figure 3.11a shows the voltammograms obtained and the arrows designate the three upper potential limits used 1.2 V; 1.3V; 1.4 V and 1.3 V for the first scan and 0.9 V for the subsequent ones to achieve the electropolymerization. The steady state voltammograms of the copolymers after ten voltammetric cycles are shown in Figure 3.11b. It is observed in this figure that the cyclic voltammograms of the

copolymer materials show differences with respect the obtained in a monomer ratio of 5, three redox transitions similar to the previous contribution but the relative currents are different. Again the amount of polymer increases with the positive potential (Figure 3.10b), moreover, the ratio Ani:PIP has an important influence in the voltammetric profile and the amount of polymer obtained.

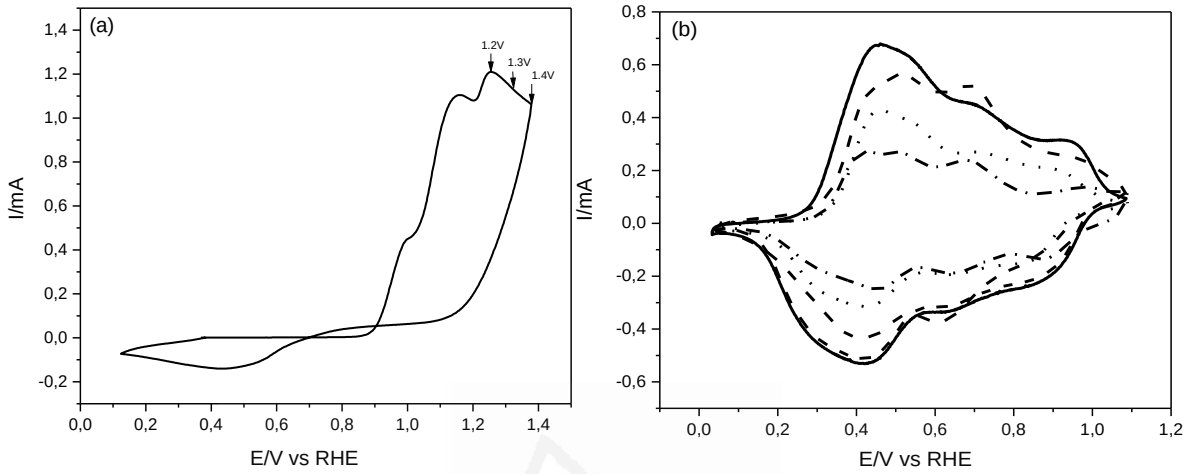

Figure 3.11. (a) First forward scan recorded for a Pt electrode during the electrochemical copolymerization of aniline and Piperazine in 0.5M: 0.5M monomer ratio (PIP/Ani=1); (b) Steady state cyclic voltammograms for the polymeric materials obtained after ten cycles up to the potential marked in: 1.3 V (solid line); 1.4 V (dashed line) 1.2 V (dotted line); and 1.3 V for the first scan, and at 0.9 V for the subsequent ones (dashed-dotted line). Background electrolyte 1M $HClO_4$ and scan rate 50 mV s−1 in all cases.

3.2.4 Effect of method of polymerization and monomer ratio.

The electrochemical behavior of the deposited copolymer was tested in an acidic background solution during the electrochemical copolymerization of aniline and piperazine at different monomer ratios 0.5M: 0.5M (PIP/Ani=1); 0.5M: 0.17M (PIP/Ani =3); 0.5M: 0.1M (PIP/Ani =5). In these conditions, the method of polymerization has been studied, and two procedures have been used: i) the limit potential is 1.3 V for the first scan, and at 0.9 V for the subsequent ones and ii) the limit potential is maintained at 1.3V for the ten cycles. The results are shown in Figure 3.12. The amount of electrochemical deposition of copolymers are strongly affected by the method of polymerization and the potential limit. The shape of cyclic voltammograms response of deposited copolymers after ten voltammetric cycles at 1.3V are very similar; however, the charge in the voltammograms is very different. Then, it can be deduced that the amount of material deposited on the surface of the electrode is considerably higher when the electrochemical copolymerization of aniline and piperazine is carried

out at 1.3 V (method ii). ; and when maintaining the potential for the first scan at 1.3 V and change it to 0.9 V for the subsequent ones; the first potential scan was carried out up to 1.3 V to generate an adequate amount of anilinium radicals, while the inversion potential was set at 0.9 V for the subsequent scans to ensure that the piperazine unbroken rings can be incorporated to the growing polymer. Figure 12 shows that this fact is observed for all the monomers ratios being the amount of polymer deposited for the higher monomer ratio (ANI/PIP=1) as it can be explained considering that when the aniline concentration is higher the formation of the copolymer is easily.

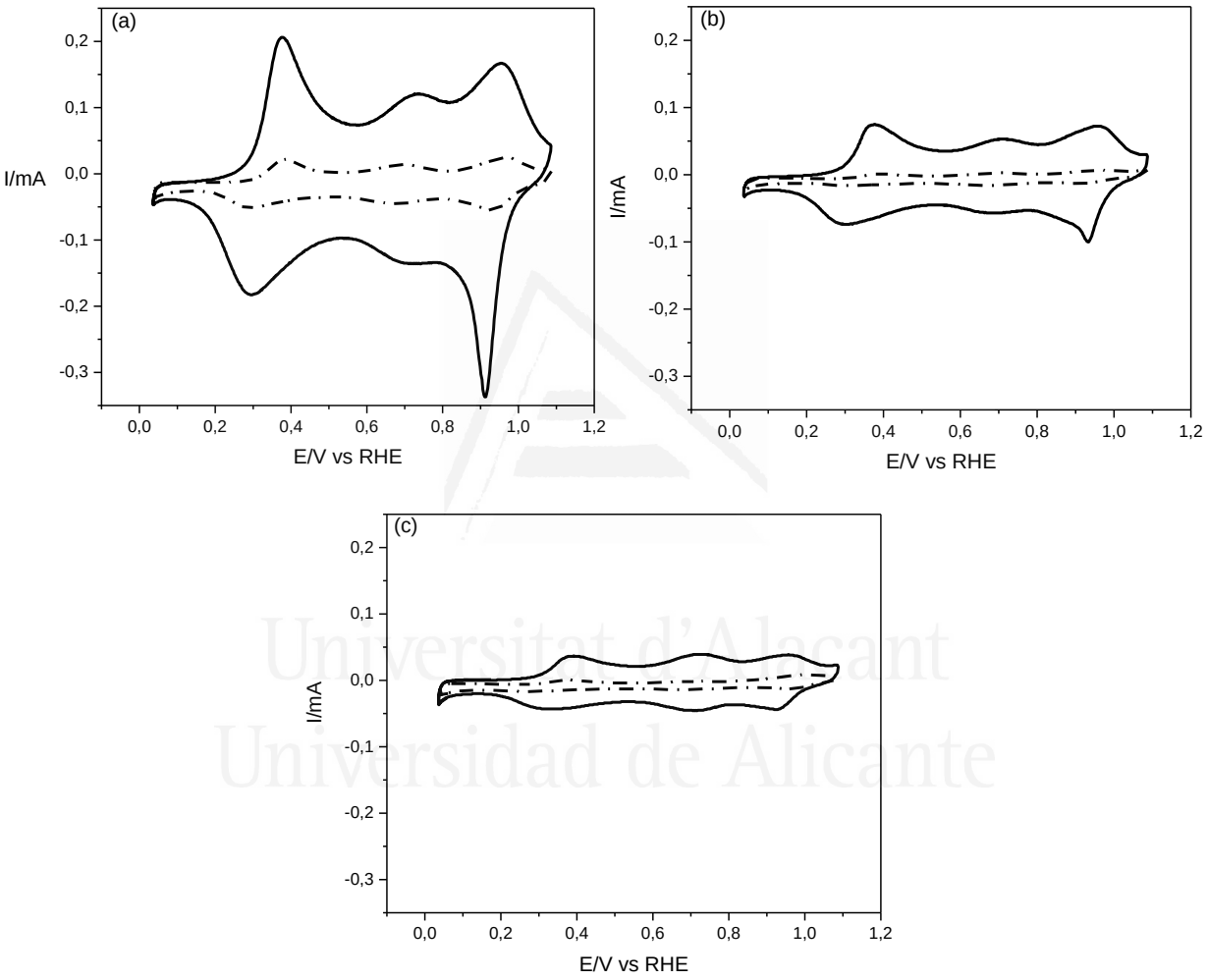

Figure 3.12. Steady state cyclic voltammograms for the poly(Ani-co-PIP) obtained after ten cycles at different molar ratios with variation of the potential (a) 0.5 M: 0.5 M piperazine and aniline at 1.3V (solid line); and 1.3 V for the first scan, and at 0.9 V for the subsequent ones (dashed-dotted line); (b) 0.5 M: 0.17 M piperazine and aniline; (c) 0.5 M: 0.1 M piperazine and aniline. Background electrolyte 1M $HClO_4$ and scan rate 50 mV s^{-1} in all cases.

In the analysis of the monomeric species, the decreasing study of the molar ratio and the effect of the potential on the copolymer formed from aniline and the Piperazine monomers are similar. Then, the study of the increasing of molar ratio (PIP/Ani) from 1 to 5 at different potentials 1.2V; 1.3V and 1.4V; the results are shown in Figure 3.13 have been performed in this section. Figure 3.13a for molar ratio 1 shows a better performance compared to the other two molar ratios 3 and 5 Figure 3.13b and c . When the monomer ratio is higher, the concentration of piperazine is also higher producing an increase in the oxidation current and the voltammetric charge decreases when the molar ratio decreases. Figure 3.14 shows the evolution of the oxidation peak current of the first redox process observed in the voltammogram with the polymerization potential limit and the monomer ratio (PIP/Ani). It can be observed that the peak current increases with the potential and the monomer ratio.

In the poly(Ani-co-PIP), there is a distribution as a function of the length of the chain, as well as according to the chemical composition; a general theory that encompasses the problem of the resulting distributions has been formulated by W.H. Stockmayer [38]. It becomes important now that the experimental methods are under development [39]; but in our case we study only the experimental side of our copolymerization rather than checking the theoretical distributions of the copolymer. This study contains many hypotheses without sufficient evidence, and the discussion is based on our electrochemical results and literature data. The main challenge of the copolymerization of our monomers is used in this work with the presence of a large amount of piperazine. However, we believe that our efforts can broaden the understanding of the main concentration patterns of polyaniline in the presence of piperazine with a higher conductivity and further develop in the field of science.

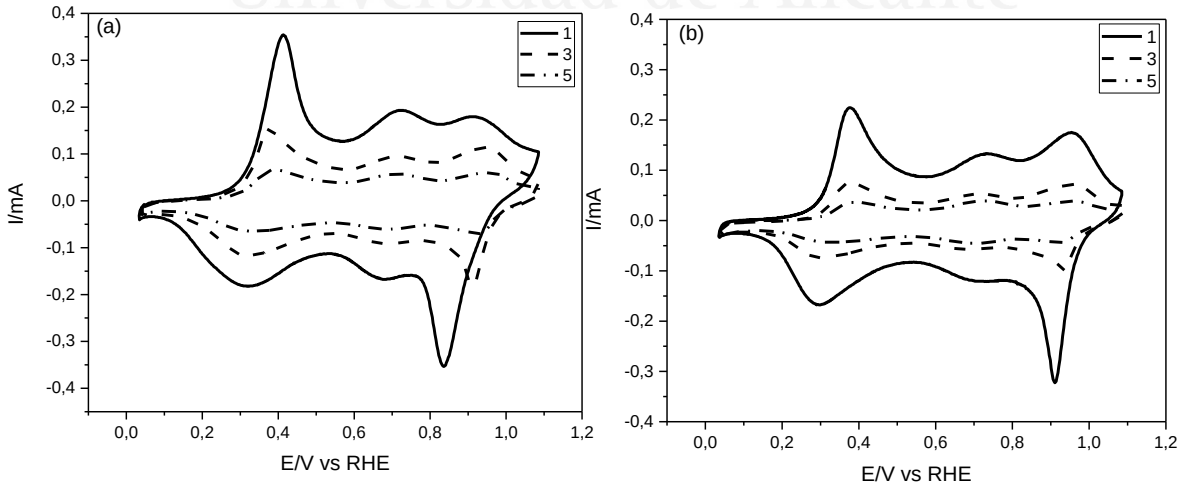

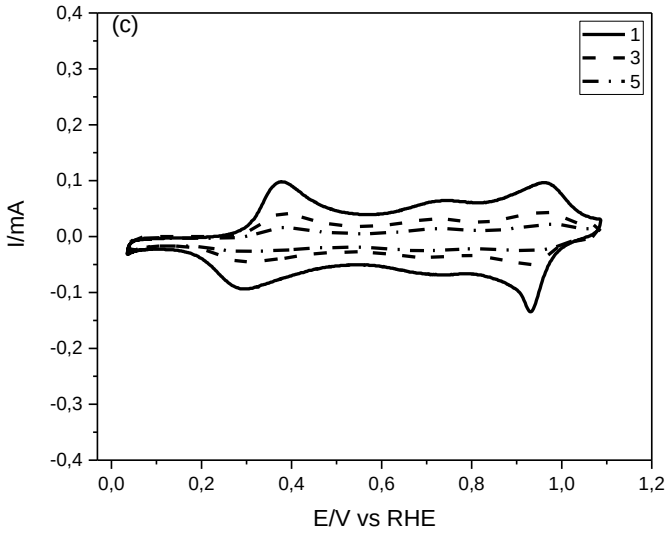

Figure 3.13. Steady state cyclic voltammograms for the poly(Ani-co-PIP) obtained after ten cycles at different monomers ratio variation by maintaining the potential (a) PIP/Ani =1 (solid line); PIP/Ani =3(dashed line) and PIP/Ani =5 (dashed-dotted line) at 1.4V; (b) the same previous monomers ratio at 1.3V;(c) at 1.2V.Background electrolyte 1M $HClO_4$ and scan rate 50 mV s^{-1} in all cases.

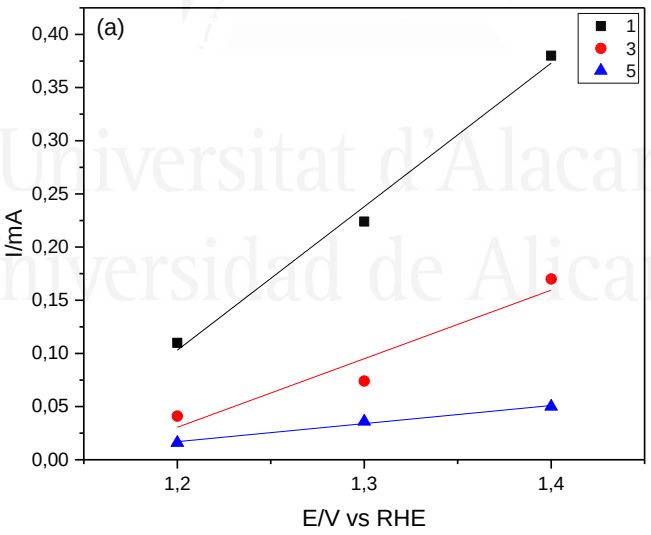

Figure 3.14. Oxidation peak currents recorded for a Pt electrode covered with poly(Ani-co-PIP)-X copolymers in 1 M of $HClO_4$ aqueous solutions versus the polymerization potential and the monomer ratio (X).

3.3 Oxidation of ascorbic acid and dopamine

Platinum electrodes coated with the copolymers synthetized in this PhD Thesis have been successfully employed to determine ascorbic acid (AA) and dopamine (DA) in synthetic samples. The following sections show the electrochemical behavior of the different copolymers in presence of ascorbic acid and dopamine in the solution.

3.3.1 Oxidation of ascorbic acid on polyaniline-modified Pt electrode

In order to compare the different copolymers for thus application the behaviour of polyaniline has been studied in the oxidation of ascorbic acid and dopamine in the same synthesis conditions. Pani is the most popularly used conducting polymer in electrochemical sensors attributed to its excellent electrocatalytic ability, conductivity, easy synthesis, high environmental stability and thermal stability [40].Ascorbic acid (AA) is a significant vitamin required for human diet and usually its concentration in extra cellular fluids is much higher (about 1000 times) than that of Dopamine (DA) [41][42]. Several modified electrodes based on nanomaterial [43], conducting polymers [1][44], metal nanoparticles [45] and metal oxides [46][47] were developed; however not all of them are ideal modifiers [48]. Figure 3.15a shows the oxidation of AA at different concentration on polyaniline obtained at 1.2V. It can be observed that the oxidation peak of AA at 0.79V increase with the concentration which is a value slightly below that usually obtained for bare Pt surfaces under similar experimental conditions [49], [50]. Figure 3.15b shows the plot of the current with the concentration of AA for two polyanilines prepared at 1.2V and 1.4V. The slopes of oxidation Peak currents containing an increasing concentration of AA from 3 mM to 30 mM show a good linearity (Figure 3.15b). From that plot, it can be derived that the polyaniline demonstrates quite a sensitive response, within the range of concentrations studied. A similar electrocatalytic effect can be observed for Pani prepared at 1.4V, in which the sensitivity is lower than the obtained with a Pani obtained at 1.2V. The oxidation peak currents are linearly increased as the concentrations of AA, the linear range is 3–30 mM for the two polyanilines and the sensitivity is defined by the respective slopes (22.78 ± 0.07and 13.27 ± 0.06) for PANI prepared 1.2V and 1.4V respectively (Table 3.3). The square of the correlation coefficient are shown in (Figure 15b) $R^2 = 0.99$; $R^2 = 0.97$ obtained at 1.2V and 1.4V respectively. It can be observed that the higher sensitivity is obtained with the Pani synthesized at 1.2V.

Table 3.3. *Sensitivity comparison of AA oxidation obtained with Pani prepared at different potential*

Copolymer	**Sensitivity (µA /mM)**
Pani 1.2V	22.78 ± 0.07
Pani 1.4V	13.27 ± 0.06

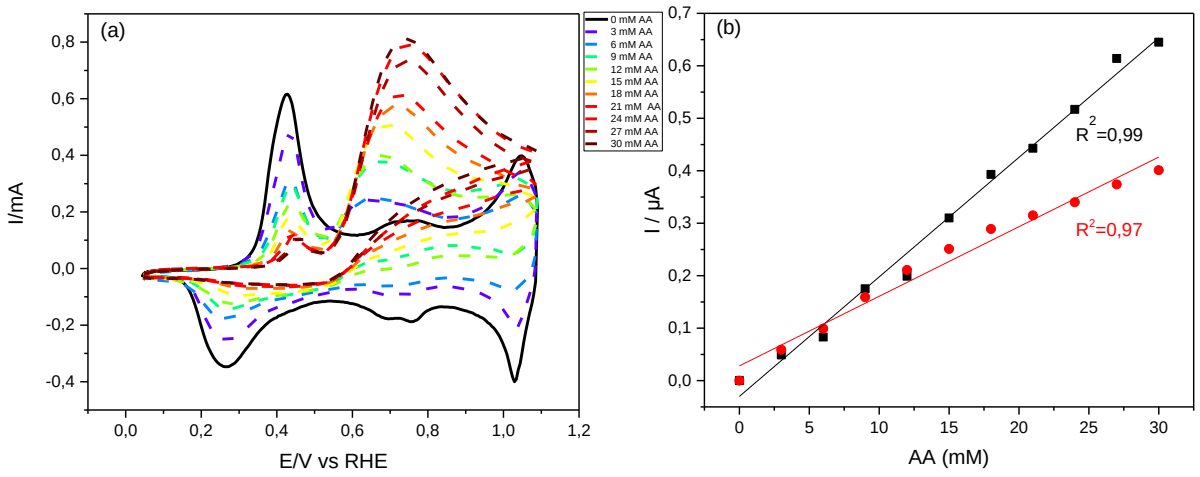

Figure 3.15 (a) cyclic voltammograms recorded during AA oxidation using a Pt electrode covered with Pani prepared in 1 M of $HClO_4$ at 1.2V. AA concentration range from 3 to 30 mM. (b) Calibration curves obtained with a Pt electrode covered with Pani obtained at 1.2V (black) and at 1.4V (red). v= 50 mV s^{-1} in all cases.

3.3.2 Oxidation of ascorbic acid on poly(Ani-co-ATA) deposited on Pt.

Platinum electrodes coated with copolymer formed from 2ATA and Ani (poly(Ani-co-ATA)) films have been employed to determine AA in synthetic samples. The sensitivity of the measurement and the catalytic performance of the copolymer have been evaluated in acidic medium. Figure 3.16a shows the cyclic voltammograms recorded with a Pt electrode covered with the copolymer and AA samples were prepared within a concentration range from 3 to 30 mM. the oxidation current appears at 0.85 V. This anodic peak potential is nearly the same as that reported in the literature for bare Pt electrodes in acidic medium [59,60] but higher than that one obtained with Pani. Figure 3.16b shows the oxidation current of ascorbic acid for two copolymers poly(Ani-co-ATA) synthesized at two potential limits (1.2V and 1.4V). The oxidation current increases linearly with analyte concentration for both copolymers. From that plot, it can be derived that the copolymer demonstrates quite a sensitive response. The linear range is between 3 and 30 mM and the sensitivity is defined by the respective slopes (Table 3.4). And the correlation coefficient are shown in (Figure 3.16b) being R^2 = 0.996; R^2 = 0.99 4 at 1.2V and 1.4V, respectively. In that case, the sensitivity is very similar; however, it is higher for the copolymers obtained at 1.2V as in the case of Pani.

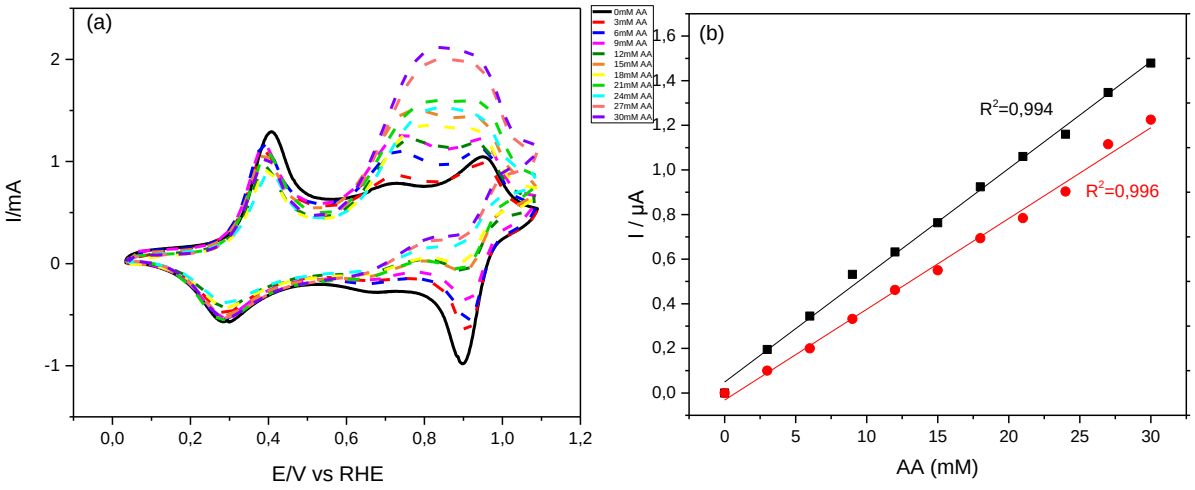

Figure 3.16 (a) cyclic voltammograms recorded during AA oxidation using a Pt electrode covered with poly(Ani-co-ATA) prepared in 1 M of $HClO_4$ at 1.4V. AA concentration range from 3 to 30 mM. (b) Calibration curves obtained with a Pt electrode covered with Pani obtained at 1.2V (red) and at 1.4V (black). v= 50 mV s^{-1} in all cases.

Table 3.4. *Sensitivity comparison of AA oxidation obtained with poly(Ani-co-ATA) obtained at different potential.*

Copolymer	Sensitivity (µA /mM)
Poly(Ani-co-ATA) 1.2V	47.87 ± 0.08
Poly(Ani-co-ATA) 1.4V	40.700 ± 0.001

3.3.3 Oxidation of ascorbic acid on poly(Ani-co-PIP) deposited on Pt.

Platinum electrodes coated with copolymer formed from piperazine and Ani (poly(Ani-co-PIP)) films have been employed to determine AA in synthetic samples. The sensitivity of the measurement and the catalytic performance of the copolymer have been evaluated in acidic medium. Cyclic voltammograms recorded at increasing concentration of AA in acidic solution are shown in Figure 3.17a for the copolymer piperazine and Ani. The oxidation of ascorbic acid starts at about 0.6 V and produces a first anodic peak centered at 0.89 V whose intensity increases linearly at increasing analyte concentrations, the copolymer demonstrates a quite sensitive response. Figure 3.17a shows cyclic voltammograms recorded with a Pt electrode covered with the copolymer poly(Ani-co-PIP) and AA samples were prepared within a concentration range from 3 to 30 mM. Figure 3.17b shows

how the oxidation current of ascorbic acid increases linearly with analyte concentration. According to this plot, it can be derived that the copolymer demonstrates quite a sensitive response. Figure 3.17b shows the calibration curves for a Pt electrode covered with copolymers obtained at 1.2V and 1.4V. The sensitivity is defined by the respective slopes (obtining 20.38 ± 0.07 and 9.87 ± 0.02 for the poly(Ani-co-PIP) respectively) (Table 3.5). And the correlation coeficient is shown in Figure 3.17b, R^2 = 0.988; R^2 = 0.994 obtained at 1.2V and 1.4V respectively.

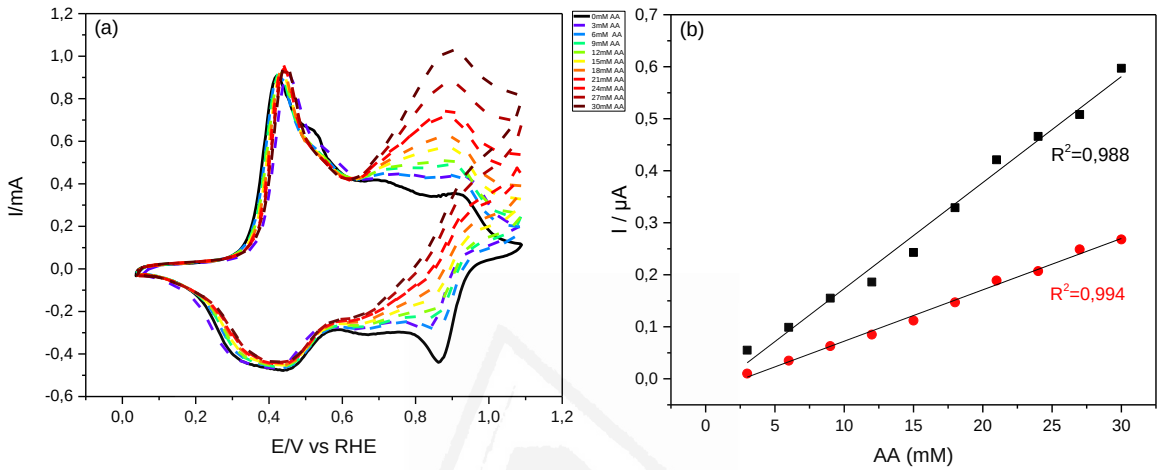

Figure.17 (a) cyclic voltammograms recorded during AA oxidation using a Pt electrode covered with poly(Ani-co-PIP) prepared in 1 M of $HClO_4$ at 1.2V. AA concentration range from 3 to 30 mM. (b) Calibration curves obtained with a Pt electrode covered with Pani obtained at 1.2V (black) and at 1.4V (red). v= 50 mV s^{-1} in all cases.

Table 3.5. *Sensitivity comparison of AA oxidation obtained with poly(Ani-co-PIP) obtained at different potential.*

Copolymer	Sensitivity (µA /mM)
Poly(Ani-co-PIP) 1.2V	20.38 ± 0.07
Poly(Ani-co-PIP) 1.4V	9.87± 0.02

3.3.4 Sensitivity comparison between Pani, poly(Ani-co-ATA) and poly(Ani-co-PIP)

In all cases, the sensitivity is higher for the polymer (Pani and copolymers (poly(Ani-co-ATA) and poly(Ani-co-PIP)) obtained at 1.2 V, for this reason the sensitivity comparison has been done with the polymers obtained at this potential. Figure 3.18 shows the calibration curves for the different polymers obtained at 1.2V. It should be noted that the value for the poly(Ani-co-ATA) is higher than the obtained with the others polymers. This can be consequence of the interaction between the AA molecule and the carboxylic groups which are deprotonated at this pH.

Table 3.6 shows the comparison of different modified electrodes for AA determination. It can be observed that the values of sensitivity obtained is very high in comparison with other materials; however the linear range of concentration is high.

Table 3.6: Comparison of sensitivity and linear range, of different polymers for determination of AA.

Electrode	AA linear range (μM)	Sensitivity (μA μM^{-1})	Refs
Polyaniline-GO[h a]	25–200	0.92	[51]
PtNP-MWCNT/GCE[b]	0.22 – 2.2	0,017	[52]
MgB_2-MWCNT[c]	200- 1000	76.6	[53]
Pani-MnO_2[d]	0 - 60	0.026	[54]
GNP/AgNR/poly (AY) NC[e]	1–200	0.88	[55]
GCE/fMWCNT/AuNP@PDDA/P[16–f]	0,005-0,075	0,064	[56]
PVP/CPE[g]	0.01-0.75	14.1	[57]
PAMAM/PNB[h]	0.17 – 1826	0.29	[58]
Pani	3000-30000	22.78	This work
poly(Ani-co-ATA)	3000-30000	47.87	This work
poly(Ani-co-PIP)	3000-30000	20.38	This work

[a]Polyaniline-GO: polyaniline-graphene oxide

[b]Platinum nanoparticles-multiwall carbon nanotubes/glassy carbon electrode.

[c]Magnesium boride-multi-walled carbon nanotube.

[d]Polyaniline- Manganese dioxide hybrid nanowires.

[e]Graphene nanoplatelets-silver nanorods/poly (4-amino-1-1 -azobenzene-3, 4 -disulfonic acid dye) (acid yellow 9, poly (AY)).

[f]Multiwall carbon nanotubes (fMWCNT), PDDAstabilized gold nanoparticles (AuNP@PDDA), and DNA bioinspired polyanions (P^{16-}).

[g]PVP/CPE: Polyvinylpyrrolidone/carbon paste electrode;

[h]PAMAM/PNB: poly(amido amine) dendrimer/ poly(Nile blue)-modified electrode

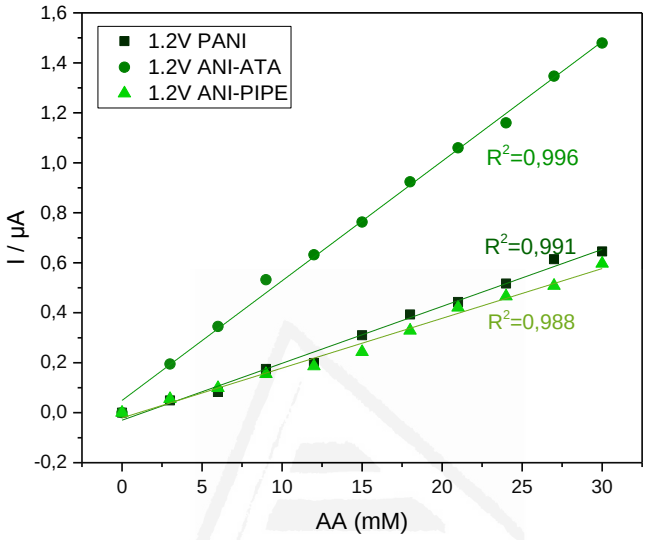

Figure 3.18 Calibration curves for the different polymers obtained at 1.2V.

3.3.5 Oxidation of dopamine on polyaniline-modified Pt electrode .

DA is one of the key neurotransmitter in mammalian central nervous systems which facilities communication between brain and neurons [59]–[61]. Therefore, sensitive determination of DA is important in clinical analysis [62]–[64]. Platinum electrodes coated with Pani have been employed to determine DA, the sensitivity and the catalytic performance of the polymer have been evaluated in acidic medium. The First, DA samples were prepared within a concentration range from 0.2 to 3.0 mM. Figure 3.19a shows the oxidation of DA at different concentration on polyaniline obtained at 1.2V for electrochemical sensing of these compounds. It can be observed that the oxidation peak of DA appears at 0.85V and its intensity increases with the DA concentration. During the negative scan, a reduction peak at around 0.7 V. Then, the oxidation peak at 0.85V corresponds to the oxidation of DA to dopaminequinone. The reduction peak of dopaminequinone to DA is observed at 0.7 V during the reverse scan. These values of peak potentials are slightly below that usually obtained for bare Pt surfaces under similar experimental conditions [49][50]. Figure 3.19b shows the calibration curve obtained for peak oxidation current with the concentration of DA for the two polyanilines prepared at 1.2V and 1.4V. It can be derived that the Pani demonstrates quite a sensitive response, within the

range of concentrations studied. The oxidation peak currents are linearly increased as the concentrations of DA, the linear range is 0.2-3.0 mM for the two polyanilines and the sensitivity is defined by the respective slopes (58, 94 ± 0.02and 89, 32 ± 0.02) for those potential 1.2V and 1.4V the results are shown in Table 3.7. And the correlation coefficients are shown in Figure 3.19.b, being R^2 = 0.98; R^2 = 0.99 at 1.2V and 1.4V, respectively. It can be observed that the higher sensitivity is obtained with the Pani synthesized at 1.4V.

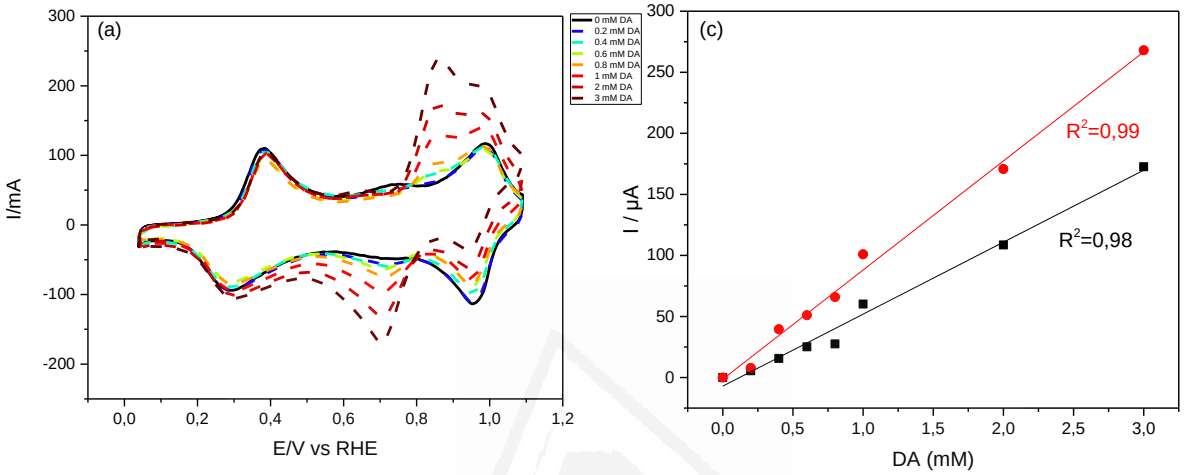

Figure 3.19 a) cyclic voltammograms recorded during DA oxidation using a Pt electrode covered with Pani prepared in 1 M of $HClO_4$ at 1.2V. DA concentration range from 0.2 to 3 mM. (b) Calibration curves obtained with a Pt electrode covered with Pani obtained at 1.2V (black) and at 1.4V (red). 1 M $HClO_4$, v= 50 mV s^{-1} in all cases.

Table 7. *Sensitivity comparison of DA oxidation obtained with Pani obtained at different potential.*

Polymer	Sensitivity (µA /mM)
Pani 1.2V	58.94 ± 0.02
Pani 1.4V	89.32 ± 0.02

3.3.6 Oxidation of dopamine on poly(Ani-co-ATA) deposited on Pt

Platinum electrodes coated with copolymer formed from 2ATA and Ani monomers (poly(Ani-co-ATA) films have been employed to determine DA in synthetic samples. The sensitivity of the measurement and the catalytic performance of the copolymer have been evaluated in acidic medium. Figure 3.20a shows the cyclic voltammograms recorded with a Pt electrode covered with poly(Ani-

co-ATA). The DA concentration is within a concentration range from 0.2 to 3.0 mM. The anodic peak at 0.84V appears at nearly the same potential that reported in the literature for bare Pt electrodes in acidic medium [65] [66], and it is similar to that obtained with Pani. The reduction peak of dopaminequinone to DA is also observed during the reverse scan. Figure 3.20b shows the oxidation current of dopamine for two copolymers synthesized at two potential limits (1.2V and 1.4V). The current peak increases linearly with DA concentration. From that plot, it can be derived that the poly(Ani-co-ATA) demonstrates quite a sensitive response. The linear range is 0.2–3.0 mM and the sensitivity is defined by the respective slopes for both synthesized potentials, 1.2V and 1.4V respectively (Table 3.8). The correlation coefficient is shown in Figure 3.20b, being R^2 = 0.986; R^2 = 0.985 at 1.2V and 1.4V respectively. In that case, the sensitivity is similar; however, the values is higher for the poly(Ani-co-ATA) obtained at 1.4V as in the case of Pani (Table 3.7).

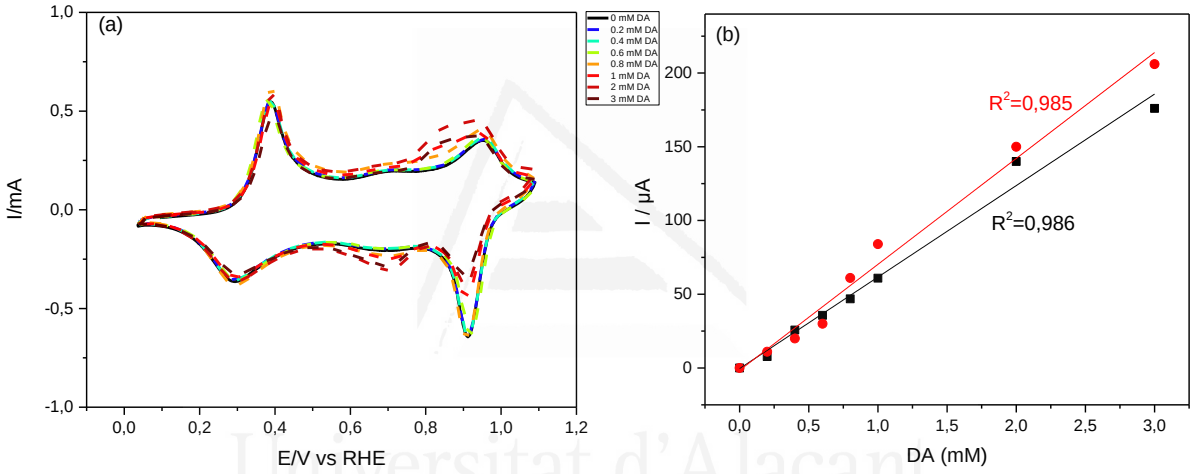

Figure 3.20 (a) cyclic voltammograms recorded during DA oxidation using a Pt electrode covered with poly(Ani-co-ATA) prepared in 1 M of $HClO_4$ at 1.4V. DA concentration range from 0.2 to 3 mM. (b) Calibration curves obtained with a Pt electrode covered with poly(Ani-co-ATA) obtained at 1.2V (black) and at 1.4V (red). 1 M $HClO_4$, v= 50 mV s^{-1} in all cases.

Table 3.8. *Sensitivity comparison of DA oxidation obtained with* poly(Ani-co-ATA) *obtained at different potential.*

Copolymer	**Sensitivity (µA /mM)**
poly(Ani-co-ATA) *1.2V*	62.04 ± 0.02
poly(Ani-co-ATA) *1.4V*	71.80± 0.03

3.3.7 Oxidation of dopamine on poly(Ani-co-PIP) deposited on Pt.

Platinum electrodes coated with copolymer poly(Ani-co-PIP) have been studied for the oxidation of DA in acidic medium. The cyclic voltammograms recorded at increasing concentration of DA are shown in Figure 3.21a with a concentration range from 0.2 to 3 mM The oxidation of dopamine starts at about 0.75 V and produces a first anodic peak centered at aroound 0.9 V whose intensity increases linearly by DA concentration. Figure 3.21b shows the calibration curves for the different poly(Ani-co-PIP) copolymers obtained at 1.2V and 1.4V. The sensitivity of the differente calibration curves are shown in Table 3.9. As in the case of Pani and poly(Ani-co-ATA) te sensitivity is higher for the polymer obtained at high potential.

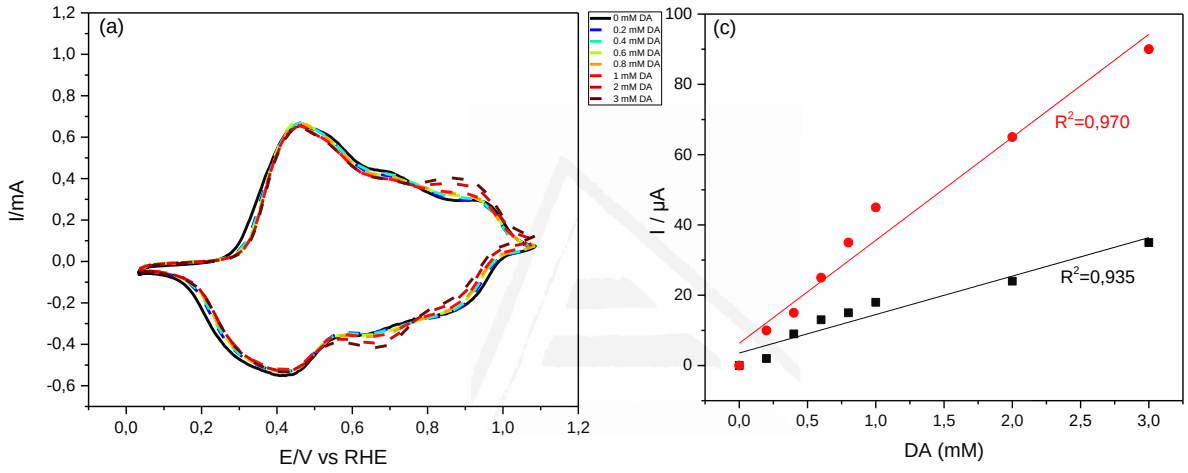

Figure.21 (a) cyclic voltammograms recorded during DA oxidation using a Pt electrode covered with poly(Ani-co-PIP) prepared in 1 M of $HClO_4$ at 1.4V. DA concentration range from 0.2 to 3 mM. (b) Calibration curves obtained with a Pt electrode covered with poly(Ani-co-ATA) obtained at 1.2V (black) and at 1.4V (red). 1 M $HClO_4$, v= 50 mV s^{-1} in all cases.

Table 3.9. *Sensitivity comparison of DA oxidation obtained with* poly(Ani-co-PIP) *obtained at different potential.*

Copolymer	Sensitivity (µA /mM)
poly(Ani-co-PIP) 1.2V	10.94± 0.01
poly(Ani-co-PIP) 1.4V	29.30±0.02

3.3.8 Sensitivity comparison between Pani and copolymers

Figure 3.22 shows the calibration curves compared for the different polymers obtained at 1.4V, because the DA oxidation shows a higher sensitivity with the polymers obtained at this potential. In that case, the Pani and poly(Ani-co-ATA) show the higher sensitivity. Table 3.10 shows the comparison of different modified electrodes for DA determination. It can be observed that the values of sensitivity obtained are similar to that obtained with other electrode materials; however, the linear range is different.

Table 3.10: Comparison of different modified electrodes for determination of DA.

Modified electrode	DA linear range (μM)	Sensitivity (μA μM^{-1})	Refs
Pani-MWCNTs[a]	50–385	1.29	[67]
Nafion–AgCl@PANI/GC[b]	0.5-4.0	0.49	[68]
Poly (4-amino-6-hydroxy-2-mercaptopyrimidine)[c]	2.5−25.0	0.207	[69]
CuO/MWNTs/Nafion[d]	1–80	3.09	[46]
PEDOT/Au nanoparticles[e]	0.15–330	0.040	[70]
Poly-β-CD(f-MWCNTs)/PANI[f]	0.5–15.0	2.12	[71]
MWCNTs/CeO2-PEDOT composite[g]	0.1−10.0; 40−400	3.669; 0.208	[72]
Polyaniline-GO[h]	2–18	2.0	[51]
PEDOT-GO[i]	6.0-200	0.10	[73]
Pani	200-3000	0.089	This work
Poly(Ani-co-ATA)	200-3000	0.072	This work
Poly(Ani-co-PIP)	200-3000	0.0293	This work

[a]Polyaniline-multiwall carbon nanotubes composite modified carbon paste electrode.

[b]The Nafion–AgCl@PANI/GC

[c]Poly (4-amino-6-hydroxy-2-mercaptopyrimidine)/ GCE

[d]Nano-sized copper oxide-multi-wall carbon nanotube/Nafion.

[e]Poly (3,4-ethylenedioxythiophene)/Au nanoparticles

[f]Poly-β-cyclodextrin incorporated f-MWCNTs/polyaniline modified glassy carbon electrode

[g]MWCNTs/ nanoceria-poly(3,4-ethylenedioxythiophene)composite modified GCE

[h]Polyanilinegraphene oxide

[i]Poly(3,4-ethylenedioxythiophene) doped with graphene oxide

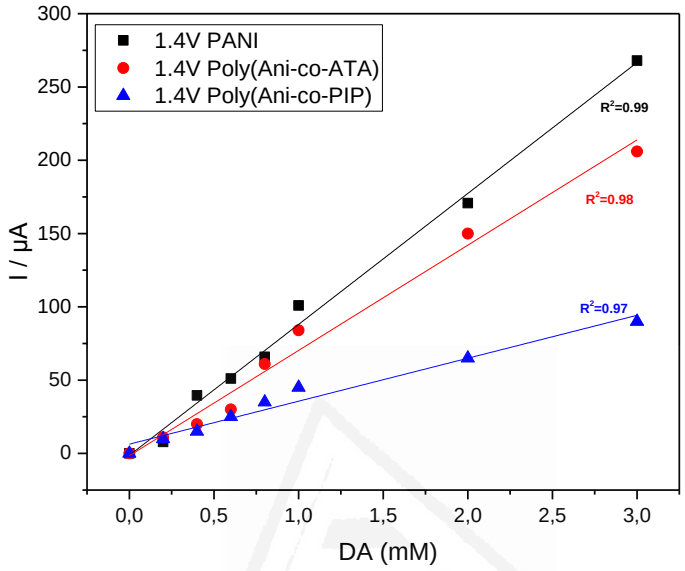

Figure 3.22 Calibration curve comparison for the oxidation of DA using the different polymers obtained at 1.4V.

4 Conclusion

The electrochemical synthesis by means of cyclic voltammetry on a platinum electrode of copolymers of aniline in an acidic medium has been studied. The different copolymers obtained are poly(Ani-co-ATA) and poly(Ani-co-PIP). It has been analyzed the upper potential limit and the monomer ratio in the electrochemical properties of the different polymers.

The voltammetric profiles show the amount of material deposited on the electrode surface is significantly higher when the electropolymerization potential limit is at 1.2 V. Obviously, such a value is too positive to correspond to the same transitions occurring when the polymer was synthesized at moderate potentials.

The electrochemical response of 2ATA shows that the electrochemical oxidation of aminoterephthalic acid does not yield an electroactive polymer on the electrode surface of Pt.

However, the 2ATA could be an interesting co-monomer for the aniline copolymerization because it contains two –COOH groups linked to the aromatic ring. Therefore, controlling the monomer ratio was a key parameter to obtain the copolymerization product and to modulate the material composition and properties.

The electrochemical oxidation of piperazine on platinum electrodes at moderate potentials (roughly below 1.0 V/RHE) preserves the ring structures and produces ketopiperazines as the main reaction product. In situ FTIR spectroscopy strongly suggested that ring opening and overoxidation occur at higher potentials to form both amides and isocyanates. As a result, it was observed that the homopolymerization of piperazine cannot be achieved in perchloric acid aqueous solution under electrochemical conditions. On the contrary, piperazine can be successfully copolymerized with aniline in acidic medium. The deposited copolymer shows some electrochemical features similar to those of pristine polyaniline, particularly those related with leucoemeraldine-to-emeraldine and emeraldine-to-pernigraniline transitions. However, a key difference arises in the intermediate potential region between both transitions. As shown by in situ FTIR and XPS spectroscopies, the intermediate redox peak is a consequence of the incorporation of piperazine units to the copolymer structure. Most of these piperazine centers undergo electrochemical oxidation during the copolymerization potential scans and, as a result, a new reversible hydroxy ⇌ ketopiperazine redox transformation seems to occur as the intermediate voltammetric feature centered at 0.68 V. It should be noted that, owing to the conservative potential program applied during the deposition process, any significant amount of overoxidation.

It was observed that the poly(Ani-co-ATA) and poly(Ani-co-PIP) show a linear response when applied to the electrochemical determination of dopamine or ascorbic acid in synthetic samples. The sensitivity of these measurements is in both analytes high enough to assure the correct quantification of analytes. The copolymers exhibited oxidation peaks for each concentration of DA and AA. It can be observed that the increase in the synthesis copolymer potential produces the increase in sensitivity.

5 Reference:

[1] J. Wang. Nanomaterial-based electrochemical biosensors. Analyst. 2005, 130, 421–426.

[2] J. L. S. Li, Y. Ge, S.A. Piletsky, Molecularly Imprinted Sensors : Overview and Applications, First Edition, 2012.

[3] D. S. K. R. Francis, Applications of polymeric Materials and Composites. Wiley-VCH Verlag, 2016.

[4] S. Dkhili, S. López-bernabeu, F. Huerta, F. Montilla, S. Besbes-hentati, and E. Morallón. A self-doped polyaniline derivative obtained by electrochemical copolymerization of aminoterephthalic acid and aniline. Synth. Met. 2018, 245, no. July, 61–66, 2018.

[5] E. Grieshaber, D.; MacKenzie, R.; Vörös, J.; Reimhult. Electrochemical Biosensors - Sensor Principles and Architectures. sensors. 2008, 8, 1400–1458.

[6] M. J. Jiri Janata. Conducting polymers in electronic chemical sensors. Nat. Mater. 2003, 2, 19–24,.

[7] T. F. Otero. Biomimetic Conducting Polymers : Synthesis , Materials , Properties , Functions , and Devices," Polym. Rev. 2013, 53(3), 311–351.

[8] M. Joulazadeh and A. H. Navarchian. Ammonia detection of one-dimensional nano-structured polypyrrole / metal oxide nanocomposites sensors. Synth. Met. 2015, 210, 404–411.

[9] T.-H. Le, Y. Kim, and H. Yoon. Electrical and Electrochemical Properties of Conducting Polymers. Polymers (Basel). 2017, 9, 150,.

[10] H. Yoon. Current Trends in Sensors Based on Conducting Polymer Nanomaterials. Nanomaterials. 2013, 3 (3), 524–549.

[11] J. Arias-Pardilla, H. J. Salavagione, C. Barbero, E. Morallón, and J. L. Vázquez. Study of the chemical copolymerization of 2-aminoterephthalic acid and aniline. Synthesis and copolymer properties. Eur. Polym. J., 2006, 42 (7), 1521–1532,.

[12] D. Gu, G. Yang, Y. He, B. Qi, G. Wang, and Z. Su. Triphenylamine-based pH chemosensor: Synthesis, crystal structure, photophysical properties and computational studies. Synth. Met. 2009, 159 (23–24), 2497–2501.

[13] K. Ghosh, D. Tarafdar, A. Samadder, and A. R. Khuda. Piperazine-based simple structure for selective sensing of Hg^{2+} and glutathione and construction of logic circuit mimicking Inhibit

gate. New J. Chem., 2013, 37, 4206–4213,.

[14] Z. Sun, H. Li, D. Guo, Y. Liu, Z. Tian, and S. Yan. A novel piperazine-bis(rhodamine-B)-based chemosensor for highly sensitive and selective naked-eye detection of Cu^{2+} and its application as an INHIBIT logic device. J. Lumin. 2015, 167, 156–162.

[15] R. Z. and H. L. Fang Zhang, Xushi Yang, Chao Liang. Piperazine-functionalized Ordered Mesoporous Polymer as Highly Active and Reusable Organocatalyst for Water-medium Organic Synthesis. Green Chem. 2013, 15 (6), 1665–1672.

[16] D. Sachdev, P. H. Maheshwari, and A. Dubey. Piperazine functionalized mesoporous silica for selective and sensitive detection of ascorbic acid. J. Porous Mater. 2016, 23, 123–129,.

[17] R. Ramachandran, S. Balasubramanian, G. Aridoss, and P. Parthiban. Polymer Synthesis and studies of semiconducting piperazine – aniline copolymer. 2006, 42, 1885–1892,.

[18] M. Abidi, S. López-Bernabeu, F. Huerta, F. Montilla, S. Besbes-Hentati, and E. Morallón. Spectroelectrochemical study on the copolymerization of o-aminophenol and aminoterephthalic acid. Eur. Polym. J. 2017, 91, 386–395.

[19] A. Benyoucef, F. Huerta, J. L. Vázquez, and E. Morallon. Synthesis and in situ FTIRS characterization of conducting polymers obtained from aminobenzoic acid isomers at platinum electrodes. Eur. Polym. J. 2005, 41(4), 843–852,.

[20] E. M. Geniès, M. Lapkowski, and J. F. Penneau. Cyclic voltammetry of polyaniline: interpretation of the middle peak. J. Electroanal. Chem. 1988, 249(1–2), 97–107.

[21] M. A. Cotarelo, F. Huerta, C. Quijada, R. Mallavia, and J. L. Vázquez. Synthesis and Characterization of Electroactive Films Deposited from Aniline Dimers. J. Electrochem. Soc. 2006, 153(7), D114–D122.

[22] G. Horanyi and I. Bakos. Experimental evidence demonstrating the occurrence of reduction processes of ClO , ions in an acid medium at platinized platinum electrodes. J. Electroanal. Chem. 1992, 331(1–2), 727–737.

[23] S. L. Wang, S. Y. Lin, and T. F. Chen. Thermal-dependent dehydration process and intramolecular cyclization of lisinopril dihydrate in solid state. Chem. Pharm. Bull. 2000, 48(12), 1890–1893.

[24] T. C. Cheam and S. Krimm. Vibrational analysis of crystalline diketopiperazine-I. Raman and i.r. spectra. Spectrochim. Acta Part A Mol. Spectrosc. 1984, 40(6), 481–501.

[25] G. Socrates, Infrared and Raman characteristic group frequencies. Tables and charts, Third

edit. Chichester: Wiley and Sons, Ltd., 2001.

[26] V. P. Pattar, P. A. Magdum, D. G. Patil, and S. T. Nandibewoor. Thermodynamic, kinetic and mechanistic investigations of Piperazine oxidation by Diperiodatocuprate(III) complex in aqueous alkaline medium. J. Chem. Sci. 2016, 128(3), 477–485.

[27] J. L. Owens and G. Dryhurst. Electrochemical reduction of tetraketopiperazine. Anal. Chim. Acta. 1976, 87(1), 37–50.

[28] Z. Ping, G. E. Nauer, H. Neugebauer, and J. Theiner. In situ Fourier transform infrared attenuated total reflection (FTIR-ATR) spectroscopic investigations on the base-acid transitions of different forms of polyaniline. 1 Base-acid transition in the leucoemeraldine form. J. Electroan, 1997, 420, 301–306.

[29] G. Louarn, M. Lapkowski, S. Quillard, A. Pron, J. P. Buisson, and S. Lefrant. Vibrational Properties of Polyaniline s Isotope Effects. J. Phys. Chem. 1996, 100(17), 6998–7006.

[30] M. Abidi, F. Huerta, F. Montilla, and E. Morallón. Electrochimica Acta The chemical and electrochemical oxidative polymerization of 2-amino. Electrochim. Acta. 2016, 212, 958–965.

[31] A. Quillard, S.; Berrada, K.; Louarn, G.; Lefrant, S.; Lapkowski, M.; Pron. In situ Raman spectroscopic studies of the electrochemical behavior of polyaniline. New J. Chem. 1995, 19, 365–374.

[32] P. J. Hendra and D. B. Powell, "The infra-red and Raman spectra of piperazine," Spectrochim. Acta. 1962, 18(3), 299–306.

[33] NIST X-ray Photoelectron Spectroscopy Database, Version 4.1 (Web Version), 2012. Available online: http: //Srdata.Nist.Gov/Xps/ (accessed on 20 January 2021)

[34] J. J. Langer. Polyaniline Micro- and Nanostructure. 1999, 7, 1–7.

[35] S. Yonezawa, K. Kanamura, and Z. Takehara. Effects of the Solvent for the Electropolymerization of Aniline on Discharge and Charge Characteristics of Polyaniline. J. Electrochem. Soc. 1995, 142(10), 3309–3313.

[36] Y.-B. Shim, M.-S. Won, and S. Park. Electrochemistry of Conductive Polymers VIII : In Situ Spectroelectrochemical Studies of Polyaniline Growth Mechanisms Electrochemistry of Conductive Polymers VIII In Situ Spectroelectrochemical Studies of Polyoniline Growth Mechanisms. J. Electrochem. Soc. 1990, 137(2), 538–544.

[37] M. A. Cotarelo, F. Huerta, C. Quijada, F. Cases, and J. L. Vázquez.The electrocatalytic

behaviour of poly (aniline-co-4adpa) thin films in weakly acidic medium. Synth. Met. 2004, 144, 207–211.

[38] W. H. Stockmayer, "Distribution of Chain Lengths and Compositions in Copolymers," J. Chem. Phys. 1945, 13, 199.

[39] and R. K. C. Gliickner, J. H. M. van den Berg, N. L. J. Meyerink, Th.G. Scholte. Macromolecules. 1984, 17, 962.

[40] S. Khalili, B. Khoshandam, and M. Jahanshahi. Synthesis of activated carbon / polyaniline nanocomposites for enhanced CO_2 adsorption. RSC Adv. 2016, 6, 35692–35704.

[41] T. Xu, Q. Zhang, J. Zheng, Z. Lv, and J. Wei. Electrochimica Acta Simultaneous determination of dopamine and uric acid in the presence of ascorbic acid using Pt nanoparticles supported on reduced graphene oxide. Electrochim. Acta. 2014, 115, 109–115.

[42] T. W. and T. Y. J. Sun, L. Li, X. Zhang, D. Liu, S. Lv, D. Zhu. Simultaneous determination of ascorbic acid, dopamine and uric acid at nitrogen-doped carbon nanofiber modified electrode. RSC Adv. 2015, 5, 11925–11932.

[43] E. Alipour, M. R. Majidi, A. Saadatirad, S. mahdi Golabi, and A. M. Alizadeh. Simultaneous determination of dopamine and uric acid in biological samples on the pretreated pencil graphite electrode. Electrochim. Acta. 2013, 91, 36–42.

[44] Y. Wu, Z. Dou, Y. Liu, G. Lv, T. Pu, and X. He. Dopamine sensor development based on the modification of glassy carbon electrode with β-cyclodextrin-poly(N-isopropylacrylamide). RSC Adv. 2013, 3, 12726–12734.

[45] C. R. Raj, T. Okajima, and T. Ohsaka. Gold nanoparticle arrays for the v oltammetric sensing of dopamine. J. Electroanal. Chem. 2003, 543, 127–133.

[46] S. Yang, G. Li, Y. Yin, R. Yang, J. Li, and L. Qu, "Nano-sized copper oxide/multi-wall carbon nanotube/Nafion modified electrode for sensitive detection of dopamine. J. Electroanal. Chem. 2013, 703, 45–51.

[47] S. Thirumalairajan, K. Girija, V. R. Mastelaro, V. Ganesh, and N. Ponpandian. Detection of the neurotransmitter dopamine by a glassy carbon electrode modi fi ed with self- assembled perovskite $LaFeO_3$ microspheres made up of nanospheres. RSC Adv. 2014, 4, 25957–25962.

[48] L. Xing and Z. Ma. A glassy carbon electrode modified with a nanocomposite consisting of MoS_2 and reduced graphene oxide for electrochemical simultaneous determination of ascorbic acid , dopamine , and uric acid. Microchim. Acta. 2016, 183, 257–263.

[49] M. Bp.Ezina, J. Koryta, And T. L. And D. Marsikov. Adsorption And Kinetics Of Oxidation Of Ascorbic Acid At Platinum Electrodes. Electroanal. Chem. Interfacial Electrochem. 1972, 40, 13–17.

[50] X. Xing, I. T. Bae, M. Shao, and C. Liu. Electra-oxidation of L-ascorbic acid on platinum in acid solutions: an in-situ FTIRRAS study. J. Electroanal. Chem. 1993, 346, 309–321.

[51] P. Manivel, M. Dhakshnamoorthy, A. Balamurugan, N. Ponpandian, D. Mangalaraj, and C. Viswanathan. Conducting polyaniline-graphene oxide fibrous nanocomposites: preparation, characterization and simultaneous electrochemical detection of ascorbic acid, dopamine and uric acid. RSC Adv. 2013, 3(34), 14428.

[52] Z. Dursun and B. Gelmez. Simultaneous determination of ascorbic acid, dopamine and uric acid at pt nanoparticles decorated multiwall carbon nanotubes modified GCE. Electroanalysis. 2010, 22(10), 1106–1114.

[53] D. Banan, W. T. Tan, Y. Sulaiman, M. F. Yusri, M. Zidan, and S. Ab Ghani. Electrochemical oxidation of ascorbic acid using MgB2-MWCNT modified glassy carbon electrode. Int. J. Electrochem. Sci. 2013, 8(12), 12519–12530.

[54] M. Chi, Y. Zhu, L. Jing, C. Wang, and X. Lu. Fabrication of oxidase-like polyaniline-MnO_2 hybrid nanowires and their sensitive colorimetric detection of sulfite and ascorbic acid. Talanta. 2017, 191, 171–179.

[55] V. Sharma, A. Sundaramurthy, A. Tiwari, and A. K. Sundramoorthy. Graphene nanoplatelets-silver nanorods-polymer based in-situ hybrid electrode for electroanalysis of dopamine and ascorbic acid in biological samples. Appl. Surf. Sci. 2017, 449, 558–566.

[56] F. Tulli, V. I. P. Zanini, J. M. Fernández, D. M. Martino, B. A. L. de Mishima, and C. D. Borsarelli. Influence of Electrostatic Interactions Induced via a Nanocomposite Film onto a Glassy Carbon Electrode Used for Highly Selective and Sensitive Ascorbic Acid Detection. J. Electrochem. Soc. 2019, 166(8), B742–B747.

[57] P. Wang, T. Gan, J. Zhang, J. Luo, and S. Zhang. Polyvinylpyrrolidone-enhanced electrochemical oxidation and detection of acyclovir. J. Mol. Liq. 2013, 177, 129–132,.

[58] L. D. ChakkaraPani, S. N. Sangilimuthu, and S. Arumugam. New electrochemical sensor for the detection of biological analytes using poly(amido amine) dendrimer and poly(Nile blue)-modified electrode. J. Electroanal. Chem. 2019, 855, 113486.

[59] V. S. Vasantha and S. Chen. Electrocatalysis and simultaneous detection of dopamine and ascorbic acid using poly (3 , 4-ethylenedioxy) thiophene film modified electrodes. J.

Electroanal. Chem. 2006, 592, 77–87.

[60] H. Sun, J. Chao, X. Zuo, S. Su, X. Liu, L. Yuwen, C. Fanab and L. Wang. Gold nanoparticle-decorated MoS_2 nanosheets for simultaneous detection of ascorbic acid, dopamine and uric acid. RSC Adv. 2014, 4, 27625–27629.

[61] R. A. Wise. Dopamine , Learning And Motivation. Nat. Rev. Neurosci. 2004, 5, 483–494.

[62] R. Devasenathipathy, V. Mani, S.-M. Chen, B. Viswanath, V. S. Vasantha, and M. Govindasamy. Electrodeposition of gold nanoparticles at pectin scaffold and its electrocatalytic application to the selective determination of dopamine. RSC Adv. 2014, 4, 55900–55907.

[63] B. Kong, A. Zhu, Y. Luo, Y. Tian, Y. Yu, and G. Shi. Sensitive and Selective Colorimetric Visualization of Cerebral Dopamine Based on Double Molecular Recognition. Angew. Chemie. 2011, 50(8), 1837–1840.

[64] C. Yang, E. Trikantzopoulos, M. D. Nguyen, C. B. Jacobs, Y. Wang, M. Mahjouri-Samani, I. N. Ivanov, and B. J. Venton. Laser Treated Carbon Nanotube Yarn Microelectrodes for Rapid and Sensitive Detection of Dopamine in Vivo Laser Treated Carbon Nanotube Yarn Microelectrodes for Rapid and Sensitive Detection of Dopamine in Vivo. ACS Sensors. 2016, 1(5), 508–515.

[65] D. A. Stern, G. N. Salaita, F. Lu, J. W. McCargar, N. Batina, D. G. Frank, L. Laguren-Davidson, C. Lin, N. Walton, J. Y. Gui, A. T. Hubbard. Studies of L-DOPA and Related Compounds Adsorbed from Aqueous Solutions at Pt (100) and Pt (ll1): Electron Energy-Loss Spectroscopy, Auger Spectroscopy, and Elect roc hemistry. Langmuir, 1988, 4, 711–722.

[66] M. Kavanoz, E. Ülker, and U. Bük. A Novel Polyaniline – Poly (3- Diaminobenzidine) Electrode for the Determination of Dopamine in Human Serum. Anal. Lett. 2014, 37–41.

[67] R. E. Sabzi, K. Rezapour, and N. Samadi. Polyaniline-multi-wall-carbon nanotube nanocomposites as a dopamine sensor. J. Serbian Chem. Soc. 2010, 75(4), 537–549.

[68] W. Yan, X. Feng, X. Chen, X. Li, and J. J. Zhu. A selective dopamine biosensor based on AgCl@polyaniline core-shell nanocomposites. Bioelectrochemistry. 2008, 72(1), 21–27.

[69] A. Kannan and R. Sevvel. A highly selective and simultaneous determination of paracetamol and dopamine using poly-4-amino-6-hydroxy-2-mercaptopyrimidine (Poly-AHMP) film modified glassy carbon electrode. J. Electroanal. Chem. 2017, 791, 8–16.

[70] A. Ali, R. Jamal, T. Abdiryim, and X. Huang. Synthesis of monodispersed PEDOT/Au hollow nanospheres and its application for electrochemical determination of dopamine and uric acid. J. Electroanal. Chem. 2017, 787, 110–117.

[71] Y. H. Chang, P. M. Woi, and Y. Alias. The selective electrochemical detection of dopamine in the presence of ascorbic acid and uric acid using electro-polymerised-β-cyclodextrin incorporated f-MWCNTs/polyaniline modified glassy carbon electrode. Microchem. J. 2019, 148, 322–330,.

[72] A. Üğe, D. Koyuncu Zeybek, and B. Zeybek. An electrochemical sensor for sensitive detection of dopamine based on MWCNTs/CeO_2-PEDOT composite," J. Electroanal. Chem. 2018, 813, 134–142.

[73] D. Li, M. Liu, Y. Zhan, Q. Su, Y. Zhang, and D. Zhang. Electrodeposited poly(3,4-ethylenedioxythiophene) doped with graphene oxide for the simultaneous voltammetric determination of ascorbic acid, dopamine and uric acid. Microchim. Acta. 2020, 187(1), 94.

Chapter 4

Synthesis and Characterization of Hydrogels Obtained from Aniline and Aminoterephthalic Acid and Piperazine Monomers

1 Introduction

Hydrogels are three-dimensional networks of hydrophilic polymers which are remarkably suitable for a wide range of applications. Although hydrogels have been demonstrated to be highly versatile platforms for different applications, their insulating nature often limits their potential. Conducting polymer hydrogels are attracting increasing attention for application in wearable and flexible strain sensors, due to their excellent conductivity and mechanical properties [1]. These electroconductive hydrogels are produced through the incorporation of conductive materials into polymeric hydrogels. Polyaniline, polypyrrole, and exceptionally poly(3,4-ethylenedioxythiophene) (PEDOT) are currently used as conducting materials, while cross-linked water-soluble polymers are the other component [2,3]. Such hydrogels are obtained by the oxidation of monomers in the presence of an anionic polyelectrolyte, and their formation depends on the concentrations of the monomer, oxidant and polyanion [4,5]. Moreover, the use of strong polyelectrolytes, such as polystyrenesulphonate (PSS), to prepare colloidal composites is a general method as the colloids can be directly transformed into processable films by a simple solution-casting process [6].

2-aminoterephthalic acid (2ATA), Figure 1, could be an interesting monomer for its copolymerization with aniline (Ani) by chemical oxidative polymerization [7]. It was found that 2ATA monomers were four times less reactive than aniline under chemical polymerization conditions, because of the deactivating effect of the carboxylic group attached to the aromatic ring; however, it constitute an attractive way for providing self-doping to the polyaniline, thus avoiding the use of external dopants [8]. A copolymer from aniline (Ani) and 2ATA monomers by chemical oxidative polymerization has been previously studied [9]. Therefore, controlling the monomer ratio was a key parameter to obtain a true copolymerization product and to modulate the composition and properties material [10].

Piperazine (PIP), also known as hexahydropyrazine (Figure 4.1), consists of a saturated cycle containing two nitrogen atoms on different sides of the cycle, which can be found in many drugs

[8,11,12]. Molecular compounds containing the piperazine group attracted great attention, due to their different applications in the industrial and drug fields [13–15]. Heterocyclic compounds containing nitrogen are of particular importance because of their ability to form hydrogen bonds, thus generating supramolecular structures [16,17]. The chemical copolymerization of aniline and piperazine was studied by Ramachandran et al [18]. Moreover, electrochemical copolymerization has also been studied, and the copolymer showed electrochemical activity [19].

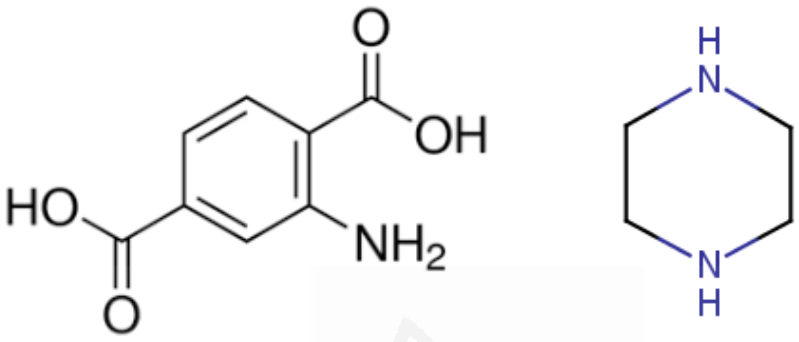

Figure 4.1. Structure of (a) 2-aminoterephthalic acid and (b) piperazine.

The goal of the present contribution is to study the chemical synthesis of hydrogels from aniline and 2-aminoterephthalic acid or aniline and piperazine in presence of PSS that can improve some of the properties of such hydrogels, like solubility and interaction with other compounds. The copolymer hydrogels (poly(Ani-co-2ATA)/PSS and poly(Ani-co-PIP)/PSS) have been characterized using different techniques. A combination of X-ray photoelectron spectroscopy (XPS), thermogravimetric analysis (TGA) and Fourier transform infrared (FTIR) spectroscopy has been used for the characterization of the hydrogels. Electrochemical techniques have been used to analyze the redox behavior of the copolymer. Finally, the conductive properties of the hydrogels have been tested with a four-point probe method. The mass swelling ratio was measured by comparing the hydrated weight with the dehydrated weight.

2 Experimental part

Aniline was previously distilled under vacuum. Piperazine (98.8%), 2-aminoterephthalic acid (Aldrich, 98%) and sodium poly(4-styrenesulfonate) (NaPSS, Mw 70,000) were used without further purification. All these compounds were supplied by Aldrich. Ammonium per sulphate (APS) (Merck,

p.a.), HCl (Merck, p.a.) and $HClO_4$ (Merck, p.a.) were obtained from Merck. The ultrapure water (18.2 MΩ cm) employed in all the experiments was obtained from an Elga Labwater Purelab system.

2.1 Synthesis of hydrogel

Various strategies have been employed in the preparation of copolymer hydrogels formed from 2ATA and PIP with aniline in the presence of PSS. Different molar ratios in concentrated solutions have been used. The hydrogels were synthesized in 1 M HCl, and different quantities of aniline and 2-aminoterephtalic acid (Ani:2ATA) at different molar ratios (0.25/0.25=1; 0.38/0.12=3; 0.42/0.08=5) were added into 20 mL of 1 M HCl aqueous solutions and NaPSS. The concentration of NaPSS in the reaction system was always 0.5 M, and the molar ratio of monomers to APS was kept at 1:1. After stirring for 10 min, 10 mL of APS (oxidant) solution were added to induce the polymerization. The resulting mixture was stirred for 1 min to ensure complete mixing and then the reaction was allowed to proceed without agitation for 12 h at room temperature. The same procedure has been used in the synthesis of aniline and piperazine hydrogels, and the same ratio monomers than in the case of 2ATA has been used (Ani:PIP). Hydrogel products were purified in a large amount of distilled water for 1 week to wash out low molecular weight components. The different samples have been called poly(Ani-co-2ATA)/PSS-X and poly(Ani-co-PIP)/PSS-X, X being the ratio of both monomers (1, 3 or 5). The Pani/PSS hydrogel has also been synthesized using the same procedure to compare with the copolymer hydrogels.

2.2 Characterization

Transmission electron microscopic (TEM) measurements were carried out using a JEOL TEM, JEM-2010 model and a GATAN acquisition camera. Thermal analysis was determined by thermogravimetry (TG) in N_2 (80 mL min^{-1}) flow, heating the sample from 25 to 920°C (heating rate: 10°Cmin^{-1}) using a Stanton Redcroft STA-780 thermobalance. FTIR spectra were collected in the transmission mode by using a Bruker Alpha spectrometer.

Elemental composition was performed using a Carlo Erba CHNS-O EA1108 analyzer. The XPS spectra were obtained with an AVG-Microtech Multilab 3000 electron spectrometer (VG Microtech Ltd., Uckfield, UK). The 300-W power radiation source was a non-monochromatized Mg-Kα, and the analysis was performed under 5×10^{-7} Pa pressure. The high-resolution spectra were obtained at 50 eV pass energy and are presented as a combination of Lorentz (30%) and Gaussian (70%) curves. The C1s line at 284.4 eV has been employed as the reference for the experimental binding energies, which were obtained with 0.2 eV accuracy.

For the determination of the swelling properties, the freshly prepared samples of hydrogels (Pani/PSS, poly(Ani-co-2ATA)/PSS-X and poly(Ani-co-PIP)/PSS-X) were weighed on the analytical balance. Subsequently the samples were placed in an oven at 80°C for 24 hours to remove water and weighed over time. The mass swelling ratio was measured by comparing the hydrated weight (Ww) with the dehydrated weight (Wi) using the following equation: mass swelling ratio (%) = ((Ww - Wi)/Ww) × 100%; and the percentage of water loss (%) = (Ww/Wi) × 100%.

The electrochemical characterization of the poly(Ani-co-2ATA)/PSS-X and poly(Ani-co-PIP)/PSS-X hydrogels was carried out in 1M $HClO_4$ electrolyte. The dispersion solutions of the different hydrogels were deposited on glassy carbon and the solvent was removed with an infrared lamp. The modified glassy carbon is used as working electrode. The counter electrode was a platinum wire. All potentials were measured against a reversible hydrogen electrode (RHE) immersed in the working solution as reference electrode. Cyclic voltammograms were recorded at 50 mV s^{-1} and at room temperature.

Electrical conductivity measurements were carried out using Lucas Lab resistivity equipment with four in-line probes. The samples were dried during 24 hours, and then pellets of 0.013 m of diameter of each one were made under 10 Tn cm^{-2} pressure.

3 Results and discussion

3.1 Poly(Ani-co-2ATA)/PSS-X hydrogels

3.1.1 Transmission electron microscopy (TEM)

Figure 4.1 shows the TEM images of the poly(Ani-co-2ATA)/PSS-1 and pani/PSS hydrogels. No significant differences were observed for the different molar ratios for the copolymer hydrogels. Moreover, the images in Figure 4.1 show that the morphology of the copolymer hydrogels is similar to that observed with the Pani/PSS hydrogel.

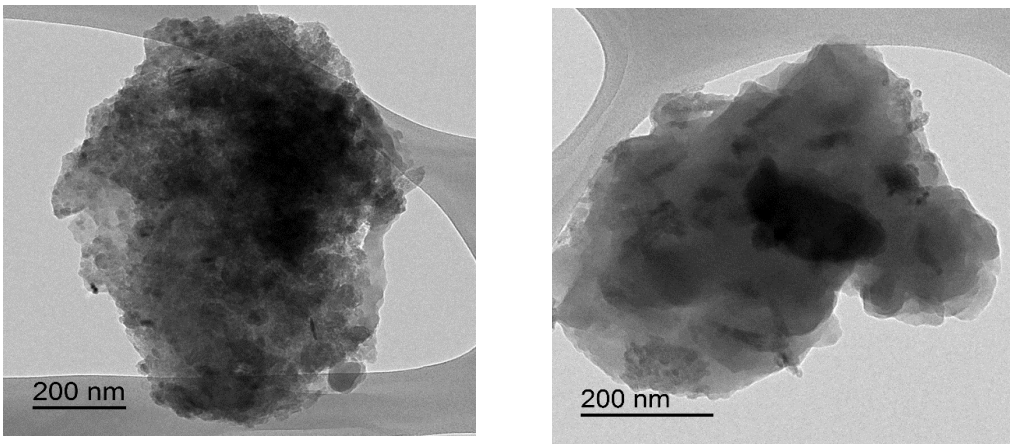

Figure 4.1. TEM images of the (a) Pani/PSS and (b) poly(Ani-co-2ATA)/PSS-1 hydrogels.

3.1.2 Thermogravimetry

The thermal stability of a conducting polymer is very important for its potential application. Thermogravimetry is a significant, useful and dynamic way to detect the degradation behavior in which the weight loss of a hydrogel sample is measured continuously while the temperature is changed at a constant rate. In this sense, the thermogravimetric analyses (TGAs) of all hydrogels have been performed in temperatures ranging from 25 to 950°C under nitrogen atmosphere at a heating rate of 10°C min^{-1}. Figure 4.2 displays the TGA profiles of the synthesized hydrogels.

The thermal behavior of the hydrogels with lower amount of 2ATA (poly(Ani-co-2ATA)/PSS-3 and poly(Ani-co-2ATA)/PSS-1) is similar to that of Pani/PSS and exhibits a four-stage decomposition pattern. In the first stage (practically from room temperature to 110ºC), the weight loss is due to the loss of water molecules and removal of solvent or dopant anions present in the samples. The second stage, at around 200ºC, is attributed to the doping of the copolymer chain. The third and fourth stages are responsible for the complete degradation and decomposition of the polymer backbone [20]. However, for the hydrogel with high amount of 2ATA, the stability increases as a consequence of the interaction between the carboxylic groups and the charged nitrogen in the structure of the polymer.

The amount of residue (percentage at 950ºC) after the decomposition is shown in Table 4.1. This table indicates that the residue for the poly(Ani-co-2ATA)/PSS-1 is higher than for the other hydrogels, confirming the high amount of ATA monomer in this copolymer.

Table 4.1. Amount of residue after thermal decomposition of copolymer hydrogels.

Samples	w_i (g) at 30°C	w_f (g) at 950°C	Δw %
PANI/PSS	0.0106	0.0028	73.6
poly(Ani-co-2ATA)/PSS-1	0.0105	0.0055	47.6
poly(Ani-co-2ATA)/PSS-3	0.0102	0.0035	65.7
poly(Ani-co-2ATA)/PSS-5	0.0105	0.0033	68.6

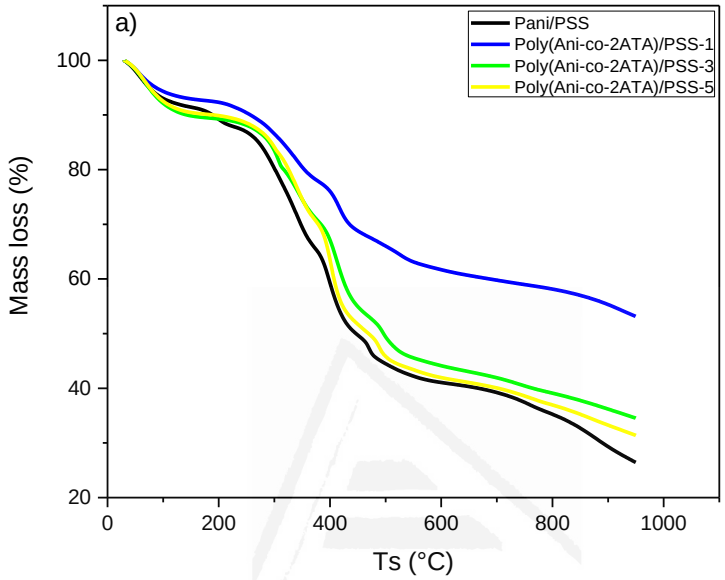

Figure 4.2. Thermogravimetric analysis curves of Pani/PSS and poly(Ani-co-ATA)/PSS-X.

3.1.3 X-ray photoelectron spectroscopy

Table 4.2 shows the XPS data obtained for each poly(Ani-co-2ATA)/PSS-X hydrogel and the Pani/PSS. It can be observed that the composition of the different copolymer hydrogels is similar. The differences are observed in the XPS data, in which the amount of S is lower in the Pani/PSS hydrogel, which is in agreement with the low amount of oxygen in comparison with the copolymer hydrogels.

Table 4.2**.** Composition of poly(Ani-co-2ATA)/PSS-X and Pani/PSS obtained by XPS.

	XPS/ wt%			
Sample	**S**	**N**	**C**	**O**
Pani/PSS	4.25	5.13	74.9	15.7
Poly(Ani-co-2ATA)/PSS-1	15.1	4.48	46.4	34.0
Poly(Ani-co-2ATA)/PSS-3	15.0	3.98	46.8	34.2
Poly(Ani-co-2ATA)/PSS-5	10.8	4.70	60.7	24.2

Figure 4.3 shows the photoelectronic spectra of C1s, N1s and S2p core levels and Table 4.3 summarizes the proposed assignments for the observed signals and the percentage of each species. Four contributions have been observed in the C1s, at 284.5, 285.4, 286.5 and 288.9 eV. The main contribution at 284.5 eV corresponds to aromatic carbon, while the 285.4 eV contribution can be assigned to aromatic carbon bonded to either amine or imine neutral nitrogen. The C1s peak at 288.9 eV corresponds to carbon atoms bonded to oxygen (C=O and C–O). Therefore, it strongly suggests the presence of carboxylic carbon in the structure of the poly(Ani-co-2ATA)/PSS-X hydrogels, which confirms the incorporation of 2ATA into the copolymer [21]. The intensity of this C1s signal, assigned to carboxylic groups, increases with the amount of 2ATA (decreasing the ratio of monomers) (Table 4.3).

Additionally, the XPS N1s spectra are shown in Figure 4.3.b. Different peaks are observed at 399.2, 400.5 and 401.7 eV. The first peak at 399.2 eV can be assigned to neutral amines and the peak around 400.5 eV to imine species which are also observed in polyaniline. The peak at 401.7 eV can be attributed to positively charged nitrogen [22–26]. The amount of this species is very high in comparison with the other peaks and increases with the amount of 2ATA. This could be a consequence of the stabilization of this positively charged nitrogen by interaction with the carboxylic group of the 2ATA, producing the self-doping in the copolymer hydrogel.

The determined amounts of S (in wt%) of the copolymer hydrogels at different molar ratios are presented in Table 4.4. Figure 4.3.c shows the XPS spectra (S2p core level) for the different poly(Ani-co-2ATA)/PSS-X hydrogels. Regarding the S2p spectra, deconvolution of the sulfur species shows doublets (2p1/2 and 2p3/2), with a peak separation of 1.16 eV, and the ratio of the intensities is 0.5. The S2p data for the poly(Ani-co-2ATA)/PSS-5 can be fitted using only one doublet (with maximum peaks at 168.1 and 169.3 eV), which reflects the S2p spin–orbit interaction. Thus, the XPS data confirm the presence of only one type of sulfur corresponding to the sulfonic group in the PSS. However, in the case of the copolymer hydrogels with lower amount of aniline (X=1 and

3), two doublets are clearly observed with maximum values at 167.7 and 169.1 eV, which indicate two different species of S. The first one can correspond to the sulfonic groups of PSS, and the second one could be a consequence of either the interaction between the sulfonic group and the positively charged nitrogen in the polymer hydrogels or to the presence of sulfate anions. These last species are only observed in two of the hydrogels and their origin can indicate that the final products were not properly washed.

Table 4.3. Summary of the XPS binding energy values (eV) obtained for hydrogels: (a) Pani@PSS, (b) poly(Ani-co-2ATA)/PSS-1, (c) poly(Ani-co-2ATA)/PSS-2 and (d) poly(Ani-co-2ATA)/PSS-5.

	Binding Energy (eV)								
	C1s				N1s			S2p	
(a)	284,57	285,61	286,66	288,84	399,47	401,30	402,51	167,84	//
(b)	284,59	285,68	286,62	289,02	399,28	400,56	401,89	167,87	169,09
(c)	284,62	285,57	286,24	289,08	399,3	400,64	401,99	167,76	169,06
(d)	284,61	285,5	286,55	289,06	399,49	401,93	400,93	168,04	//
Assignments	C–C C=C C–H C–S	C–N	C=N C–OH	C=O O=C– OH	=N–	–NH– –NC–	$-N^{+}-$ $=N^{+}-$	–S–C S=O	$-SO_4^{2-}$

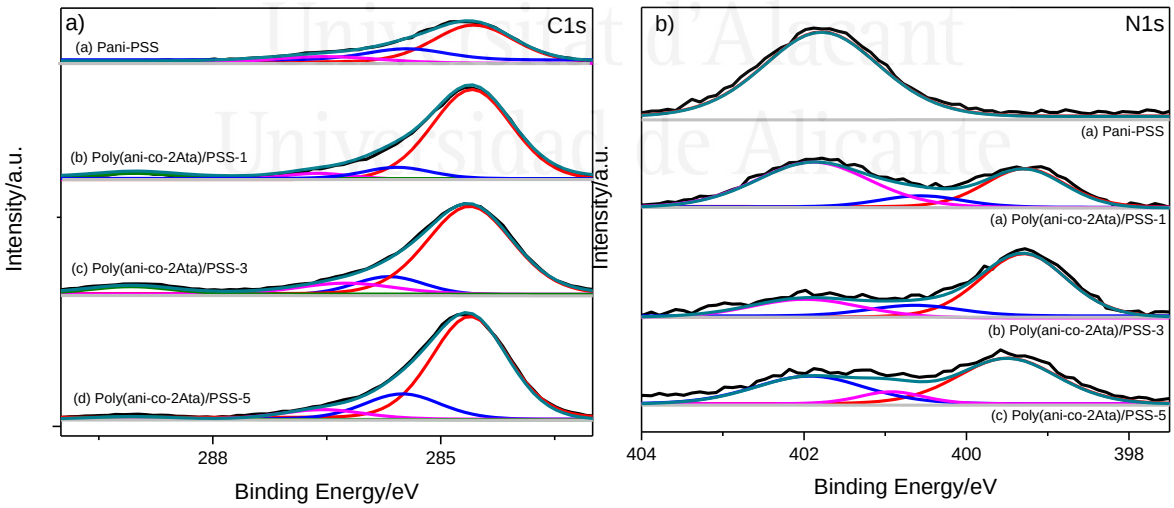

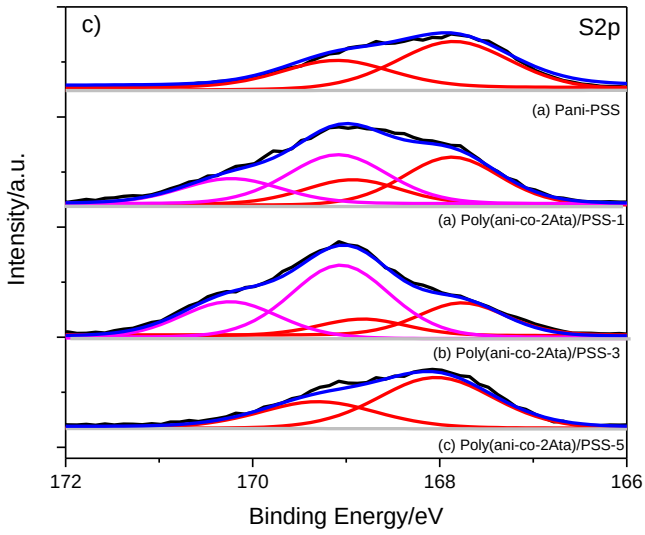

Figure 4.3. C1s; N1s and S2p XPS spectra of poly(Ani-co-2ATA)/PSS-X hydrogels.

3.1.4 Swelling ratio

To estimate the swelling degree it was assumed that the freshly synthesized hydrogel is maximally swelled by water [4]. To obtain the quantity of water in the hydrogel, the wet and dried samples were weighed during the drying time. The swelling ratio and the percentage of water loss in the Pani/PSS hydrogel and the poly(Ani-co-2ATA)/PSS-X hydrogels are shown in Figure 4.4. The water content is thus very high in all hydrogels. Furthermore, the swelling capacity of the hydrogel and hydrogel copolymers is much higher.

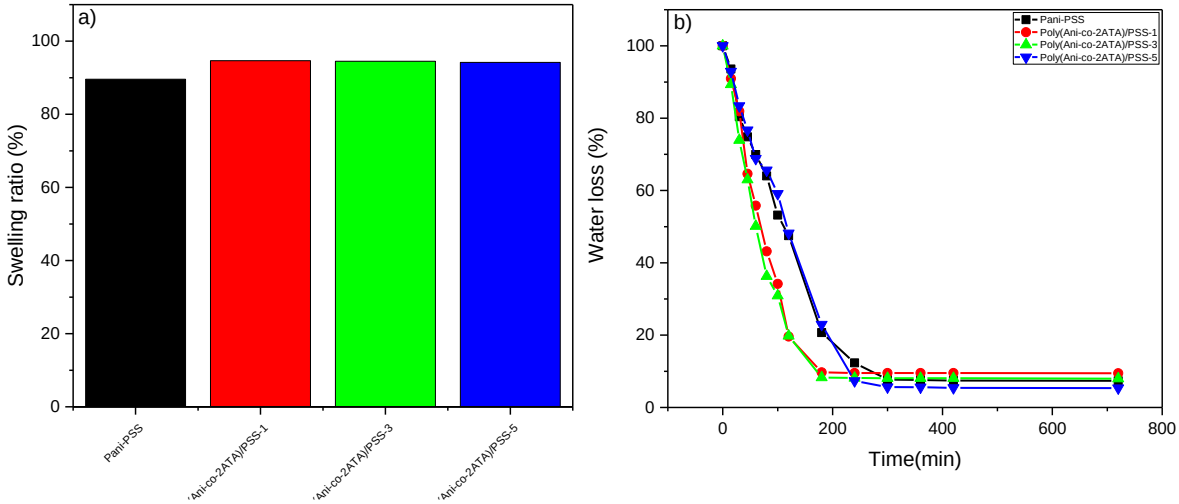

Figure 4.4. (a) Swelling ratios of the poly(Ani-co-2ATA)/PSS-X hydrogels; (b) water loss percentage after 24h drying.

3.1.5 Conductivity

Table 4.4 shows the conductivity values measured with a four-probe method. It can be observed that the conductivity values of all materials are between 0.03 and 0.8 S cm^{-1}. When the molar ratio of aniline is lower (X=1 and 3), the conductivity is one order of magnitude smaller than Pani/PSS. These values are similar to those obtained with self-doped polyanilines [33]. When the amount of aniline increases, so does the conductivity.

Table 4.4**.** Conductivity of poly(Ani-co-2ATA)/PSS-X and Pani/PSS hydrogels.

Sample	**Conductivity(S cm^{-1})**
Pani/PSS	0.787
Poly(Ani-co-2ATA)/PSS1	0.037
Poly(Ani-co-2ATA)/PSS-3	0.085
Poly(Ani-co-2ATA)/PSS-5	0.112

3.1.6 *Electrochemical Characterization.*

The electroactivity and electrochemical behavior of the synthesized copolymer hydrogels have also been analyzed to explore the use of these materials as electrodes. Films of the copolymer were deposited on glassy carbon to produce modified electrodes. Figure 4.5.a shows the cyclic voltammograms studied in the 1 M $HClO_4$ aqueous solution of the different poly(Ani-co-2ATA)/PSS-X hydrogels in powder form (dry form). The deposited material was tested in an acidic background solution that was free of any monomer species. The voltammetric behavior is similar to those obtained in substituted polyanilines with the presence of two redox processes, corresponding to the leucoemeraldine–emeraldine transition (first peak) and the emeraldine–pernigraniline transition (second peak) [34]. However, the second peak, which is less intense, has been usually interpreted as and clearly related to the emeraldine–pernigraniline transition of the copolymer hydrogel, the obtained results are similar to Pani/PSS under the same experimental conditions (solid line). The potential value that appears at the second peak is slightly lower than Pani films. The similarly shifted redox potentials are observed in cyclic voltammograms of oligoanilines [35]. Consequently, the differences between the redox potentials of the copolymer hydrogel and the Pani/PSS hydrogel films suggest that copolymer hydrogels are composed of oligomeric species. The

first peak potential appears at more negative values than Pani/PSS and the amount of 2ATA units in the copolymer increases. This effect is due to the presence of the carboxylate group, which withdraws electrons from the aromatic rings, making amine units more difficult to oxidize. On the other hand, the second peak potential appears at lower positive values than in Pani as the amount of 2ATA units increases [36]. This effect has been observed in sulfonated polyanilines [37]. Interestingly, when the amount of 2ATA decreases, the voltammetric charge increases. Figure 4.5.b shows the cyclic voltammograms of wet hydrogels; it can be observed that the voltammetric profile is different to those obtained with the dry hydrogels. However, the materials maintain their electroactivity in acidic conditions. Also noteworthy is that the voltammetric charge is higher than that obtained with the dry hydrogels, which could indicate that the electrochemical surface area is larger in these conditions.

The first redox peak is broader for Pani/PSS; moreover, its potential is shifted in the anodic direction compared to typical electropolymerized Pani films, with potential values in the range of 0.34 V for poly(Ani-co-2ATA)/PSS-X in comparison with Pani/PSS. A similar higher position of the first redox pair has been observed for other polymers, for example, Pani/PSS colloidal particles [38] and Pani/PSS halloysite nanocomposites [39].

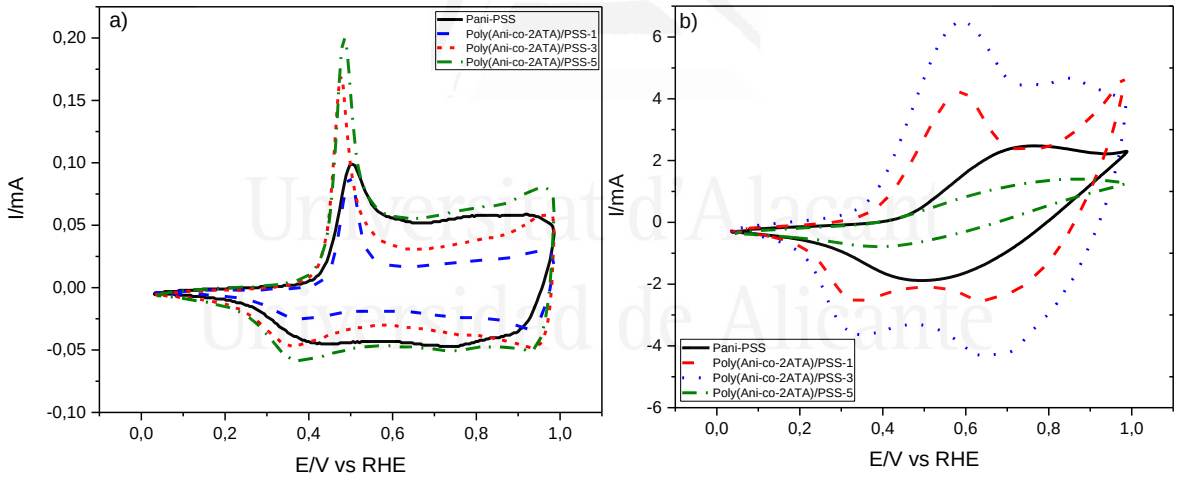

Figure 4.5. (a) cyclic voltammograms of dried Pani/PSS and poly(Ani-co-2ATA)/PSS-X hydrogels, and (b) cyclic voltammograms of wet hydrogels. Scan rate= 50 mV s^{-1} in all cases. 0.1 M $HClO_4$

3.2 Poly(Ani-co-PIP/PSS-X hydrogels

3.2.1 Transmission electron microscopy (TEM)

Figure 4.6 shows the TEM images of the hydrogels (Pani/PSS and poly(Ani-co-PIP)/PSS-X), in which a different morphology than that detected with the copolymer with 2ATA and Pani/PSS can be observed. In the present case, bars can be seen in the structure of the copolymer.

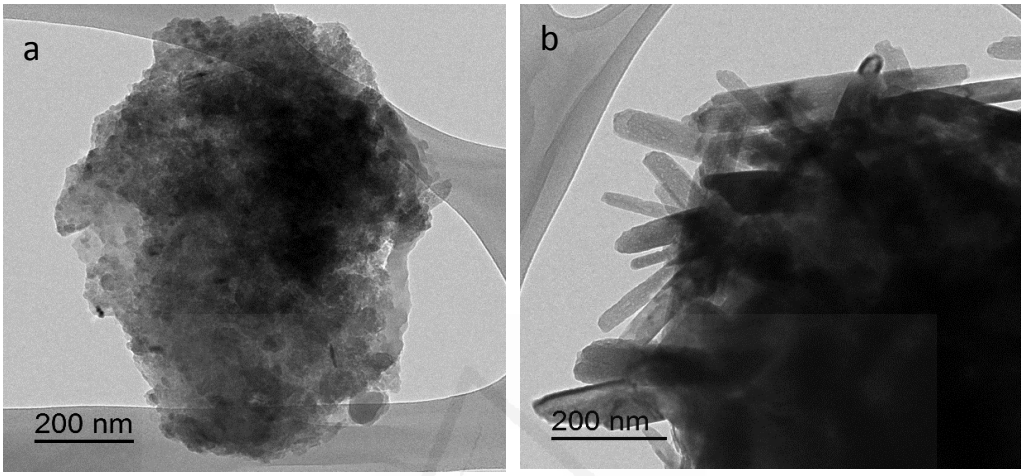

Figure 4.6. TEM images of the hydrogel: (a) Pani/PSS; (b) poly(Ani-co-PIP)/PSS.

3.2.2 Thermogravimetry

Figure 4.7 displays the TGA profiles of the poly(Ani-co-PIP)/PSS-X hydrogels. It can be observed that the behavior of all copolymer hydrogels is similar to that of Pani/PSS hydrogel, indicating that the piperazine monomer is incorporated into the copolymer in a low amount. Similar zones to those observed in Figure 4.2 for poly(Ani-co-PIP)/PSS hydrogels with low amount of 2ATA are observed for these poly(Ani-co-PIP)/PSS hydrogels. The Figure 4.7 shows that the amount of residue after the decomposition of the hydrogels is higher for the poly(Ani-co-PIP)/PSS-1, in which the amount of piperazine monomer is higher. These results confirm the incorporation of piperazine into the copolymer hydrogels (Table 4.5).

Table 4.5. Amount of residue after thermal decomposition of copolymer hydrogels.

Samples	Δw %
Pani/PSS	26.4
Poly(Ani-co-PIP)/PSS-1	35.8
Poly(Ani-co-PIP)/PSS-3	29.5
Poly(Ani-co-PIP)/PSS-5	30.7

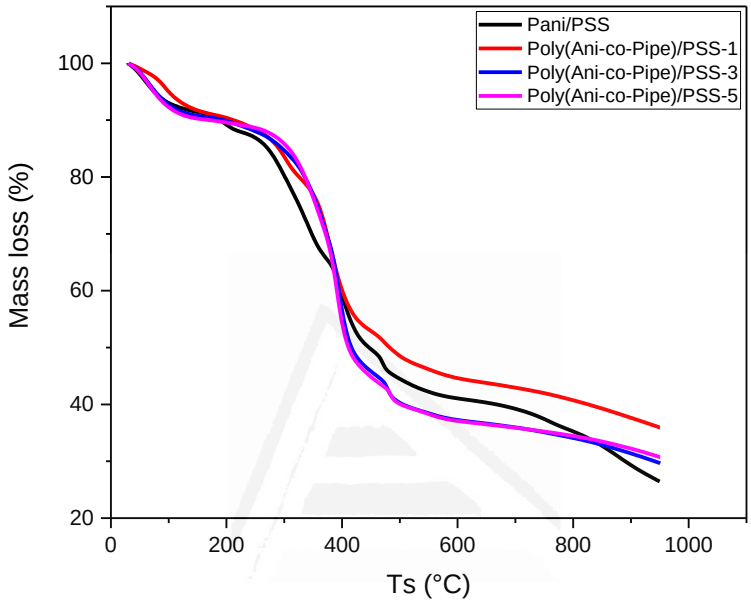

Figure 4.7. A thermogravimetric analysis curves for Pani/PSS and Poly(Ani-co-PIP)/PSS-X hydrogels

3.2.3 X-ray photoelectron spectroscopy (XPS)

To study the chemical composition of the different copolymer hydrogels, they were characterized by X-ray photoelectron spectroscopy (XPS). Table 4.6 shows the composition obtained for the different poly(Ani-co-PIP)/PSS-X hydrogels and differs from each other in their elemental composition. When the molar ratio decreases (that is, when the amount of aniline monomer decreases), the amount of nitrogen increases, which is in agreement with the increases in piperazine in the structure of the polymer.

Table 4.6. Composition of poly(Ani-co-PIP)/PSS-X and Pani/PSS obtained by XPS.

	XPS/ wt%			
Sample	**S**	**N**	**C**	**O**
Pani/PSS	4.25	5.13	74.9	15.7
Poly(Ani-co-PIP)/PSS-1	14,51	9,08	54,07	22,30
Poly(Ani-co-PIP)/PSS-3	16,97	4,74	52,01	26,25
Poly(Ani-co-PIP)/PSS-5	13,65	4,90	62,97	18,45

Figure 4.8 shows the C1s, O1s and S2p XPS spectra of the different poly(Ani-co-PIP)/PSS hydrogels. The C1s signal can be fitted with two characteristic peaks of carbon bonds. A large peak at 284.5 eV corresponded to aromatic carbon. Moreover, a contribution at 285.6 eV of quinonimine units and another contribution at 286.9 eV due to charged species of carbon bonded to positive nitrogen and a delocalized π–π* electron of the aromatic network in poly(Ani-co-PIP)/PSS (290.9 eV) were also detected [43–45]. The latter contribution is compatible with the presence of a small amount of carbonyl carbon, which was probably associated with the ketopiperazine centers [19]. Additionally, a high-resolution N1s core-level spectrum of poly(Ani-co-PIP)/PSS (Figure 4.8.c) appears noisier than C1s. The best curve fit for this element comprised at least two distinct nitrogen atoms at 399.4 eV and 401.7 eV which are attributed to C-N in the amine group and oxidized nitrogen, respectively [22,24,30]. The contribution around 400.6 eV, which could be assigned to the– NH_3^+ group resulting from the protonated secondary amine –NH, is discernable in the signal delivered by nitrogen photoelectrons [46,47]. Table 4.7 summarizes the proposed assignments for the observed signals obtained by XPS.

Regarding the S2p spectra in Figure 4.8.b, two separate peaks can be fitted, one at about 168.8 eV that corresponds to sulfur in the $-SO_3H$ group and arises from the presence of PSS in the hydrogel as reported in [48–50] [51]. [52].

Table 4.7. The percentage (%) of each species for different poly(Ani-co-PIP)/PSS hydrogels.

	Binding Energy (eV)								
	C1s				N1s			S2p	
(a)	284,57	285,61	286,66	288,84	399,47	401,30	402,51	167,84	//
(b)	284,63	285,29	286,43	//	399,41	401,66	//	167,92	169,28
(c)	284,63	285,81	286,98	//	399,55	401,89	400.65	167,84	169,13
(d)	284,56	285,66	286,94	290.96	399,45	401,83	400.62	167,77	169,89
Assignments	C–C C=C C–H C–S	C–N	C=N C–OH	C=O O=C– OH	=N–	–NH– –NC–	$-N^{+}-$ $=N^{+}-$	–S–C S=O	$-SO_4^{2-}$

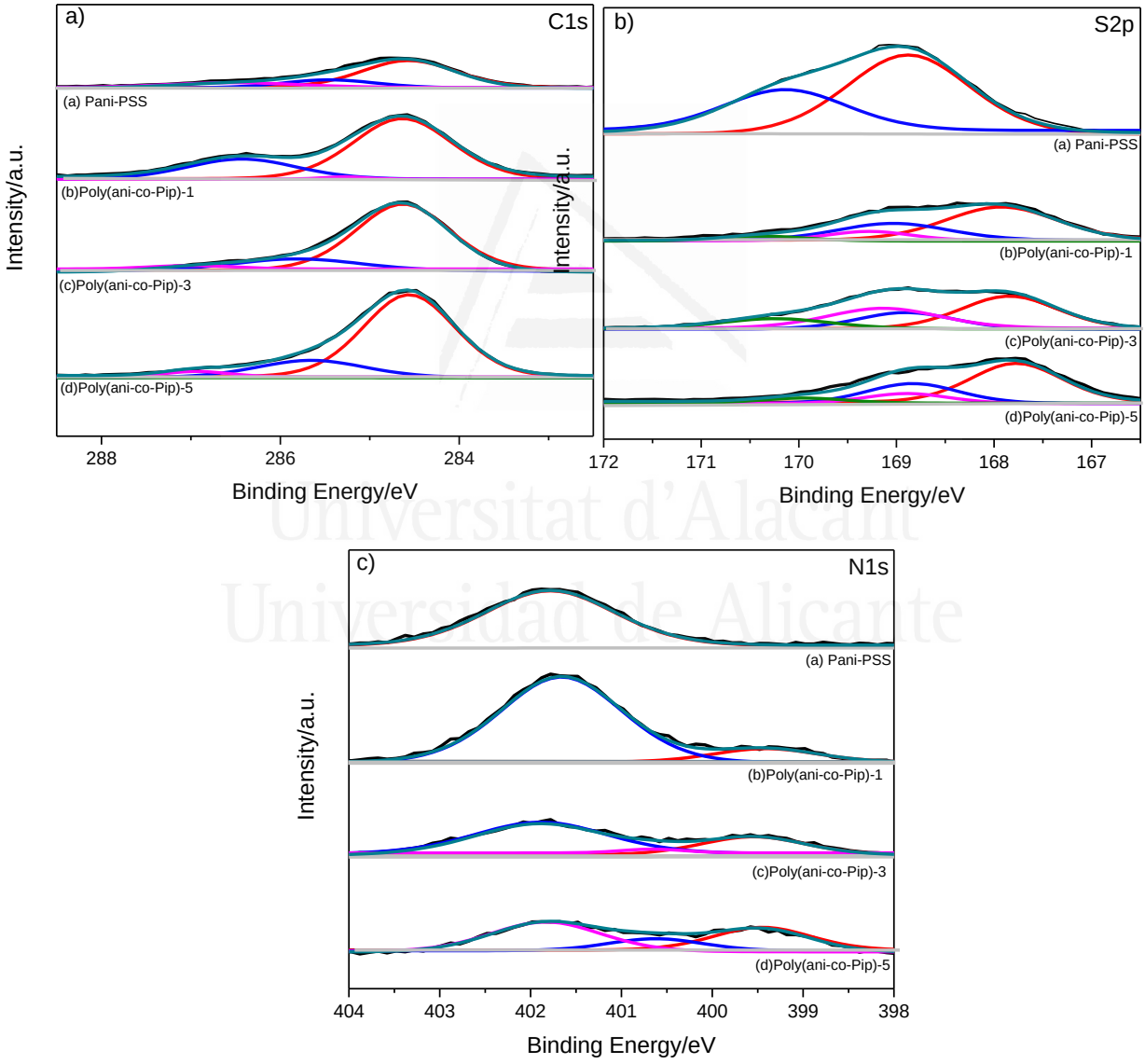

Figure 4.8. Deconvoluted a) C1s, b) S2p and c) N1s XPS of poly(Ani-co-PIP)/PSS-X copolymer hydrogels.

3.2.4 Swelling ratio

To estimate the swelling degree it was assumed that the freshly synthesized hydrogel is maximally swelled by water [4]. To obtain the quantity of water in the hydrogel, the wet and dried samples were weighed. The swelling ratio and the percentage of water loss in the Pani/PSS hydrogel and the hydrogel copolymers poly(Ani-co-PIP)/PSS are shown in Figure 9. The water content is thus very high in all hydrogels. Furthermore, the swelling capacity of the hydrogel and hydrogel copolymers is much higher and similar, as shown in Figure 9.a; and the water loss is clearly observed after 24h drying, as shown in Figure 4.9.b.

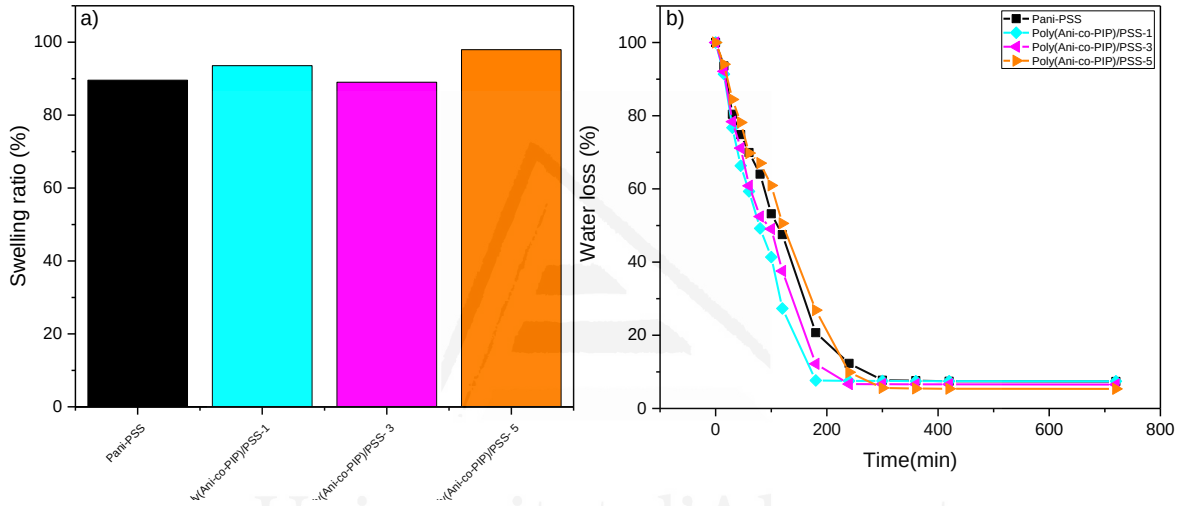

Figure 4.9. (a) Swelling ratios of the poly(Ani-co-PIP)/PSS-X hydrogels; (b) water loss percentage after 24h drying.

3.2.5 Electrochemical Characterization

Electrochemical characterization is utilized to estimate the electrochemical behavior of the dried hydrogel Pani/PSS and Poly(Ani-co-PIP)/PSS-X at different molar ratiosss in powder and characterized as suspension deposited on glassy carbon (Figure 4.10.b) and also in wet hydrogel (Figure 4.10.d); Figure 4.10 shows the cyclic voltammograms studied in 1 M $HClO_4$ in aqueous solution; the deposited material was tested in an acidic background solution that was free of any monomer species. Figure 4.10.b, shows CVs for the poly(Ani-co-PIP)/PSS-X hydrogels in aqueous solutions containing 0.1 M $HClO_4$. The shapes of the voltammograms of copolymer hydrogels (Figure 4.10 b) seems like a typical cyclic voltammogram of Pani films [34], the potential of the first redox process is equal to 0.5V/0.49V, and it can be assigned to a leucoemeraldine–emeraldine

transformation similar to the Pani. The second one, which is less intense, can be interpreted and related to the emeraldine–pernigraniline transition of the poly(Ani-co-PIP)/PSS hydrogel, which is similar to Pani/PSS under the same experimental conditions (solide line). The similarly shifted redox potentials are observed in cyclic voltammograms of oligoanilines [35]. Consequently, the differences between the redox potentials of the poly(Ani-co-PIP)/PSS copolymer hydrogel and Pani/PSS hydrogel suggest that copolymer hydrogels are composed of oligomeric species, there is two redox processes corresponding to the leucoemeraldine and emeraldine transition (first peak) and the emeraldine to pernigraniline transition (second peak). As shown in Figure 4.10.b the second redox peak may be related to the existence of redox transitions involving hydroxypiperazine ⇌ ketopiperazine species within the copolymer structure [19,53].

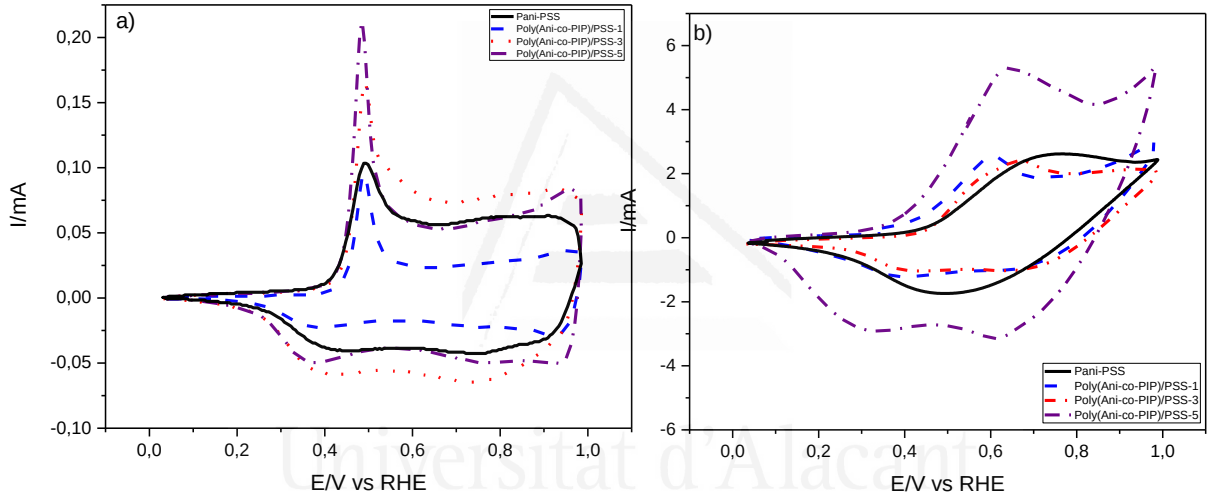

Figure 4.10. (a) cyclic voltammograms of dried Pani/PSS hydrogel (solid line) and poly(Ani-co-PIP)/PSS-X; (b) cyclic voltammograms of wet hydrogels. Scan rate= 50 mV s^{-1} in all cases. 0.1 M $HClO_4$

Figure 4.10.b shows the cyclic voltammograms of wet Pani/PSS hydrogel. It can be observed that the voltametric charge is relatively smaller than poly(Ani-co-PIP)/PSS hydrogel. The first redox peak is broader for Pani/PSS, suggesting that Pani chains with various lengths might be formed. The presence of slightly shorter Pani chains might also cause the shift in the position of the oxidation peak. The transformation of emeraldine into the fully oxidized pernigraniline occurs at 0.75 V. The middle redox pair is probably related to the phenazine sites [54,55]. The potential of the first couple is shifted in the anodic direction compared to typical electropolymerized Pani films, while the potential of the poly(Ani-co-PIP)/PSS is shifted in the cathodic direction by 0.6 V compared to

Pani/PSS hydrogel. A similar higher position of the first redox pair has been observed for other other authors for Pani/PSS materials, for example, Pani/PSS colloidal particles [38] and Pani/PSS halloysite nanocomposites [39].

Nevertheless, as shown in the CV of poly(Ani-co-PIP)/PSS hydrogel, the shape of the CV is rather similar to that of the Pani/PSS hydrogels. In the case of the poly(Ani-co-PIP)/PSS hydrogels, it is found that the two peaks shift, which is caused by the influence of the neighboring groups of piperazine on the Pani/PSS hydrogels [56]. Figure 4.10.a shows that the introduction of piperazine in the polymer influences the electrochemical redox process. The samples of poly(Ani-co-PIP)/PSS hydrogel at different molar ratios exhibit a single redox processes centered near 0.6 V, but the charge of the redox process differs significantly when the molar ratio increase. Such differences might be explained by various ion-exchange properties and the differences in the structure of the hydrogels.

3.2.6 Conductivity

Table 4.8 shows the conductivity obtained with the different poly(Ani-co-PIP)/PSS-X hydrogels. It can be observed that the conductivity increases in comparison to Pani/PSS. Therefore, the higher content of PIP increases the conductivity of the poly(Ani-co-PIP)/PSS-X hydrogel.

Table 4.8. Conductivity of poly(Ani-co-PIP)/PSS-X and Pani/PSS hydrogels.

Sample	**Conductivity S·cm^{-1}**
Pani/PSS	0.787
Poly(Ani-co-PIP)/PSS-1	1.458
Poly(Ani-co-PIP)/PSS-3	1.078
Poly(Ani-co-PIP)/PSS-5	1.756

4 Conclusion

Conducting polymer hydrogels represent an emerging class of materials with a high application potential, especially in energy conversion and storage, but also in many other applications. Conducting polymers, such as Pani, provide electronic conductivity, and redox activity; moreover, the aqueous phase in the hydrogel ensures ionic conductivity and the resulting combination of properties is unique. This chapter has described an effective approach for the fabrication of conducting polymer hydrogels based on Pani via supramolecular self-assembly. The study of the chemical structure of copolymer hydrogels (poly(Ani-co-2ATA)/PSS and poly(Ani-co-PIP)/PSS) and their characterization with a combination of X-ray photoelectron spectroscopy (XPS)

shed more light on the chemical surface of synthesized materials. The electrochemical characterizaion were used to characterize the redox behavior of the copolymer hydrogels and their electroactivity in acid medium. Finally, the conductive properties of the copolymer hydrogels were tested to compare the electrical conductivity between the following hydrogels. In the case of poly(Ani-co-2ATA)/PSS-X the conductivity is lower than in the case of Pani/PSS as consequence of the presence of carboxylic groups in the Pani; however, in the case of poly(Ani-co-PIP)/PSS-X the conductivity is higher than Pani/PSS. The mass swelling ratio of the different copolymer hydroges was measured by comparing the hydrated weight with the dehydrated weight and compare with Pani/PSS. Thermogravimetric analyses (TGAs) were also performed with the aim of evaluating the thermal stability of the hydrogel copolymers, which are very important for the potential application of these materials.

5 References

[1] J. Stejskal, Conducting polymer hydrogels, Chem. Pap. 2017, 71, 269–291. doi:10.1007/s11696-016-0072-9.

[2] J. Stejskal, O.E. Bogomolova, N. V. Blinova, M. Trchová, I. Šeděnková, J. Prokeš, I. Sapurina. Mixed electron and proton conductivity of polyaniline films in aqueous solutions of acids: Beyond the 1000 S cm_{-1} limit. Polym. Int. 2009, 58, 872–879. doi:10.1002/pi.2605.

[3] A. Malti, J. Edberg, H. Granberg, Z.U. Khan, J.W. Andreasen, X. Liu, D. Zhao, H. Zhang, Y. Yao, J.W. Brill, I. Engquist, An Organic Mixed Ion – Electron Conductor for Power Electronics. 2016, 3, 1–9. doi:10.1002/advs.201500305.

[4] A. Jab, B. Pa, Effect of the polymerization bath on structure and electrochemical properties of polyaniline-poly (styrene sulfonate) hydrogels, 2017, 784, 115–123. doi:10.1016/j.jelechem.2016.11.050.

[5] T. Dai, Y. Jia, Supramolecular hydrogels of polyaniline-poly (styrene sulfonate) prepared in concentrated solutions, Polymer (Guildf). 2011, 52, 2550–2558. doi:10.1016/j.polymer.2011.04.006.

[6] J. Sun, W.W. Gerberich, L.F. Francis. Transparent, conductive polymer blend coatings from latex-based dispersions, Prog. Org. Coatings. 2007, 59, 115–121. doi:10.1016/j.porgcoat.2007.01.019.

[7] J. Arias-Pardilla, H.J. Salavagione, C. Barbero, E. Morallón, J.L. Vázquez, Study of the chemical copolymerization of 2-aminoterephthalic acid and aniline. Synthesis and copolymer properties. Eur. Polym. J. 2006, 42, 1521–1532. doi:10.1016/j.eurpolymj.2006.02.003.

[8] M. Abidi, S. López-Bernabeu, F. Huerta, F. Montilla, S. Besbes-Hentati, E. Morallón. Spectroelectrochemical study on the copolymerization of o-aminophenol and aminoterephthalic acid. Eur. Polym. J. 2017, 91, 386–395. doi:10.1016/j.eurpolymj.2017.04.024.

[9] D. Gu, G. Yang, Y. He, B. Qi, G. Wang, Z. Su. Triphenylamine-based pH chemosensor : Synthesis , crystal structure, photophysical properties and computational studies. Synth. Met. 2009, 159, 2497–2501. doi:10.1016/j.synthmet.2009.08.040.

[10] S. Dkhili, S. López-bernabeu, F. Huerta, F. Montilla, S. Besbes-hentati, E. Morallón. A self-doped polyaniline derivative obtained by electrochemical copolymerization of aminoterephthalic acid and aniline, Synth. Met. 2018, 245, 61–66. doi:10.1016/j.synthmet.2018.08.005.

[11] M. Wikström, P. Holmgren, J. Ahlner, A2 (N-Benzylpiperazine) a New Drug of Abuse in Sweden. J. Anal. Toxicol. 2004, 28, 67–70. doi:10.1093/jat/28.1.67.

[12] D. De Boer, I.J. Bosman, E. Hidvégi, C. Manzoni, A.A. Benkö, L.J.A.L. Dos Reys, R.A.A. Maes. Piperazine-like compounds: A new group of designer drugs-of-abuse on the European market, Forensic Sci. Int. 2001, 121, 47–56. doi:10.1016/S0379-0738(01)00452-2.

[13] M. Yarim, M. Koksal, I. Durmaz, R. Atalay. Cancer Cell Cytotoxicities of 1-(4-Substitutedbenzoyl)-4-(4-chlorobenzhydryl)piperazine Derivatives. Int. J. Mol. Sci. 2012, 13, 8071–8085. doi:10.3390/ijms13078071.

[14] S.Ikeda,T.Yoshioka,S.Nankai, Biosensor and method for quantitative measurement of a substrate using the same, Google Patents, 1999.

[15] C.S. Ananda Kumar, S. Nanjunda Swamy, N.R. Thimmegowda, S.B. Benaka Prasad, G.W. Yip, K.S. Rangappa. Synthesis and evaluation of 1-benzhydryl-sulfonyl-piperazine derivatives as inhibitors of MDA-MB-231 human breast cancer cell proliferation, Med. Chem. Res. 2007, 16, 179–187. doi:10.1007/s00044-007-9022-y.

[16] N. Jamai, M. Rzaigui, S.A. Toumi, Piperazine-1,4-diium bis(hexahydroxidoheptaoxidohexaborato- κ3O,O′,O″)cobaltate(II) hexahydrate, Acta Crystallogr. Sect. E Struct. Reports Online. 2014, 70. doi:10.1107/S1600536814007090.

[17] L. Zhang, X.M. Peng, G.L.V. Damu, R.X. Geng, C.H. Zhou. Comprehensive Review in Current Developments of Imidazole-Based Medicinal Chemistry. Medicinal Research Reviews, Med. Res. Rev. 2013, 34, 340–437. doi:doi:10.1002/med.21290.

[18] R. Ramachandran, S. Balasubramanian, G. Aridoss, P. Parthiban. Polymer Synthesis and studies of semiconducting piperazine – aniline copolymer. 2006, 42, 1885–1892. doi:10.1016/j.eurpolymj.2006.02.010.

[19] S. Dkhili, S. López-Bernabeu, C.N. Kedir, F. Huerta, F. Montilla, S. Besbes-Hentati, E. Morallon. An electrochemical study on the copolymer formed from piperazine and aniline monomers, Materials (Basel). 2018, 11, 1012 . doi:10.3390/ma11061012.

[20] M.C.G. and S.S. Umare, Studies on Poly(o-methoxyaniline). Macromolecules. 1992, 25, 138–142. doi:doi:10.1021/ma00027a023.

[21] M. Khaldi, A. Benyoucef, C. Quijada, A. Yahiaoui, E. Morallon. Synthesis, Characterization and Conducting Properties of Nanocomposites of Intercalated 2-Aminophenol with Aniline in Sodium-Montmorillonite. J Inorg Organomet Polym. 2014, 267–274. doi:10.1007/s10904-013-9998-3.

[22] M. González-Torres, M.G. Olayo, G.J. Cruz, L.M. Gómez, V. Sánchez-Mendieta, F. González-Salgado, XPS Study of the Chemical Structure of Plasma Biocopolymers of Pyrrole and Ethylene Glycol, Adv. Chem. 2014, 2014, 1–8. doi:10.1155/2014/965920.

[23] L.P. Dong, C. Deng, R.M. Li, Z.J. Cao, L. Lin, L. Chen, Y.Z. Wang, Poly(piperazinyl phosphamide): A novel highly-efficient charring agent for an EVA/APP intumescent flame retardant system. RSC Adv. 2016, 6, 30436–30444. doi:10.1039/C6RA00164E.

[24] P. Rannou, D. Rouchon, Y.F. Nicolau, M. Nechtschein, A. Ermolieff, Chemical degradation of aged CSA-protonated PANI films analyzed by XPS, Synth. Met. 1999, 101, 823–824. doi:10.1016/S0379-6779(98)01186-2.

[25] J. Quílez-bermejo, A. Ghisolfi, D. Grau-marín, E. San-fabián, E. Morallón, D. Cazorla-amorós, Post-synthetic efficient functionalization of polyaniline with phosphorus- containing groups. Effect of phosphorus on electrochemical properties, Eur. Polym. J. 2019, 119 272–280. doi:10.1016/j.eurpolymj.2019.07.048.

[26] F. Quintero-jaime, D. Cazorla-amor, E. Morall, Electrochimica Acta Electrochemical functionalization of single wall carbon nanotubes with phosphorus and nitrogen species, 2020, 340. doi:10.1016/j.electacta.2020.135935.

[27] L. Zhang, M. Wan, Synthesis and characterization of self-assembled polyaniline nanotubes doped with D-10-camphorsulfonic acid, in: Nanotechnology, 2002, 750–755. doi:10.1088/0957-4484/13/6/311.

[28] S. Trakhtenberg, Y. Hangun-Balkir, J.C. Warner, F.F. Bruno, J. Kumar, R. Nagarajan, L.A. Samuelson, Photo-cross-linked Immobilization of Polyelectrolytes for Enzymatic Construction of Conductive Nanocomposites, J. Am. Chem. Soc. 2005, 127, 9100–9104. doi:10.1021/ja042438v.

[29] L.J. Bredas, S. Stafstrom, A.J. Epstein, H.S. Woo, B.D. Tanner, W. Huang, A.G. MacDiarmid, Polaron lattice in highly conducting PANI: optical and theoretical studies, Phys. Rev. Lett. 59, 1987.

[30] Y. Wu, Y.X. Chen, J. Yan, D. Quinn, P. Dong, S.W. Sawyer, P. Soman, Fabrication of conductive gelatin methacrylate-polyaniline hydrogels, Acta Biomater. 2016, 33, 122–130. doi:10.1016/j.actbio.2016.01.036.

[31] K. Xu, K. Li, P. Khanchaitit, Q. Wang, Synthesis and characterization of self-assembled sulfonated poly (styrene-b-vinylidene fluoride-b-styrene) triblock copolymers for proton conductive membranes, Chem. Mater. 2007, 19, 5937–5945. doi:10.1021/cm071626s.

[32] A. Słoniewska, B. Pałys, Supramolecular polyaniline hydrogel as a support for urease, Electrochim. Acta. 2014, 126, 90-97. doi:10.1016/j.electacta.2013.10.164.

[33] C. Sanchís, H.J. Salavagione, J. Arias-Pardilla, E. Morallón, Tuning the electroactivity of conductive polymer at physiological pH, Electrochim. Acta. 2007, 52, 2978–2986. doi:10.1016/j.electacta.2006.09.031.

[34] B. Pałys, P. Celuch, Redox transformations of polyaniline nanotubes. Cyclic voltammetry, infrared and optical absorption studies, Electrochim. Acta. 2006, 51, 4115–4124. doi:10.1016/j.electacta.2005.11.030.

[35] D. Chao, L. Cui, Z. Li, X. Lu, H. Mao, W. Zhang, Y. Wei, Electroactive copolymers with oligoanilines in the main chain via oxidative coupling polymerization, Macromol. Chem. Phys. 2006, 207, 1691–1696. doi:10.1002/macp.200600280.

[36] J. Arias-Pardilla, H.J. Salavagione, C. Barbero, E. Morallón, J.L. Vázquez, Study of the chemical copolymerization of 2-aminoterephthalic acid and aniline. Synthesis and copolymer properties. Eur. Polym. J. 2006, 42, 1521–1532. doi:10.1016/j.eurpolymj.2006.02.003.

[37] J. Yue, Z.H. Wang, K.R. Cromack, A.J. Epstein, A.G. MacDiarmid. Effect of Sulfonic Acid Group on Polyaniline Backbone. J. Am. Chem. Soc. 1991, 113 2665–2671. doi:10.1021/ja00007a046.

[38] M.K. Park, K. Onishi, J. Locklin, F. Caruso, R.C. Advincula, Self-assembly and characterization of polyaniline and sulfonated polystyrene multilayer-coated colloidal particles and hollow shells. Langmuir. 2003, 19, 8550–8554. doi:10.1021/la034827t.

[39] H. Huang, J. Yao, H. Chen, X. Zeng, C. Chen, X. She, L. Li, Facile preparation of halloysite/polyaniline nanocomposites via in situ polymerization and layer-by-layer assembly with good supercapacitor performance, J. Mater. Sci. 2016, 51, 4047–4054. doi:10.1007/s10853-016-9724-y.

[40] G. Socrates, Infrared and Raman characteristic group frequencies. Tables and charts, Third edit, Wiley and Sons, Ltd., Chichester, 2001. doi:10.1002/jrs.1238.

[41] V.P. Pattar, P.A. Magdum, D.G. Patil, S.T. Nandibewoor, Thermodynamic, kinetic and mechanistic investigations of Piperazine oxidation by Diperiodatocuprate(III) complex in aqueous alkaline medium, J. Chem. Sci. 2016, 128, 477–485. doi:10.1007/s12039-016-1044-x.

[42] J. Ostrowska, A. Narebska, Infrared study of hydration and association of functional groups in a perfluorinated Nafion membrane, Part 1, Colloid Polym. Sci. 1983, 261, 93–98. doi:10.1007/BF01410686.

[43] H.S.O. Chan, S.C. Ng, W.S. Sim, K.L. Tan, B.T.G. Tan. Preparation and Characterization of Electrically Conducting Copolymers of Aniline and Anthranilic Acid: Evidence for Self-Doping by X-ray Photoelectron Spectroscopy. Macromolecules. 1992, 25, 6029–6034. doi:10.1021/ma00048a026.

[44] R. Rajagopalan, J.O. Iroh. Characterization of polyaniline-polypyrrole composite coatings on low carbon steel: A XPS and infrared spectroscopy study. Appl. Surf. Sci. 2003, 218, 58–69. doi:10.1016/S0169-4332(03)00579-8.

[45] J.S. Stevens, S.J. Byard, S.L.M. Schroeder. Characterization of Proton Transfer in Co-Crystals by X-ray Photoelectron Spectroscopy (XPS), Cryst. Growth Des. 2010, 10, 1443–1450. doi:10.1021/cg901545k.

[46] J.S. Stevens, S.J. Byard, C.C. Seaton, G. Sadiq, R.J. Davey, S.L.M. Schroeder, Proton transfer and hydrogen bonding in the organic solid state: A combined XRD/XPS/ssNMR study of 17 organic acid-base complexes, Phys. Chem. Chem. Phys. 2014, 16, 1150–1160. doi:10.1039/c3cp53907e.

[47] J.S. Stevens, L.K. Newton, C. Jaye, C.A. Muryn, D.A. Fischer, S.L.M. Schroeder, Proton transfer, hydrogen bonding, and disorder: Nitrogen near-edge X-ray absorption fine structure and X-ray photoelectron spectroscopy of bipyridine-acid salts and co-crystals, Cryst. Growth Des. 2015, 15 1776–1783. doi:10.1021/cg5018278.

[48] M. Liu, S. Jia, Y. Gong, C. Song, X. Guo, Effective hydrolysis of cellulose into glucose over sulfonated sugar-derived carbon in an ionic liquid, Ind. Eng. Chem. Res. 2013, 52, 8167–8173. doi:10.1021/ie400571e.

[49] K.S. Siow, L. Britcher, S. Kumar, H.J. Griesser. XPS study of sulfur and phosphorus compounds with different oxidation states. Sains Malaysiana. 2018, 47, 1913–1922. doi:10.17576/jsm-2018-4708-33.

[50] J.W. Han, H. Lee, Direct conversion of cellulose into sorbitol using dual-functionalized catalysts in neutral aqueous solution, Catal. Commun. 2012, 19, 115–118. doi:10.1016/j.catcom.2011.12.032.

[51] G. Zotti, S. Zecchin, G. Schiavon, F. Louwet, L. Groenendaal, X. Crispin, W. Osikowicz, W. Salaneck, M. Fahlman. Electrochemical and XPS studies toward the role of monomeric and polymeric sulfonate counterions in the synthesis, composition, and properties of poly(3,4-ethylenedioxythiophene). Macromolecules. 2003, 36, 3337–3344. doi:10.1021/ma021715k.

[52] M. Kozłowski. XPS study of reductively and non-reductively modified coals. Fuel. 2004, 83,

259–265. doi:10.1016/j.fuel.2003.08.004.

[53] J.L. Owens, G. Dryhurst, Electrochemical reduction of tetraketopiperazine. Anal. Chim. Acta. 1976, 87, 37–50. doi:10.1016/S0003-2670(01)83118-4.

[54] P.N. Bartlett, P.R. Birkin, F. Palmisano, G. De Benedetto. A study on the direct electrochemical communication between horseradish peroxidase and a poly(aniline) modified electrode. J. Chem. Soc. - Faraday Trans. 1996, 92, 3123–3130. doi:10.1039/ft9969203123.

[55] E.M. Geniès, M. Lapkowski, J.F. Penneau. Cyclic voltammetry of polyaniline: interpretation of the middle peak. J. Electroanal. Chem. 1988, 249, 97–107. doi:10.1016/0022-0728(88)80351-6.

[56] C. Dispenza, C. Lo Prsti, C. Belfiore, G. Spadaro, S. Piazza, Electrically conductive hydrogel composites made of polyaniline nanoparticles and poly(N-vinyl-2-pyrrolidone), Polymer (Guildf). 2006, 47, 961–971. doi:10.1016/j.polymer.2005.12.071.

Chapter 5

Hybrid Supercapacitors from Supramolecular Hydrogels

1 Introduction

Electrochemical energy storage devices such as batteries and supercapacitors have attracted considerable attention from the scientific community due to the rapidly increasing demand for energy from green renewable technologies [2]. Batteries and fuel cells have a high specific energy density but a relatively low specific power density. The development of electrode materials with large surface area, electroactive functional groups and high electrochemical stability is crucial for the improvement of the energy density and durability of these devices [3,4]. The preparation method of conducting polymer hydrogels (CPHs) and their specific application components in supercapacitors can be used to provide high power [5] in a short time when vehicles accelerate, and to recover energy when they brake [6,7]. Conducting polymers (CPs) can be used as electrode materials in supercapacitors [8]. Given their redox properties, they have been employed as electrode materials in rechargeable batteries since the 1980s [9]. Among CPs, polyaniline (Pani) has received much attention from researchers, as its properties include electrical conductivity, electrochemical activity, ease of synthesis and low cost. However, this material undergoes volume changes due to the diffusion of ions inside its structure, which means it has poor mechanical properties and its cycle stability is reduced [8]. Conducting polymer hydrogels are gels containing a conducting polymer along with a supporting polymer as components, and they are swollen with water or electrolyte solutions [10]. Polyaniline, polypyrrole, and exceptionally poly(3,4-ethylenedioxythiophene) (PEDOT) are currently used as conductive part, while water-soluble cross-linked polymers on the other part [11]. Such hydrogels are obtained by the oxidation of monomers in the presence of an anionic polyelectrolyte [12]. The hydrogel formation depends on the concentration of the monomer, oxidant and polyanion. Reagent concentrations that are too low yield colloidal solutions of complexes of polyaniline (Pani) and polyanion [13,14]. It was found that ATA monomers were four times less reactive than aniline under chemical polymerization conditions, because of the deactivating effect of the carboxylic group attached to the aromatic ring. This makes the formation of ATA homopolymers

very difficult. The copolymerization with aniline controlling the monomer ratio was a key parameter to obtain a true copolymerization product and to modulate the composition and properties of the material [15].

On the other hand, the chemical copolymerization of aniline and piperazine was studied by Ramachandran et al [16]. The present chapter will study the application of the different hydrogels prepared in the previous chapter as electrodes in capacitors in aqueous solution.

2 Experimental part

2.1 Materials

Aminoterephthalic acid, piperazine and polytetrafluoroethylene (PTFE) were provided by Sigma-Aldrich. Multiwall carbon nanotubes (MWCNTs) were obtained from Cheap Tubes and Vulcan XC-72 CABOT. Sulfuric acid (H_2SO_4) was obtained from Merck. The ultrapure water (18.2 MΩ cm) employed in all the experiments was obtained from a Millipore MilliQ system.

2.2 Electrochemical characterization

The electrochemical characterization of the different hydrogel materials was done using a standard three-electrode cell configuration. Ag/AgCl/KCl (3M) was used as reference electrode in all cases. The different samples have been called poly(Ani-co-2ATA)/PSS-X and poly(Ani-co-PIP)/PSS-X, X being the ratio of both monomers (1, 3 or 5). The hydrogel containing only aniline (Pani/PSS) has also been studied.

The electrochemical characterization of all samples was done by cyclic voltammetry (CV) using a Biologic VSP 300 potentiostat at different scan rates. For the electrochemical characterization of the two-electrode cell symmetric capacitors an Arbin SCTS potentiostat was used, and the galvanostatic charge-discharge measurements at various current densities were performed at 0.8 V.

Symmetric capacitors (in mass) were assembled for the different hydrogels. Current density and specific capacitance were defined based on the total weight of the active material included in both electrodes. The energy density and power density were calculated as described elsewhere [17]. The measurements were repeated twice.

The specific capacitance of the different hydrogel materials was calculated from the voltammogram obtained in the three-electrode cell, according to the following equations:

$$Q = \int_{E0}^{E} I\, dt \qquad (1)$$

Where Q is the charge calculated in the voltammogram (C), I is the current (A), E and E_0 are the potentials at the limit of the voltammogram, and t is the time (s). Then,

$$C_g = Q/m\Delta U \qquad (2)$$

Where C_g (F g^{-1})is the specific capacitance, *v* is the scan rate, *m* (g) is the mass of electroactive material in the electrode, and ΔU (V) is the potential window ($E-E_0$) used in the determination of the voltammetric charge.

The specific capacitance Cg (F g^{-1}) of the symmetric capacitors prepared with the hydrogels has been calculated from galvanostatic charge-discharge profiles obtained with the two-electrode cell as follows:

$$C_g = It/(m\Delta U) \qquad (3)$$

In which *I* is the constant current (A), *m* (g) is the total mass of the two electrodes, *U* (V) is the voltage, and *t* (s) is the discharge time. The volumetric capacitance (C_v) was calculated considering the dimensions of the electrodes.

$$C_v = It/V$$

Where V is the volume of one electrode.

The energy density values *E* (W h kg^{-1}) of half cells and supercapacitors were calculated by the integration of the graph during the discharge process according to the following formula:

$$E = \int U dQ \qquad (4)$$

In which *U* (V) is the voltage and Q is the charge in the discharge process.

The power density values *P* (W kg^{-1}) of half cells and supercapacitors were calculated according to the equation:

$$P = E/t \qquad (5)$$

In which *t* (s) is the discharge time.

2.3 Preparation of the symmetrical two-electrode cell capacitors

Symmetric capacitors were constructed by pressing two electrodes against each other and separating them by a nylon membrane filter (pore size: 320 nm). The method used is shown in Figure 5.1. The electrodes were prepared by mixing the hydrogel material with a binder and a conductivity promoter. The weight ratio of each of them is the following: the hydrogel copolymers poly(Ani-co-2ATA)/PSS and poly(Ani-co-PIP)/PSS (in powder form) (97 wt%) were mixed with 3 wt% polytetrafuorethylene (PTFE) as binder in a ratio of 97:3 (w/w). Thus, the total weight of the electrode is around 12 mg. Another composition was 92 wt% of hydrogel copolymer powder, 3 wt%

polytetrafuorethylene (PTFE), and 5 wt% of conductivity promoter as multiwall carbon nanotubes (MWCNTs) or carbon black (Vulcan XC-72) in a ratio of 92:3:5 (w/w). The weight of the electrodes was around 8 mg. The electrodes were attached to a stainless steel collector by using a conducting adhesive (Figure 1). The size of the electrodes was around 6 mm in diameter and 150 µm in thickness.

2.4 Preparation of electrolyte

Using aqueous electrolytes for a supercapacitor makes it more environment-friendly compared to those where organic electrolytes are employed.

1M sulfuric acid was used as electrolyte. It was prepared in 20 ml of distilled water by putting one drop on a nylon membrane. The membrane is a separator, the disc film electrode that will be attached to the current collector.

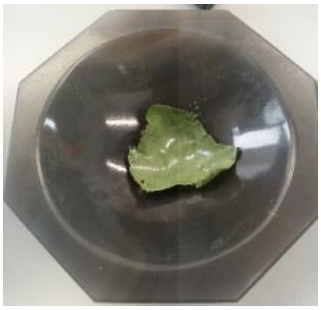

(a)Forming the film electrode

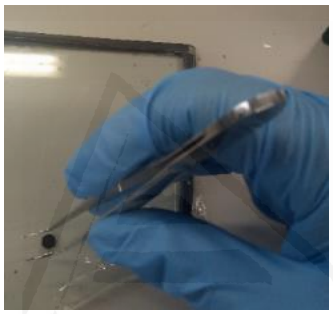

(b) disc film electrode

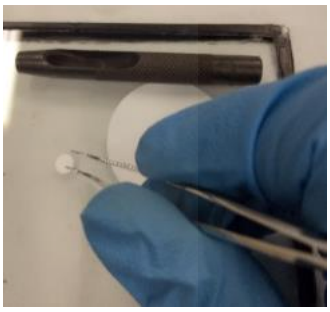

(c) nylon separator membrane.

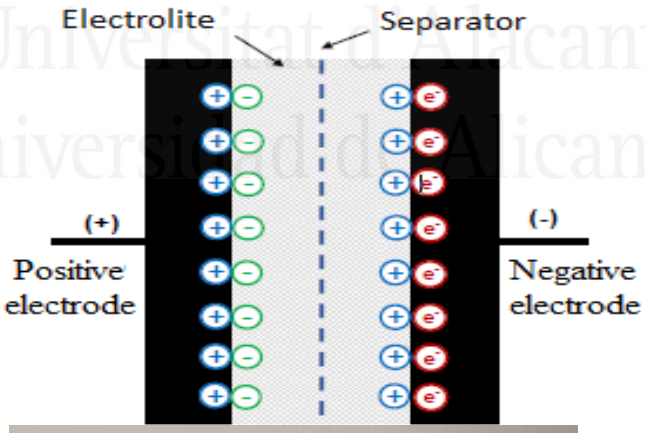

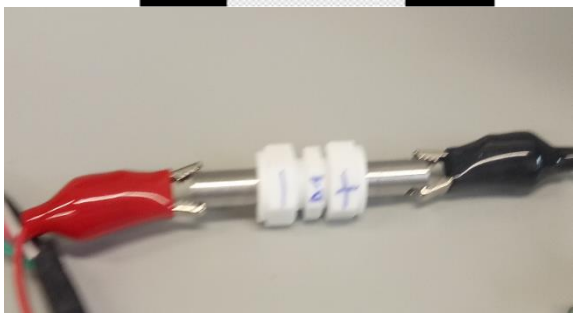

Figure 5.1. Building a cell with two electrodes.

3 Results and discussion

3.1 Poly(Ani-co-2ATA)/PSS-X hydrogels

3.1.1 Electrochemical characterization ofthe poly(Ani-co-2ATA)/PSS-X hydrogels

The Pani/PSS hydrogel and copolymer hydrogels were fabricated without using any binders and could be directly employed to carry out electrochemical measurements with a conventional three-electrode system. Figure 5.2 shows the cyclic voltammograms studied in the 1 M H_2SO_4 aqueous solution for the different poly(Ani-co-2ATA)/PSS-X hydrogels. The hydrogel materials were tested in an acidic solution that was free of any monomer species; the comparison between the Pani/PSS hydrogel and the poly(Ani-co-2ATA)/PSS-X hydrogel electrodes was done at several scan rates, ranging from 5 to 500 mV s^{-1}. The CV curve shows the redox peaks associated with the redox processes of polyaniline-type polymers, suggesting that the capacitance mainly consists of redox processes of Pani [18]. The representative redox peaks, which are ascribed to the transformation between leucoemeraldine base (LB), emeraldine salt (ES), and pernigraniline base (PB), are clearly observed in the voltammograms. No deviation of the potential peaks is observed even at high scan rates (500 mV/s), indicating their fast rate capability [19]. By comparing the CV curves of all the hydrogel copolymers, it can be seen that the voltammetric charge of poly(Ani-co-2ATA)/PSS-5 is the largest, indicating the highest specific capacitance of this sample. Moreover, the redox processes are clearly obtained even at high scan rates. With increased scan rates, the cathodic peaks right-shift to higher voltages, and the anodic peaks shift to lower values. This is due to the large time constant (t=RC) determined by the large resistance or capacitance, due to the pseudo-reversible redox kinetics of Pani [18,20]. The increased aniline content could bring about a significant increment of current density and a corresponding increase in capacitance. However, with the increased scan rate, the capacitance of hydrogel electrodes fabricated with different molar ratios (1;3;5) decreases sharply and delivers poor rate capability (capacitance retention of 1.48%) [18].

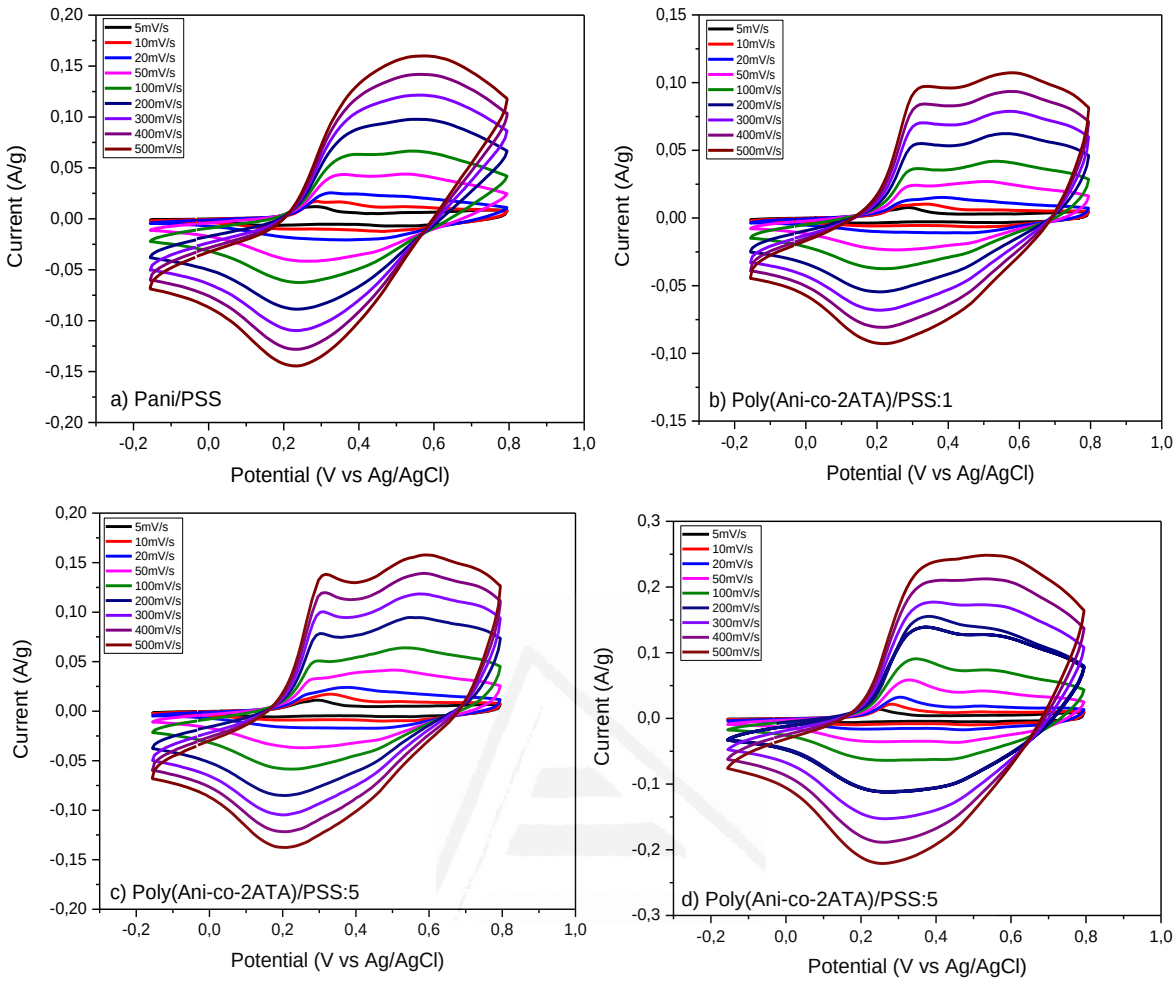

Figure 5.2. Voltammograms for (a) Pani/PSS, (b) poly(Ani-co-2ATA)/PSS-1, (c) poly(Ani-co-2ATA)/PSS-3 and (d) poly(Ani-co-2ATA)/PSS-5 electrodes deposited on glassy carbon at different scan rates ranging from 5 mV s^{-1} to 500 mV s^{-1}. 1 M H_2SO_4 solution.

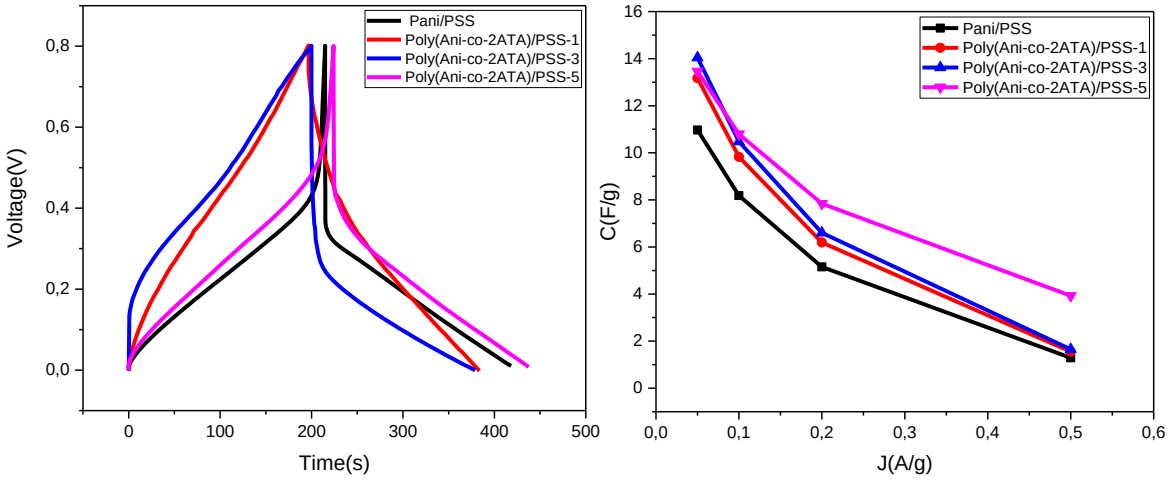

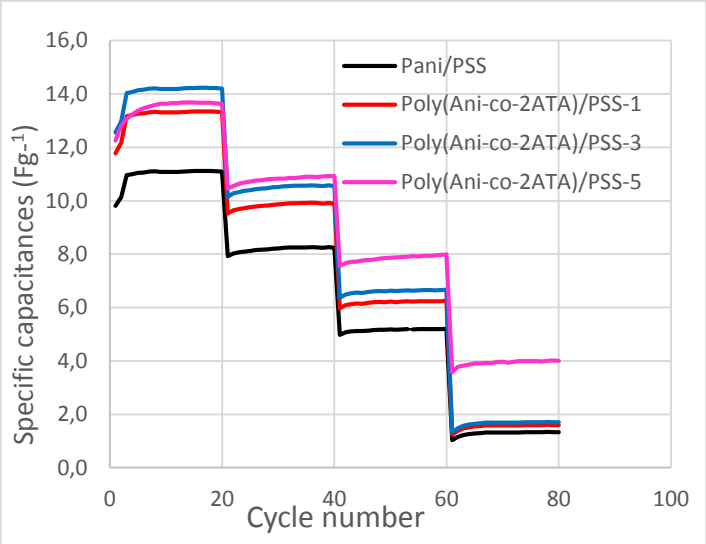

Figure 5.3. (a) Galvanostatic charge-discharge profiles of Pani/PSS and poly(Ani-co-2ATA)/PSS-X symmetric capacitors at 0.05 A g^{-1}. 1 M H_2SO_4 solution; (b) specific capacitances of Pani/PSS and poly(Ani-co-2ATA)/PSS-X capacitors versus current densities; (c) discharge-charge capacitances versus cycle numbers tested at different current densities. 1 M H_2SO_4.

3.1.2 Symmetric capacitors prepared with poly(Ani-co-2ATA)/PSS-X hydrogels

The characterization of the symmetric capacitors by chronopotentiometry was carried out to further study the specific capacitance and rate performance of the Pani/PSS and hydrogel copolymer electrodes. Figure 5.3a shows the galvanostatic charge-discharge curves of the different capacitors called poly(Ani-co-2ATA)/PSS-X and the aniline hydrogel (Pani/PSS) at 0.05 A/g. The diffusion of ions through the hydrogels is different depending of the interactions of the aniline monomer with the aminoterephthalic acid and piperazine monomers. It plays a key role in controlling the supercapacitive performance [21]. The resistance (IR) drops in these GCD curves are very important, owing to the low conductivity of the hydrogels, which is probably a consequence of the high amount of PSS. The corresponding specific capacitances at different specific currents are shown in Figure 5.3.b. At 0.05 A/g a similar value of specific capacitance around 38 F/cm^3 is obtained for the capacitors prepared with the copolymer hydrogels; this value is higher than that obtained with the symmetric capacitor prepared with Pani/PSS (33 F/cm^3). These values are lower than those of all previously reported Pani-based electrodes [2,22]. Table 5.1 shows the values of capacitance, energy density, maximum power density and energy for the different capacitors. The values are very low and very small differences are observed between the four symmetric capacitors, indicating that the efficiency performance is very similar. According to Figure 5.3.b, the capacitance retention for Pani/PSS is only 18% at 0.5 A/g and the energy density is very low. However, poly(Ani-co-

2ATA)/PSS-5 hydrogel has a capacitance retention of 30% in the same conditions, which shows the advantage of using the copolymer in comparison to Pani/PSS (Table 5.1). Figure 5.3.c shows the capacitance during 20 cycles and at different current densities. The capacitance is stable with the cycles but decreases with the increase in current density.

Table 5.1. Gravimetric capacitance (Cg), energy density (E), maximum power density (P) and energy efficiency and capacitance retention determined by Pani/PSS hydrogel and poly(Ani-co-2ATA)/PSS copolymer hydrogel electrodes. Pani/PSS and poly(Ani-co-2ATA)/PSS-X symmetric capacitors by galvanostatic charge-discharge cycles. 1M H_2SO_4. j= 0.05A/g.

Samples	**Cg (F/g)**	**C_v (F/cm^3)**	**E (Wh/kg)**	**P_{max} (W/kg)**	**Energy efficiency(%)**	**Capacitance retention(%)**
Pani-PSS	11	33	0.5	0.008	53	18
poly(Ani-co-2ATA) /PSS-1	13	38	0.6	0.010	53	15
poly(Ani-co-2ATA) /PSS-3	14	38	0.64	0.011	53	14
poly(Ani-co-2ATA) /PSS-5	14	35	0.55	0.009	58	30

3.2 Poly(Ani-co-PIP)/PSS-X hydrogels

3.2.1 Electrochemical characterization of poly(Ani-co-PIP)/PSS-X hydrogels

Figure 5.4 shows the cyclic voltammograms of the Pani/PSS and hydrogel copolymers obtained with piperazine (poly(Ani-co-PIP)/PSS-X). As in the case of ATA copolymers, the redox processes which are ascribed to the transformation between leucoemeraldine base (LB), emeraldine salt (ES), and pernigraniline base (PB) are observed [19]. The introduction of piperazine at different amounts influences the redox transitions involving hydroxypiperazine ⇌ ketopiperazine species within the copolymer structure [23]. The redox processes are clearly observed even at high scan rates, suggesting a good capacitive behavior was still retained even at 500 mV/s. In all cases, the capacitance decreases with the scan rate until reaching a very low value. The increased aniline content could bring about a significant increment of current density and a corresponding increase in capacitance. However, with the increased scan rate, the capacitance of hydrogel electrodes fabricated with different molar ratios (1;3;5) increases and delivers a medium rate capability (capacitance retention of around 43%) [18].

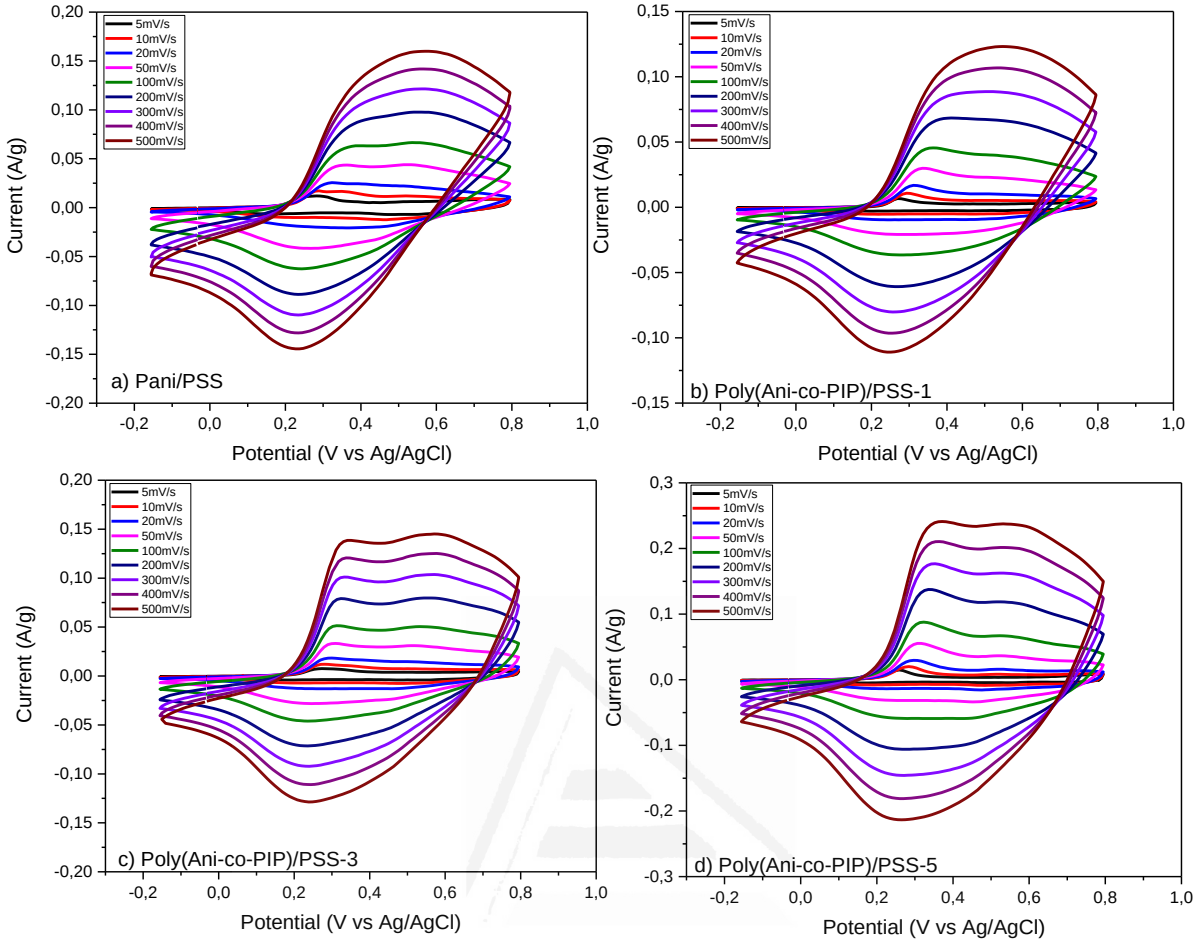

Figure 5.4. Voltammograms for (a) Pani/PSS, (b) poly(Ani-co-PIP)/PSS-1, (c) poly(Ani-co-PIP)/PSS-3 and (d) poly(Ani-co-PIP)/PSS-5 on glassy carbon electrode at different scan rates ranging from 5 mV s^{-1} to 500 mV s^{-1}. 1 M H_2SO_4 solution.

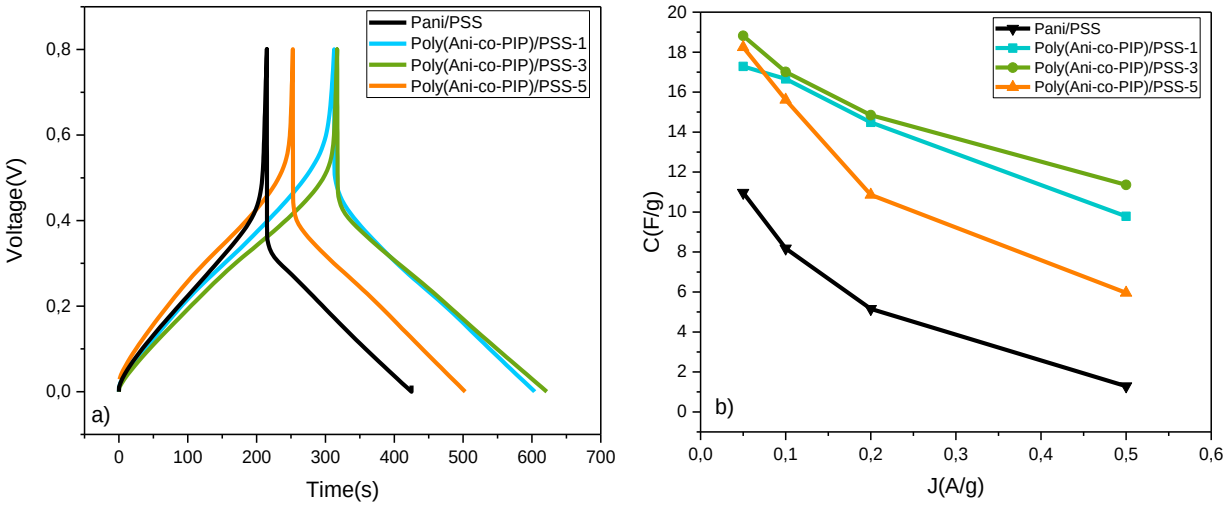

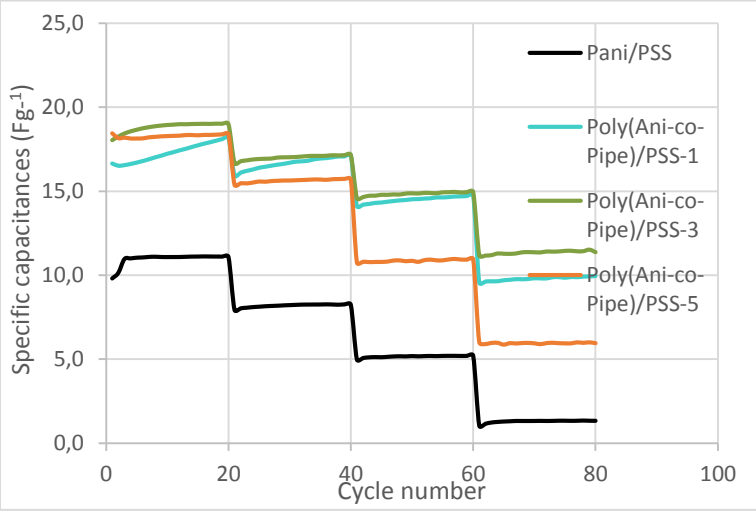

Figure 5.5. (a) Galvanostatic charge-discharge profiles of Pani/PSS and poly(Ani-co-PIP) copolymer hydrogel electrodes tested under a current density of 0.05 A g^{-1} at room temperature and 1 M H_2SO_4 solution; (b) specific capacitances of Pani/PSS hydrogel and poly(Ani-co-PIP)-X hydrogel electrodes versus current densities; (c) discharge-charge capacitances of Pani/PSS hydrogel and poly(Ani-co-PIP)-X hydrogel electrodes versus cycles tested at different current densities. 1 M H_2SO_4 solution.

3.2.2 Symmetric capacitors prepared with poly(Ani-co-PIP)/PSS-X hydrogels

The same tests that had been performed with the 2ATA copolymer hydrogels were carried out with PIP copolymer hydrogels to study the specific capacitance and rate performance of symmetric capacitors prepared with these copolymers. Figure 5.5.a shows the galvanostatic charge-discharge curves of the different symmetric capacitors at 0.05 A/g. The Pani/PSS hydrogel and poly(Ani-co-PIP)-X hydrogels show a triangular form with a high resistance. The specific capacitance was calculated based on the GCD data and the corresponding values at different current densities, as shown in Figure 5.5.b (Table 5.2). The gravimetric capacitance, energy density, maximum power density, energy efficiency and capacitance retention are shown in Table 5.2 for the three symmetric capacitors prepared with the three poly(Ani-co-PIP)-X copolymer hydrogels. Similar values are obtained around 52 F/cm^3 at 0.05 A/g for the three poly(Ani-co-PIP)-X hydrogels. The values obtained for gravimetric capacitance are higher than that obtained with the Pani/PSS hydrogel and poly(Ani-co-ATA)-X copolymer hydrogels (Table 5.1). Moreover, the capacitance retention is also higher in all cases reaching a value of up to 63% for poly(Ani-co-PIP)/PSS-3.

Table 5.2. Gravimetric capacitance (Cg), energy density €, maximum power density (P) and energy efficiency and capacitance retention determined for Pani/PSS hydrogel and poly(Ani-co-PIP)/PSS-

X copolymer hydrogel electrodes symmetric supercapacitors by galvanostatic charge-discharge cycles. 1M H_2SO_4. j= 0.05 A/g.

Samples	Cg (F/g)	C_v (F/cm^3)	E (Wh/kg)	P_{max} (W/kg)	Energy efficiency(%)	Capacitance retention(%)
Pani-PSS	11	33	0.5	0.008	53	18
poly(Ani-co-PIP) /PSS-1	17	50	0.83	0.011	66	59
poly(Ani-co- PIP) /PSS-3	19	52	0.91	0.011	69	63
poly(Ani-co- PIP) /PSS-5	18	52	0.82	0.020	60	38

3.3 Comparison of the parameters obtained for poly(Ani-co-2ATA)/PSS and poly(Ani-co-PIP)/PSS

In this section, the capacitors prepared with the different copolymer hydrogels synthesized and with the Pani/PSS have been compared. Figure 5.6 shows the comparison of the gravimetric capacitance and their performance with the current density and number of cycles for the best copolymers. It can be observed that the capacitors prepared with the poly(Ani-co-2ATA)-5 and poly(Ani-co-PIP)-3 copolymer hydrogels have better performance than the Pani/PSS capacitor, especially the capacitor prepared with the poly(Ani-co-PIP)-3 hydrogel, as its capacitance value is more than 70% higher and its capacitance retention increases 2.5 times.

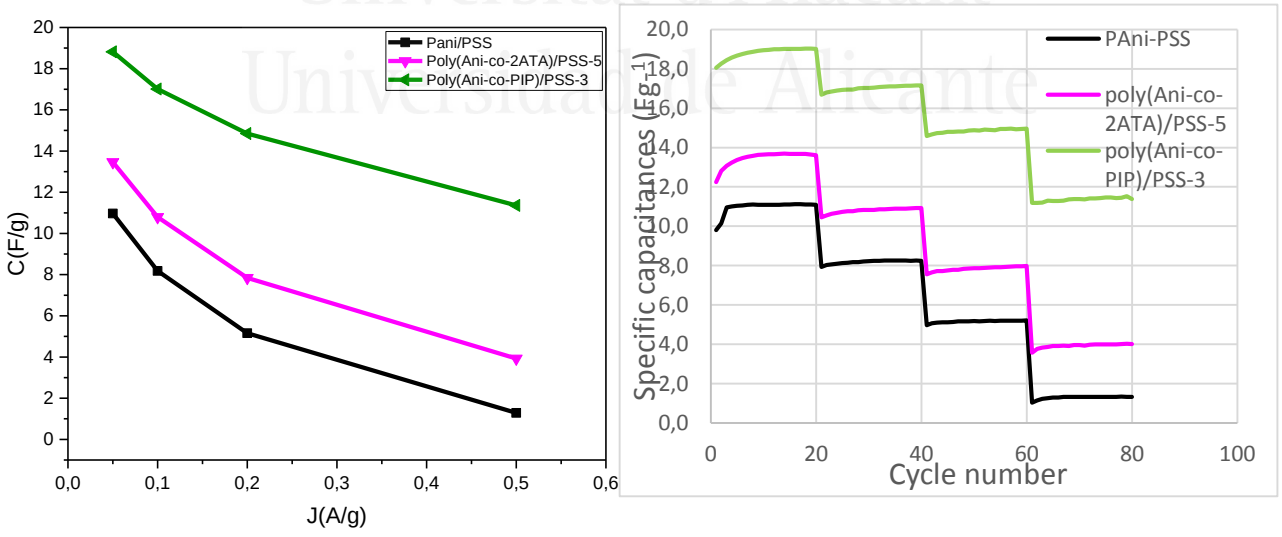

Figure 5.6. Comparison of (a) specific capacitance versus specific current density and (b) capacitance retention when current density ranges from 0.05 A/g to 0.5 A/g. 1 M H_2SO_4 solution.

3.4 Symmetric capacitors prepared with hydrogels and carbon materials

To improve the performance of the capacitors, the addition of either a carbon black (Vulcan) or multiwall carbon nanotube (MWCNT) has been studied. Figure 5.7 shows the charge-discharge curves for the capacitors prepared with poly(Ani-co-2ATA)-MWCNTs/PSS-5 and poly(Ani-co-2ATA)-Vulcan/PSS-5. The capacitors with Pani/PSS and the same carbon materials have also been studied for comparison purposes (Pani-MWCNTs-PSS and Pani-Vulcan-PSS samples). It can be observed that the performance of the poly(Ani-co-2ATA)-MWCNTs/PSS-5 capacitor is better than the capacitor prepared with Vulcan, and both show a decrease in resistance that can be associated with an increase in the conductivity of the samples. Therefore, the capacitance values are higher in the presence of carbon materials, and higher than the Pani/PSS capacitor. The same behavior has been observed with the poly(Ani-co-PIP)-X hydrogels. Figure 5.7.b shows the charge-discharge curves for the different samples and in the presence of carbon materials. The results revealed that the charge-discharge and specific capacitance of the devices were dependent on the current density (Figure 5.7.d) and composition of the hydrogel copolymers. The devices demonstrated that the discharge time and specific capacitance decreased with increasing current density. This is due to the insufficient time for the ions from the hydrogel copolymers to penetrate the structure at high current rates. At low current rates, the ions can be able to penetrate to the interior of the electrodes, thus, longer discharge times were observed [37,38].

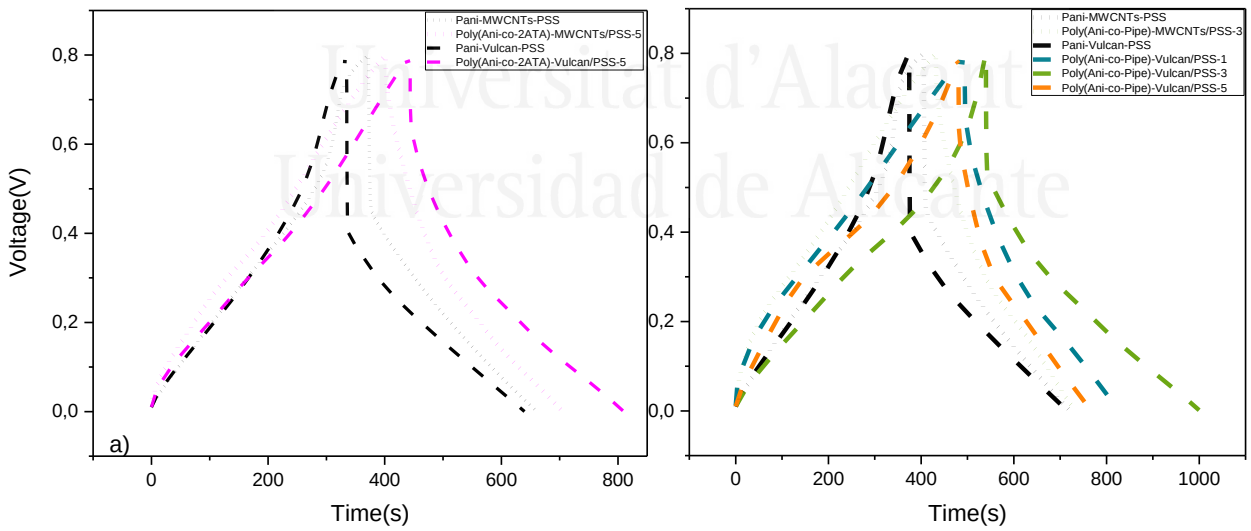

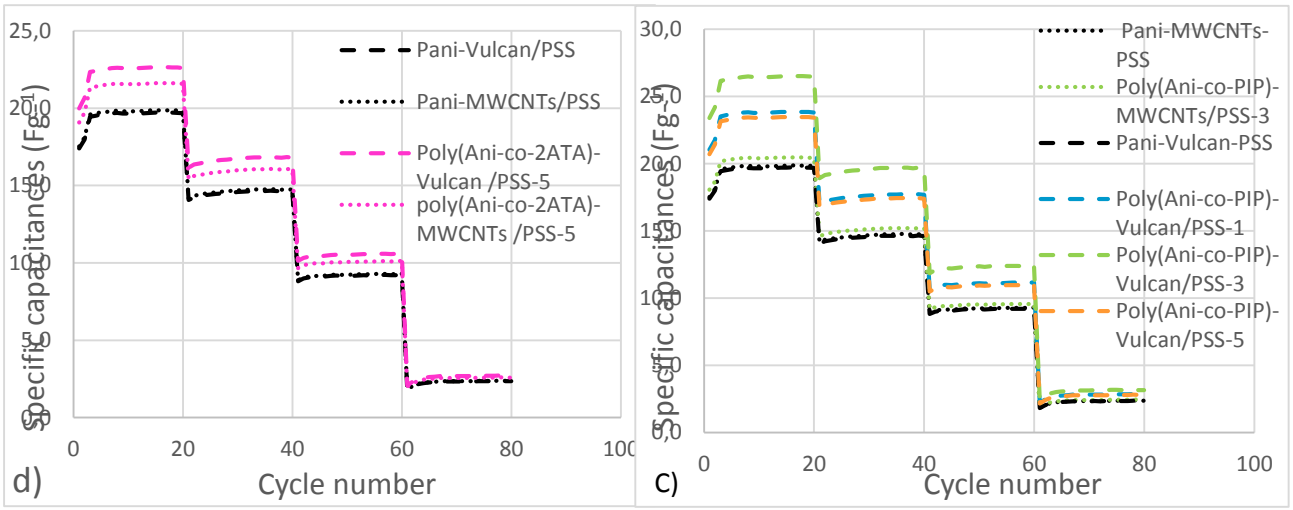

Figure 5.7. Charge-discharge curves for (a) Pani-MWCNTs-PSS; poly(Ani-co-2ATA)-MWCNTs/PSS-5; and Pani-Vulcan-PSS; poly(Ani-co-2ATA)-Vulcan/PSS-5 and (b) poly(Ani-co-PIP)-MWCNTs/PSS-X; and Pani-Vulcan-PSS; poly(Ani-co-PIP)-Vulcan/PSS-X at 0.05 A g^{-1}; (c) and (d) discharge-charge capacitances of Pani/PSS hydrogel and copolymer electrodes versus cycle numbers tested at different current densities. 1 M H_2SO_4 solution.

Table 5.3. Comparison of capacitor parameters using the different hydrogels and carbon materials.

Samples	Cg (F/g)	C_v (F/cm^3)	E (Wh/kg)	P_{max} (W/kg)	Energy efficiency (%)	Capacitance retention (%)
Pani/PSS	11	33	0.5	0.008	53	18
Pani-MWCNTs/PSS	20	41	0.89	0.015	53	12
Pani-Vulcan/PSS	20	36	0.88	0.015	53	12
poly(Ani-co-2ATA) /PSS-5	14	35	0.55	0.009	58	30
poly(Ani-co-2ATA)-MWCNTs/PSS-5	21	41	0.97	0.017	53	12
poly(Ani-co-2ATA)-Vulcan/PSS-5	22	41	1.01	0.017	53	12
poly(Ani-co-PIP) /PSS-3	19	52	0.91	0.011	69	63
poly(Ani-co-PIP)-MWCNTs/PSS-3	20	41	0.91	0.016	53	12
poly(Ani-co-PIP) Vulcan/PSS-3	26	47	1.19	0.020	53	12

Table 5.3 shows the parameters for the different capacitors prepared in the presence of carbon materials and the comparison with the capacitors in the absence of carbon materials. It can be observed that specific capacitance increases in the presence of carbon materials and the increase is higher with Vulcan. These results can be a consequence of the increase in conductivity, but also of the increase in surface area.

Table 5.4 compares the values obtained in this chapter with the values of specific capacitance and energy density previously published by other authors with hydrogel electrodes. Specific capacitance values are difficult to compare because this parameter is rarely included. However, the volumetric capacitance and specific capacitance are similar to or in some cases higher than the values obtained in previous studies with other materials and design methods of recent hydrogel electrolytes for supercapacitors [24,25]. However, the energy density is very low.

Table 4. Comparison of capacitance and energy density for different symmetric capacitors prepared with different conducting polymers.

Conductive Polymer Materials	**Hydrogel Matrix or Gelation Agent**	**Specific Capacitance (F/g)**	**Energy density (Wh /kg)**	**Ref**
Pani	Polyvinyl alcohol	928 mF/cm^2 at 0.5 A/g	13.6	[26]
Pani	H_2SO_4-polyvinyl alcohol	488 mF/cm^2 at 0.2 A/g	42	[27]
PEDOT:PSS/CNTs	APS	227 mF/cm^2 at 0.5 mV/s		[28]
PEDOT:PSS/cellulose	PVA/KOH	50.4 F cm^{-3} at 0.05 A cm^{-3}	13.2	[29]
PEDOT:PSS/CNT film	PVA/H_3PO_4	64 mF cm^{-2} at 0.2 mA cm^{-2}	8.89	[30]
PVA–PANI–MLG hydrogel	HCl-APS			[31]
PA/PANI	PVA/H_2SO_4	311.3 F cm^{-3} at 1 A g^{-1}	49.9	[32]
CNT film	Poly(AMPS-co-DMAAm)/ LAPONITE®/GO nanocomposite GPE	180 mF cm^{-2} at 0.5 mA cm^{-2}		[33]

PAD/H2SO4–PANI hydrogel	PAD/H_2SO_4 GPE	430 mF cm^{-2} at 0.5 mA cm^{-2}		[34]
PPy@CNT paper	Al-alginate/PAAm hydrogel	94.7 mF/cm^{-2} at 0.1 mA cm^{-2}		[35]
MWCNT film	LiCl/PEI–PVA–Bn	16.7 mF cm^{-2} at 0.05 mA cm^{-2}	3.13	[36]
Pani/PSS	H_2SO_4-APS-Poly (4-styrenesulfonate)	11 F/g 33 F/cm^3 at 0.05 A g^{-1}	0.5	This work
Pani-MWCNTs/PSS	H_2SO_4-APS-Poly (4-styrenesulfonate)	20 F/g 41 F/cm^3 at 0.05 A g^{-1}	0.89	This work
poly(Ani-co-PIP)/PSS-3	H_2SO_4-APS-Poly (4-styrenesulfonate)	19 F/g 52 F/cm^3 at 0.05 A g^{-1}	0.91	This work
poly(Ani-co-2ATA)-Vulcan /PSS-5	H_2SO_4-APS -Poly (4-styrenesulfonate)	22 F/g 41 F/cm^3 at 0.05 A g^{-1}	0.97	This work
poly(Ani-co-PIP)Vulcan /PSS-3	H_2SO_4-APS-Poly (4-styrenesulfonate)	26 F/g 47 F/cm^3 at 0.05 A g^{-1}	1.19	This work

4 Conclusions

Symmetric supercapacitors based on conducting polymer hydrogels have been studied. A supramolecular assembly of polyaniline and aminoterephthalic acid and piperazine with designed structures and different electrochemical properties has been used as an application for supercapacitors. In this chapter, the copolymer hydrogels in the presence of carbon materials (multiwall carbon nanotubes and Vulcan) have been studied as electrodes in supercapacitors. It has been observed that the copolymer hydrogels show better performance than the polyaniline hydrogel. Furthermore, the presence of carbon materials improves the conductivity of the electrodes and the electrochemical performance of the capacitor obtaining the better results with Vulcan. The capacitance retention increases for the copolymers in comparison with Pani/PSS obtaining a high capacitance retention with poly(Ani-co-PIP)-3 copolymer hydrogel. The volumetric capacitance values are higher than or similar to those obtained by other authors.

5 References:

[1] Y. Han, L. Dai. Conducting Polymers for Flexible Supercapacitors. Macromol. Chem. Phys. 2019,220, 1–14. doi:10.1002/macp.201800355.

[2] Y. Gao, Y. Li, H. An, Y. Feng, W. Feng. Copolymers of aniline and 2-aminoterephthalic acid as a novel cathode material for hybrid supercapacitors. RSC Adv. 2017, 7, 8762–8770. doi:10.1039/c6ra27900g.

[3] P. Simon, Y. Gogotsi. Materials for electrochemical capacitors. Nat. Mater. 2008, 7, 845–854.

[4] F. Béguin, E. Frackowiak, Carbons for Electrochemical Energy Storage and Conversion Systems, First Edition, CRC Press, 2009.

[5] X. Han, G. Xiao, Y. Wang, X. Chen, G. Duan, Y. Wu, X. Gong, H. Wang. Design and fabrication of conductive polymer hydrogels and their applications in flexible supercapacitors. J. Mater. Chem. A. 2020, 8, 23059–23095. doi:10.1039/d0ta07468c.

[6] A. Chu, P. Braatz. Comparison of commercial supercapacitors and high-power lithium-ion batteries for power-assist applications in hybrid electric vehicles: I. Initial characterization. J. Power Sources. 2002, 112, 236–246. doi:10.1016/S0378-7753(02)00364-6.

[7] E. Faggioli, P. Rena, V. Danel, X. Andrieu, R. Mallant, H. Kahlen, Supercapacitors for the energy management of electric vehicles, J. Power Sources. 1999, 84, 261–269. doi:10.1016/S0378-7753(99)00326-2.

[8] G.A. Snook, P. Kao, A.S. Best. Conducting-polymer-based supercapacitor devices and electrodes. J. Power Sources. 2011, 196, 1–12. doi:10.1016/j.jpowsour.2010.06.084.

[9] P.J. Nigrey. Lightweight Rechargeable Storage Batteries Using Polyacetylene, (CH)[sub x] as the Cathode-Active Material. J. Electrochem. Soc. 1981, 128,1651. doi:10.1149/1.2127704.

[10] J. Stejskal, Conducting polymer hydrogels, Chem. Pap. 2017, 71, 269–291. doi:10.1007/s11696-016-0072-9.

[11] A. Malti, J. Edberg, H. Granberg, Z.U. Khan, J.W. Andreasen, X. Liu, D. Zhao, H. Zhang, Y. Yao, J.W. Brill, I. Engquist. An Organic Mixed Ion – Electron Conductor for Power Electronics. Advanced Science. 2016, 3, 1–9. doi:10.1002/advs.201500305.

[12] A. Jabłońska, B. Pałys. Effect of the polymerization bath on structure and electrochemical properties of polyaniline-poly(styrene sulfonate) hydrogels. J. Electroanal. Chem. 2017, 784, 115–123. doi:10.1016/j.jelechem.2016.11.050.

[13] T. Dai, Y. Jia. Supramolecular hydrogels of polyaniline-poly (styrene sulfonate) prepared in concentrated solutions. Polymer (Guildf). 2011, 52 2550–2558. doi:10.1016/j.polymer.2011.04.006.

[14] D. Gu, G. Yang, Y. He, B. Qi, G. Wang, Z. Su. Triphenylamine-based pH chemosensor: Synthesis, crystal structure, photophysical properties and computational studies. Synth. Met. 2009, 159, 2497–2501. doi:10.1016/j.synthmet.2009.08.040.

[15] S. Dkhili, S. López-bernabeu, F. Huerta, F. Montilla, S. Besbes-hentati, E. Morallón. A self-doped polyaniline derivative obtained by electrochemical copolymerization of aminoterephthalic acid and aniline. Synth. Met. 2018, 245, 61–66. doi:10.1016/j.synthmet.2018.08.005.

[16] R. Ramachandran, S. Balasubramanian, G. Aridoss, P. Parthiban. Polymer Synthesis and studies of semiconducting piperazine – aniline copolymer. Eur Polym J. 2006, 42, 1885–1892. doi:10.1016/j.eurpolymj.2006.02.010.

[17] M.J. Mostazo-López, R. Ruiz-Rosas, E. Morallón, D. Cazorla-Amorós. Nitrogen doped superporous carbon prepared by a mild method. Enhancement of supercapacitor performance. Int. J. Hydrogen Energy. 2016, 41, 19691–19701. doi:10.1016/j.ijhydene.2016.03.091.

[18] Z. Yang, D. Shi, W. Dong, M. Chen. Self-Standing Hydrogels Composed of Conducting Polymers for All-Hydrogel-State Supercapacitors. Chem. - A Eur. J. 2020, 26, 1846–1855. doi:10.1002/chem.201904357.

[19] H. Guo, W. He, Y. Lu, X. Zhang. Self-crosslinked polyaniline hydrogel electrodes for electrochemical energy storage. Carbon N. Y. 2015, 92, 133–141. doi:10.1016/j.carbon.2015.03.062.

[20] J. Wu, Q. Zhang, J. Wang, X. Huang, H. Bai, A self-assembly route to porous polyaniline/reduced graphene oxide composite materials with molecular-level uniformity for high-performance supercapacitors. Energy Environ. Sci. 2018, 11, 1280–1286. doi:10.1039/c8ee00078f.

[21] A. Sikdar, S.K. Deb, A. Gogoi, A. Majumdar, P. Dutta, K.A. Reddy, U.N. Maiti. Polyaniline-Graphene Hydrogel Hybrids via Diffusion Controlled Surface Polymerization for High Performance Supercapacitors. ACS Appl. Nano Mater. 2020, 3, 12278–12287. doi:10.1021/acsanm.0c02749.

[22] K. Wang, X. Zhang, C. Li, H. Zhang, X. Sun, N. Xu, Y. Ma. Flexible solid-state supercapacitors based on a conducting polymer hydrogel with enhanced electrochemical performance. J. Mater. Chem. A. 2014, 2, 19726–19732. doi:10.1039/c4ta04924a.

[23] S. Dkhili, S. López-Bernabeu, C.N. Kedir, F. Huerta, F. Montilla, S. Besbes-Hentati, E. Morallon. An electrochemical study on the copolymer formed from piperazine and aniline monomers. Materials (Basel). 2018, 11, 1012. doi:10.3390/ma11061012.

[24] C.Y. Chan, Z. Wang, H. Jia, P.F. Ng, L. Chow, B. Fei. Recent advances of hydrogel electrolytes in flexible energy storage devices. J. Mater. Chem. A. 2021, 9, 2043–2069. doi:10.1039/d0ta09500a.

[25] W. Li, X. Li, X. Zhang, J. Wu, X. Tian, M.J. Zeng, J. Qu, Z.Z. Yu. Flexible Poly(vinyl alcohol)-Polyaniline Hydrogel Film with Vertically Aligned Channels for an Integrated and Self-Healable Supercapacitor. ACS Appl. Energy Mater. 2020, 3 9408–9416. doi:10.1021/acsaem.0c01794.

[26] W. Li, H. Lu, N. Zhang, M. Ma. Enhancing the properties of conductive polymer hydrogels by freeze-thaw cycles for high-performance flexible supercapacitors, ACS Appl. Mater. Interfaces. 2017, 9, 20142–20149. doi:10.1021/acsami.7b05963.

[27] K. Wang, X. Zhang, C. Li, X. Sun, Q. Meng, Y. Ma, Z. Wei. Chemically Crosslinked Hydrogel Film Leads to Integrated Flexible Supercapacitors with Superior Performance. Adv. Mater. 2015, 27, 7451–7457. doi:10.1002/adma.201503543.

[28] Z. Chen, J.W.F. To, C. Wang, Z. Lu, N. Liu, A. Chortos, L. Pan, F. Wei, Y. Cui, Z. Bao. A three-dimensionally interconnected carbon nanotube-conducting polymer hydrogel network for high-performance flexible battery electrodes. Adv. Energy Mater. 2014, 4, 1–10. doi:10.1002/aenm.201400207.

[29] D. Zhao, Q. Zhang, W. Chen, X. Yi, S. Liu, Q. Wang, Y. Liu, J. Li, X. Li, H. Yu. Highly Flexible and Conductive Cellulose-Mediated PEDOT:PSS/MWCNT Composite Films for Supercapacitor Electrodes. ACS Appl. Mater. Interfaces. 2017, 9, 13213–13222. doi:10.1021/acsami.7b01852.

[30] Y. Zhu, N. Li, T. Lv, Y. Yao, H. Peng, J. Shi, S. Cao, T. Chen. Ag-Doped PEDOT:PSS/CNT composites for thin-film all-solid-state supercapacitors with a stretchability of 480%. J. Mater. Chem. A. 2018, 6, 941–947. doi:10.1039/c7ta09154k.

[31] H. Joo, H. Han, S. Cho. Fabrication of Poly(vinyl alcohol)-Polyaniline Nanofiber/Graphene Hydrogel for High-Performance Coin Cell Supercapacitor. Polymers (Basel). 2020, 12, 928. doi:doi:10.3390/polym12040928.

[32] X. Chu, H. Huang, H. Zhang, H. Zhang, B. Gu, H. Su, F. Liu, Y. Han, Z. Wang, N. Chen, C. Yan, W. Deng, W. Deng, W. Yang. Electrochemically building three-dimensional supramolecular polymer hydrogel for flexible solid-state micro-supercapacitors. Electrochim. Acta. 2019, 301, 136–144. doi:10.1016/j.electacta.2019.01.165.

[33] H. Li, T. Lv, H. Sun, G. Qian, N. Li, Y. Yao, T. Chen. Ultrastretchable and superior healable supercapacitors based on a double cross-linked hydrogel electrolyte, Nat. Commun. 2019, 10, 1–8. doi:10.1038/s41467-019-08320-z.

[34] Y. Shi, Y. Zhang, L. Jia, Q. Zhang, X. Xu. Stretchable and Self-Healing Integrated All-Gel-State Supercapacitors Enabled by a Notch-Insensitive Supramolecular Hydrogel Electrolyte. ACS Appl. Mater. Interfaces. 2018, 10, 36028–36036. doi:10.1021/acsami.8b13947.

[35] Z. Liu, G. Liang, Y. Zhan, H. Li, Z. Wang, L. Ma. A soft yet device-level dynamically super-tough supercapacitor enabled by an energy-dissipative dual-crosslinked hydrogel electrolyte.

Nano Energy. 2019, 58, 732–742. doi:10.1016/j.nanoen.2019.01.087.

[36] J. Liu, J. Huang, Q. Cai, Y. Yang, W. Luo, B. Zeng, Y. Xu, C. Yuan, L. Dai/ Design of Slidable Polymer Networks: A Rational Strategy to Stretchable, Rapid Self-Healing Hydrogel Electrolytes for Flexible Supercapacitors. ACS Appl. Mater. Interfaces. 2020, 12, 20479–20489. doi:10.1021/acsami.0c03224.

[37] D.S. Silvaraj, S. Bashir, M. Hina, J. Iqbal, S. Gunalan, S. Ramesh, K. Ramesh. Tailorable solid-state supercapacitors based on poly (N-hydroxymethylacrylamide) hydrogel electrolytes with high ionic conductivity. J. Energy Storage. 2021, 3. doi:10.1016/j.est.2021.102320.

[38] M.Z. Bidin, N. Hon Ming, F.S. Omar, K. Ramesh, S. Ramesh. Solid terpolymer electrolyte based on poly(vinyl butyral-co-vinyl alcohol-co-vinyl acetate) incorporated with lithium salt and tetraglyme for EDLCs. J. Appl. Polym. Sci. 2018, 135, 1–7. doi:10.1002/app.45902.

Chapter 6
General Conclusions

This PhD Thesis has focused on the electrochemical synthesis of conducting polymers based on polyaniline modified with 2-aminoterephthalic acid and piperazine, and their behaviour in the oxidation of Dopamine (DA) and Ascorbic acid (AA) oxidation, and their possible application as electrochemical sensors. In addition, the chemical synthesis of hydrogels of the different copolymers based on aniline, 2-aminoterephthalic acid and piperazine has been studied. The hydrogels have studied as electrodes in supercapacitors. The main conclusions derived from this PhD Thesis are summarized.

An Electrochemical Study on the Copolymers formed from 2-Aminoterephthalic Acid, Piperazine, and Aniline Monomers Testing their Sensitivity towards Dopamine and Ascorbic Acid

- 2-Aminoterephthalic acid (2ATA) could be an interesting co-monomer for the aniline copolymerization because it contains two carboxylic groups linked to the aromatic ring. The electrochemical oxidation of aminoterephthalic acid on platinum electrodes in perchloric acid medium does not yield an electroactive polymer on the electrode surface; however, in presence of aniline the copolymer is obtained. Therefore, the monomer ratio and the oxidation potential are key parameters to obtain copolymerization product and to modulate the material composition and properties.

- The electrochemical oxidation of piperazine on platinum electrodes at moderate potentials (roughly below 1.0 V/RHE) preserves the ring structures and produces ketopiperazines as the main reaction product. In situ FTIR spectroscopy strongly suggested that ring opening and overoxidation occur at higher potentials to form both amides and isocyanates. As a result, it was observed that the homopolymerization of piperazine could not be achieved in perchloric acid aqueous solution under electrochemical conditions. On the contrary, piperazine can be successfully copolymerized with aniline in acidic medium. A reversible hydroxy ⇌ ketopiperazine redox transformation seems to occur as the intermediate voltammetric feature centered at 0.68 V. It should be noted that, owing to the conservative

potential program applied during the deposition process, any significant amount of overoxidation.

- The electrochemical synthesis of copolymers based on aniline and 2ATA and PIP, by means of cyclic voltammetry on a platinum electrode, in an acidic medium produces the synthesis of different copolymers (poly(Ani-co-2ATA) and poly (Ani-co-PIP)). The voltammetric profiles show the amount of material deposited on the electrode surface is significantly higher when the electropolymerization potential limit is at 1.2 V. Moreover, the decrease in the monomer ratio (PIP/Ani and 2ATA/Ani) produces the same effect, that is, the increase in the voltammetric charge associated with the polymers as a consequence of an increase in the amount of polymer obtained. This effect is a consequence of the higher reactivity of aniline compared to the other two monomers.

- The poly(Ani-co-2ATA) and poly (Ani-co-PIP) copolymers show a linear response during oxidation of both dopamine and ascorbic acid in synthetic samples. The coplymer electrodes exhibited oxidation peaks for each concentration of DA and AA and the sensitivity of these measurements is in both cases high enough to assure the correct quantification of analytes. The increase in the synthesis potential of copolymers by cyclic voltammetry increases the sensitivity.

- The higher sensitivity for AA determination is obtained with poly(Ani-co-2ATA) as consequence of the increase in interaction between the carboxylic groups and the AA molecule. In the case of DA the higher sensitivity is obtained with poly(Ani-co-PIP).

Synthesis and Characterization of Hydrogels Obtained from Aniline and Aminoterephthalic Acid and Piperazine Monomers

- An effective approach has been studied for the synthesis of hydrogels and copolymer hydrogels via supramolecular self-assembly between PSS and conducting polymers. Pani/PSS, poly(Ani-co-ATA/PSS)-X and poly(Ani-co-PIP/PSS-X have been synthesized using different molar ratios. The different synthesized copolymer hydrogels have been characterized by different electrochemical and physicochemical techniques like XPS, FTIR, etc. The redox behavior of the copolymers has been studied by cyclic voltammetry.

- The conductive properties of the different synthesized hydrogels were measured by determining the electrical conductivity. The mass swelling ratio, thermogravimetric analyses were performed; with the objective of evaluating the reactivity and thermal stability of hydrogel copolymers.

Hybrid Supercapacitors from Supramolecular Hydrogels Obtained from Aniline and Aminoterephthalic Acid and Piperazine Monomers

- The electrochemical characterization of the poly(Ani-co-2ATA)/PSS-X and poly(Ani-co-PIP)/PSS-X copolymer hydrogels show a higher specific capacitance than Pani/PSS hydrogel.

- The gravimetric capacitance and their performance with the current density and number of cycles are higher for the copolymer hydrogels with respect to that obtained with Pani/PSS hydrogel.

- Symmetric capacitors were assembled with all the hydrogels synthetized in this PhD Thesis and were characterised in acidic medium and, their electrochemical behaviour have been related to the synthesis parameters, such as chemical molar ratio. Electrochemical characterisation revealed that piperazine groups significantly contributed to the pseudocapacitance in these copolymer hydrogels and produced a high capacitance retention with the current density in comparison to the Pani/PSS capacitor.

- Symmetric supercapacitors based on conducting polymers hydrogels were prepared in presence of carbon materials (multiwall carbon nanotubes and Vulcan) by physical mixing. It has been observed that the copolymer hydrogels show better performance than the Pani/PSS hydrogel. The presence of carbon materials improves the conductivity of the electrodes and the electrochemical performance of the capacitor increases. The values of volumetric capacitance are higher or similar to that obtained by other authors.

Chapter 7

Resumen y conclusiones generales.

Esta Tesis Doctoral ha sido realizada en los grupos de investigación Electrocatálisis y Electroquímica de Polímeros (GEPE) del Departamento de Química Física y perteneciente al Instituto de Materiales de la Universidad de Alicante, España (IUMA) y en el Laboratorio de Química Orgánica, y Materiales Macromoleculares de la Universidad de Mascara, Argelia (LCOMM) en cotutela internacional.

1 Introducción

Hoy en día es imposible desconocer la importancia de los polímeros en el desarrollo de nuevas tecnologías, están presentes en todos los ámbitos debido a su gran aplicación, desde la alimentación hasta la industria aeroespacial pasando por la cosmética. Son ligeros, sencillos de implementar y tienen un coste mucho menor que el de la mayoría de los materiales que son sus competidores; incluso se puede considerar que estarán en el centro de la próxima revolución industrial. Dentro de los polímeros, los polímeros conductores son de gran interés, y se han escrito un gran número de artículos, reseñas, libros y tesis doctorales sobre este tipo de polímeros, que a menudo se enfocan en diferentes perspectivas, desde la Química, o desde la Física hasta desde la Ciencia de Materiales y la Ingeniería. Una mirada a la naturaleza en busca de inspiración indica que la complejidad, más que la simplicidad, es a menudo el resultado de un proceso evolutivo. Una revisión de la sección de la revista Faraday Discussion de la Chemical Society, de hace casi dos décadas, sobre la transferencia de carga en los polímeros sugiere que polímeros con la misma composición rara vez se comportan exactamente de la misma manera. Esto nos indica, las dificultades en la reproducibilidad en los materiales. Sin embargo, la investigación de nuevos materiales y una mejor comprensión de las propiedades y características de este tipo de polímeros conductores ha permitido y permitirá el desarrollo de nuevos materiales.

Los polímeros conductores son la generación de polímeros más reciente y prometedora. Tienen muchas de las propiedades deseables generalmente asociadas con los polímeros convencionales, pero también exhiben propiedades eléctricas similares a las de los metales y semiconductores inorgánicos. Este tipo de polímeros han desempeñado un papel central en el último desarrollo tecnológico y la ampliación de las propiedades de los polímeros, que está ganando campos de aplicación sin precedentes.

La polianilina (Pani) es uno de los polímeros conductores más estudiados debido a su bajo coste, fácil síntesis y fácil dopaje/desdopado. La Pani, también conocida como negro de anilina, se descubrió por primera vez como tinte y se ha estudiado durante más de 100 años. La polianilina tiene múltiples formas estructurales, mediante dopaje presenta una alta conductividad y además, tiene una buena estabilidad ambiental. Además, puede sintetizarse fácilmente por oxidación química o electroquímica de la anilina. La Pani es un polímero de anillos aromáticos (fenilenos) enlazados con un grupo –NH–, lo que la hace flexible. La Pani puede encontrarse en varios estados de oxidación, la forma totalmente oxidada se llama pernigranilina y la reducida se conoce como leucoemeraldina, mientras que el estado intermedio se llama emeraldina, siendo esta estructura semioxidada la que presenta los valores de conductividad más altos.

La polianilina tiene algunos inconvenientes, como son su baja solubilidad en disolventes comunes y por lo tanto su procesabilidad es baja. Para evitar estos problemas, se ha estudiado la incorporación de grupos funcionales en la cadena del polímero, disminuyendo las interacciones fuertes entre cadenas y aumentando la solubilidad. Hay tres métodos para introducir grupos funcionales:

(i) Posfuncionalización del Pani una vez sintetizada.

(ii) Homopolimerización de anilinas sustituidas

(iii) Copolimerización de anilina con anilinas sustituidas.

Dado que no es posible controlar el grado de modificación en la postmodificación, los dos últimos métodos parecen ser los más efectivos para obtener un polímero con las propiedades deseadas. Al elegir entre uno y otro, se deben tener en cuenta las propiedades químicas (principalmente reactividad) del monómero. La copolimerización en principio se utiliza normalmente para la síntesis de derivados de anilina cuando no es posible obtenerlos por homopolimerización. En general, los monómeros utilizados para obtener polianilina modificada se pueden clasificar en tres categorías, según la posición ocupada por los grupos funcionales, en todos los casos, el método de polimerización es similar, pero las propiedades de los polímeros obtenidos son muy diversas.

Los compuestos moleculares que contienen el grupo piperazina han atraído una gran atención, debido a sus diferentes aplicaciones en los campos industrial y farmacéutico. Estos compuestos heterocíclicos que contienen nitrógeno tienen especial importancia debido a su capacidad para formar enlaces de hidrógeno generando estructuras supramoleculares. La electropolimerización de compuestos de piperazina ha sido objeto de mucha atención por parte de varios investigadores debido a los diferentes campos de aplicación de la piperazina. Así, la copolimerización química de 1,4-bis(3-aminopropil)piperazina con N-metil-2-pirrolidona (NMP), catalizada por un líquido iónico, produce polímeros con pesos moleculares controlados y baja polidispersidad. Por tanto, la modificación de la polianilina con este compuesto puede dar lugar a polímeros con aplicaciones en diferentes campos.

El ácido 2-aminotereftálico (2ATA) también conocido como (ácido 2-amino 1,4-bencenodicarboxílico) puede ser un monómero muy interesante para su copolimerización con anilina. El 2ATA contiene dos grupos carboxílicos, y constituye un monómero muy interesante para obtener copolímeros autodopados, evitando así el uso de dopantes externos en la polianilina. En un trabajo anterior en el grupo de investigación se han obtenido copolímeros de anilina y monómeros 2ATA por polimerización oxidativa química. Se encontró que los monómeros 2ATA son cuatro veces menos reactivos que la anilina en las condiciones de polimerización química, debido al efecto desactivador de los grupos carboxílicos unidos al anillo aromático. Sin embargo, la síntesis electroquímica puede ser de gran interés en la preparación de polianilina modificada con este monómero.

Los hidrogeles son redes poliméricas tridimensionales hidrofílicas capaces de absorber grandes cantidades de agua sin perder su estructura. Las redes están compuestas por homopolímeros o copolímeros, y son insolubles debido a la presencia de entrecruzamientos químicos (uniones covalentes) o entrecruzamientos físicos. La alta hidrofilicidad de los hidrogeles se debe a la presencia de motivos hidrofílicos tales como grupos carboxilo, amida, amino e hidroxilo distribuidos a lo largo de la estructura de las cadenas poliméricas, los cuales son capaces de ionizarse en presencia de agua. Los hidrogeles se hinchan en presencia de agua, que generalmente representa más del 80% de la masa total del gel, lo que le confiere propiedades de biocompatibilidad. Los hidrogeles de polímero conductor son geles que se hinchan con agua y contienen un polímero conductor junto con un polímero de soporte como constituyentes.

Los hidrogeles contienen diferentes propiedades: i) conductividad eléctrica mixta (conductividad electrónica e iónica); ii) reversibilidad electroquímica entre formas oxidadas y reducidas del polímero conductor; iii) transición entre conductor (forma de sal) y aislante (forma de

base) en los polímeros conductores; iv) buena flexibilidad e integridad mecánica; v) material no tóxico y compatible; vi) alta porosidad y superficie específica; vii) homogeneidad macroscópica y morfología controlada.

La síntesis de hidrogeles se puede realizar según dos vías principales. La primera se considera la polimerización y reticulación simultáneas de los monómeros. La segunda es mediante la formación del gel por reticulación de macromoléculas lineales ya formadas, posiblemente funcionalizadas durante un primer paso de síntesis mediante reacción química. La estructura obtenida es más homogénea pero el método es menos versátil y más difícil que la síntesis de copolímeros.

A continuación, se describirán las aplicaciones estudiadas en la Tesis Doctoral. Una de ellas ha sido el uso de los materiales sintetizados como sensores electroquímicos. Así, un sensor es un dispositivo que puede detectar una cantidad física, química o bioquímica y convertirla en una señal, que puede ser analizada por un observador o un instrumento. Los sensores se han utilizado ampliamente en muchas áreas, como la monitorización medioambiental, la obtención de imágenes, la fabricación, aplicaciones médicas y biológicas, etc. Parte de la clasificación de los sensores es la siguiente: 1) electroquímicos, 2) ópticos, 3) electromecánicos y 4) térmicos. La oxidación electroquímica del ácido ascórbico (AA) se ha estudiado ampliamente en la literatura, debido a la importancia de su detección en bioquímica y en su aplicación en el diagnóstico clínico. La oxidación electroquímica en electrodos convencionales está muy documentada, sin embargo, la baja reproducibilidad obtenida en la oxidación electroquímica directa del ácido ascorbico sobre los electrodos convencionales ha llevado a estudiar el uso de mediadores y electrodos modificados para mejorar y catalizar la oxidación electroquímica. Así el empleo de diferentes electrodos modificados ha dado lugar a un amplio campo de investigación. Por otro lado, la dopamina (DA) se produce en muchas partes del sistema nervioso y la determinación de sus niveles en fluidos biológicos es de especial importancia en el diagnostico de determinadas enfermedades. Por tanto el desarrollo de sensores electroquímicos para esta aplicación es de gran importancia. Así, la Pani surge en estos estudios como un electrocatalizador eficaz en la oxidación de dopamina, y demuestra ser un potencial transductor para el desarrollo de sensores electroquímicos.

Los condensadores electroquímicos (también llamados supercondensadores) son una clase de dispositivos de almacenamiento electroquímico de energía, muy adecuados para el almacenamiento y liberación rápidos de energía. Los materiales más usados como electrodos en los supercondensadores son carbones activados, óxidos metálicos y polímeros conductores. Estos dispositivos constan de dos electrodos en contacto con un electrolito y separados por una membrana porosa que permite el contacto eléctrico en la disolución. La energía se almacena debido a la

formación de una doble capa eléctrica en la interfase electrodo-disolución. Durante el proceso de carga del condensador electroquímico, en el electrodo negativo (cátodo en proceso de carga) se produce la adsorción de los cationes y sobre el electrodo positivo (ánodo en proceso de carga) se produce la adsorción de los aniones. Por tanto, la carga se acumula por la adsorción de los iones del electrolito en la interfase electrodo/electrolito. Este mecanismo es el predominante cuando utilizamos materiales de carbón de alta porosidad como electrodos. En el caso de utilizar polímeros conductores, además aparece el fenómeno denominado pseudocapacidad, en el que almacenamiento de energía viene dada también por reacciones farádicas reversibles que ocurren en la superficie del electrodo. La contribución a la capacidad de estos procesos redox rápidos superficiales es un factor que es relevante en la investigación de nuevos materiales para supercondensadores. Por tanto, la adición de grupos funcionales en los polímeros conductores puede, además, tener diferentes efectos beneficiosos tales como aumentar la humectabilidad del material. Por el contrario, también pueden afectar negativamente el comportamiento del material al reducir la estabilidad del material y disminuir la conductividad eléctrica.

Se obtiene un condensador simétrico cuando el dispositivo está formado por dos electrodos de igual material y masa. Este es el formato de implementación industrial más frecuente y simple, aunque no tiene por qué ser el más óptimo en términos de energía y potencia para el material utilizado como electrodo. Este será la disposición que se ha utilizado en la Tesis Doctoral.

2 Objetivos de la Tesis Doctoral

El principal objetivo de esta Tesis Doctoral es la síntesis de polímeros conductores del tipo polianilina modificados con piperazina y ácido aminotereftalico y sus aplicación como sensores electroquímicos. Además, se plantea como objetivo la síntesis de hidrogeles de estos polímeros sintetizados y su aplicación en el almacenamiento electroquímico de energía. En base a este objetivo, se presentan los siguientes objetivos específicos:

- Síntesis electroquímica de copolímeros a partir de anilina y los monómeros piperazina y ácido aminotereftalico. Caracterización mediante espectroscopía FTIR in situ.

- Síntesis química de hidrogeles de polianilina y copolímeros anilina y los monómeros piperazina y ácido aminotereftálico.

- Caracterización fiscicoquímica, morfológica y electroquímica de los diferentes polímeros conductores y copolímeros hidrogeles sintetizados.

 Evaluar la aplicabilidad de los copolímeros obtenidos mediante métodos electroquímicos como sensores electroquímicos para la detección de dopamina y ácido ascórbico.

 Evaluar la aplicabilidad de los copolímeros hidrogeles como electrodos en supercondensadores.

3 Técnicas y Metodología.

En este capítulo describe los diferentes reactivos, técnicas y métodos estadísticos empleados durante la Tesis Doctoral. Se presenta un resumen de los principales conceptos de cada técnica empleada para la caracterización fisicoquímica, morfológica y electroquímica. Además, los diferentes procedimientos, la determinación precisa de las especies de interés, las diferentes ecuaciones y los métodos estadísticos empleados para la validación y confiabilidad de los resultados obtenidos, se describen en detalle en este capítulo.

Las técnicas utilizadas han sido para la caracterización morfológica como microscopía electrónica de transmisión (TEM), microscopía electrónica de barrido (SEM), como de análisis fisicoquímico como termogravimetría, espectroscopía FTIR, espectroscopía fotoelectrónica de Rayos-X (XPS). Además, se ha determinado la conductividad eléctrica de los materiales mediante medidas en cuatro puntas, y por último se ha utilizado técnicas electroquímicas para la síntesis de los polímeros y para su caracterización y aplicaciones, así se han utilizado voltametría cíclica y cronopotenciometría.

3.1 Estudio electroquímico de la síntesis de copolímeros de ácido 2-aminotereftálico, piperazina y anilina. Sensores electroquímicos de dopamina y ácido ascórbico.

En este capítulo se realiza el estudio de la oxidación electroquímica de piperazina y su copolimerización electroquímica con anilina en medio ácido. Se encontró que la homopolimerización de piperazina no se puede lograr en condiciones electroquímicas acopladas a espectroscopía FTIR. Mediante FTIR in situ y XPS se ha realizado la caracterización de la estructura química, así como del comportamiento redox de los polímeros sintetizados.

Por tanto, este capítulo se centra en la preparación y caracterización de diferentes polímeros conductores, especialmente copolímeros para sensores electroquímicos . El capítulo se ha dividido en dos partes dependiendo de los métodos de los materiales sintetizados:

Una síntesis electroquímica de copolímeros formados a partir de monómeros de ácido 2-aminotereftálico, piperazina y anilina que prueban su comportamiento electroquímico frente a la oxidación de dopamina y de ácido ascórbico en un electrolito acuoso. Se ha estudiado el efecto del

potencial positivo del barrido de potencial y la relación de la concentración de monómeros.El electrodo modificado con los diferentes copolímeros sintetizados electroquímicamente exhibió picos de oxidación para cada concentración de DA y AA, y cuando el potencial correspondiente al límite superior del voltagrama aumenta, la sensibilidad también aumenta. Los copolímeros sintetizados muestran una respuesta lineal con la concentración de dopamina y ácido ascórbico, la sensibilidad de estas medidas es en ambos casos lo suficientemente alta para asegurar la correcta cuantificación de ambos analitos. Además, el copolímero poli(Ani-co-2ATA) es más sensible que el copolímero de poli(Ani-co-PIP).

Los resultados obtenidos en este capítulo sugieren que la copolimerización de piperazina con anilina debe llevarse a cabo utilizando el potencial más bajo posible, con el fin de minimizar la oxidación irreversible de la primera. Sin embargo, se sabe que los cationes de anilinio (que se originan en potenciales superiores a 1,2 V frente a RHE) son necesarios para producir el depósito de polímeros derivados de polianilina. Por tanto, se necesita un compromiso entre las condiciones de polimerización más favorables para obtener un material (polímero) poco degradado y las condiciones reales para obtener un depósito. Debido a la mayor reactividad del monómero de anilina, la disolución de copolimerización contenía una concentración relativa anilina: piperazina baja de 0,2 en 1 M de $HClO_4$. En estas condiciones, se llevó el primer barrido hasta 1,3 V para generar una cantidad adecuada de radicales de anilinio, y los siguientes barridos de potencial se fijaron en 0,9 V para asegurar que los anillos de piperazina se puedan incorporar al polímero en crecimiento. La presencia y aumento de de procesos redox dentro de la región de potencial de 0.05-0.9 V evidencia el crecimiento de una especie polimérica electroactiva. Después de 10 ciclos, el electrodo de Pt se retiró de la disolución y su superficie apareció cubierta por una película de color azul oscuro.La formación de cetopiperazinas tras la oxidación de la piperazina a potenciales anódicos muy bajos demuestra que el material depositado podría incorporar una pequeña cantidad de las estructuras quinoides previamente formadas. Sin embargo, la alta intensidad relativa de la onda voltamétrica a 0,68 V sugiere que la principal contribución a los procesos redox involucran unidades de piperazina que se oxidan después de que se incorporan a la cadena del copolímero. En consecuencia, el segundo pico redox que se observa en el copolímero de anilina y piperazina, puede estar relacionado con la existencia de transiciones redox que involucran especies de hidroxipiperazina ⇌ cetopiperazina dentro de la estructura del copolímero.

Se estudió el efecto del potencial de polimerización en una disolución de ambos monómeros con una relación de 5. Se observan dos picos de oxidación claros en el barrido de potencial positivo, las flechas indican los potenciales utilizados para la copolimerización. Por otro lado, para entender este comportamiento, los copolímeros de anilina-piperazina se depositaron usando cuatro límites superiores de potencial diferentes 1,2 V; 1,3 V; 1,4 V y 1,1 V para el primer escaneo y 0,9 V para

los siguientes. Se ha podido observar que el comportamiento electroquímico de los copolímeros está fuertemente influido por el potencial superior en el barrido utilizado durante la síntesis. Los perfiles voltamétricos muestran que la cantidad de material depositado en la superficie del electrodo de Pt es significativamente mayor cuando el límite superior de potencial es superior a 1,3 V.

Además, el copolímero electrodepositado se examinó durante la copolimerización electroquímica de anilina y piperazina en una relación de monómero de 0,5 M: 0,5 M (ANI / PIP=1). Se ha observado en los voltamogramas cíclicos de los materiales obtenidos diferencias con respecto a las obtenidas en una relación de monómeros de 5, obteniéndose un perfil voltamétrico similar pero con mayores corrientes relativas (mayor carga). Nuevamente la cantidad de polímero aumenta con el potencial positivo. Además, la relación anilina: piperazina tiene una influencia importante en el perfil voltamétrico y la cantidad de polímero obtenido también. Por tanto, podemos concluir de estos resultados que cuando la relación de monómeros (PIP/Ani) es mayor, la concentración de piperazina también es mayor produciendo un aumento en la corriente de oxidación, y una disminución de la carga voltamétrica, esto indica que la oxidación se debe a la oxidación irreversible de la piperazina y que se produce una menor incorporación en el polímero. .

Se ha estudiado la oxidación de ácido ascórbico sobre el electrodo de Pt modificado con polianilina, con el fin de comparar el comportamiento con los diferentes copolímeros. El efecto electrocatalítico se puede observar para diferentes potenciales de síntesis de los polímeros, a 1,4 V y a 1,2 V. Las corrientes de pico de oxidación aumentan linealmente como las concentraciones de AA, el rango lineal es de 3 a 30 mM para las dos polianilinas y la sensibilidad se define por las pendientes respectivas (22,78 ± 0,07 y 13,27 ± 0,06) para Pani preparadas a 1,2V y 1,4 V, respectivamente. Se puede observar que la mayor sensibilidad se obtiene con la Pani sintetizada a 1.2V. En el caso de la oxidación de la DA, se puede observar un efecto electrocatalítico similar.. Las corrientes pico de oxidación aumentan linealmente como las concentraciones de DA, el rango lineal es 0.2-3.0 mM para las dos polianilinas y la sensibilidad está definida por las pendientes respectivas (58, 94 ± 0.02 y 89, 32 ± 0.02) para esos potenciales 1,2 V y 1,4 V, respectivamente. Se puede observar que la mayor sensibilidad se obtiene con la Pani sintetizada a 1.4V.

En el caso de los copolímeros, se puede observar un efecto electrocatalítico similar. Los copolímeros de polianilina y anilina-ácido aminotereftálico y anilina-piperazina muestran una respuesta lineal cuando se aplican a la determinación electroquímica de ácido ascórbico y dopamina en muestras sintéticas. La sensibilidad de estas mediciones es en ambos casos lo suficientemente alta como para asegurar la correcta cuantificación de analitos. El electrodo modificado exhibió picos de oxidación agudos para cada concentración de DA y AA. Este material de electrodo debe ser probado en muestras reales, pero de acuerdo con los resultados presentados, muestra una aplicación potencial

en sensores DA y AA, debido a su fácil síntesis, alta estabilidad química y respuesta lineal reproducible.

3.2 Síntesis y caracterización de hidrogeles obtenidos de monómeros de anilina y ácido aminotereftálico y piperazina.

Los hidrogeles son redes tridimensionales de polímeros hidrófilos que son notablemente adecuados para una amplia gama de aplicaciones. Los hidrogeles de polímeros conductores representan una clase emergente de materiales con un alto potencial de aplicación, especialmente en la conversión y almacenamiento de energía, pero también en muchas otras aplicaciones. Los polímeros conductores, como Pani, proporcionan conductividad electrónica y actividad redox; además, la fase acuosa del hidrogel asegura la conductividad iónica y esta combinación da lugar a propiedades únicas. En este capítulo se ha realizado un estudio de la síntesis química de hidrogeles de los copolímeros estudiados en el anterior capítulo mediante el autoensamblaje supramolecular. La síntesis química de hidrogeles a partir de anilina y ácido 2-aminotereftálico o anilina y piperazina puede permitir la obtención de materiales que mejoren algunas de las propiedades de los hidrogeles basados en Pani, como la solubilidad y la interacción con otros compuestos. Por tanto, se ha realizado un estudio de la síntesis mediante métodos químicos de hidrogeles basados en polímeros conductores (Pani/PSS, poli(Ani-co-ATA)/PSS y poli(Ani-co-PIP)/PSS) con diferentes relaciones molares. Los materiales sintetizados se han caracterizado mediante diferentes técnicas. Los copolímeros (poli(Ani-co-2ATA)/PSS y poli(Ani-co-PIP)/PSS) se han caracterizado utilizando diferentes técnicas.

La caracterización electroquímica se utilizó para caracterizar el comportamiento redox de los hidrogeles copolímeros y su electroactividad en medio ácido. Finalmente, se probaron las propiedades conductoras de los hidrogeles de copolímero para comparar la conductividad eléctrica. En el caso de poli(Ani-co-2ATA)/PSS-X la conductividad es menor que en el caso de Pani/PSS como consecuencia de la presencia de grupos carboxílicos en la estructura del polímero; sin embargo, en el caso de poli(Ani-co-PIP)/PSS-X la conductividad es más alta que Pani/PSS. También se realizaron análisis termogravimétrico (TGA) con el objetivo de evaluar la estabilidad térmica de los copolímeros de hidrogel, los cuales son muy importantes para la potencial aplicación de estos materiales. Además, se estudió la capacidad de hinchamiento midiendo el peso hidratado y el peso deshidratado.

3.3 Supercondensadores híbridos de hidrogeles supramoleculares

Los dispositivos de almacenamiento de energía electroquímica, como las baterías y los supercondensadores, han atraído una atención considerable de la comunidad científica debido al rápido aumento de la demanda de energía procedente de tecnologías ecológicas renovables. Por tanto, en este capítulo se evaluó la aplicabilidad de diferentes hidrogeles preparados en el capítulo

anterior como electrodos en condensadores en solución acuosa, para lo que se prepararon y probaron condensadores simétricos trabajando a un voltaje de 0.8 V en medio ácido.

La caracterización de los condensadores simétricos por cronopotenciometría (CP) se llevó a cabo para estudiar la capacidad específica. Las curvas de carga-descarga galvanostática a 0.05 A/g de los diferentes condensadores obtenidos con poli(Ani-co-2ATA)/PSS-X y el preparado con Pani/PSS muestran valores de capacidad muy bajos y se observan diferencias muy pequeñas entre los cuatro condensadores simétricos. La retención de capacidad con el aumento de la densidad de energía para el condensador preparado con Pani/PSS es solo del 18% a 0.5 A/g. Sin embargo, el condensador preparado con poli(Ani -co-2ATA)/PSS-5 presenta un 30% de retención de capacidad en las mismas condiciones, lo que muestra la ventaja de usar el copolímero en comparación con Pani. En el caso de los condensadores preparados con poli(Ani-co-PIP)-X también se observa un valor de retención de la capacidad superior al obtenido con los otros polímeros (Pani/PSS y poli(Ani-co-ATA)/PSS). El mayor valor de retención de capacidad se obtiene con poli(Ani-co-PIP)/PSS-3, que alcanza un valor del 63%. Por tanto, podemos concluir que todos los condensadores preparados con los hidrogeles de copolímero ofrecen una mejora de casi 1,5 veces la capacidad gravimétrica con respecto al hidrogel de Pani, además, la potencia máxima y la estabilidad mediante ciclado son adecuadas, lo que indica las ventajas de los hidrogeles copolímeros poli(Ani-co-PIP)/PSS y poli(Ani-co-2ATA)/PSS para esta aplicación en comparación con Pani/PSS.

Para mejorar el rendimiento de los condensadores asimétricos, se ha estudiado la adición de negro de carbón (Vulcan) y nanotubos de carbono de paredes múltiples (MWCNT). En todos los casos se han mezclado los hidrogeles con estos materiales carbonosos y se han probado en las mismas condiciones. Los resultados obtenidos muestran que los condensadores simétricos preparados en presencia de materiales de carbón presentan una capacidad específica mayor que la obtenida en ausencia de los materiales carbonosos, y el aumento es mayor en presencia de Vulcan. Estos resultados pueden ser consecuencia del aumento de la conductividad, pero también del aumento de la superficie específica. La retención de capacidad aumenta para los copolímeros en comparación con Pani/PSS obteniendo una mayor retención de capacidad con hidrogel del copolímero poli(Ani-co-PIP)-3. Los valores de capacidad volumétrica son superiores o similares a los obtenidos por otros autores.

4 **Conclusiones generales**

Esta Tesis Doctoral se ha centrado en la síntesis electroquímica de polímeros conductores basados en polianilina modificada con ácido 2-aminotereftálico y piperazina, y comportamiento frente a la oxidación de dopamina (DA) y ácido ascórbico (AA) y su posible aplicación como sensores electroquímicos. Además, se ha estudiado la síntesis química de hidrogeles de los copolímeros desarrollados y su aplicación como electrodos en supercondensadores. A continuación se resumen las principales conclusiones derivadas de esta Tesis Doctoral.

Estudio electroquímico de los copolímeros formados a partir de monómeros de ácido 2-aminotereftálico, piperazina y anilina que prueban su sensibilidad a la oxidación de la dopamina y al ácido ascórbico

• El ácido 2-aminotereftálico (2ATA) puede ser un monómero interesante para la copolimerización con anilina porque contiene dos grupos –COOH unidos al anillo aromático. La oxidación electroquímica del ácido 2-aminotereftálico en medio ácido no produce un polímero electroactivo en la superficie del electrodo de Pt; sin embargo, en presencia de anilina, se obtiene el copolímero. Por tanto, controlar la proporción de monómeros y el potencial de oxidación son parámetros clave para obtener un producto de copolimerización y modular la composición y propiedades del material.

• La oxidación electroquímica de piperazina sobre electrodos de platino a potenciales moderados (aproximadamente por debajo de 1.0 V / RHE) preserva la estructura del anillo de piperazina y produce ketopiperazinas como el principal producto de reacción. La espectroscopía FTIR in situ sugirió que la apertura del anillo y la sobreoxidación de este monómero ocurren a potenciales más altos para formar amidas e isocianatos. Como resultado, se observó que la homopolimerización de piperazina no se podía lograr en disolución acuosa de ácido perclórico en condiciones electroquímicas. Por el contrario, la piperazina se puede copolimerizar con éxito con anilina en medio ácido. El perfil voltamétrico del copolímero muestra un proceso redox a 0,68V que puede asociarse a la transformación reversible de hidroxi ↔ ketopiperazina. Cabe señalar que, debido al programa de potencial aplicado durante el proceso de polimerización no se observa una sobreoxidación significativa del mismo.

• La síntesis electroquímica mediante voltametría cíclica sobre un electrodo de platino de los monómeros de piperazina y ácido aminotereftalico con anilina en medio ácido produce la formación de diferentes copolímeros (poli(Ani-co-2ATA) y poli(Ani-co-PIP)). Los perfiles voltamétricos muestran que la cantidad de material depositado en la superficie del electrodo es significativamente mayor cuando el límite superior de potencial en la electropolimerización está en 1,2 V. De igual forma, la disminución en la relación de monómeros (PIP/Ani y 2ATA/Ani) produce el mismo efecto, es decir, el aumento en la carga voltamétrica asociada a los polímeros consecuencia de un aumento

en la cantidad de polímero obtenido. Este efecto es consecuencia de la mayor reactividad de la anilina en comparación con los otros dos monómeros.

• Los copolímeros poli(Ani-co-2ATA) y poli(Ani-co-PIP) muestran una respuesta lineal de la corriente de oxidación con la concentración de DA y AA en muestras sintéticas. El electrodo de Pt modificado con los copolímeros muestra procesos de oxidación para cada concentración de DA y AA y la sensibilidad de estas medidas es en ambos casos lo suficientemente alta para asegurar la cuantificación correcta de ambos analitos por separado. El aumento del límite superior del potencial en la síntesis de los copolímeros mediante voltametría cíclica aumenta la sensibilidad en la detección de DA y AA.

Síntesis y caracterización de hidrogeles obtenidos a partir de monómeros de anilina y ácido aminotereftálico y piperazina

• Se ha estudiado la síntesis química de hidrogeles y copolímeros de hidrogel mediante el auto-ensamblaje supramolecular entre las cadenas de polímero y copolímero. Se ha sintetizado el hidrogel de Pani/PSS y los hidrogeles de los copolímeros poli(Ani-co-2ATA)/PSS-X y poli(Ani-co-PIP)/PSS-X con diferentes relaciones molares. Los diferentes hidrogeles de los copolímeros se han caracterizado por diferentes técnicas como XPS, FTIR, etc. El comportamiento redox de los copolímeros se ha estudiado mediante técnicas electroquímicas (voltametría cíclica). Se realizaron análisis termogravimétricos; con el objetivo de evaluar la reactividad y la estabilidad térmica de los copolímeros de hidrogeles.

• Se medido las propiedades conductoras de los diferentes hidrogeles sintetizados, mediante la determinación de la conductividad eléctrica. Además, se ha calculado el hinchamiento de los hidrogeles comparando el peso hidratado con el peso deshidratado.

Supercondensadores híbridos de hidrogeles supramoleculares obtenidos de monómeros de anilina y ácido aminotereftálico y piperazina

• La caracterización electroquímica de los hidrogeles de los copolímeros poli(Ani-co-2ATA)/PSS-X y poli(Ani-co-PIP)/PSS-X muestran una capacidad prometedora en comparación con el hidrogel Pani/PSS.

• La comparación de los condensadores simétricos preparados con los hidrogeles de los copolímeros, muestra un aumento en la capacidad gravimétrica y un mejor comportamiento con la densidad de corriente con respecto al condensador obtenido con el hidrogel Pani/PSS.

• Se ensamblaron y caracterizaron condensadores simétricos con todos los hidrogeles sintetizados en esta Tesis Doctoral en medio ácido y, su comportamiento electroquímico se ha relacionado con los parámetros de síntesis, como la relación molar utilizada en la síntesis química. La caracterización electroquímica reveló que los grupos piperazina contribuyen significativamente a la pseudocapacidad en los hidrogeles de copolímeros con presencia de piperazina, obteniéndose una mayor retención de la capacidad específica con el aumento en la corriente, en comparación al condensador preparado con Pani/PSS.

• Se prepararon supercondensadores simétricos basados en polímeros conductores hidrogeles a partir de copolímeros hidrogeles en presencia de materiales de carbono (nanotubos de carbono de paredes múltiples y Vulcano). Se ha observado que los hidrogeles de copolímero muestran un mejor comportamiento que el hidrogel de polianilina. Y la presencia de negro de carbón mejora la conductividad de los electrodos y aumenta el rendimiento electroquímico del condensador. Los valores de capacitancia volumétrica son superiores o similares a los obtenidos por otros autores.

• Se prepararon supercondensadores simétricos basados en los hidrogeles de polímeros conductores en presencia de materiales de carbono (nanotubos de carbono de paredes múltiples y negro de carbón) mediante mezcla física. Se ha observado que los hidrogeles de los copolímeros muestran un mejor comportamiento que el hidrogel de Pani/PSS. La presencia de materiales de carbono mejora la conductividad de los electrodos y aumenta el rendimiento electroquímico del condensador. Los valores de capacidad volumétrica son superiores o similares a los obtenidos por otros autores.